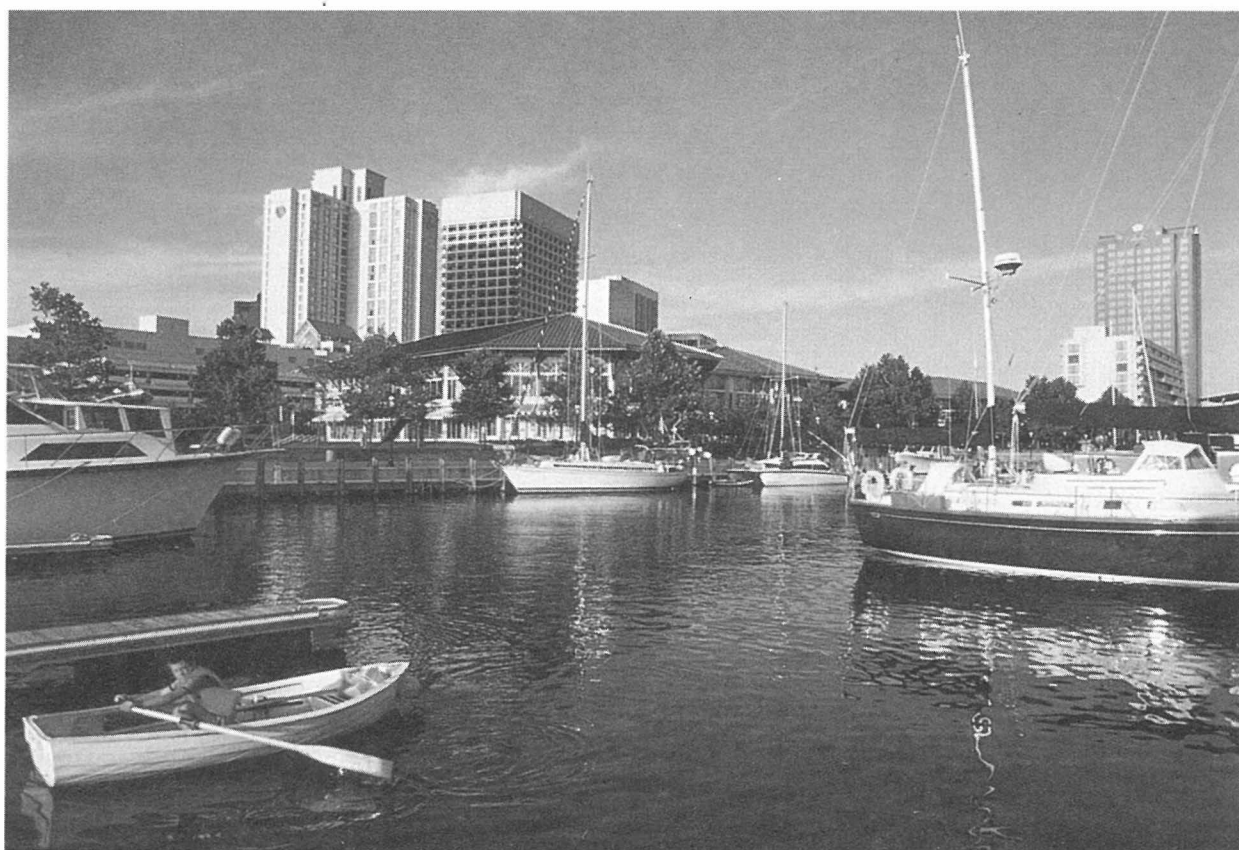


BULLETIN

OF THE AMERICAN PHYSICAL SOCIETY

PROGRAM OF THE 52ND ANNUAL
GASEOUS ELECTRONICS CONFERENCE



Norfolk, Virginia
October 5-8, 1999

October 1999
Volume 44, No. 4

BULLETIN

OF THE AMERICAN PHYSICAL SOCIETY

Coden BAPSA6

ISSN: 0003-0503

Series II, Vol. 44, No. 4

October 1999

APS COUNCIL 1999

President

Jerome Friedman, * *Massachusetts Institute of Technology*

President-Elect

James S. Langer, * *University of California, Santa Barbara*

Vice-President

George Trilling, * *Lawrence Berkeley National Laboratory*

Executive Officer

Judy R. Franz, * *University of Alabama, Huntsville*

Treasurer

Thomas McIlrath, * *University of Maryland*

Editor-in-Chief

Martin Blume, * *Brookhaven National Laboratory*

Past-President

Andrew M. Sessler, * *Lawrence Berkeley Laboratory*

General Councillors

Daniel Auerbach, Beverly Berger, Philip Bucksbaum, L. Craig Davis, S. James Gates, * Donald Haman, * Leon Lederman, Cynthia McIntyre, Roberto Peccei, Paul Peercy, * Helen Quinn, Susan Seestrom, * James Trefil, Virginia Trimble, * Ronald Walsworth, Sau Lan Wu

Chair, Nominating Committee

Daniel Kleppner

Chair, Panel on Public Affairs

Denis McWhan

Division and Forum Councillors

Steven Holt (*Astrophysics*), Eric Heller, * Harold Metcalf (*Atomic, Molecular, and Optical*), Robert Callender (*Biological*), Stephen Leone (*Chemical*), E. Dan Dahlberg, David Aspnes, * Arthur Hebard, Zachary Fisk* (*Condensed Matter*), Warren Pickett (*Computational*), Jerry Gollub (*Fluid Dynamics*), James Wynne (*Forum on Education*), Gloria Lubkin (*Forum on History of Physics*), Matt Richter (*Forum on Industrial and Applied Physics*), Myriam Sarachik (*Forum on International Physics*), Dietrich Schroer (*Forum on Physics and Society*), Andrew Lovinger (*High Polymer*), Daniel Grischkowsky (*Laser Science*), Howard Birnbaum (*Materials*), John Schiffer, John D. Walecka (*Nuclear*), Robert Kohn, Sally Dawson (*Particles and Fields*), Robert Siemann (*Physics of Beams*), Richard Hazeltine, William Krueger (*Plasma*)

**Members of APS Executive Board*

ADVISORS

Sectional Representatives

George Rawitscher, *New England*; William Standish, *New York*; Perry P. Yaney, *Ohio*; Joseph Hamilton, *Southeastern*; Stephen Baker, *Texas*

Representatives from Other Societies

Thomas O'Kuma, *AAPT*; Marc Brodsky, *AIP*

Editor: Donna Baudrau

Meeting Publications Coordinator:

Vinaya K. Sathyasheelappa

APS MEETINGS DEPARTMENT

One Physics Ellipse

College Park, MD 20740-3844

Telephone: (301) 209-3200

FAX: (301) 209-0866

Donna Baudrau, *Meetings Manager*

Terri Adorjan, *Assistant Meetings Manager*

Karen MacFarland, *Meetings Coordinator*

Don Wise, *Registrar*

Staff Representatives

Barrett Ripin, *Associate Executive Officer*; Irving Lerch, *Director of International Affairs*; Ramon Lopez, *Director of Education and Outreach*; Robert L. Park, *Director, Public Information*; Michael Lubell, *Director, Public Affairs*; Stanley Brown, *Administrative Editor*; Charles Muller, *Director of Editorial Office Services*; Michael Stephens, *Controller and Assistant Treasurer*

The *Bulletin of The American Physical Society* is published 9X in 1999, March, June, July, October (2X), November (3X), and December, by The American Physical Society, through the American Institute of Physics. It contains information about meetings of the Society, including abstracts of papers to be presented, as well as transactions of past meetings. Reprints of papers can be obtained only by writing directly to the authors.

The *Bulletin* is delivered, on subscription, by Periodicals mail. Complete volumes are also available on microfilm. **APS Members** may subscribe to individual issues, or for the entire year. **Nonmembers** may subscribe to the *Bulletin* at the following rates: Domestic \$470; Foreign Surface \$490; Air Freight \$515. Information on prices, as well as subscription orders, renewals, and address changes, should be addressed as follows: **For APS Members**—Membership Department, The American Physical Society, One Physics Ellipse, College Park, MD 20740-3844. **For Nonmembers**—Circulation and Fulfillment Division, The American Institute of Physics, Suite 1NO1, 2 Huntington Quadrangle, Melville, NY 11747-4502. Allow at least 6 weeks advance notice. For address changes, please send both the old and new addresses, and, if possible, include a mailing label from a recent issue. Requests from subscribers for missing issues will be honored without charge only if received within 6 months of the issue's actual date of publication.

The *Bulletin of The American Physical Society* (ISSN: 0003-0503) is published ten times a year for The American Physical Society by the American Institute of Physics. 1999 subscription rate is \$470 for domestic nonmembers. Postmaster: Send address changes to *Bulletin of The American Physical Society*, AIP, Suite 1NO1, 2 Huntington Quadrangle, Melville, NY 11747-4502. Periodicals postage paid at Huntington Station, NY, and additional mailing offices.

On the Cover: A waterview of Norfolk, courtesy of the Norfolk Convention & Visitors Bureau.

BULLETIN

OF THE AMERICAN PHYSICAL SOCIETY

Vol. 44, No. 4, October 1999

52nd Annual Gaseous Electronics Conference

TABLE OF CONTENTS

General Information	3
<i>Arranged oral and poster sessions</i>	3
<i>Presentations</i>	3
<i>Lab Tours</i>	3
GEC Student Award for Excellence	3
Special Workshop	4
<i>High Pressure Light Sources</i>	4
<i>Low Pressure Light Sources</i>	4
<i>Light Source Diagnostics</i>	4
<i>Modeling of Light Sources</i>	5
Registration	5
<i>Opening Reception</i>	5
<i>Conference Banquet</i>	5
<i>E-mail and Other Business Services</i>	5
<i>Audiovisual Equipment</i>	5
<i>Dining Options</i>	5
Guest Program	5
Call for Nominations for GEC General and Executive Committees	6
GEC Executive Committee	6
Please Note	6
Epitome	7

Main Text	9
<i>Tuesday</i>	9
<i>Wednesday</i>	37
<i>Thursday</i>	65
<i>Friday</i>	76
Author Index	83
Map and Floor Plans	At End of Issue
Condensed Epitome	Back Covers

52nd Annual
Gaseous Electronics Conference
October 5 – 8, 1999; Norfolk, Virginia

GENERAL INFORMATION

Welcome to the 52nd Annual Gaseous Electronics Conference (GEC), a topical conference of the American Physical Society. The GEC99 program will include a GEC Foundation Talk, a Will Allis Memorial Session, and the annual GEC Student Award for Excellence. Oral sessions of both invited and contributed papers and two poster sessions will address a broad range of topics. The Sheraton Norfolk Waterside Hotel will serve as headquarters for the conference.

The **GEC Foundation Talk** will be given by **Alex Dalgarno**, *Historical Evolution of Cross Section Calculations*.

The **Will Allis Memorial Session (Session GW2)** will feature presentations by **James E. Lawler**, *Resonance Radiation Transport in Low Pressure Discharges* and **Graeme Lister**, *Recent Developments in Modeling and Diagnostics of Fluorescent Lamps*.

Arranged oral and poster sessions include:

- Electron-Atom Collisions (*Session IWP3*)
- Electron-Molecule Collisions (*Sessions AT1 and ETP1*)
- Electron Collisions with Excited Atoms and Molecules (*Session JW1*)
- Electron Impact Ionization (*Session MR1*)
- Dissociation and Ionization (*Session NR1*)
- Negative Ion Formation (*Session RF2*)
- Recombination and Heavy Particle Collisions (*Session LR1*)
- Heavy Particle Collisions (*Session ETP1*)
- Glows (*Sessions AT2, ETP3, IWP4, and NR2*)
- RF Glows (*Session FW2*)
- DC Glows (*Session QF2*)
- Inductively Coupled Plasmas (*Session AT2*)
- Sheaths and Instabilities (*Session BT1*)
- Simulations and Modeling (*Session JW2*)
- Transport Effects (*Session IWP1*)
- Surface Wave Plasmas (*Session MR2*)
- Magnetically-Enhanced Plasmas (*Sessions IWP6 and ORI*)
- Dusty Plasmas (*Sessions ETP6 and OR2*)

- Plasma Processing and Surface Modifications (*Session IWP10*)
 - Plasma-Surface Interactions (*Sessions IWP7 and RF1*)
 - Diagnostics (*Sessions DT1 and QF1*)
 - Electrical Discharges (*Session IWP12*)
 - Mass Spectrometry (*Session IWP12*)
 - Etching (*Session BT2*)
 - Lighting and Plasma Displays (*Session DT2*)
 - Lighting Related Discharges (*Session IWP8*)
 - High Intensity Light Sources (*Session ETP4*)
 - Deposition/Materials Processing (*Session FW1*)
 - Chemistry and Transport Processes (*Session GW1*)
 - Laser Media and Thermal Plasmas (*Session IWP5*)
 - High Pressure Lighting Plasmas (*Session LR2*)
 - Environmental Applications (*Session IWP11*)
 - Innovative Plasma Applications (*Sessions IWP13 and RF2*)
 - Gas Phase Chemistry (*Session IWP2*)
 - Plasma Displays (*Session IWP9*)
 - Spark Channel Temporal Variations (*Session ETP5*)
 - Optical Diagnostics (*Session ETP7*)
- There will also be a post-deadline poster session.

Presentations

Papers that have been accepted for presentation are listed in the daily schedule of technical sessions. Additional postdeadline papers will be distributed at the meeting. Oral contributed presentations are allotted 12 minutes, with an additional 3 minutes for discussion. Invited papers are 25 minutes in length, with 5 minutes for discussion.

Lab Tours

A tour of the physics and engineering laboratories on the Old Dominion University campus will take place Wednesday, October 6, from 8:00 PM to 10:00 PM. The University is a ten minute drive from the Sheraton. Transportation to and from campus will be provided. Shuttle busses will begin leaving from the hotel at approximately 7:30 PM.

**GEC STUDENT AWARD
FOR EXCELLENCE**

In order to recognize and encourage the outstanding contributions students make to the Gaseous Electronics Conference, the GEC will continue to present an award

for the best paper presented by a student. A subcommittee of the GEC executive committee will choose the award winner. Students competing for the \$500 award are:

Bernd E. E. Kastenmeier, SUNY, Albany, **BT2 5**: *Etching Mechanism of Silicon Nitride in Remote Plasmas Containing Fluorine, Oxygen, and Nitrogen.*

John Kline, West Virginia University, **OR1 2**: *Ion Heating in the HELIX Helicon Plasma Source.*

Yunlong Li, University of Arkansas, **DT1 5**: *Absorption Measurements of 4s State Number Density for a Microwave Argon Plasma.*

Philippe Mérel, University of Quebec, INRS, **FW1 3**: *Development and Characterization of an Atomic Nitrogen Source for the Epitaxial Growth of GaN.*

Yaoxi Wu, UC Berkeley, **AT2 5**: *The Influence of Antenna Configuration and Standing Wave Effects on Density Profile in a Large Area Inductive Plasma Source.*

SPECIAL WORKSHOP

A special one-day workshop on Non-Coherent Light Sources will be held Monday, October 4, 1999. The workshop will take place at the Sheraton Norfolk Waterside Hotel and will begin at 9:00 AM. The registration desk will be open from 8:00 AM to 10:00 AM. Registration for the Workshop is \$50. Participants are encouraged to preregister for the workshop, using the conference registration form.

The workshop will be comprised of four tutorials:

High Pressure Light Sources
Low Pressure Light Sources
Light Source Diagnostics
Modeling Of Light Sources

High Pressure Light Sources
Tutorial leader: Klaus Günther

Electronic Stabilization of HID Lamps

The photometric properties of High Intensity Discharge (HID) lamps are carefully optimized to the field of their application. They should be stabilized during their lifetime as much as possible. This can be accomplished in two ways: (i) suppressing all aging and corroding processes leading to changing conditions of the radiating plasma by means of a proper combination of the lamp components and operation conditions, and (ii) the electronic detection of all deviations from the designed operation point and their compensation by a modification of the electric circuit parameters. The procedure is discussed for different types of HID lamps.

Low Pressure Light Sources

Tutorial leader: John Waymouth

Low Pressure Discharge Light Sources

Part I: Plasma Phenomena

I will discuss the plasma phenomena of importance to the high efficiencies of production of resonance radiation in low-pressure discharges used for general lighting applications: mercury-rare-gas fluorescent lamps, and low-pressure sodium lamps. I will highlight the unique properties of mercury that underlie the 60-percent-plus efficiency of generation of 254-nm 3P1-mercury resonance radiation.

Part II: Electrode phenomena

Hot cathodes in low-pressure discharge lamps deliver 10-50 amp/cm² of electron emission for tens of thousands of hours at an energy cost of about 10 watts/ampere. I will discuss physical phenomena responsible for this remarkable technical performance. I will also discuss potential improvements in these performance figures which may be permitted by recent developments in lamp operating circuitry that substantially reduce cathode damage at ignition.

Light Source Diagnostics

Tutorial leaders: J. J. Curry & J. E. Lawler

Advanced X-ray Diagnostics of HID Lamps

J. J. Curry & J. E. Lawler

X-ray diagnostic techniques for High Intensity Discharge (HID) lamps will be reviewed. HID lamps are a particular challenge for diagnosticians. The low optical quality and strong curvature of standard fused silica arc tubes limits the utility of optical and UV diagnostic experiments. Spatially resolved optical or UV diagnostics are impossible in translucent Polycrystalline Alumina (PCA) arc tubes for metal halide HID lamps. A recent X-ray experiment using a new detector technology will be described. Opportunities for much more ambitious X-ray diagnostics experiments on HID lamps using modern synchrotron radiation sources such as the Advanced Photon Source, and using modern detector technologies such as phosphor image plates and Charge Coupled Device detector arrays will be emphasized.

Light Source Diagnostics

J. E. Lawler & J. J. Curry

Diagnostic techniques for glow and high intensity discharge (HID) lamps will be reviewed, with emphasis on spectroscopic techniques. Capabilities of emission, absorp-

tion, laser induced fluorescence, and laser optogalvanic techniques will be compared. New technologies which enhance diagnostic techniques including new types of lasers, detector arrays, and synchrotron radiation facilities will be discussed. Microwave interferometry and probe techniques will be discussed. The kinds of information as well as the spatial and temporal resolution provided by various diagnostic methods will be compared.

Modeling Of Light Sources

Tutorial leader: Graeme Lister

Modeling of

Low Pressure Discharges for Lighting

This lecture will principally deal with the modeling of fluorescent lamps, in particular the positive column of the discharge, which is the major source of useful radiation. Fluorescent lamps are gas discharges containing a few mtorr of mercury vapor in a rare gas at pressures of a few torr. Mercury atoms radiate principally in the UV and this is converted to visible light by means of a phosphor. The models described include the influence of radiation trapping, pumping of mercury from the center of the discharge (cataphoresis) through ambipolar diffusion and the electron energy distribution function in both the "local" and "non local" approximations. The data requirements for the models will also be discussed, together with the calculation of relevant transport coefficients. Modeling of the new generation of "electrodeless" lamps, in which electrical power is inductively coupled to the discharge by radio-frequency fields, will also be considered. Finally, modeling of pure rare gas discharges and discharges in which elements other than mercury are used (sodium and barium) will be described.

Modeling of

High Pressure Discharges for Lighting

This lecture will describe the modeling of metal halide lamps, which typically operate at a few atmospheres pressure of mercury and contain a small amount of metal halide salts to augment the visible radiation from mercury atoms, which is principally green. The influence of convection flows, thermal conduction, radiation transport and species separation by cataphoresis (de-mixing) will be described. The data required to implement these models will be reviewed, and supporting models which describe the thermodynamic properties and transport coefficients will be discussed. The use of 1D, 2D and 3D models will also be assessed.

REGISTRATION

The conference registration desk is located on the Promenade. Registration hours will be 8:00 AM to 10:00 AM and 6:00 PM to 9:00 PM on Monday, October 4, and from 7:30 AM to 3:30 PM October 5-7. The regular conference fee is \$220 (\$270 after September 3), and \$120 for students and retirees.

OPENING RECEPTION

Old Dominion University will sponsor an Opening Reception for GEC participants and their guests. The Reception will take place on Monday, October 4, from 7:00 PM to 9:00 PM in the Stratford Hall of the Sheraton.

CONFERENCE BANQUET

There will be a banquet held on the evening of Thursday, October 7 for conference attendees and their guests in Sheraton Norfolk Waterside Hotel. The banquet will be held in the Stratford Hall of the Sheraton, preceded by a reception starting at 6:30 PM on the Promenade.

E-MAIL AND OTHER BUSINESS SERVICES

Free e-mail access is available to conference participants. FAX, photocopy services, and office supplies are also available at the Business Center of the Sheraton Hotel.

AUDIOVISUAL EQUIPMENT

Each room is equipped with an overhead projector and slide projector. If additional equipment is required, please contact the conference secretary.

DINING OPTIONS

A wide variety of dining options exist for conference participants. A bar and restaurant are located in the Sheraton Hotel. The Waterside Festival Marketplace, adjacent to the Sheraton, houses an extensive food court. Restaurants and a food court are located in the newly opened MacArthur Center, about three blocks from the Sheraton. In addition, many fine restaurants, in a variety of price ranges, are located within walking distance of the hotel.

GUEST PROGRAM

The Sheraton Waterside Hotel is within walking distance of a number of historical and cultural attractions. These include the acclaimed Chrysler Museum of Art, the Harrison Opera House, Nauticus - the National Maritime Center, the d'Art Center, St. Paul's Church (built in 1739), the Moses Meyers House, and the General Dou-

glas MacArthur Memorial. The Norfolk Botanical Gardens, Norfolk Naval Base, and the Virginia Zoological Park are all a short drive from the Hotel. The Virginia Beach oceanfront is about a 25 minute drive, and Colonial Williamsburg is about 45 minutes away.

CALL FOR NOMINATIONS FOR GEC GENERAL AND EXECUTIVE COMMITTEES

The GEC Executive Committee (ExComm) is the governing body of the GEC. It is the responsibility of ExComm to oversee all aspects of the conference. This includes selection of meeting sites, budgetary decisions, selection of special topics and invited speakers, accepting/rejecting abstracts and arranging the program. The ExComm formally meets three times a year: the General Committee and ExComm meetings during the GEC, and the Summer ExComm Meeting where the program of the next GEC is arranged. There are numerous communications between members of the ExComm (usually e-mail) during the year to see to the successful completion of their duties. We have been fortunate over the years to have a dedicated group of volunteers who have been willing to take on these very necessary roles.

The bylaws of the Gaseous Electronics Conference describe the process whereby members of the ExComm are elected. At the GEC Business Meeting (to be held on Wednesday, October 6, at 11:30 AM) nominations are accepted for members of the GEC General Committee (GenComm). The GenComm consists of the ExComm and six at-large members elected at the Business Meeting. The eligible voting membership of the GEC (defined as those attending the Business Meeting) elect these six at-large members. The GenComm then meets to fulfill its only duty: to elect new members of ExComm.

The ExComm membership consists of the Chair, Treasurer, Past-Secretary, Secretary, Secretary-elect, past or incoming Chair and four at-large members. The Chair is a 4-year term (1-year incoming, 2-years chair, 1-year past-chair), the secretary is a 3-year term (1-year incoming, 1-year secretary, 1-year past- secretary), and all other ExComm members serve two years. (The secretary is the person who manages the local arrangements for the meeting and is usually "recruited" and appointed to the ExComm.)

The ExComm welcomes nominations, including self-nominations, for both the GenComm and ExComm. Becoming a GenComm and/or ExComm member pro-

vides a unique opportunity to see both how the GEC is run and to influence its future direction by helping to define the programs and choose future sites. Please submit your nominations to the GEC Chair or any member of the ExComm (listed below). The ExComm also welcomes inquiries on hosting the GEC.

GEC EXECUTIVE COMMITTEE

Gerry Hays, Chair
Sandia National Laboratories
Leposava Vuškovic, Secretary
Old Dominion University
Mark J. Kushner, Past-Chair
University of Illinois
Charles Fledderman, Past-Secretary
University of New Mexico
Demetre Economou, Secretary-Elect
University of Houston
Kristen Steffens, Treasurer
NIST, Gaithersburg
Tim Gay, *University of Nebraska*
Gerrit Kroesen, *Technische Univ. Eindhoven*
Kunihide Tachibana, *Kyoto University*
Tom Rescigno, *Livermore National Laboratory*
Helen Hwang, *Thermosciences Institute*
Bob Piejak, *OSRAM Sylvania Inc.*

Conference Secretary

Further information on the conference may be obtained from the conference secretary at the following address:

Professor Leposava Vuškovic
Old Dominion University
Department of Physics
4600 Elkhorn Ave.
Norfolk, VA 23529-0116USA
757 683-4611 (Voice)
757 683-3038 (FAX)
email: vuskovic@physics.odu.edu

PLEASE NOTE

The APS has made every effort to provide accurate and complete information in this *Bulletin*. Changes or corrections, however, may occasionally be necessary, and may be made without notice after the date of publication. To ensure that you receive the most up-to-date information, please check the meeting *Corrigenda* distributed with this *Bulletin*.

Epitome of the 1999 GEC Meeting

8:00 TUESDAY MORNING 5 OCTOBER

- AT1 **Electron-Molecule Collisions**
Chutjian, Burrow
Stratford Room
- AT2 **Glows: Inductively Coupled
Plasmas**
Wendt, Godyak
York Room

10:30 TUESDAY MORNING 5 OCTOBER

- BT1 **Sheaths and Instabilities**
Stratford Room
- BT2 **Etching**
York Room

13:30 TUESDAY AFTERNOON 5 OCTOBER

- CT1 **Foundations of Gaseous
Electronics**
Dalgarno
York and Stratford Rooms

15:00 TUESDAY AFTERNOON 5 OCTOBER

- DT1 **Diagnostics I**
Döbele, Herman
Stratford Room
- DT2 **Lighting and Plasma Displays**
York Room

19:30 TUESDAY EVENING 5 OCTOBER

- ETP1 **Electron-Molecule Collisions**
Poplar Room
- ETP2 **Heavy Particle Collisions**
Poplar Room
- ETP3 **Glows I**
Poplar Room
- ETP4 **High Intensity Light Sources**
Poplar Room

- ETP5 **Spark Channel Temporal
Variations**
Poplar Room

- ETP6 **Dusty Plasmas**
Poplar Room

- ETP7 **Optical Diagnostics**
Poplar Room

8:00 WEDNESDAY MORNING 6 OCTOBER

- FW1 **Deposition/Materials Processing**
Grapperhaus
Stratford Room

- FW2 **RF Glows**
York Room

10:15 WEDNESDAY MORNING 6 OCTOBER

- GW1 **Chemistry and Transport
Processes**
Stratford Room

- GW2 **Will Allis Memorial Session**
Lawler, Lister
York Room

11:30 WEDNESDAY MORNING 6 OCTOBER

- HW1 **Business Meeting**
York Room

13:30 WEDNESDAY AFTERNOON 6 OCTOBER

- IWP1 **Transport Effects**
Poplar Room

- IWP2 **Gas Phase Chemistry**
Poplar Room

- IWP3 **Electron-Atom Collisions**
Poplar Room

- IWP4 **Glows II**
Poplar Room

- IWP5 **Laser Media and
Thermal Plasmas**
Poplar Room

- IWP6 **Magnetically-Enhanced Plasmas**
Poplar Room
- IWP7 **Plasma-Surface Interactions**
Poplar Room
- IWP8 **Lighting-Related Discharges**
Poplar Room
- IWP9 **Plasma Displays**
Poplar Room
- IWP10 **Plasma Processing and Surface
Modifications**
Poplar Room
- IWP11 **Environmental Applications**
Poplar Room
- IWP12 **Electrical Diagnostics and Mass
Spectrometry**
Poplar Room
- IWP13 **Innovative Plasma Applications**
Poplar Room

**16:00 WEDNESDAY AFTERNOON
6 OCTOBER**

- JW1 **Electron Collisions With Excited
Atoms and Molecules**
Lin, Kouchi, Khakoo
Stratford Room
- JW2 **Simulations and Modeling**
Lieberman, Graves, Kushner, Kim
York Room

**20:00 WEDNESDAY EVENING
6 OCTOBER**

- KW1 **Laboratory Tours**
Old Dominion University Campus

**8:00 THURSDAY MORNING
7 OCTOBER**

- LR1 **Recombination and
Heavy Particle Collisions**
Guberman, Mitchell
Stratford Room
- LR2 **High Pressure Lighting Plasmas**
Schoenbach, Guenther
York Room

**10:30 THURSDAY MORNING
7 OCTOBER**

- MR1 **Electron Impact Ionization**
Schmidt, McCurdy, Pindzola
Stratford Room
- MR2 **Surface Wave Plasmas**
Moisan, Shivarova
York Room

**13:30 THURSDAY AFTERNOON
7 OCTOBER**

- NR1 **Dissociation and Ionization**
Cocke, Cosby
Stratford Room
- NR2 **Glows**
Yasuoka
York Room

**15:45 THURSDAY AFTERNOON
7 OCTOBER**

- OR1 **Magnetically-Enhanced Plasmas**
Stratford Room
- OR2 **Dusty Plasmas**
Goree, Sato
York Room

**18:30 THURSDAY EVENING
7 OCTOBER**

- PR1 **Reception and Banquet**
York and Stratford Rooms

**8:00 FRIDAY MORNING
8 OCTOBER**

- QF1 **Diagnostics II**
Stratford Room
- QF2 **DC Glows**
York Room

**10:30 FRIDAY MORNING
8 OCTOBER**

- RF1 **Plasma-Surface Interactions**
Oehrlein, Möller
Stratford Room
- RF2 **Innovative Plasma Applications/
Negative Ion Formations**
Eden, Ratner
York Room

SESSION AT1: ELECTRON-MOLECULE COLLISIONS

Tuesday morning, 5 October 1999; Stratford Room Sheraton Waterside Hotel at 8:00

T.N. Rescigno, Lawrence Livermore National Laboratory, presiding

Invited Papers

8:00

AT1 1 Ultralow Energy Electron Attachment at Sub-Millielectron Volt Resolution.ARA CHUTJIAN,* *Jet Propulsion Laboratory, California Institute of Technology, Pasadena, CA*

The technique of rare-gas photoionization¹ has been extended² by use of direct laser ionization to electron energies ϵ in the range 0-100 meV, with a resolution $\Delta\epsilon$ of 0.4-0.5 meV (FWHM). Tunable UV light at $\lambda 276$ nm is produced using a pulsed Nd:YAG laser and nonlinear mixing techniques. The beam is frequency tripled in a pulsed jet of xenon. The VUV radiation, tunable at $\lambda 92$ nm, is then used to photoionize Xe at its $^2P_{1/2}$ threshold (single-photon ionization). The photoelectrons produced interact with admixed target gas to generate negative ions through the *s*-wave capture process. Recent results in electron attachment to SF₆ will be reported which show resonance structure at the opening of the ground-state vibrational channels.³ This structure corresponds to the process of vibrational excitation + attachment, which is superimposed on the underlying *s*-wave (direct) capture process. It should be a general phenomenon, present in a wide variety of zero-energy electron attaching molecules.

*In collaboration with A. Kortyna, M. R. Darrach and P-T. Howe. This work was carried out at JPL/Caltech, and was supported through the NSF AMOP Program through agreement with NASA.

¹J. M. Ajello and A. Chutjian, *J. Chem. Phys.* **65**, 5524 (1976).

²A. Kortyna, M. Darrach and A. Chutjian, *Bull. Am. Phys. Soc.* **43**, 1336 (1998).

³H. Hotop et al., *AIP Conf. Proc. Ser. 360* (AIP, New York, 1995), and private communication.

8:30

AT1 2 Dissociative Attachment in Chlorine-substituted Hydrocarbons .*PAUL D. BURROW, *University of Nebraska-Lincoln, Lincoln, NE 68588.*[†]

The dissociative attachment process, $e + AB \rightarrow AB^- \rightarrow A + B^-$, plays a role in a variety of gas phase, surface and liquid environments. The central problem in studies of DA in complex systems is to link DA cross sections to the structure of the target molecules. Our approach is to examine the connection between the DA cross sections and the vertical attachment energies (VAEs) for formation of the temporary negative ion intermediates. In a series of saturated hydrocarbons substituted with one, two or three Cl atoms, we find that with few exceptions the peak DA cross sections decline exponentially with increasing VAE, a result that should be useful for modeling purposes. The role of unsaturation in hydrocarbons will also be discussed briefly.

*Supported by the National Science Foundation, CHE-9710076.

[†]Work carried out in collaboration with K. Afatooni and G.A. Gallup.

Contributed Papers

9:00

AT1 3 Theoretical Study of the Effects of Nuclear Motion on Low-Energy Electron-CO₂ Scattering* W.A. ISAACS, *LBNL*

T.N. RESCIGNO, *LLNL* C.W. McCURDY, *LBNL* We report the results of variational calculations on the scattering of low-energy electrons by CO₂ over the energy range from 0 to 10 eV. The calculations use the complex Kohn formalism and include electron-target correlation and polarization in a completely *ab initio* fashion. We will concentrate on the two features that dominate the low-energy electron scattering for this system, namely, the 3.8 eV shape resonance and the virtual state enhancement of the elas-

tic cross sections below 2 eV. In particular, we will investigate how these features change when the nuclear motion of the target is properly accounted for and we will present cross sections that reflect the inclusion of bending and stretching degrees of freedom.

*Work performed under auspices of USDOE by LLNL under contract W-7405-ENG and LBNL under contract DE-AC03-76F00098

9:15

AT1 4 Ubiquitous Low Energy Structures in Differential Elastic Electron Molecule Scattering STEPHEN J. BUCKMAN,

LEWIS T. CHADDERTON, *Atomic and Molecular Physics Laboratories, Australian National University, Canberra.* In recent years detailed, low energy, elastic electron-molecule scattering experiments in our laboratory and others, have revealed alluring

structures in angular differential cross sections which occur at scattering angles around 20-50°. They take the form of a shallow minimum/maximum which develops, and then disappears, over a very small impact energy range, typically between 3-7 eV. They have been observed in a variety of molecules - diatomic and polyatomic, closed and open shell, polar and non-polar (e.g. N₂, O₂, NO, CO, N₂O, CO₂) and only in a few cases is there even a marginal correspondence with contemporary quantum scattering theory. Their origin is puzzling but we are persuaded that they are due to a fully wave-mechanical double (or triple etc.), sequential atomic scattering. In electron scattering from N₂, for example, the primary scattered wave from the first atom falls on the second atom in the near-field. Secondary scattering of this first atom image by the second atom takes place and a second, focused image is established. The experimental observations are described in terms of a "rainbow" component of this molecular steric scattering which, perhaps surprisingly, survives angular averaging over stochastic molecular orientations.

9:30

AT1 5 Absolute Elastic Electron Scattering from Benzene
ROBERT GULLEY, STEPHEN BUCKMAN, *Australian National University* Absolute differential cross-sections for vibrationally elastic electron scattering from benzene (C₆H₆) have been measured, for the first time, in the energy range from 4 to 20 eV and for scattering angles between 15° and 130°, using a crossed-beam apparatus. The cross-sections are characterised by strong forward-angle scattering due to the large dipole polarizability of the molecule and large-angle oscillations due to the effect of shape resonances. Favourable comparisons are made with a recent the-

oretical calculation¹ which uses a parameter-free, exact-static-exchange-correlation-polarization (SECP) potential to treat the electron-molecule interaction in all scattering symmetries. To our knowledge, this is the only contemporary calculation of differential elastic electron-C₆H₆ scattering.

¹F.A. Gianturco and R.R. Lucchese, *J. Chem. Phys.* **108** 6144, (1998).

9:45

AT1 6 Low Energy Dissociative Electron Attachment to Ozone
GILBERT SENN, *Institute of Ion Physics, University of Innsbruck* JAN DUSAN SKALNY, *Department of Plasma Physics, Comenius University, Bratislava* ALEKSANDAR STAMATOVIC, *Faculty of Physics Beograd* NIGEL MASON, *University College London* PAUL SCHEIER, *Institute of Ion Physics, University of Innsbruck* TILMANN MARK, *Institute of Ion Physics, University of Innsbruck* The production of O⁻ and O₂⁻ by dissociative electron attachment to ozone is reported. A high resolution trochoidal electron monochromator developed recently in our laboratory was used to prepare an electron beam with small electron energy distributions. The electron energy in this monochromator is adjustable from close to zero up to 10 eV. A previously unobserved sharp structure is observed in the formation of the O⁻ ions at zero incident energy, with an 1/E energy dependence, which is characteristic for a s-wave electron capture. This large additional cross section peak implies also large attachment rate coefficient at thermal energies. This has important consequences for the role of ozone in the anion formation processes in the D layer of the ionosphere.

SESSION AT2: GLOWS: INDUCTIVELY COUPLED PLASMAS

Tuesday morning, 5 October 1999; York Room Sheraton Waterside Hotel at 8:00; Peter Ventzek, Motorola/Austin, presiding

Invited Papers

8:00

AT2 1 Modulated Discharges in Processing Applications.

A. E. WENDT, *Univ. of Wisconsin - Madison*

S.-B. WANG, *Univ. of Wisconsin - Madison*

J. WERKING, *SEMATECH*

Discharge pulsing has recently been touted as a promising method to address a number of problems in plasma etching for semiconductor fabrication. These include control of selectivity, particulate contamination, substrate heat loads, device damage and feature profiles. An overview will be given of research on discharge pulsing including physical mechanisms involved and how they can improve etching processes. Particular attention will be paid to the "electron shading" effect, localized surface charging on high aspect ratio features that can lead to distortion of feature profiles and gate oxide damage. Recent work shows that these problems can be avoided by appropriate discharge pulsing, due to charge neutralization during sheath collapse when the discharge power is periodically extinguished. Another type of pulsing will also be presented, in the form of a new method for controlling the ion energy distribution function (IEDF) at the substrate using a tailored, pulsed voltage waveform on the substrate electrode. By maintaining a nearly constant substrate voltage, with periodic spikes to collect electrons (and prevent continuous charge accumulation on the substrate surface), a nearly monoenergetic IEDF can be achieved. IEDF control has significant implications for selectivity, feature profile control, and the study of the influence of ion bombardment energy in processing environments.

8:30

AT2 2 Low Frequency Inductive Discharges.

VALERY GODYAK, *OSRAM Sylvania, 71 Cherry Hill Drive, Beverly, MA 01915*

The rf inductive discharge or inductively coupled plasma (ICP) continues to attract growing attention as an effective plasma source in many industrial applications, the best known of which are plasma processing and lighting technology. Although most practical ICPs operate at 13.56 MHz, the trend to reduce the operating frequency is clearly recognizable from recent ICP developments. The use of a lower operating frequency simplifies and reduces cost of rf matching systems and rf generators and can eliminate capacitive coupling between the inductor coil and plasma, which could be a strong factor in wall erosion and plasma contamination. The transition to a lower operating frequency also brings with it changes in ICP physics. The most remarkable feature of low frequency rf inductive discharges is the manifestation of non-linear interaction between the electromagnetic fields and the plasma. This non-linear behavior originates from two quite different effects. The first is associated with periodic modulation of the plasma conductivity due to changes in plasma density and electron temperature when the rf field frequency approaches the characteristic frequency of electron energy exchange and/or the ionization frequency. The second kind of non-linearity is originated by rf Lorentz force and brings about a variety of new effects. It has been shown that the rf magnetic field may modulate the electron density at the second harmonic with its associated rf field, modify the steady-state plasma density distribution and generate plasma currents at the second harmonic in a direction normal to the main discharge current at the fundamental frequency. All these phenomena are attributed to the non-linear skin effect and are expected to be more pronounced at lower rf frequency. This lecture presents a systematic experimental study of low frequency cylindrical rf discharges with a planar coil operated at 450 and 900 kHz. Discharge electrical characteristics, the electron energy distribution function and the spatial distribution of the rf electromagnetic fields and rf currents on fundamental and higher harmonics has been measured over a wide range of argon gas pressure (1, 10 and 100 mTorr) and at discharge powers ranging between 50 and 400W. In the mTorr range of gas pressure we found that at these frequencies the Lorentz force can be much larger than electric one, and we were able to observe and characterize a variety of non-linear effects originated by the rf Lorentz force.

TUESDAY MORNING / AT2

Contributed Papers

9:00

AT2 3 ICP Reactor Modeling: CF₄ Discharges DEEPAK BOSE, *Thermosciences Institute* T.R. GOVINDAN, *NASA Ames Research Center* M. MEYYAPPAN, *NASA Ames Research Center* Inductively coupled plasma (ICP) reactors are widely used now for etching and deposition applications due to their simpler design compared to other high density sources. Plasma reactor modeling has been playing an important role since it can, in principle, reduce the number of trial and error iterations in the design process and provide valuable understanding of mechanisms. Fluorocarbon precursors have been the choice for oxide etching. We have data available on CF₄ from our laboratory. These are current voltage characteristics, Langmuir probe data, UV-absorption, and mass spectrometry measurements in a GEC-ICP reactor. We have developed a comprehensive model for ICP reactors which couples plasma generation and transport and neutral species dynamics with the gas flow equations. The model has been verified by comparison with experimental results for a nitrogen discharge in an ICP reactor. In the present work, the model has been applied to CF₄ discharge and compared to available experimental data.

9:15

AT2 4 Two-dimensional Experimental Characterization of an Inductive Discharge and Comparison to a Kinetic Plasma Model using Parallel Computing UWE KORTSHAGEN, BRIAN HEIL, *Mechanical Engineering, University of Minnesota, MN 55455** Two-dimensionally resolved measurements of electron distribution functions, electron density profiles, and plasma potential profiles have been performed in an inductively coupled plasma. Different coil configurations and aspect ratios have been studied in argon and oxygen plasmas. Experimental results are compared to results of a spatially two-dimensional, kinetic plasma model. A parallel code for the determination of the electron distribution function by solution of the Boltzmann equation was de-

veloped. The code can be run on workstation clusters supporting the MPI protocol.

*Supported by the NSF under grant ECS 97-13137 and the Univ. of Minnesota Supercomputing Center

9:30

AT2 5 The Influence of Antenna Configuration and Standing Wave Effects on Density Profile in a Large Area Inductive Plasma Source* YAOXI WU, M. A. LIEBERMAN, *University of California at Berkeley* A large area inductive plasma source driven by a 13.56 MHz traveling wave has been investigated. Launching a traveling wave by a tuning network eliminates standing wave effects to obtain a uniformly excited processing plasma. The designed tuning network is capable of launching a wave with any standing wave ratio. The influence of standing wave effects on plasma density profile is thus studied under various operating conditions. The influence of antenna configuration on the density distribution is examined by varying the number of powered rods and the way in which the exciting wave is launched. The plasma properties, such as ion density profile, electron temperature, and plasma potential are measured using a Langmuir probe and a capacitive probe. Our experimental results show that both the antenna configuration and voltage standing wave ratio are crucial in controlling the plasma density profile. A comparison of experimental results with theoretical analysis is performed.

*Funded by NSF and UC-Smart Contract 97-01

9:45

AT2 6 Determination of Species Concentrations and Temperatures in Chlorine Inductively Coupled Plasmas MIKHAIL V. MALYSHEV, VINCENT M. DONNELLY, NICHOLAS C. M. FULLER, KATHERINE H. A. BOGART, *Bell Laboratories, Lucent Technologies* IRVING P. HERMAN, *Columbia University* Concentrations of neutral (Cl and Cl₂) and charged (n_e , n_{Cl}^+ , $n_{Cl_2}^+$) species are determined for a broad range of pressure and power conditions in an inductively-coupled plasma reactor by a combi-

nation of optical emission spectroscopy, Langmuir probe, and laser-induced fluorescence. In the plasmas operated in a capacitively-coupled mode (at low source power) the dominant ion is Cl_2^+ . When power is increased and the plasma is operated in an inductively-coupled mode, the dominant ion is Cl^+ . This is mainly a consequence of a low degree of dissociation of molecular chlorine at low power and higher degree of dissociation at high power. We also carried out zero-dimensional modeling for both neutral and charged species that reproduced their dependence on pressure and power. The density of negative ions is determined both from experiment (through the difference of positive ion and electron densities) and modeling. Electron temperature (T_e) is determined by Langmuir probe and trace-rare gases optical emission spectroscopy. Differences in values of T_e between the two techniques are explained through derivations of the electron energy distribution function from Maxwellian behavior.

SESSION BT1: SHEATHS AND INSTABILITIES

Tuesday morning, 5 October 1999

Stratford Room Sheraton Waterside Hotel at 10:30
M. Riley, Sandia National Laboratories, presiding

10:30

BT1 1 Effect of electron and ion transport on the charge build-up of a microscopic structure exposed to plasma.* T. MAKABE, J. MATSUI, N. NAKANO, *Keio University at Yokohama, Japan* Plasma-induced charging damage, caused by the local charging on a patterned wafer surface, prevents us developing a fine pattern etching with space of $0.25\mu\text{m}$ by using a high density plasma. There is few theoretical studies considering the phase space transport of electrons/ions incident to the microscopic structure under charge accumulation from the sheath in plasma etching. We have developed the numerical model to investigate the effect of the transport of electrons/ions on the charge build-up of microstructure by tracing electrons/ions in conjunction with Poisson's equation. We studied the surface charging of a sub micrometer scale trench on SiO_2 . Time constant for charging in the trench is discussed as a function of external plasma conditions. As a result, in the case of high energy ions incident to the wafer, the time constant for charging t_c is larger and the position dependence is strong. The peak of surface potential moves from the center of the trench bottom to the edge with increasing of ion energy. The surface potential on the insulator without charge migration oscillates during etching due to the great difference of the electron drift velocity with ions, in addition to a much less momentum relaxation.

*This work is supported by STARC in Japan.

10:45

BT1 2 Ion Transport Modeling in Non-Collisional RF Sheaths DEEPAK BOSE, *Thermosciences Institute* T.R. GOVINDAN, *NASA Ames Research Center* M. MEYYAPPAN, *NASA Ames Research Center* A reactor scale ICP plasma model does not adequately resolve the sub-millimeter scale rf sheaths due to severe disparities in length and times scales. These non-collisional sheaths determine the spread in the ion bombardment energy distribution on the wafer. Analytical models based on "damped potential" has been used by various authors to simplify sheath modeling. However, inherent in these models are some assumptions that may be invalid. In this work we show that simplifying as-

sumptions such as a uniform ion flux may be in error by as much as 200% at 13.56MHz. This work involves solving ion transport in non-collisional rf sheaths. A comprehensive study of the dependence of ion flux and energy on uncertainties in the sheath-presheath (i.e. sheath thickness) boundary will also be done.

11:00

BT1 3 Plasma -Sheath Interface Problem NATALIA STERNBERG, *Dept. of Mathematics and Computer Science, Clark university, Worcester, Mass. 01610* MARSHALL SLEMROD, *Center for Mathematical Sciences, University of Wisconsin, Madison, WI. 53715* For a collisional bounded plasma problem, it is necessary to model the plasma and sheath separately because of the different scales in each region. We specify the plasma boundary by Godyak's criterion and sheath boundary by Bohm's criterion. We connect the plasma and sheath by a viscous interfacial region where the electric field is approximately constant. The approach enables us to develop and solve universal models for each of the three regions, and combine the solutions continuously to approximate the solution to the bounded plasma problem. Comparison of combined solutions with corresponding solution to the bounded plasma problem yields relative error at wall for ion density of 9%, ion velocity 10%, electric field 19%. All these errors are within experimental range. When the interface is neglected and the plasma and sheath are combined, the relative errors are ion density 40%, ion velocity 30%, electric field 19%. Although the interface region is very small it greatly improves the result.

11:15

BT1 4 Bohm Criterion for Sheaths and Shocks with Two Ion Species* NOAH HERSHKOWITZ, *University of Wisconsin-Madison* It is well known that in single ion species plasmas with low collisionality, ions are lost at the Bohm velocity and the Bohm velocity is equal to the ion acoustic velocity. When two or more ion species are present, it is usually assumed that each ion species is lost at their individual Bohm velocity. However, neither of these velocities is equal to the ion sound velocity of the combined system. Riemann has derived a Bohm criterion for systems with multiple ions which depends explicitly on the both ion at the sheath edge. Possible solutions include one with each ion species lost at its own Bohm velocity and another for which all species are lost at the ion sound velocity of the system. The former can be achieved by a plasma potential drop of $T_e/2$ in a collisionless presheath while the latter corresponds to the situation in a collisionless shock wave. In previous work collisionless electrostatic shocks have been argued to be moving double layers. Double layers have potential structures similar to sheaths. With cold plasma, in the shock frame, all ions approach the shock at the same speed, somewhat greater than the ion sound velocity. For the sheath, the ion energies match, while for the shock, the ion velocities match.

*Work supported by USDOE grant DE-FG02-97ER54437

11:30

BT1 5 Modeling of the Field Reversal in a Capacitive RF Sheath* H.-B. VALENTINI, *IPHT Inc, Jena, Germany* D. KAISER, *IAM FSU, Jena* Measurements^{1,2} have shown that in rf discharges near the powered electrode an electric field occurs pointing in towards the plasma during a short interval of each period when the rf amplitude exceeds a threshold. To describe this phenomenon the standard model of the collisionless sheath³ is modified. The electron current is limited by the minimum of the potential in front of the electrode when the field reversal exists. A corresponding boundary value problem is solved numerically by

various methods. The resulting threshold is relatively small. Results are discussed and compared with experimental results^{1,2}.

¹A.H. Sato and M.A. Lieberman, *J.Appl.Phys.* 68, 6117, (1990)

²U. Czarnetzki et al., *Plasma Sources Sci. Technol.* 8, 230 (1999)

³J. Gierling and K.-U. Riemann, *J.Appl.Phys.* 83, 3521 (1998)

*Work supported in part by SFB 191 of German Science Foundation

11:45

BT1 6 Ponderomotive instability of inductive discharges in argon M. M. TURNER, *Dublin City University, Ireland* G. CUNGE, *Université Joseph Fourier, Grenoble, France* B. CROWLEY, D. VENDER, *Dublin City University, Ireland* There is a widespread assumption that inductive discharges in electropositive gases such as argon are free of macroscopic instabilities, although there are contrary indications¹. In experiments reported elsewhere at this meeting, we show that this is not true, and that under some conditions periodic perturbations of plasma density appear and grow to large amplitude ($\sim 50\%$ of the unperturbed plasma density) over a pressure range from 60 mTorr upwards. These perturbations are parallel to the induced electric field lines. In this paper we show that this instability is caused by a ponderomotive effect, and we develop a model showing that the instability occurs when the induced electric field amplitude exceeds a critical value. B probe measurements show that this critical value is exceeded in our experiments. The growth of the instability is described by a nonlinear diffusion equation. Two dimensional numerical solutions of this equation are in reasonably good agreement with the experimentally observed perturbations of the plasma.

¹J. A. Stittsworth and A. E. Wendt, *IEEE Trans. Plasma Sci.* 24, 125 (1996)

12:00

BT1 7 Ponderomotive Instability of Inductive Discharges in Electronegative Gases M. M. TURNER, *Dublin City University, Ireland* Informal reports of instabilities in low pressure inductive discharges in electronegative gases are widespread, although the literature is sparse¹. Elsewhere at this meeting we have presented experimental and theoretical evidence that inductive radiofrequency discharges can be unstable because of ponderomotive effects, even in electropositive gases. In this paper we will discuss the implications of these results for electronegative discharges. In particular, we will show that the threshold electric field amplitude required to initiate the instability is not increased substantially in electronegative gases. However, since the instability produces perturbations of the plasma potential of the order of the electron temperature, considerably more severe disruptions of the discharge structure can be expected in electronegative gases relative to electropositive gases, owing to the sensitivity of the relatively cold negative ions to variations in the plasma potential.

¹M. Tuszewski, *J. Appl. Phys.* 79, 8967 (1996)

12:15

BT1 8 Instabilities in Electronegative Inductive Discharges* A. M. MARAKHTANOV, M. A. LIEBERMAN, A. J. LICHTENBERG, *University of California at Berkeley* Instabilities in a transformer coupled plasma (TCP) have been studied. A cylindrical inductive discharge has been created by a 13.56 MHz rf-driven planar using O_2 and SF_6 and their mixtures with Ar. Plasma instabilities have been observed at frequencies 1 Hz - 0.9 MHz for pressures of 2.5-20 mTorr and an absorbed power of 150-600 W. The positive ion and electron current oscillations were detected by a biased Langmuir probe. For the ion and electron saturation cur-

rent the modulations have reached 10% and 30% respectively. The same frequencies of plasma fluctuations were measured by a photomultiplier tube and a frequency analyzer. A volume-averaged model for the plasma instabilities has been developed. The particle and energy balance equations have been considered for the transition from capacitive (E) to inductive (H) discharge regime where the plasma instabilities take place. The relaxation oscillations in E-H transition cause modulations of charged particle densities, electron temperature, and plasma potential. In some cases, strong oscillations lead to potential collapse and negative ion flow to the walls.

*Funded by NSF and UC-Smart Contract 97-01

SESSION BT2: ETCHING

Tuesday morning, 5 October 1999

York Room Sheraton Waterside Hotel at 10:30

Justine Johannes, Sandia National Laboratories, presiding

10:30

BT2 1 Validation Issues in Oxide Etch Plasma Source Models P VENTZEK, S RAUF, D CORONELL, V ARUNACHALAM, T SPARKS, M HARTIG, *Motorola Inc.* H ANDERSON, K WATERS, *University of New Mexico* H HWANG, *Thermosciences Inst. NASA Ames* Mathematical models and process simulations of plasma sources for oxide etch applications are highly complex, but should provide a very valuable tool to develop advanced process technology. Accurate mechanism development must rely on the comparison and feedback of experimental data to the simulations. Typical mechanism approximations assume that the electron energy distribution function, gas flow, and plasma power are the primary parameters. The results of a comprehensive study of these issues as they pertain to the modeling of the GEC Reference Cell and a commercial plasma source will be presented. Specifically, the impact of these approximations on C4F8 oxide etch chemistry and other model chemistries will be presented. These will also be validated with system and wafer level experiments. Further, the sensitivity of these results will be discussed in terms of their impact on feature scale analysis

10:45

BT2 2 Modeling of Oxide Etch Charging Effects HELEN HWANG, *Thermosciences Institute* DEEPAK BOSE, *Thermosciences Institute* T.R. GOVINDAN, *NASA Ames Research Center* Charging of insulating films, such as SiO_2 , is potentially a significant aspect during etching of semiconductor devices. The electron flux toward the wafer is isotropic, while the positive ions are directed anisotropically by the electric fields. In narrow trenches, charging on the sidewalls and bottom can occur due to these differences in angular distributions. If charging is significant, electric fields in the trench can be perturbed, and subsequently the ion trajectories can be altered. It has been postulated that microtrenching is a result of these altered ion trajectories. We will present a model that calculates charging on oxides using an electron and ion Monte Carlo method. Electrons and ion trajectories are tracked in the plasma above an oxide layer. The surface charges when the ions and electrons bombard and stick to the oxide. Discharging via surface currents is accounted for using a drift-diffusion model on the oxide surface. Poisson's equation is solved to obtain the electric fields. We will demonstrate the effects of charging on a num-

ber of different trench geometries. The modified electric fields and charged particle trajectories will be presented.

11:00

BT2 3 Effect of SF₆ Addition to BCl₃ Etching Plasmas YAO-SHENG LEE, KAUSHAL UPADHYAYA, PRASAD GOGINENI, KAREN NORDHEDEN, *Plasma Research Laboratory, University of Kansas* Plasmas in gas mixtures such as BCl₃/SF₆ are often used for the selective etching of GaAs over AlGaAs. A dramatic increase in the GaAs etch rate has been observed with the addition of SF₆ to BCl₃ plasmas. Optical emission intensities of molecular and atomic chlorine also increase with SF₆ addition, indicating an increase in the dissociation of the BCl₃, and hence an increase in the available etch species. Actinometry was performed with argon, and the emission intensity at 750 nm increased significantly with the addition of SF₆. However, microwave interferometry indicated that the average electron density decreases with increasing SF₆ addition. It is believed that the increase in etch species, and hence etch rate, is due to an increase in the electron temperature.

11:15

BT2 4 Effect of Rare Gas Dilution of SF₆ Plasma on RIE Etching Characteristics of SiC J.D. SCOFIELD, B.N. GANGULY, P. BLETZINGER, *ISSI, Dayton, OH* The etch rates and the anisotropy of etched features of hexagonal 6H-SiC have been measured in a capacitively coupled rf discharge using SF₆+Ar and SF₆+He diluted gas mixtures. These measurements provide evidence for the generic nature of utilizing gas mixtures to modify electrical characteristics of rf discharges to optimize power coupling efficiency, although etch rates and surface morphology do not necessarily scale only with the plasma power coupling efficiency. In spite of the measured lower power deposition with He dilution compared to Ar, He diluted SF₆ plasma resulted in 1.5 greater etch rates (up to 300 nm/min) with 50% He dilution, with better anisotropy and surface texture than comparable SF₆+Ar mixtures. Superior SiC etch performance was obtained with He dilution, compared to Ar, over the entire 10% up to 90% range despite lower power coupling efficiency and the notion that Ar⁺ ions are expected to enhance ion assisted etch mechanism. The differences in dc self bias and volume plasma E/n leading to the conversion of SF₅⁺ ions to SF₃⁺ along with Penning ionization of SF₆ by metastable He atoms may be responsible for the observed superior etch characteristics.

11:30

BT2 5 Etching Mechanism of Silicon Nitride in Remote Plasmas Containing Fluorine, Oxygen and Nitrogen BERND E.E. KASTENMEIER, PETER J. MATSUO, GOTTLIEB S. OEHRLEIN, *Department of Physics, State University of New York at Albany, Albany, NY 12222* ROBERT E. ELLEFSON, LOUIS C. FREES, *Leybold Inficon Inc., East Syracuse, NY 13057-9714* The etch rate of silicon nitride (Si₃N₄) in the afterglow of fluorine containing plasmas is strongly enhanced when both nitrogen and oxygen are added to the discharge. This effect is attributed to the formation of nitric oxide NO, which we identify as a highly reactive precursor for the etching of Si₃N₄. The Si₃N₄ etch rate, surface oxidation and the depletion of the surface of N atoms show a linear dependence on the NO density. In order to determine the products of the NO reaction at the Si₃N₄ surface, mass spectrometry was performed in immediate proximity to the surface with a specially designed movable sampling orifice. Both SiF₄ and N₂ are

the primary etch products, but a smaller amount of N₂O was also detected. We suggest that NO enhances the removal of N from the Si₃N₄ surface by the formation of gaseous N₂, and leaving behind an O atom. This modified surface reacts more readily with F atoms than the Si₃N₄ surface.

11:45

BT2 6 Measurement of Ion Flux passing through A Real-Contact-Hole-Size Capillary for SiO₂ etching N. OZAWA, S. NODA, H. TSUBOI, Y. HIKOSAKA, K. KINOSHITA, M. SEKINE, *Association of Super-Advanced Electronics Technologies (ASET)* Ion flux that hits the bottom of a high-aspect contact hole (HARC) is a key factor in clarifying the etching mechanism of HARC. It has been reported that an IFED (Ion Flux Energy Distribution) at a low rf power (Vdc=-125 V) has been measured through a large capillary plate (CP) that had a diameter and aspect ratio of 10 μm and 20, respectively¹. However, an IFED through real holes (~0.2 μm diameter) has never been measured. In our study, the IFED of ions striking the rf-biased electrode were investigated through a real contact hole size CP in an actual SiO₂ etching. The CP has 0.2 μm diameter SiO₂ through-hole patterns, and its aspect ratio was varied from 0 to 7. An Ar/C₄F₈/CH₂F₂/O₂ gas mixture was used at a gas pressure of 5 mTorr. The Vdc on the CP set on the rf-biased (2-MHz) electrode was -500 V. We were able to accurately measure the IFED by using an rf-floating ion energy analyzer equipped with a sector-type energy filter. The IED measured at a low-aspect ratio was composed of two peaks (the so-called bimodal distribution) that were about 970 eV and 50 eV. The IED obtained at a high-aspect ratio has only the higher energy peak, and the peak position shifted to lower energy than that at low-aspect ratio. The ion flux decreased drastically with an increasing aspect ratio even at an rf power higher than that of the previous study. This result suggested that not only the aspect ratio but also the hole size affects the ion transportation through HARC. This work was supported by NEDO.¹

¹K. Kurihara and M. Sekine, *Plasma Source Sci. Technol.* 5 (1996) 121

12:00

BT2 7 Fabrication of Real-Contact-Hole-Size Capillary Plate to Study SiO₂ Etching Mechanism S. NODA, Y. HIKOSAKA, N. OZAWA, H. TSUBOI, K. KINOSHITA, M. SEKINE, *Association of Super-Advanced Electronics Technologies (ASET)* To clarify the etching mechanisms inside deep and narrow contact holes, we fabricated a real-contact-hole-size capillary plate to observe incident species into the holes. We expected to obtain a lot of useful information using this capillary plate, such as information on ions and radicals flux arriving at the bottom surface, ion flux energy distribution (IFED), charge build-up in the holes, and the sticking coefficient of radicals on the side wall, in a realistic dimension regime of the contact hole etching process. The capillary plate was made of a 1.5-μm-thick SiO₂ membrane with many through holes (> 0.15 μm diameter) on the whole surface. The holes were patterned by an EB multi-layer resist process and were etched with dual frequency RIE on thermally oxidized Si wafers. The membrane structure was formed by removing the backside Si substrate in diluted hydrazine. Generally, formation of a large SiO₂ membrane is very difficult because of the compressive stress of the SiO₂. The SiO₂ membrane must be kept below 50 μm square to avoid buckling. Using this capillary plate, we measured the CF⁺ flux and IFED through 0.2 μm diameter holes with rf floating ion energy analyzer (IEA) in a SiO₂ etching condition. At this time, the opened area ratio of the capillary plate is so small

(2.7 %) that it makes the transmitted ion flux very small. However, the IFED profiles of transmitted ions were successfully measured throughout a wide energy range using an IEA with a high-transmittance-sector type energy filter. This work was supported by NEDO.

12:15

BT2 8 Absolute sputtering yields of Au due to Ar⁺ impact at energies of 33 to 1000 eV THOMAS STEPHEN, *University of Denver* BERT VAN ZYL, *University of Denver* The absolute sputtering yield of a polycrystalline Au target due to normally incident Ar⁺ has been measured for ion impact energies of 33 to

1000 eV. These measurements were made using a modified quartz crystal microbalance. This technique has allowed for the measurement of sputtering yields down to the 10⁻⁴ range. The experimental results are compared with previous work, as well as with analytical theory and computer simulations. The present measurements agree with previous measurements down to approximately 60 eV. There are very little published data at energies lower than 60 eV and there is marked disagreement with present results. The sputtering yields fall off at a higher energy than theory predicts, with a sputtering threshold at an energy below that predicted by simulations. This work was supported in part by NASA/Goddard Space Flight Center NAG5-3386, the Air Force Office of Scientific Research and the William F. Marlar Foundation

SESSION CT1: FOUNDATIONS OF GASEOUS ELECTRONICS

Tuesday afternoon, 5 October 1999; York and Stratford Rooms Sheraton Waterside Hotel at 13:30

Gerry Hays, Sandia National Laboratories, presiding

13:30

CT1 1 Historical Evolution of Cross Section Calculations.

A. DALGARNO, *Harvard-Smithsonian Center for Astrophysics, Cambridge, MA 02138*

An account will be presented of the history of atomic and molecular collision theory and the influence of the development of computing systems will be described. Some examples will be given of the concomitant increase in sophistication of the construction of theoretical models of astrophysical plasmas.

SESSION DT1: DIAGNOSTICS I

Tuesday afternoon, 5 October 1999; Stratford Room Sheraton Waterside Hotel at 15:00

Vasgen A. Shamamian, Naval Research Laboratory, presiding

Invited Papers

15:00

DT1 1 *In-situ* Diagnostics of Highly Excited Hydrogen Molecules by LIF in the Vacuum UV.

H.F. DÖBELE, *Institut für Laser- und Plasmaphysik, Universität GH Essen, 45117 Essen, Germany*

The population dynamics of low-temperature hydrogen plasmas, though extensively treated in simulations, is still lacking complete experimental verification. This applies especially to the role of highly excited molecules in the electronic ground state, since the population of states with $v'' > 8$ - considered of decisive importance for the generation of negative ions by the process of dissociative attachment - has been inaccessible for *in-situ* diagnostics so far. Spatially resolved quantitative determination of their population in the plasma of a magnetic multipole source has now become possible by Laser Induced Fluorescence spectroscopy (LIF) in the vacuum UV. Populations with rotational resolution are obtained up to $v'' = 13$ with good signal-to-noise ratio. It is furthermore possible to follow the decay of the populations as a function of time after fast current shut-off. $1/e$ times ranging from milliseconds at small v'' down to several 10 microseconds at the highest states are found.

15:30

DT1 2 Optical Diagnostics of the Plasma and Surface during Inductively Coupled Plasma Etching.

IRVING P. HERMAN, *Columbia University**

The use of optical diagnostics to analyze the etching of Si, Ge, and InP by chlorine in an inductively coupled plasma (ICP) is investigated. Optical probes, along with other conventional plasma diagnostics, are used to characterize the process through measurements of the constituents of the plasma and the surface composition to obtain a more complete picture of the etching process. Neutral Cl₂ and Cl densities are determined by optical emission actinometry by following optical emission from Cl₂. The absolute densities of Cl₂⁺ and Cl⁺ are determined by laser-induced fluorescence (LIF) of Cl₂⁺ and Langmuir probe measurements of the total positive ion density. The surface is probed by using laser-induced thermal desorption with an XeCl laser (308 nm) to desorb the steady-state adlayer and optical methods to detect these desorbed species. The development of a new method to detect optically these laser desorbed (LD) species is detailed, that

of examining transient changes in the plasma-induced emission (PIE). This LD-PIE method is more universal than the previously reported detection by LIF (LD-LIF), but requires more calibration due to varying electron density and temperature with varying plasma conditions. This is detailed for Si etching, for which LD-PIE and LD-LIF results are compared. The calibration methods are seen to be valid when the surface is analyzed as the rf power supplied to the reactor is varied. The electron density - needed for LD-PIE calibration - is measured by microwave interferometry. An improved understanding of the etching mechanism is obtained by combining the results of each of these measurements. This work was supported by NSF Grant No. DMR-98-15846.

*The presented work is a collaboration with J.Y. Choe and N.C.M. Fuller of Columbia University, and V.M. Donnelly, M.V. Malyshev, and K.H.A. Bogart of Bell Laboratories, Lucent Technologies.

Contributed Papers

16:00

DT1 3 A new plasma uniformity monitor based on optical tomography ERIC BENCK, *NIST* Optical emission measurements of a plasma do not provide a direct measure of the plasma uniformity, since each measurement is actually equal to the plasma emissivity integrated along the line of sight through the plasma. In order to determine the actual plasma emissivity distribution, without assuming cylindrical symmetry, optical emission measurements are inverted using computer aided tomography (CAT) with Tikhonov regularization. Results from a new sensor array designed for CAT will be presented. The new sensor utilizes a fiber optic array coupled to an intensified CCD camera with an electronically tuned narrow band pass filter. The sensor simultaneously records the light output from 82 separate channels and is designed to observe the plasma through two small optical ports. Measurements for a variety of different plasma conditions will be made on an inductively coupled plasma source built in a modified GEC RF Reference Cell.

16:15

DT1 4 Time-resolved Emission Spectroscopic Determination of Rotational Temperatures in a Hydrogen RF Discharge V. SCHULZ-VON DER GATHEN, T. KAWETZKI, H.F. DÖBELE, *Universität GH Essen, Institut für Laser- und Plasmaphysik, 45117 Essen, Germany* Spectroscopic gas temperature determination in hydrogen plasmas is commonly based on molecular line intensity ratio measurements of the diagonal bands ($\Delta v = 0$) of the Fulcher- α system ($d^3\Pi_u \rightarrow a^3\Sigma_g$). We have studied - in contrast to earlier work where only time-averaged intensities were measured - the temporal behavior of the rotational state distribution along the discharge axis of a CCRF plasma source ($P = 10 - 100$ W, $p = 10 - 100$ Pa) with a novel intensified CCD camera. This camera is synchronized to the transceiver frequency and allows measurements with time resolution of $\Delta t = 3$ ns using each rf cycle. Rotational temperatures inferred on the basis of collisional excitation from the ground state indicate strong variations during one cycle rising from about 400 K by more than e.g. 100 K at high pressures. We conclude that either more elaborate population models have to be applied or a time interval has to be selected by time-resolved spectroscopy where the underlying assumptions are fulfilled to allow the application of this otherwise very convenient diagnostic. This work is supported by the DFG in the frame of the SFB191.

16:30

DT1 5 Absorption Measurements of 4s State Number density for a Microwave Argon Plasma YUNLONG LI, *Mechanical Engineering, University of Arkansas* MATTHEW GORDON, *University of Arkansas* LARRY ROE, *University of Arkansas* KHALED HASSOUNI, *University of Paris* Optical emission and continuum measurements have been performed to characterize microwave argon plasmas. A Wavemat (model MPDR-3135) micro-

wave diamond deposition system was used to generate the argon plasma at 5 Torr with an argon flow rate of 300 sccm. In a previous study, three excited states number densities (4p, 5p, and 5d) were obtained from the emission measurements. These data were used to validate our zero-dimensional (with diffusion) Collisional-Radiative Model (CRM) by matching these three excited state number densities with the prediction from the CRM. An energy balance study showed that the energy absorbed by the argon plasma was far less than the reading from the power meters, also in agreement with our CRM predictions. To better characterize the plasma, we have recently measured the 4s population through absorption at 7635. The light source was a low-pressure AC argon lamp. To calculate the 4s number density, the lineshapes of the argon lamp and the argon plasma are needed. The lineshape of the argon lamp was taken from previous work which used a similar lamp. However, the plasma lineshape depends on the electron number density, the number densities of related excited states, the electron and gas temperatures, etc. For our microwave plasma system, these parameters cannot be measured directly. Therefore, the plasma lineshape was calculated based on the parameters predicted from the CRM. The 4s state number density calculated from this lineshape matches the predicted one from the CRM within the experimental uncertainty, further validating our model.

16:45

DT1 6 Development of Vacuum Ultraviolet Absorption Spectroscopy using High Pressure H₂ Microdischarge Hollow Cathode Lamp for Measurements of H Atom Density in Plasmas SEIGOU TAKASHIMA, MASARU HORI, AKIHIRO KONO, TOSHIO GOTO, *Nagoya University* MASAFUMI ITO, *Wakayama University* KATSUMI YONEDA, *Nippon Laser & Electronics LAB.* H atoms play an important role in process plasmas. We have newly developed a high pressure H₂ microdischarge hollow cathode lamp (MHCL) as a light source for vacuum ultraviolet absorption spectroscopy (VUVAS). The transition line used for the measurement was Lyman α . For MHCL, He gas containing a small amount of H₂ gas were employed. The total gas pressure was about 88k Pa. MHCL generates a point-source-like emission from the hollow 0.1 mm in diameter. MHCL was designed to prevent the emission profile broadening due to fast H atoms arising from the dissociation of H₂. Moreover, the self-absorption of MHCL was successfully reduced by decreasing the H₂ partial pressure below 7.0 Pa. From the measured results of the absorption intensity at Lyman α as a function of the RF power in inductively coupled H₂ plasmas (H₂-ICPs), the spectral profile of MHCL was estimated to be the Voigt profile with the Doppler width corresponding to a H atom temperature of 300 K and the Lorentz width two times as large as the Doppler width. Using VUVAS employing MHCL, absolute densities of H atoms in H₂-ICPs were measured. The absolute density of H atoms was $6 \times 10^{11} \text{ cm}^{-3}$ in H₂-ICP at a pressure of 1.33 Pa and a RF power of 100W.

17:00

DT1 7 Spatial distribution measurements of absolute CF_x (x = 1-2) radical densities using single path infrared diode laser absorption spectroscopy and laser-induced fluorescence technique MASAFUMI ITO, MASA YUKI NAKAMURA, MASARU HORI, TOSHIO GOTO, *Nagoya University* NOBUO ISHII, *Tokyo Electron Ltd.* We have developed a novel measurement method for obtaining spatial distributions of absolute radial densities in plasma reactors. This measurement method consists of a laser-induced fluorescence (LIF) technique and a single path infrared laser absorption spectroscopy (SP-IRLAS). The measurements using the SP-IRLAS and the LIF can be carried out at the same time only by changing the laser beams. The laser beam for the SP-IRLAS goes through the same path as the beam for the LIF does in the plasma reactor. Therefore, the absolute densities obtained by the SP-IRLAS are the values averaged on the exact same optical path as the LIF laser beam goes through. By using these values, the relative spatial distributions obtained by the LIF are easily converted to the absolute ones with high reliability. This method has been successfully applied to the spatial distribution measurement of absolute CF and CF₂ radicals in electron cyclotron resonance C₄F₈ plasmas. From the results obtained, it was found that CF radical densities were higher than CF₂ ones in the plasma region while lower out of the region.

17:15

DT1 8 Temperature Measurements in Glow Discharges Using Ultraviolet Filtered Rayleigh Scattering* AZER YALIN, YURIY IONIKH, RICHARD MILES, DEPT. OF MECH. AND AEROSPACE ENG., PRINCETON UNIV. TEAM, We report temperature measurements obtained in low pressure (order 50 torr) glow discharges by ultraviolet filtered Rayleigh scattering (UV FRS). FRS uses an optically thick, atomic mercury absorption filter to suppress elastic background (from stray laser scatter and window scatter), and may be used in cases where the background would otherwise obscure the Rayleigh signal. The Rayleigh scattered light is broad in frequency compared to the elastic scatter (FWHM ~ 100MHz), so the wings of the scattering lineshape are transmitted, while the narrower elastic component is strongly absorbed. About 35% of the Rayleigh scattered light is transmitted, while less than ~ 0.001% of the elastic scatter is transmitted, hence strong background suppression is achieved. Measurements of radial profiles of temperature have been performed in a 50 torr, 20 mA argon discharge, with uncertainties of ~ 5%. The measurements have a spatial resolution of ~ 1mm. The temperature range across the profile was found to be about 300 K near the wall, up to about 650 K on the centerline. All experimental measurements are in reasonable agreement with computed values.

*Work supported by Air Force Plasma Ramparts MURI and New World Vista programs.

SESSION DT2: LIGHTING AND PLASMA DISPLAYS

Tuesday afternoon, 5 October 1999

York Room Sheraton Waterside Hotel at 15:00

Robert Piejak, OSRAM Sylvania Inc., presiding

15:00

DT2 1 Nonequilibrium in Fluorescent Lamp Discharges. J. D. MICHAEL, *GE-CRD, One Research Circle, Niskayuna, NY 12309* J. H. INGOLD, *One Bratenahl Place #610, Bratenahl, OH 44108* Typical fluorescent lamps are low pressure discharge devices comprised of a few mTorr of Hg and a few Torr of rare gas such as Ar. It has long been customary to simulate fluorescent

lamp behavior with computer models based on the concept of equilibrium, meaning that energy given to electrons by the axial electric field is exactly balanced by elastic and inelastic collisions with neutral atoms in each volume element of the discharge [1]. The purpose of this work is to examine conditions for which equilibrium is expected to prevail in fluorescent lamps. Qualitatively, the criterion for equilibrium to prevail is that electron energy relaxation length be small compared with characteristic dimension of the discharge [2]. Quantitatively, the criterion is that divergence of radial energy flow be small compared with Joule heating, so that Joule heating and collision loss are equal in each volume element of the discharge [3]. Based on application of this criterion to fluorescent lamp discharges, it is concluded that lamps of standard diameter are very likely not in equilibrium and lamps of smaller diameter are almost certainly not in equilibrium. [1]R. B. Winkler, J. Wilhelm, & R. Winkler, *Annalen der Physik* **40**, 90 & 119 (1983); M. Yousfi, G. Zissis, A. Alkaa, & J. J. Damelincourt, *Phys. Rev. A* **42**, 978 (1990). [2]J. L. Blank, *Phys. Fluids* **11**, 1686 (1968). [3]J. H. Ingold, *Phys. Rev. E* **56**, 5932 (1997).

15:15

DT2 2 A new method for changing the color of fluorescent lamps LEON BAKKER, *Eindhoven University of Technology* GERRIT KROESEN, *Eindhoven University of Technology* Recently, there's a growing interest in lamps with a variable color. In the past, several options for changing the color of a fluorescent lamp were proposed. Most of these options use radio frequency or pulsed excitation of the gas discharge. By changing the electrical excitation, the electron energy distribution function changes. This causes the output spectrum of the lamp to change. A disadvantage of such a lamp is the expensive power sources that are required. Especially the pulsed excitation is costly; it demands electrical pulses on microsecond scale with several different pulse shapes. We propose a new lamp with a variable color. This lamp is more efficient than the lamps mentioned above, it has the same construction as a normal fluorescent lamp, and it doesn't need expensive rf sources and pulsed power sources.

15:30

DT2 3 Nonlinear Thermal Balance and Cathode Spot Formation in Cylindrical Thermionic Cathode YAN-MING LI, *OSRAM SYLVANIA Development Inc., 71 Cherry Hill Drive, Beverly, MA 01915* It is well known that the transfer of discharge current from plasma to the thermionic cathode can occur in diffuse and spot modes. In [1], Benilov has shown that the thermal conduction problem for thermionic cathode heated by nonlinear heat flux derived from the plasma, can exhibit multiple steady state solutions under certain conditions. With simplified formulation, further analytical and numerical studies of diffuse-spot mode transition with discharge current were also made [1]. We decided to study the nonlinear thermal balance in more realistic terms, where the nonlinear heat flux applied to one end of the electrode as well as to the side cylindrical surface. Nonlinear radiative cooling is also added. The two dimensional steady state solutions are determined numerically using nonlinear finite element method. Indeed, under certain parameter range, multiple solutions do exist. Three modes are identified: spot mode with localized high temperature on axis, diffuse mode with monotonic increasing temperature towards the edge, and the third mode peaked on axis with a smaller local maximum at the edge. A general form of the nonlinear heat flux function [2], is assumed in the present computations. This function could be replaced by self-consistent heat flux function based on hot cathode-glow discharge model [3]. [1] M. S. Benilov, "Non-linear surface heating of a plane sample and modes of current transfer to hot arc cathode," *Phys. Rev. E*, Vol. 58, p. 6480 (1998) [2] M. S. Benilov, "A Self-Consistent Analytical Model of Arc

Spots on Electrodes," IEEE Trans. Plasma Sci., Vol. 22, No. 1, p. 73 (1994) [3] Byszewski W. W., Gregor P. D., Budinger A. B., Li Y. M., "Tungsten radiation measurement during starting of metal halide lamps," J. Ill. Eng. Soc., Vol. 21, p. 85 (1992)

15:45

DT2 4 Radiation Transport in Cylindrical Discharges with Radial Inhomogeneities* JOHN J. CURRY, J. E. LAWLER, *Department of Physics, University of Wisconsin* G. G. LISTER, *OSRAM Sylvania, Inc., Beverly, Massachusetts* We have studied the transport of radiation in cylindrical systems with radially symmetric, inhomogeneous distributions of absorbing atoms. These studies are applicable to radiation transport in cylindrical glow discharge plasmas exhibiting non-uniform neutral atom densities produced by ambipolar (radial) cataphoresis or by temperature gradients. These studies are also applicable to trapping of radiation by plasma ions or excited neutral atoms. Numerical solutions of the Holstein-Biberman transport equation and Monte Carlo simulations of resonance photon scattering have both been used to study the effect of radially symmetric distributions of absorbing atoms on the spatial distribution of emitting atoms and on the associated trapped decay rate. The use of two distinct numerical methods provides a robust cross-check of the results. We have examined three limiting cases of interest that lead to complete frequency redistribution: (i) a Doppler broadened atomic lineshape, (ii) a Lorentz atomic lineshape produced by foreign gas broadening, and (iii) a Lorentz atomic lineshape produced by resonance collision broadening. We found that for many conditions of interest, the fundamental mode trapped decay rate is reasonably well characterized by the radially-averaged density of absorbing atoms.

*Funded by OSRAM Sylvania and the Electric Power Research Institute.

16:00

DT2 5 A Comparison of AC and Short-Pulse Excitation for Xe Excimer Barrier Discharge Lamps R.P. MILDREN, *Dept. of Physics, Macquarie University* R. MORROW, *CSIRO* R.J. CARMAN, *Macquarie University* Dielectric barrier discharge excitation of rare-gas and rare-gas halide excimers provides an efficient scheme for generating intense VUV radiation for applications including lighting, ozonisation, and photochemical surface treatment. Typically, lamps employ AC (sinusoidal) voltage excitation in which case VUV emission is produced from short-lived micro discharges (streamers) distributed stochastically over the dielectric. However, it has been recently demonstrated that significantly increased efficiency (by factor 2-3) can be obtained from Xe lamps when using short excitation pulses separated by idle periods[1]. In this paper, we report an investigation into the mechanisms which bring about improved efficiency by comparing the electrical, spectral and spatial emission characteristics of a small-scale Xe lamp excited by short pulses (100ns) with that of conventional AC excitation. The results reveal that pulsed excitation produces a homogenous glow-like discharge in which the electron density and temperature are more favourable for efficient excimer production. [1] RP Mildren et al, IVth Int. Conf. Atom. and Molec. Pulsed Lasers, Tomsk, Siberia Sept. (1999); F Vollkommer and L Hitzschke, Proc. 8th Int. Symp. Sci. Tech. Light Sources, Greifswald, Germany, '98, IL-07, pp51-59 (1998)

16:15

DT2 6 Processes in Microwave-Excited Lamps Containing Mercury and Noble Gas Based Excimers M. CEKIC, *Fusion UV Systems, Gaithersburg, MD* S. POPOVIC, *Old Dominion U., Norfolk, VA* Numerous applications require efficient light sources that are able to radiate simultaneously in multiple bands distributed over the spectral range of 170 to 300 nm. Several spectral bands of mercury and noble gas based gas excimer mixture are evenly distributed over this spectral range. Thus, the prospect of obtaining a high-intensity, optically thin radiation emitted in the vacuum ultraviolet and ultraviolet region, led to the development of the lamps containing mercury and noble gas based excimer mixtures. Influence of microwave power density and initial gas composition on axial and radial distribution of radiation, stability of operation and the effects of discharge filamentation was studied in order to obtain the optimal parameters of the lamp and microwave cavity design. The experiments were performed with a special lamp design with an excimer-grade quartz window for end-on observation. The lamp was directly attached to VUV spectrometer. Possibility of controlling the kinetics of the complex mercury - excimer mixtures in the available power density range was studied.

16:30

DT2 7 Dynamic Behavior of Excited Xe(1s₄, 1s₅) Atoms in a Pixel of AC-PDP Studied by Spectroscopic Microscopy K. TACHIBANA, S.-J. FENG, *Kyoto University* T. SAKAI, *Hyundai Electronics Japan* Two dimensional spatio-temporal behavior of excited Xe atoms in the 1s₄ resonance state and the 1s₅ metastable state have been measured in a unit cell of AC-type PDP by a laser absorption technique using an optical microscope. The measured density of Xe(1s₅) have two large peaks on both temporal anode and cathode sides. The peak at the anode has a narrower spatial distribution while the peak at cathode is distributed over the electrode area. In the temporal behavior, the anode peak rises slightly faster than the peak at the cathode and decays faster at the beginning of afterglow, but both the peaks tend to have the same decay rate in the later period. The behavior of Xe(1s₄) shows a similar feature, but the decay rate is much larger corresponding to the effective lifetime of imprisoned resonance radiation. The maximum densities of Xe(1s₅) and Xe(1s₄) are 5×10^{13} and 2×10^{13} cm⁻³, respectively. The emission from Xe(2p) atoms has also been observed, which nearly follows the current waveform.

16:45

DT2 8 Simulation of Micro-Discharges in Plasma Addressed Liquid Crystal Displays GERJAN HAGELAAR, *Eindhoven University of Technology, Dept. of Physics* GERRIT KROESEN, *Eindhoven University of Technology, Dept. of Physics* PALC (Plasma Addressed Liquid Crystal) is one of the most promising technologies for large size flat panel displays. In this technology micro-discharges are used as electrical switches for the addressing of a liquid crystal layer. In view of the small size of the micro-discharges, discharge modelling is an indispensable tool for the optimisation of their properties. In this work we present a two-dimensional fluid model for the simulation of DC discharges and afterglows in the PALC geometry. The model comprises continuity equations and drift-diffusion equations for reactive particle species, a balance equation for the electron energy, and Poisson's equation for the electric field. Simulation results are in good agreement with experimental results.

17:00

DT2 9 Frequency characteristics in a micro-cell plasma in Xe by using RCT model* M. KURIHARA, T. MAKABE, *Keio University, Japan* Plasma display panel (PDP) is one of the flat display devices, expected to be a large size, hanging, and high-definition TV monitor. One of the disadvantages of the present PDP is a low efficiency of UV radiation inherent in the low frequency discharge. We had already reported the effect of pd and fd in a micro-cell plasma. In this work, we numerically investigate the dependence of frequency on a micro-cell plasma in pure Xe by using RCT model. There are different characteristics between high and low input power under the same pressure. Under a high input power, the efficiency of UV radiation decreases as increasing the frequency, because the power spent in heating ions will increase due to a high sheath field caused by a high plasma density. On the other hand, under a low input power, the efficiency can be improved as increasing the frequency. In this case, plasma is sustained by the ionization of electron accelerated in the sheath region. Furthermore we will show the effect of the gas mixture between Ne and Xe.

*Supported by MESCS in Japan, B(2)-09450146 and -9555111.

**SESSION ETP1: POSTER SESSION:
ELECTRON-MOLECULE COLLISIONS
Tuesday evening, 5 October 1999
Poplar Room Sheraton Waterside Hotel at 19:30**

ETP1 1 Low-Energy Electron Scattering from Nitrous Oxide ROBERT GULLEY, JENNIFER GIBSON, STEPHEN BUCKMAN, *Australian National University* Absolute differential cross-sections for vibrationally elastic scattering of electrons from nitrous oxide (N_2O) have been measured in the energy range of 2 to 20 eV and scattering angles between 15° and 130° . Comparisons are made with recent experimental results and theoretical calculations, including the R-matrix and Schwinger variational techniques. In general, the agreement with the most recent experiment is excellent. Indeed, agreement with other previous experimental results are generally good. Comparison between the present results and theoretical calculations show good agreement for energies of 10 eV and above. However, large discrepancies are found at energies below 10 eV, especially around 5 eV (although the agreement somewhat improves at 2 eV). The present results show a sharp minimum in the differential cross section at forward angles and low energies (4 to 8 eV). Similar forward angular behaviour has been observed in a wide range of molecular species and it continues to provide a challenge to the description of long-range interactions in most theoretical models.

ETP1 2 Electron-Impact Excitation of Nitric Oxide* R. SCOTT SCHAPPE, ROBERT EDGELL, ANDREW KUCHE-RIAVY, STEVE WILLIAMS, *Lake Forest College* Despite its important roles in the atmosphere, very little work has been done on nitric oxide (NO). We have measured absolute electron-impact cross sections for the β system ($B^2\Pi - X^2\Pi$) of NO. To overcome the difficulties of working with such a reactive gas, we use a room temperature molecular beam crossed with a monoenergetic electron beam. This arrangement also reduces concerns of radia-

tion trapping. We present apparent cross sections for several of the B - X vibrational transitions as determined by the optical method. We have also measured the energy dependence of these cross sections from threshold to 700 eV.

*This research was supported by an award from Research Corporation

ETP1 3 Analysis of Optical Emissions Following Electron Impact on C2F6 K.E. MARTUS, *William Paterson University, Wayne, USA* P. KURUNCZI, K. BECKER, *Stevens Institute of Technology, Hoboken, USA* Low-temperature plasmas using gas mixtures which contain fluorocarbon species such as CF₄, C₂F₆, or C₃F₈ are widely used in the semiconductor industry for the etching of silicon. Optical emissions from these plasmas can be used for diagnostics purposes. While the optical emissions from electron-impact excited CF₄ have been studied extensively in the past for emissions from the vacuum ultraviolet (90 nm) to the near-infrared (900 nm) by several groups, no such studies have been carried out for C₂F₆ and C₃F₈. We report a comprehensive measurement of absolute photoemission cross sections and appearance energies for emissions produced by controlled electron impact on C₂F₆ from the VUV, where the F resonance lines around 95 nm are the most prominent emission features, to the 600 - 800 nm range, where F emissions resulting from transitions between excited atomic fluorine state occur. In general, we found that the intensity of the optical emissions from C₂F₆ was weaker than what was observed for the same emissions from CF₄. In addition, we found no evidence in C₂F₆ of the prominent emission continuum from 200 to 500 nm that dominates the CF₄ emission spectrum. *Work supported by the NSF.

ETP1 4 Total and elastic cross sections of CF3I by electron and positron impacts MINEO KIMURA, *Yamaguchi University* OSAMU SUEOKA, *Yamaguchi University* AKIRA HAMADA, *Yamaguchi University* HIROSHI TANAKA, *Sophia University* MASASHI KITAJIMA, *Sophia University* As one of possible candidates for the next generation plasma-etching gases, CF₃I has attracted much of experimental and theoretical attention recent years since the life time of this gas is relatively short compared to other types of fluorine-substituted hydrocarbons. Total and elastic cross sections for CF₃I by electron and positron impacts have been measured in the energy region from 0.9 eV to 600 eV for electron and from 0.7 eV to 600 eV for positron, respectively. Total cross section measurements were carried out by using the time-of-flight apparatus with 600 mm length. As electron and positron sources, a ²²Na radioisotope was employed. For elastic cross sections from 0.2 eV to 100 eV, the electron beam emerging from the monochromator was crossed at 90° with a molecular beam. The analyzer measures the scattered electrons. The analyzer can rotate mechanically around the scattering center covering the angular range from 10° to 130° with respect to the incident electron beam. We have also employed the continuum multiple-scattering method for theoretical analysis. Furthermore, we have carried out the experimental study on positronium (Ps) formation.

ETP1 5 Measurement of Total Electron Scattering Cross Sections for SO₂* M.E. JOHNSTON, J.A. BERGER, J.P. HEGGEMEIER, T.M. KLEIN, *University of St. Thomas, St. Paul MN* In space sulphur dioxide (SO₂) plays an important role in the atmospheres of Jupiter and Venus and interstellar clouds. On Earth it is

responsible for acid rain and climate effects. In modeling these systems, electron impact data is needed. In this poster we present absolute total electron impact cross sections from 2 eV to 200 eV. The measurements were made using the linear transmission method. The apparatus consists of an unselected electron gun (+0.5 eV) coupled to a scattering cell. Energy resolution is enhanced by time-of-flight detection techniques. The results are compared to earlier experimental and theoretical work.

*Research supported by Minnesota Space Grant, the Research Corporation and the University of St. Thomas

ETP1 6 Electron Interactions with SF₆ LOUCAS CHRISTOPHOROU, JAMES OLTHOFF, RALPH SIEGEL, *NIST* MAKOTO HAYASHI, *GEI, Japan* YOSHIHARU NAKAMURA, *Keio University, Japan* Experimental data on electron collisions with SF₆ have been reviewed and assessed. Recommended or suggested data will be presented for the cross sections for total, elastic, and differential electron scattering, for total and partial ionization, and for electron attachment. Similarly, recommended or suggested data will be presented as a function of E/N for the electron drift velocity, and the coefficients for electron diffusion, ionization, and attachment. Assessed data will be presented also on the electron attachment rate constant as a function of E/N in the pure gas and in mixtures with rare gases and N₂, and as a function of the mean electron energy and gas temperature.

ETP1 7 Electron Collisions with Hexafluorobenzene, C₆F₆ CARL WINSTEAD, VINCENT MCKOY, *California Institute of Technology* MARCIO H. F. BETTEGA, *Universidade Federal do Paraná* We report elastic electron collision cross sections for C₆F₆, hexafluorobenzene, computed using the Schwinger multi-channel method. Polarization effects are systematically treated so as to obtain accurate resonance positions. The resonance structure in the C₆F₆ cross section is explored in detail and compared to that observed in benzene and in other fluorocarbons. We compare our results to available experimental data.

ETP1 8 Effects of Molecular Vibrational Excitation in Low Pressure Processing Discharges W.L. MORGAN, *Kinema Research & Software, L.L.C.** Modeling calculations exploring the degree of molecular vibrational excitation and its effects on other atomic and molecular processes in low pressure processing discharges are presented. Gases such as O₂, N₂O, HBr, and NF₃, which are common in plasma processing, are known to have dissociative attachment cross sections that have strong temperature dependences, *i.e.* increase dramatically with the degree of vibrational excitation. The vibrational states of molecules are readily excited by electrons in a discharge. The steady state vibrational temperature, which can be a function of spatial position, results from a balance of this excitation versus losses due to electron collisions, diffusion to the walls, and vibrational energy transfer processes. Different processes dominate the balance as one changes pressure and, to some degree, rf power input. Further details can be found on the KR&S Web site.

*This work was supported by SEMATECH, Inc. through the Caltech Department of Chemistry

ETP1 9 Dissociation Cross Sections for C₂F₆, c-C₄F₈, C₃F₈, CHF₃, and TEOS W.L. MORGAN, *Kinema Research & Software, L.L.C.** Extensive use is made of beam measurements, ab initio calculations, and electron swarm measurements in deriving total cross sections for dissociation of C₂F₆, c-C₄F₈, C₃F₈, CHF₃, and TEOS into neutral fragments. Use is made of a numerical optimization algorithm for scaling measured or computed cross sections and manipulating model cross sections in order to satisfy the measured electron transport data. These are molecules that are important in plasma processing because they readily dissociate into reactive radical fragments. Although swarm analyses cannot tell us what the specific radical fragments are, they can provide an accurate estimate of the cross section and, hence, rate coefficient for dissociation. Further details can be found on the KR&S Web site.

*This work was supported by SEMATECH, Inc. through the Caltech Department of Chemistry

ETP1 10 Electron Impact Dissociation of Silane and Methane Probed by Laser-Induced Fluorescence Techniques N. ABRAMZON, K. BECKER, *Stevens Institute of Technology, Hoboken, USA* K.E. MARTUS, *William Paterson University, Wayne, USA* We employed a combination of electron scattering and laser-induced fluorescence (LIF) techniques in an absolute determination of neutral molecular dissociation cross sections. The feasibility of this technique has recently been shown in an absolute determination of the final-state-specific N₂⁺(X) ionization cross section. This cross section now serves as a calibration standard for the present experiments. Specifically, in the present experiments we determine the absolute cross section for the formation of Si atoms following electron-impact dissociation of silane, SiH₄ and the formation of CH free radicals following the electron-impact dissociation of methane, CH₄. The Si atoms are probed by LIF of the Si 389 nm transition followed by emission of the Si 288 nm line. The CH radicals are probed by LIF of the so-called "430 nm" band. Both neutral dissociation processes are important in low-temperature processing plasmas. * Work supported by NSF and NASA.

ETP1 11 Electron-Impact Ionization of C₂F₆ and C₂F₅ V. TARNOVSKY, K. BECKER, *Stevens Institute of Technology, Hoboken, USA* H. DEUTSCH, *Univ. Greifswald, Germany* R. BASNER, M. SCHMIDT, *INP Greifswald, Germany* The C₂F₆ molecule is widely used in the semiconductor industry as a constituent of low-temperature processing plasmas for the etching of silicon and silicon-based materials. We have completed a systematic study of the ionization properties of the C₂F₆ parent molecule and the C₂F₅ free radical which is one of the abundant secondary species produced in C₂F₆-containing processing plasmas. Two experimental techniques were employed, a mass spectrometric technique which uses a well-characterized time-of-flight mass spectrometer for the measurements in C₂F₆ and the fast-neutral-beam technique for the C₂F₅ free radicals. A complete account of the absolute partial ionization cross sections and appearance energies will be given for both targets. Comparisons with calculated total ionization cross sections will also be presented. In the case of C₂F₆, our total C₂F₆ ionization cross section is in very good agreement with other available data. *Work supported in part by the US DOE.

ETP1 12 Electron-Impact Ionization of $TiCl_x$ ($x=1-4$) V. TARNOVSKY, K. BECKER, *Stevens Institute of Technology, Hoboken, USA* H. DEUTSCH, *Univ. Greifswald, Germany* R. BASNER, M. SCHMIDT, *INP Greifswald, Germany* Titanium-tetrachloride, $TiCl_4$, is the precursor of choice for the plasma-assisted chemical vapor deposition of TiN. Efforts to understand and model the key plasma-chemical reactions that lead to the deposition of TiN require a knowledge of the ionization properties of the $TiCl_4$ parent molecule as well as of the $TiCl_x$ ($x=1-3$) radicals that are produced in the plasma as secondary species. We report the result of absolute ionization cross section measurements for $TiCl_4$ and the $TiCl_x$ ($x=1-3$) radicals from threshold to several hundred electronvolts. Two mass spectrometric techniques using either a high-resolution double-focusing mass spectrometer or a time-of-flight mass spectrometer and the fast-beam technique were employed in the experiments. A complete account of all relevant ionization cross sections and appearance energies will be presented at the Conference together with a comparison of the measured cross sections with predictions from semi-empirical and semi-classical calculations. *Work supported in part by the US DOE and by the VW Stiftung, Germany.

ETP1 13 Total Ionization Cross Sections of WF_x , $x=1-5$, Determined Using RECP* WINIFRED HUO, *NASA Ames Research Center* The electron collision cross sections of the radicals WF_x , $x=1-5$, have not been studied experimentally or theoretically. These radicals can be generated by electron-impact dissociation or dissociative ionization of WF_6 . Their structures have been determined by quantum chemistry calculations¹ based on the density functional theory. Several radicals in this group have been found to have low-lying excited states very close to the ground state. Thus any study must include contributions from these states. To determine the total ionization cross sections of these radicals, Complete-Active-Space SCF calculations for the radicals, including relevant low-lying excited states and their ions, have been carried out. A relativistic effective core potential was used to describe the inner shell electrons of tungsten. The parameters deduced from these calculations have been used to determine the total ionization cross sections of these radicals based on the Binary-Encounter-Bethe Model². The trend in the cross sections with increasing number of F will be discussed.

*Research supported by the NASA Ames IPT on devices and nanotechnology

¹K. G. Dyall, to be submitted

²Y.-K. Kim and M. E. Rudd, *Phys. Rev. A* **50**, 3954 (1994).

ETP1 14 Magnetic and Electric Field Induced Enhancements in Laser Induced Anion Formation* KANNADAGULI NAGESHA, *ORNL* LAL PINNADUWAGE, *ORNL/UT* Efficient negative ion formation from molecules laser excited to energies above the ionization threshold is understood to occur by dissociative attachment of low energy photoelectrons to simultaneously produced core-excited Rydberg molecules¹ as well as by dissociative capture of a bound electron from one Rydberg molecule by another Rydberg molecule.² We have observed further substantial enhancements in anion formation in the presence of external electric and magnetic fields. Our results were obtained in a crossed excimer laser pulse - molecular pulse experiment employing a

focusing time-of-flight mass spectrometer. These enhancements are likely to be due to the field induced stabilization of Rydberg states.³ Due to the concurrent field ionization of high-lying Rydberg states, electric fields induced much lesser enhancements compared to magnetic fields.

*Research sponsored by the DOE-EMSP program. ORNL is managed by the Lockheed Martin Energy Research Corporation for the US DOE under contract number DE-AC05-96OR22464.

¹L. A. Pinnaduwege and P. G. Datskos, *J. Appl. Phys.*, **81** (1997) 7715.

²K. Nagesha and L. A. Pinnaduwege, *J. Chem. Phys.*, **109** (1998) 7124.

³A. Muhlplfordt, U. Even, E. Rabani, and R. D. Levine, *Phys. Rev. A*, **51** (1995) 3922.

ETP1 15 Ionization of Trimethylgallium C. Q. JIAO, *Mobium Enterprises, Inc., Dayton, OH* C. A. DEJOSEPH, JR., A. GARSCADDEN, *Air Force Research Laboratory, Wright-Patterson AFB, OH* We report the cross sections for ionization of Trimethylgallium (GaC_3H_9) by electron impact and rates for gas-phase ion-molecule collisions, measured by Fourier transform mass spectrometry. Electron impact ionization of GaC_3H_9 over the energy range of 10-70 eV produces the molecular ion and 7 fragment ions, with a total cross section of $1.1 \pm 0.1 \times 10^{-15} \text{ cm}^2$ at 50 eV, and approximately constant to 70 eV. Absolute cross sections are determined by adding Ar to the gas sample for signal comparison with the known Ar ionization cross section. All of the observed ions contain Ga, and more than 97% of the ion population consists of $GaC_2H_6^+$, Ga^+ and $GaCH_3^+$ within the energy range studied. The results illustrate the preferential methyl abstractions. Gas-phase ion-molecule collisions in the 10^{-7} Torr · s range produce $GaC_2H_6^+$ and Ga^+ at the expense of other ionic species. Ar^+ is found to react with GaC_3H_9 also forming mainly $GaC_2H_6^+$ and Ga^+ . No significant clustering reactions have been observed, implying that gas-phase ionic polymerization does not contribute to the Ga film formation.

ETP1 16 Comparative studies of dissociative electron attachment to methyl halides* R.S. WILDE, G.A. GALLUP, I.I. FABRIKANT, *University of Nebraska* Methyl halides belong to the class of polyatomic molecules for which nuclear dynamics relevant to low-energy electron scattering can be treated relatively simply by assuming that only one vibrational mode is influenced by collisions. At the same time dissociative attachment cross sections for these compounds vary in enormous range from the virtually unmeasurable 10^{-23} cm^2 for methyl chloride at room temperature to the much larger 10^{-14} cm^2 for methyl iodide. In the present work we supplement our previous studies by calculations of dissociative attachment to methyl bromide and compare results for all methyl halides studied so far. The rate as a function of temperature for all methyl halides exhibit the exponential dependence on $1/T$ (Arrhenius law) with the activation energy lowest for methyl iodide and largest for methyl chloride. The cross section as a function of electron energy exhibits structure at vibrational excitation thresholds associated with vibrational Feshbach resonances observed previously for methyl iodide¹.

*Supported by the National Science Foundation

¹A. Schramm, I. I. Fabrikant, J. M. Weber, E. Leber, M. -W. Ruf, H. Hotop, *J. Phys. B*, to be published.

ETP1 17 Stability and Electron Loss Rate Control in Optically Pumped Plasmas E. PLOENJES, P. PALM, I.V. ADAMOVIĆ, J.W. RICH, *Dept. of Mechanical Engineering, The Ohio State University, Columbus, OH 43210-1107* The paper discusses recent ionization, recombination, and electron attachment measurements in optically pumped plasmas. Optical pumping of gas mixtures (CO, N₂, O₂, NO, and Ar) occurs via excitation of the low vibrational quantum states of CO by resonant absorption of the CO laser radiation, with subsequent vibrational energy transfer to other diatomic species by vibration-vibration (V-V) energy exchange. Optical pumping produces nonequilibrium steady-state vibrational energy distributions at the low pump laser powers (10-100 W c.w.), low gas temperatures (T=300-1500 K), and high pressures (up to 1 atm). At these conditions, the vibrational temperatures of the optically pumped species are a few thousand degrees each. Ionization in optically pumped molecular gases is dominated by the associative ionization mechanism, resulting in steady state free electron concentrations in the range $n_e \sim 10^{10}$ - 10^{11} cm⁻³. The rates of electron-ion attachment are inferred from independent measurements of the electron production rate, and of the steady state electron concentration. It is shown the recombination rate is reduced by adding small amounts of NO (~ 0.1%), which increases the electron density by an order of magnitude. A similar effect is observed in the presence of small amounts of O₂, despite the fact that oxygen is known to be an efficient electron attacher.

**SESSION ETP2: POSTER SESSION:
HEAVY PARTICLE COLLISIONS**

Tuesday evening, 5 October 1999

Poplar Room Sheraton Waterside Hotel at 19:30

ETP2 18 Ion-Molecule Reactions in CHF₃ Discharges B. L. PEKO, *University of Denver* I. V. DYAKOV, *College of William and Mary* R. L. CHAMPION, *College of William and Mary* M. V. V. S. RAO, *NASA/Ames* J. K. OLTHOFF, *NIST* In an effort to enhance the database drawn upon for analysis and modeling of CHF₃ discharges, absolute cross sections for ion-molecule reactions have been measured. The reactions investigated include collision induced dissociation, electron detachment, and dissociative electron transfer resulting from collisions of CF₃⁺, F⁺, and F⁻ with CHF₃. Impact energies range from a few eV to a few hundred eV. The cross sections are more complex than observed previously for CF₄, with a large number of possible species produced. The measured cross sections are used to analyze relative fluxes and energies that were measured for positive ions sampled from dc Townsend discharges in CHF₃. The ion-molecule collision cross sections explain an observed decrease in expected CF₃⁺ and F⁺ fluxes in the discharge, and a corresponding increase in other ions, such as CHF₂⁺, CHF⁺, CF⁺, and C⁺. This work was supported in part by the Division of Chemical Sciences, Office of Basic Energy of the U. S. Department of Energy.

ETP2 19 Gas-Phase Ion-Molecule Reactions in Perfluoropropane C. Q. JIAO, P. D. HAALAND, *Mobium Enterprises, Inc., Dayton, OH* C. A. DEJOSEPH, JR., A. GARSCADDEN, *Air Force Research Laboratory, Wright-Patterson AFB, OH* Ions in the gas phase generated by the electron impact ionization of perfluoropropane (C₃F₈) at 25 and 50 eV, respectively, were studied

to measure their reactions with the parent molecule at room temperature in the 10⁻⁷ Torr range. Among the ions observed, CF₃⁺, C₂F₄⁺ and C₂F₅⁺ were found to be unreactive (rate constant < 10⁻¹² cm³s⁻¹) with C₃F₈, while CF⁺ and CF₂⁺ reacted forming mainly C₃F₇⁺ with rate constants of 1.5 ± 0.2 × 10⁻¹¹ and 7.0 ± 0.5 × 10⁻¹¹ cm³s⁻¹, respectively, and C₃F₇⁺ reacted to form CF₃⁺ and C₂F₅⁺ with a rate constant of 8.6 ± 0.5 × 10⁻¹¹ cm³s⁻¹. Ar⁺ (formed by electron impact on Ar) has also been studied and found to react with C₃F₈ to yield mainly C₃F₇⁺ and CF₃⁺, with a rate constant of 3.9 ± 0.4 × 10⁻¹⁰ cm³s⁻¹. The reactivity of all of the ions appears to be independent of whether the reactant ions were generated by electron impact at 25 or 50 eV. The product distribution of each ion reaction was also studied as a function of the reactant translational energy. In summary, the data indicate that CF₃⁺ will be the dominant ion in the ion flux reaching a substrate surface under many plasma conditions at the mTorr and higher pressures using C₃F₈ and C₃F₈/Ar mixtures.

ETP2 20 Electron Capture in Proton Collisions with CO.* P.

C. STANCIL, D. R. SCHULTZ, *Oak Ridge National Laboratory* M. KIMURA, *Yamaguchi Univ., Japan* J.-P. GU, G. HIRSCH, R. J. BUENKER, Y. LI, *University of Wuppertal, Germany* Electron capture by protons following collisions with carbon monoxide is studied with a variety of theoretical approaches including quantal and semiclassical molecular-orbital close-coupling (MOCC) and classical trajectory Monte Carlo (CTMC) techniques. The MOCC treatments utilize potential surfaces and couplings computed for a range of H⁺-CO orientation angles and C-O separations. Results including integral, differential, electronic state-selective, and vibrational state-selective cross sections will be presented for low- to intermediate-energies. Comparison with experiment will be made where possible and the relevance of the reaction in astrophysics and atmospheric physics will be discussed.

*Work supported by NASA UVGA Program (P.C.S.), US DOE Contract DE-AC05-96OR22464 (D.R.S.), Ministry of Education, Japan (M.K.), and by The Deutsche Forschungsgemeinschaft, grant Bu 450/7 (J.-P.G., G.H., R.J.B., and Y.L.).

ETP2 21 Electron capture in collisions of Si⁴⁺ ions with He atoms below 1 keV/u MINEO KIMURA, *Yamaguchi University*

REIKO SUZUKI, *Hitotsubashi University* AYAKO WATANABE, *Ochanomizui University* HIROSHI SATO, *Ochanomizui University* PHIL STANCIL, *Oak Ridge National Laboratory* JIAN-PING GU, *Universitaet Wuppertal* GERHARD HIRSCH, *Universitaet Wuppertal* ROBERT J. BUENKER, *Universitaet Wuppertal* There have been three rigorous theoretical studies on electron capture in collisions of Si⁴⁺ ions with He atoms at low energies below 10 eV/u. Large discrepancies in rate coefficients calculated have been found, and the origin of these discrepancies has remained unresolved. More recently one experimental attempt has been reported, but the experimental rate constant was found to be smaller by a few orders of magnitude than any of theoretical results thus making the situation much more confusing. Therefore, we have undertaken an ab initio theoretical investigation for electron capture in collisions of Si⁴⁺ ions with He atoms below 1 keV/u. The theoretical approach is based on a molecular orbital expansion method within a fully quantum mechanical formulation. The preliminary result obtained agrees reasonably well with the recent theory by Stancil et al., and disagrees with the experiment.

ETP2 22 Reactions of O^+ with N_2 and NO : recoil velocity measurements in a guided-ion beam experiment DALE LEVANDIER, *Boston College, Newton, MA 02159* YU-HUI CHIU, *Boston College, Newton, MA 02159* STEVE PULLINS, *Air Force Research Laboratory, Hanscom AFB, MA 01731* RAINER DRESSLER, *Air Force Research Laboratory, Hanscom AFB, MA 01731* Previous studies of the reactions of O^+ with N_2 and NO indicate very small rates at thermal energies, with dramatic increases in reaction efficiency at higher collision energy. Recent interest in high pressure air plasmas and other extreme environments has led to the need for better characterization of these unusual exothermic reactions in the near-thermal to hyperthermal energy range, especially with regard to product state distributions. We have used the octopole guided-ion beam method to measure time-of-flight (TOF) spectra of the NO^+ produced in the reactions of ground state $O^+ + N_2$ and $O^+ + NO$. The velocity-transformed TOF data indicate more than one mechanism for both reactions. This presentation will discuss the more remarkable features of these results, including the complex-mediated $O^+ + N_2$ mechanism at hyperthermal collision energies. Where possible, the results are analyzed with the aid of the oscillating complex model of chemical reaction and are compared to statistical theory.

ETP2 23 Spectroscopy of $Na + Noble Gas$ Mixtures: Precise Measurements of Absorption Cross-Section MAX SHURGALIN, JIM BABB, HYUN-KYUNG CHUNG, *Harvard-Smithsonian Center for Astrophysics, Cambridge MA 02138, USA* WALTER LAPATOVICH, *Osram Sylvania Central Research, Beverly, MA 01915, USA* The absorption and emission of light by gases at high pressures are significantly influenced by atomic collisions, which result not only in atomic line broadening but also lead to very broad, essentially molecular spectra with rich rotational-vibrational structure and satellite features due to formation of molecules and quasi-molecules. We report new experimental results on the spectroscopy of sodium vapor and noble gas mixtures, which are compared with recent theoretical calculations. In order to perform the most stringent tests of the theoretical calculations, absolute values of absorption cross-section are measured in the range 410 to 780 nm with better than 0.01 nm resolution. A special absorption cell was designed for this purpose. To determine accurately the sodium concentration in the mixture, the cell is placed in the test arm of a Mach-Zender interferometer and the 'hook' method in the vicinity of the Na line is applied. The concentration of noble gas is determined from pressure and temperature measurements. Supported in part by the NSF and Osram Sylvania Inc.

ETP2 24 A bi-dimensional model of a Cu-HBr laser plasma. FRÉDÉRIC GIRARD, *CEA ERICK LE GUYADEC, CEA* A two-dimensional (radial and longitudinal) model is developed in order to simulate the behaviour of the plasma column constituting the active medium of a CuHBr laser. Species taken into account by the code are Cu, Ne, Br, H atoms and H_2 , HBr and CuBr molecules. We take all this species and Cu_3Br_3 to assess their densities at the thermal equilibrium. The molecules may be dissociated by collision with an electron or thermally. Neon atoms assist the thermal dissociations. For association, atom-atom reactions or atom-molecule reactions are considered: $\langle\langle \dots \rangle\rangle$ or $\langle\langle \dots \rangle\rangle$. Moreover, HBr can be involved in the electron dissociative attachment process: $\langle\langle \dots \rangle\rangle$ which has got a maximum reaction rate value of $2.5 \cdot 10^{-15} m^3 \cdot s^{-1}$ at an electronic temperature of 0.2 eV. It may be excited toward vibrational levels $v=1,2,3$ which have higher dis-

sociative attachment rates than $v=0$. The electron density is reduced by dissociative attachment process during post-discharge much more than by three bodies recombination. Within the central zone, HBr can be thermally dissociated and electron recombination is slowed down. Excitation of $HBr(v=0)$ creates an important amount of $HBr(v=1)$ at the half radius of the tube. There are then many Br- and few electrons there. Negative ions Br- density is reduced by charge neutralisation with copper ions in the afterglow. This leads to an important electron density gradient. In conclusion, creation of $HBr(v=1)$ is favoured at the middle of the radius and causes a fast electron reduction. Hence, the recombination processes produce a confinement of the plasma column at the centre of the tube and the heat deposition is then not uniform. The laser emission only occurs in the inner zone of the tube.

ETP2 25 Initial energy dependence of EED in PDP Cell T. FUKUYAMA, H. ITOH, *Chiba Inst. of Tech.* In the previous paper¹, we described on the electron transport and driven rate coefficients in a PDP cell. The calculation were carried out using the Monte Carlo simulation (MCS) method. We also verified that the local field approximation (LFA)² was not necessarily suitable for a more detailed analysis, including the strong nonequilibrium regions in the PDP cell. This paper describes the influence of initial energy of electrons on the electron energy distribution (EED) in the PDP cell. Calculations are carried out under the same conditions as in the actual PDP cell, 300 Torr in gas pressure and 0.02 cm in gap length. Hayashi³ are also used. Spatial distribution of electron transport and driven rate coefficients are obtained with two types of the initial energy distribution of electrons at the cathode. One is the distribution formed uniformly 0~ 0.1 eV, and the other is the experimental result which used a $He^+, Xe^+/Ni$ cathode⁴. The results of the electron transport and driven rate coefficients at the equilibrium region almost agree, but large differences are found in the nonequilibrium region, particularly near the cathode. Therefore, no influences on EED by initial energy of electrons were proven by this calculation except for increase of the back scattering of ejected electrons.

¹T.Fukuyama, H.Itoh, Y.Murakami and H.Matsuzaki : Bull. of the Am. Phys. Soc., Vol.43, No.5, 1469 (1998)

²Y.Murakami et al., Proceedings of Euro Display '93, P.555 (1993)

³Handbook of Plasma Material Science (in Japanese), Ohm-sha (1992)

⁴H.D.Hagstrum : Phys. Rev., Vol.104, 317~ 318 (1956)

ETP2 26 A Determination of the Symmetric Charge Transfer Cross Sections for Ar^+ and Xe^+ at Ion Thruster Conditions. STEVE PULLINS, *Air Force Research Laboratory* DALE LEVANDIER, *Boston College* YU-HUI CHIU, *Boston College* RAINER DRESSLER, *Air Force Research Laboratory* Symmetric charge transfer cross sections for Ar^+ and Xe^+ in their respective neutral gases are determined in a guided ion beam instrument for collision energies up to 400 eV. The cross sections are determined using two independent methods. In the first method, attenuation of the primary ion beam in the presence of the neutral gas is measured. The second method is a time-of-flight technique in which both the primary ions and charge transfer product intensities are measured based on their temporal separation. The results are compared to previous experimental work as well as to theoretical calculations.

ETP3 27 Solutions to the Spatially Inhomogeneous Boltzmann Equation in Rare Gases and Rare Gas-Molecular Gas Mixtures

WM. F. BAILEY, C. G. SMITHTRO, *Air Force Institute of Technology* A two-dimensional model of the electron kinetics within a glow discharge positive column has been developed, based on the formalism of Uhrlandt and Winkler¹. The model establishes a steady state solution, such that the net ionization rate is exactly balanced by the wall loss. After summarizing the analytic development, we present the numerical techniques used to solve the resulting elliptic partial differential equation, discussing an efficient method to treat sparse banded matrices. The model is first validated against published results in rare gases, examined in the limits of the local and nonlocal kinetic approximations and also compared to a previous Monte Carlo treatment. Current flow within the solution area of a neon column is examined. The model is then extended to consider the influence of the addition of a molecular gas, nitrogen, to the rare gas, neon. Current flow and ranges of applicability of the local and nonlocal approximations in the mixture are contrasted with the pure neon results.

¹Uhrlandt, D. and Winkler, R. "Radially Inhomogeneous Electron Kinetics in the DC Column Plasma," *J. Phys. D: App. Phys.*, 29:155-120 (1996).

ETP3 28 DC Plasma Column Kinetics in a Longitudinal Magnetic Field

DIRK UHRLANDT, ROLF WINKLER, *Institut für Niedertemperatur-Plasmaphysik Greifswald, Germany* The cylindrical column plasma in a neon dc glow discharge at about 100 Pa pressure under the influence of a weak longitudinal magnetic field is investigated. An extended, fully self-consistent model of the column plasma has been used to determine the kinetic quantities of electrons, ions and excited atoms, the radial space charge field and the axial electric field for given discharge conditions. The model includes a nonlocal kinetic treatment of the electrons by solving their spatially inhomogeneous kinetic equation taking into account the radial space charge potential and the magnetic field. This treatment is based on the two-term expansion of the velocity distribution and comprises the determination of its isotropic and anisotropic components in the axial, radial and azimuthal direction. The electron kinetic behavior, which is distinctly nonlocal in that example without a magnetic field, changes to a local behavior by increasing the magnetic field up to a field strength of about 200 Gauss. At first, a slight increase of the axial electric field with the magnetic field has been found. Then the axial field and the wall potential decrease with a further increase of the magnetic field.

ETP3 29 an Efficient Discretization Scheme to Solve the Spatially Inhomogeneous Electron Boltzmann Equation

C. PUNSET, *CFP, IST (Portugal)* L.L. ALVES, *CFP, IST (Portugal)* G. GOUSSET, *LPGP, Univ. Paris-Sud (France)* C.M. FERREIRA, *CFP, IST (Portugal)* The steady-state radially inhomogeneous electron Boltzmann equation (EBE) is solved for a cylindrical dc positive column in He, at intermediate pressures. The EBE is written using the classical two-term approximation in (r, u) phase space, where r is the radial position and u the electron kinetic energy. The numerical treatment of the space boundary conditions was improved¹ in order to satisfy the electron continuity equation in the vicinity of the discharge boundaries. This correction can

change the *eigenvalue* solution NR by about 50%. The EBE is discretized in energy following Rockwood², and in space by adopting an exponential scheme^{3,4}. The latter scheme is especially well suited to support large space-charge field gradients at the discharge wall, which permits to obtain a self-consistent solution, by coupling the EBE with the ion transport equations and Poisson's equation.

¹L.L. Alves, G. Gousset and C.M. Ferreira, *J. Phys. IV 7*, 143 (1997)

²S.D. Rockwood, *Phys. Rev. A 8*, 2348 (1973)

³D.L. Scharfetter, H.K. Gummel, *IEEE Trans. ED-16*, 64 (1969)

⁴J.S. Chang and G. Cooper, *J. Comp. Phys. 6*, 1 (1970)

ETP3 30 Abnormal-glow discharges in Ar: Experiments and models.

A. V. PHELPS, *JILA, CU and NIST* We review measured and calculated voltages and cathode-fall thicknesses versus the current density normalized to the square of the pressure for parallel-plane Ar glow discharges in the above-normal current range. Local-field models¹ are used to explore a wide range normalized current densities, models of ionization coefficient versus E/n , and effective electron yields per positive ion reaching the cathode. For a given normalized current density and cathode yield, non-local field models² lead to both larger and smaller cathode-fall voltages than do local-field models. The calculated and measured effects of gas heating will be compared. For a given cathode and normalized current density, experimental cathode-fall voltages usually vary by a factor of two or more, presumably because of varying cathode properties. Tests of a proposed technique for the separation of the effects of electron production at the cathode and in the gas using measured discharge parameters will be presented.

¹A. L. Ward, *J. Appl. Phys. 33*, 2789 (1962); I. Pèrés and L.C. Pitchford, *J. Appl. Phys. 78*, 774 (1995).

²I. Pèrés et al, 6th Int'l. Symp. on the Sci. and Tech. of Light Sources, Budapest 1992; A. Bogaerts and R. Gijbels, *J. Appl. Phys. 78*, 6427 (1995); V. V. Serikov and K. Nanbu, *J. Appl. Phys. 82*, 5948 (1997).

ETP3 31 Electron Density and Temperature Measurements in an Atmospheric Pressure Air Plasma by Heterodyne Interferometry

FRANK LEIPOLD, ROBERT H. STARK, AHMED EL-HABACHI, KARL H. SCHOENBACH, *Old Dominion University, Norfolk, VA 23529* Measurements of the electron density and gas temperature in a microhollow cathode supported (MCS) glow discharge in 1 atmosphere air have been performed by means of a heterodyne CO₂-laser Mach-Zehnder interferometer. The index of refraction contains contributions from both electrons and heavy particles, and therefore information on the electron density and the density of the neutral and ionized atoms and molecules, respectively. In order to separate the information on electron density and gas temperature we have measured the temporal development of the index of refraction during the ignition phase of the discharge. Since the generation of electrons occurs on a much faster time scale than heating of the gas, the initial fast decay of the index of refraction was assumed to be due to changes in electron density, the following slower decay to be due to increase in temperature. In first experiments on MCS atmospheric pressure air discharges electron densities of 10^{13} to 10^{14} cm⁻³ have been measured. The gas temperature at steady-state was found to be between 1500 K and 2500 K. — This work was funded by the Air Force Office of Scientific Research in Cooperation with the DDR&E Air Plasma Ramparts MURI Program and the National Science Foundation.

ETP3 32 Cd-Ne DC glow discharge: an efficient source of UV radiation TSVETELINA PETROVA, *University of Sofia, Sofia, Bulgaria* ALEXANDER OGOYSKI, *Technical University, Varna, Bulgaria* GEORGE PETROV, *University of Montreal, Montreal, Canada* ALEXANDER BLAGOEV, *University of Sofia, Sofia, Bulgaria* A Cd-Ne DC glow discharge has been investigated theoretically and experimentally. A complete data set has been compiled and a detailed collisional radiative model has been made. The electron Boltzmann equation and the heavy particle kinetics are solved simultaneously and the discharge properties are calculated selfconsistently. The electron density and the populations of Cd resonance and metastable states have been measured. The model and experiment are in fair agreement. Investigation of the resonance radiation from both Cd resonance states Cd (5p3P1) and Cd (5p1P1) showed that up to 60 per cent of the input power can be converted into resonance radiation which suggests that Cd-Ne DC glow discharge can be an efficient light source.

ETP3 33 ArF Excimer Emission from Microhollow Cathode Discharges WENHUI SHI, AHMED EL-HABACHI, KARL H. SCHOENBACH, *Old Dominion University, Norfolk, VA 23529* Microhollow cathode discharges (MHCD) in Ar and Xe have been shown to emit excimer radiation at 128 nm and 172 nm, respectively, with an efficiency (in case of Xe) of approximately 8% [1,2]. In order to extend the wavelength range towards longer wavelengths we have studied MHCD in argon fluoride mixtures (1% F, 5% Ar, 94% He). We were able to generate stable dc discharges in flowing gas at pressures ranging from 100 Torr to atmospheric pressure. The discharge voltage was approximately 500 V, the discharge current in these experiments was 10 mA. Whereas the spectrum at 300 Torr was dominated by atomic lines, at 700 Torr only excimer radiation peaking at 193 nm is observed in the spectral range from 120 nm to 300 nm. Absolute measurements of ArF excimer emission provided a value of approximately 3% in efficiency, or a total optical power of the excimer radiation of 150 mW. The peak power at 193 nm is 17 mW/nm. This is higher by a factor of 2 to 3, compared to xenon excimer emitters, due to the small FWHM of the 193nm ArF line (4 nm) compared to that of the Xe excimer line (24 nm). [1] Karl H. Schenbach, Ahmed El-Habachi, Wenhui Shi, and Marco Ciocca, *Plasma Source Science and Technology* 6, 468 (1997). [2] Ahmed El-Habachi and Karl H. Schoenbach, *Appl.Phys.Lett.* 73, 885 (1998). This work was funded by the DOE, Advanced Energy Division, and by the National Science Foundation.

ETP3 34 Electron Temperature Control in an MMT RF Plasma TETSUJI SHIMIZU, YUNLONG LI, KOHGI KATO, SATORU IIZUKA, NORIYOSHI SATO, *Department of Electrical Engineering, Tohoku University, Sendai 980-8579, Japan* Control of the electron temperature is of crucial importance for generating and selecting radical species in the processing plasma. In the high electron temperature plasma, the reactive gas is highly dissociated to provide many kinds of radical species. Therefore, the electron temperature should be decreased to choose suitable radical species necessary for chemical reaction. We propose a new method for controlling electron energy in a large-diameter modified magnetron-typed (MMT) RF discharge [1]. Two cylindrical mesh grids connected axially are placed inside the MMT RF electrode, which separate plasma production region from processing region radially. By varying the slot-width between the grids, the electron temperature in the process region is controlled continuously in a range of 0.5 eV ~ 3.0 eV. This method using a grid at floating potential is available in the reactive plasma where the grid might be covered with high resistance film. It is observed that

uniform radial profiles of the plasma parameters (electron temperature, ion flux, plasma potential) are formed over 30 cm in diameter in the processing region. The effects of the electron temperature control on the chemical reaction such as radical formation and film deposition are also investigated in H₂ / CH₄ plasmas. [1] Y.Li, S.Iizuka and N.Sato: *Appl. Phys. Lett.* 65 (1994) 28.

ETP3 35 Influence of Gas Composition on the Dissociative Excitation Rate of CO₂ in RF Discharges T. DINH, S. POPOVIĆ, R. L. ASH, L. VUSKOVIĆ, *Old Dominion U., Norfolk, VA* Dissociative excitation of carbon dioxide by electron impact is the controlling process for CO₂ decomposition in RF discharges. The process was studied in an RF discharge using a gas mixture that contained carbon dioxide. The amplitude of the reduced electric field was between 5 and 60 Td. The corresponding cross sections and rate coefficients were evaluated by solving numerically the appropriate transport equations, taking into account changes in the gas composition. The time evolution of the coupled dissociation and recombination of carbon dioxide was derived using a model¹ which employs a selective interaction of major neutral species and accounts for the change in gas composition during the process. The model was compared with experimental data. Special attention was given to a gas mixture representing the Martian atmospheric gas, but various initial gas mixtures were used in order to determine the optimal conditions for decomposition of carbon dioxide.

¹L. Vušković, R. Ash, S. Popović, T. Dinh, and A. Van Orden, *AIAA Paper 98-3304* (Cleveland, July 1998).

ETP3 36 2D+1 PIC-MCC Modelling in a capacitive RF GEC cell* E COSTA I BRICHA, C.M.O. MAHONY, P.G. STEEN, W.G. GRAHAM, *Dept. of Pure and Applied Physics, The Queens University of Belfast, BT7 INN, Northern Ireland.* Modelling is a powerful tool to understand and predict plasma behaviour. Here, a two-dimensional Particle In Cell (PIC) code is used to describe a capacitively coupled GEC reference cell. These two dimensions plus another of symmetry allow us to model the plasma considering ion losses to the sides, which in the GEC configuration is the main ion loss mechanism. The present code is a modified version of XOOPIC¹, which was developed by the UC Berkeley group. A blocking capacitor has been simulated to reflect the GEC external circuit and so allow ab initio development of the DC bias. The main objective is to model the response to particular diagnostic tools. At present this has focused on the Electron Energy Distribution Function (EEDF), the plasma potential and the DC bias. These outputs are time resolved. Comparison with time averaged argon experimental data at 13.3 Pa and a driven voltage amplitude of 100 V shows a good fit to the shape of the EEDF. At the present the simulated electron density is about a factor of 10 lower than the measured value. There is good agreement with plasma potential and DC bias measurements. Present work involves the incorporation of metastables and the role of secondary electron emission.

*Supported by EU BRITE grant EURAMCT 960365

¹<http://www.ptsg.eecs.berkeley.edu/xoopic/xoopic.html>

ETP3 37 Object Oriented Monte Carlo Multi Dimensional Simulations of Parallel Plate Capacitively Coupled Discharges I HORIE, *Hokkaido Inst. of Technology* Y OHMORI, *Sapporo Univ.* PLG VENTZEK, *Motorola Inc.* K KITAMORI, *Hokkaido Inst. of Technology* This presentation deals with a continuation of work on object oriented models programmed using Java. The motivation is to develop a suite of Java-based physics models that

lend themselves to parallelization (i.e. execution on distributed systems). Overall, the work is an object oriented based Monte Carlo simulation of a parallel plate discharge in 1D with mobile ions and electrons. The discharge gap is broken down into uniform slabs. Each slab corresponds to a stand-alone Monte Carlo simulation of the plasma species in that slab. After a time-step, statistics are collected using a Legendre Polynomial Weighted Sampling object and the simulation continued by an object that does a B-Spline fit to those statistics. Stable execution of this method in reasonable times depends on the sampling technique. Therefore, the presentation details the development a three-dimensional sampling method that allows better capture of the role of secondary electrons in the discharge. Results illustrating program performance will be shown for rf discharges in silane and argon and compared with fluid simulation results.

ETP3 38 Sampling and Statistics Issues in Parallelized Java Object Oriented Monte Carlo Simulations

T SUZUKI, *Hokkaido Inst. of Technology* S NAKAMURA, *Hokkaido Polytechnic Coll.* PLG VENTZEK, *Motorola Inc.* K KITAMORI, *Hokkaido Inst. of Technology* This presentation focuses on the statistics and sampling issues associated with parallelized Monte Carlo simulations that treat both the ions and electrons as mobile particles. Legendre Polynomial Weighted Sampling is used to collect information about particle spatial and velocity distributions to keep particle number at a minimum. The method is at the same time parallelizable and is implemented on an array of PC grade computers using Javas remote method invocation. While particle number is minimized, it is done at the cost of adding computational load since sampling and particle re-initialization is done frequently. This has made the scaling with the number of processors distinctly sub-linear. A bi-cubic spline technique has been combined with a very efficient random number generation scheme (Marsene Twister) to mitigate the consequences of these added tasks. The performance of this scheme will be illustrated using the simulation of rf parallel plate discharges in Ar and Silane as examples.

ETP3 39 An Investigation of Selective Promotion of Electron-Molecule Reactions by Impulse Field Electron Acceleration*

H. SUGAWARA, T. SHIMODA, Y. SAKAI, *Hokkaido University, Japan* Selective promotion of a particular electron-molecule reaction in weakly ionized gases is simulated. By applying an intense electric field E_{imp} to low energy electrons for a short time T_{imp} , the electrons are accelerated instantaneously in short-distance collisionless flight. The increase in the electron velocity is $\Delta v = (e/m)E_{imp}T_{imp}$ (e and m , the electron charge and mass). This process appears a parallel shift of the electron distribution function $f(v)$ in velocity space. If $f(v)$ before acceleration is concentrated around $v = 0$ due to low electron energy as is in a plasma bulk, $f(v)$ after acceleration is then concentrated around $v = \Delta v$, i.e. mono-energetic electrons are provided. By choosing appropriate values of E_{imp} and T_{imp} , we can aim an energy band in which the collision cross section of the target reaction is large, that would realize high selectivity. This method was applied to promotion of SiH_3 radical production in the bulk of an SiH_4 RF (13.56 MHz) plasma as a demonstration. The energy efficiency of this process was higher than those in DC/RF-driven cases without E_{imp} when their time-averaged E/N values are equal.

*Work in part supported by Grant-in-Aid 10750201 of The Ministry of Education, Science, Sports and Culture, Japan.

ETP3 40 Automated Sensor for 3-D Reconstruction of Optical Emission from RF Plasmas

COREY COLLARD, *University of Michigan* S. SHANNON, *University of Michigan* M. L. BRAKE, *University of Michigan* JAMES PAUL HOLLOWAY, *University of Michigan* Three dimensional images are obtained by using an automated scanning sensor which collects optical emission from a RF (13.56 MHz) discharge in a capacitively coupled GEC cell. The sensor scans a plane parallel to the electrode surface and transmits the plasma spectral emission through a fiber optic cable to a monochromator. The fiber optic is attached to a motorized rotational stage attached to a manual vertical translational stage. Wedges of light (argon at 750.4 nm) are collected as the fiber scans across the plasma. The data is digitized and stored so that it can be input into an algorithm, which uses a Tikhonov regularization method to reconstruct the emissivity as a function of radial position. By varying the height of the sensor, a 3-D plot of the plasma emission can be obtained. Three dimensional plots of plasmas run at 75, 100, 150 and 200 peak to peak voltage at pressures of 100, 250, 500 and 1000 mTorr were obtained. The non-uniformity of the light emission as a function of pressure and power will be discussed.

ETP3 41 Mass spectrometric investigations of ionic species in rf discharges in CHF_3 , C_2F_6 , C_4F_8 , and their mixtures with Ar

YICHENG WANG, *National Institute of Standards and Technology* MARTIN MISAKIAN, *National Institute of Standards and Technology* JAMES OLTHOFF, *National Institute of Standards and Technology* We report the measured ion fluxes and ion energy distributions in radio-frequency (rf) discharges in CHF_3 , C_2F_6 , C_4F_8 , and their mixtures with Ar. A Gaseous Electronic Conference rf reference cell with an inductively-coupled plasma source is used to produce the discharges, with the gas pressure ranging from 0.67 to 4.0 Pa and applied rf powers from 100 to 300 W. Ions are sampled through a 10 μm diameter orifice in the center of the ground electrode and analyzed with a 45 degree electrostatic energy selector in tandem with a quadrupole mass spectrometer. The total ion fluxes through the orifice are measured by configuring the first few electrostatic elements of the mass-energy analyzer system to form a Faraday cup. The dominant ion in a pure C_2F_6 discharge at 250 W, 2.7 Pa is C_2F_5^+ . Surprisingly, the dominant ion in a pure CHF_3 discharge under similar conditions has a mass of 28 u, attributed to the secondary ions CO^+ and/or Si^+ .

ETP3 42 Parametric Study of the Radial Contraction of Atmospheric Pressure Discharges Sustained by Surface Waves

Y. KABOUZI, *Universite de Montreal, Montreal, Quebec* M.D. CALZADA, *Departamento de fisica aplicada, Universidad de Cordoba, Spain* M. MOISAN, *Universite de Montreal, Montreal, Quebec* K.C. TRAN, *Universite de Montreal, Montreal, Quebec* C. TRASSY, *EPM-Madylam, ENSHMG, France* We consider that a plasma column is constricted radially when the radius of its glow is smaller than the radius of the tube containing it. The plasma filament radius can be small, as is the case with heavy mass noble gases, or large with helium and molecular gases such as oxygen and nitrogen. The efficient use of gaseous discharges at atmospheric pressure to chemically transform molecules depends on the degree of interaction of the molecules with the carrier gas, and therefore is affected by plasma constriction. Determining the influence of operating conditions (gas nature, wave frequency and tube radius) on the degree of constriction of the plasma column is therefore essential for its proper use in the remediation of given gases. We have achieved an experimental parametric study of plasma constriction as a function of discharge conditions over an extremely large range of values thanks to the surface-wave discharge flexibility.

ETP3 43 Laser Scattering Diagnostics of a Microwave Discharge Plasma S. NARISHIGE, S. TOKUYAMA, M. A. MAN-SOUR, M. D. BOWDEN, K. UCHINO, K. MURAOKA, *Kyushu University* T. SAKODA, *Kitakyushu National College of Technology* J. KHACHAN, B. W. JAMES, *University of Sydney* In order to understand reaction processes in a microwave discharge plasma for the diamond thin film fabrication, laser scattering diagnostic techniques have been used to measure densities and temperatures of various particles. The plasma was produced by a microwave at a frequency of 2.45 GHz and the power of 700W. The total pressure of a mixture of H₂ and CH₄ were set at 20 Torr. Molecular densities and temperatures of H₂ and CH₄ were measured by the laser Raman scattering method. Measured temperatures were more than 1500 K in the plasma center and about 300 K near the chamber wall. On the other hand, H₂ densities were at 20 prefilled H₂ density in the plasma center and almost 100 at the chamber wall. These results showed that pressure profile of H₂ was flat from the center of the chamber to the wall and the density decrease of H₂ was caused by the increase of temperature. For the case of CH₄ molecules, the situation was quite different. The measured density of CH₄ at the plasma center was less than 5 density. This means that the CH₄ density profile was largely affected by the dissociation. Measurements of electron densities and temperatures by laser Thomson scattering are in progress. Results of these measurements will be used to analyze reaction processes in the plasma quantitatively.

ETP3 44 Inductive Electromotive Force Measurements in Inductively Coupled Plasma KEN-ICHI TAKAGI, KAZUKI IWATANI, YUKINORI KUROKI, *Kyushu University, Japan* Recently, an inductively coupled plasma (ICP) was investigated to apply to several fabrication processes. The ICP source can produce efficiently over 10^{11}cm^{-3} high-density plasma using a simple structure. An inductive electromotive force (IEMF) is thought to contribute to this plasma production mechanism. In this experiment, we measured the IEMF using a magnetic probe in Argon plasma and made a comparison between the IEMFs of different single-loop antennas without a matching network modification. The IEMF at the quartz window did not depend on the facing area to the plasma at the same discharge power. However, the IEMF in the region over away 10mm from the quartz window was closely related to the plasma production efficiency. It indicates that only the IEMF value at the quartz window is not a dominant factor for the plasma production. On the other hand, in the antenna with a large facing area to the plasma, the IEMF at the antenna edge was larger than that of the antenna center in the region away from the quartz window. It supposes that the antenna edge is an important antenna part for the ICP production.

ETP3 45 EEDFs Measured in Ar-Electronegative Gas ICP Discharges C.M.O. MAHONY, *Dept of Physics, The Queen's University of Belfast, Northern Ireland* O.A. OKPALUGO, *Electrical & Electronic Engineering Dept., University of Ulster at Jordanstown, Northern Ireland* W.G. GRAHAM, *Dept of Physics, The Queen's University of Belfast, Northern Ireland* S. LAVERTY, P.D. MAGUIRE, *Electrical & Electronic Engineering Dept., University of Ulster at Jordanstown, Northern Ireland* There have been few fundamental studies of inert gas-electronegative gas discharges particularly in ICP systems. Here we investigate the effects of electro-negative gas addition to argon plasmas on the electron energy distribution function (eedf), an important influence on plasma chemistry. We drive an rf-inductively-coupled plasma with a 18 cm diam. 6 turn pancake coil above a 1 cm thick quartz window. The adjustable 15 cm

diam. lower, grounded electrode is 8.5 cm below the quartz window. The rf psu power was 50 W at 14 MHz, and gas pressure 50 mTorr in Ar-H₂ and 80 mTorr in Ar-Cl₂. The eedfs are measured using a compensated Langmuir probe near the gap centre. In Ar-H₂, the eedfs approximate Maxwellians, and as the H₂, they again approximate Maxwellians but show little variation in Ne ($\sim 4 \times 10^{11} \text{m}^{-3}$) or Te ($\sim 2\text{eV}$) for additions of up to 5% Cl₂. This contrasts sharply with the Ar-H₂ above and our previous Ar-Cl₂ CCP data where < 1% Cl₂ reduced Ne tenfold. This work is supported by the EPSRC Technological Plasma Initiative.

ETP3 46 RF Electric Field and Current Density Measurements in an Inductive discharge with a \vec{B} Probe: Experimental Evidence of Collisionless Heating Mechanisms G. CUNGE, *Université Joseph Fourier, Grenoble, France* B. CROWLEY, D. VENDER, M. M. TURNER, *Dublin City University, Ireland* In inductively coupled discharges, power is transferred from the oscillating electric field to the plasma electrons in a skin depth layer near the plasma boundary. This power is dissipated both Ohmically and by a collisionless process, usually called "stochastic heating." This collisionless mechanism has been recently the subject of considerable attention and is expected to be a transit time heating effect due to electron thermal motion in the inhomogeneous rf induced field. We have determined the radial distributions of electric field and current density in an inductively coupled argon plasma (cylindrical "re-entrant" geometry) using a \vec{B} probe over a wide range of plasma parameters. The field distributions are typical of the anomalous skin effect, and a strong spatial dispersion of the plasma conductivity is observed due to the diffusion of rf currents from the skin layer. Following Godyak *et al*¹ we have separated the Ohmic and stochastic parts of the dissipated power, demonstrating that stochastic heating is dominant at pressures below 5 mTorr. Our results will be systematically compared with those obtained by Godyak *et al* in a completely different geometry.

¹V. A. Godyak, R. B. Piejak, B. M. Alexandrovich and V. I. Kolobov, *Phys. Rev. Lett.* 80, 3264 (1998).

ETP3 47 On Nonlinear Effects in Inductively Coupled Plasmas* A. I. SMOLYAKOV, A. DUFFY, I. KHABIBRAKHMANOV, *Department of Physics and Engineering Physics, University of Saskatchewan, Saskatoon S7N 5E2 Canada* V. GODYAK, *OSRAM SYLVANIA Inc.* Effects analyzed in this work are associated with the nonlinear modification of the Ohm's law due to the induced magnetic field \vec{B} . The regime when Lorentz force (Hall term) is important in the electron momentum balance equation and the ion motion can be neglected is commonly referred as electron (Hall) magnetohydrodynamic (EMH). We review various nonlinear effects that may occur in inductively coupled discharges within the framework of electron magnetohydrodynamic^a. Curvature of the magnetic field is identified as a direct source of the nonlinear generation of the azimuthal magnetic field at the second harmonic in a planar discharge. Expressions for azimuthal magnetic field B_ϕ are obtained in terms of the axial B_z and radial B_r components. This may also lead to an enhanced penetration of the magnetic field due to secondary nonlinear effects associated with finite B_ϕ . Plasma inhomogeneities are also identified as a probable cause of the convective transport of the magnetic field into the plasma. ^aA.V. Gordeev, A.S. Kingsep and L.I. Rudakov, *Phys. Reports* 243, 215 (1994).

*Supported by NSERC of Canada

ETP3 48 Influence of varying dielectric window thickness on the relative inductive and capacitive coupling in a planar ICP M. WATANABE, H. UCHIYAMA, D. M. SHAW, G. J. COLLINS, *Dept. of Electrical Engineering, Colorado State University, Fort Collins, Colorado, 80523* In inductively coupled plasmas, the dielectric window separating the rf coil and the plasma volume influences both the purposeful inductive and the parasitic capacitive coupling to the plasma. We have experimentally investigated the relative contributions of both inductive and capacitive coupling in a planar inductively coupled plasma source when varying dielectric window thickness and window composition. Experimental conditions are 1 - 20 mTorr of argon feed stock gas and 40 - 750 W of absorbed plasma power. Increasing the window thickness reduces the inductive coupling, requiring increased current through the rf coil to maintain the same plasma density. Reduced inductive coupling decreases the power transfer efficiency as predicted by the air core transformer model for the ICP of Piejak et al. On the other hand, increased window thickness and lower permittivity dielectric window material reduces the capacitive coupling component, which reduces the bulk rf plasma potential as measured by a capacitive probe. Interestingly, the increased rf coil voltage, required to drive more rf current through the excitation coil due to lower inductive coupling efficiency, tends to offset the decrease in capacitive coupling due to the thicker dielectric window.

ETP3 49 Effect of bounce resonance heating on electron energy distribution function CHIN-WOOK CHUNG, SANG-HUN SEO, HONG-YOUNG CHANG, The EEDF (Electron Energy Distribution Function) measurement is made in a solenoidal ICP (Inductively Coupled Plasma). A 2-turn copper coil is wound around a pyrex tube with an inner radius of 3.2 cm. The coil is powered by tens W, 10.4 MHz. It is found that with increasing rf power, the EEDF by an rf compensated Langmuir probe evolves into a Druyvesteyn-like EEDF at the low pressure of 1 mTorr in the small solenoidal ICP. The spatial profiles of the rf fields in the ICP against rf power are also measured by a B-dot probe. When the EEDF has a Maxwellian EEDF, the skin depth is comparable to the chamber radius at low rf power and the rf fields deeply penetrates into the center with a considerable amplitude. As rf power increases, the skin depth starts to be localized within the skin layer and then the EEDF transforms into a Druyvesteyn-like EEDF. The transition of EEDF implies that there is an effective electron heating in low energy range. Electron bounce resonance is introduced to explain the EEDF transition against rf power. The energy diffusion coefficients which describe the electron heating in plasma and determine the shape of the EEDF in elastic energy range are calculated with and without the electron bounce resonance. To our knowledge, This work is the first experimental evidence of the electron bounce resonance in ICP.

ETP3 50 Evolution of the electron energy distribution function in planar inductive discharges using rare gases SANG-HUN SEO, S. S. KIM, JUNG-IN HONG, C. S. CHANG, HONG-YOUNG CHANG, *Department of Physics, Korea Advanced Institute of Science and Technology, Taejon 305-701, South Korea* N. S. YOON, *Korea Basic Science Institute, Taejon 305-333, South Korea* Measurements of the electron energy distribution functions (EEDFs) are performed over a wide range of discharge conditions in a planar and electrostatically unscreened inductive discharge. The EEDFs in the rf discharges using three different rare gases of argon, neon, and helium are investigated in the pressure range of 1-100 mTorr and the rf power range of 40-500 W. The rf compensated Langmuir probe with the reference probe and

two LC resonant filters and the AC superposition method are used to exactly measure the second derivative of probe current which is proportional to the electron energy probability function (EEDF). Such discharge parameters as electron density, effective electron temperature, and plasma potential are obtained through the EEDF measurement. The detail structures of the EEDFs for three rare gases are presented and in particular, various EEDF transitions against rf power (E-H mode transition) and gas pressure (EEDF transition into a Druyvesteyn-like distribution) can be observed. The energy diffusion coefficient which describes electron heating is calculated using 2-D simulation for each discharge condition. The observed transitions are explained with the energy dependence of the energy diffusion coefficient and various electron collision processes.

ETP3 51 Characterization of Inductively Coupled Discharges in C2F6 and CHF3 GREG HEBNER, *Sandia National Laboratories, Albuquerque NM* The chloro-fluorocarbon gases C2F6 and CHF3 are used in a number of microelectronic plasma processing systems for both oxide etch and surface passivation. To provide data on the fundamental plasma characteristics as well as plasma species, microwave interferometry has been used to measure the line integrated electron density, photodetachment spectroscopy was used to measure the negative ion density, and laser induced fluorescence (LIF) was used to measure the spatially resolved CF density. The measurements were performed in a GEC rf reference chamber with an inductive coil plasma source and rf wafer bias. Photodetachment measurements of the negative ions as a function of wavelength are consistent with the dominant negative ion being F-. Different trends between the negative ion density and the electron density show that the negative ion precursor species density depends on power, pressure and rf wafer bias, but not on the feed gas. By pulse modulating the plasma power, negative ion - positive ion recombination rates have been determined. Spatially resolved LIF measurements show the CF density peaking in the center of the C2F6 discharge but a more uniform radial distribution in CHF3. CF density scaling with power, pressure, rf bias and surface material will be shown. This work was performed at Sandia National Laboratories and supported by SEMATECH and the United States Department of Energy (DE-AC04-94AL85000).

ETP3 52 Negative ion boundary layers in Inductively Coupled Plasmas PETER VITELLO, *Lawrence Livermore National Laboratory* Partially ionized plasmas at low neutral pressure and high plasma density may exhibit strong ion-ion coupling through space charge and Coulomb scattering effects. For electronegative plasmas this can lead to large scale irregularities in the ion density, temperature, and flux. In this regime, the force on ions due to ion-ion Coulomb scattering may dominate that from ion scattering with neutrals. This can lead to the formation of a negative ion boundary layer containing the bulk of the negative ions. Commercial Inductively Coupled Plasma reactors used in the semiconductor industry typically operate at low pressure and high plasma density. Simulations, including a detailed treatment of ion temperatures, are presented for a Chlorine discharge in the GEC reactor modified for Inductively Coupled operation. Results show that ion-ion coupling can induce large variations in the plasma, and that accurate modeling of spatial plasma structure should include these effects. This work was performed under the auspices of the U. S. Department of Energy at the Lawrence Livermore National Laboratory under contract W-7405-ENG-48.

ETP3 53 Experimental Observations of Instability in Inductive Discharges G. CUNGE, *Université Joseph Fourier, Grenoble, France* M. M. TURNER, B. CROWLEY, D. VENDER, *Dublin City University, Ireland* In this paper we report on experimental observations of instabilities in an inductive discharge in argon. The geometry is "re-entrant" or internal coil, so the plasma is approximately toroidal and the experiment has nominal cylindrical symmetry. The instability is manifested as a perturbation of the plasma density which is periodic in the azimuthal direction, i.e. the perturbation is parallel with the induced electric field lines. This perturbation reaches an amplitude of about 50 % of the average plasma density, and there is a corresponding perturbation of the order of a few Volts in the plasma potential. We will present experimental results for a range of pressures and excitation frequencies, including Langmuir probe measurements and \bar{B} probe measurements, and compare these data with the predictions of the explanatory model that we discuss elsewhere at this meeting.

ETP3 54 RF Current Density Measurements and Mode Coupling in Helicon Discharges T.G. MADZIWA, D.D. BLACKWELL, D. ARNUSH, F.F. CHEN, *Department of Electrical Engineering, UCLA, Los Angeles, CA* It has been suggested that the high RF power absorption efficiency in helicon discharges is due to the transfer of energy to electron cyclotron waves called Trivelpiece-Gould (TG) modes.¹ To test this theory, measurements have been performed using magnetic and current density probes to detect TG waves. The experiments are performed in a 10-cm diam chamber with $B_0 = 25\text{--}55$ G, $n = 10^{11}\text{--}10^{12}$ cm⁻³, $p = 3$ mTorr of argon, and $P_{rf} = 0.2\text{--}1$ kW at 11 MHz. A two-turn $m = 0$ antenna is used to excite the helicon wave plasma. Measurements are compared with a numerical code developed by Arnush and Chen² which calculates the wave profiles given the antenna geometry, plasma density profile, and neutral pressure. The results show that, as predicted by theory, the RF current density is strongly influenced by the TG mode, causing broadening and ripples in the profile, while the magnetic field is influenced to a lesser extent.

¹K. P. Shamrai, V. P. Pavlenko, and V. B. Taranov, *Plasma Phys. Control. Fusion* **39**, 505 (1997).

²D. Arnush and F. F. Chen, *Phys. Plasmas* **5**, 1239 (1998).

ETP3 55 VUV-Emission from He-Xe-Glow Discharges HARTMUT LANGE, DIRK UHRLANDT, *Institut für Niedertemperatur-Plasmaphysik Greifswald, Germany* Discharge lamps with an emission in UV and VUV are used in many industrial applications as for instance UV oxidation of organic compounds, pollutions and UV synthesis of chemicals or as fluorescent lamps. A possible realization of such radiation-sources is the low-pressure-direct current discharge in Xe-He-mixtures with the resonance-radiation of xenon at 147 nm. Data to the radiation power of this resonance-radiation as well as their efficiency in the column plasma of low-pressure glow discharges are available only insufficiently. The absolute radiance of the 147 nm-resonance radiation has been studied as a function of the discharge parameters by means of the comparison with the radiance of a radiometric source standard. Simultaneously, the atom density of the lowest excited Xe-resonance level has been measured by means of laser-atom-absorption-spectroscopy. Thus a calculation of the absolute radiation power became possible. The experimental data are compared with the results of the theoretical description based on the solution of the electron kinetic equation and the balances of the excited states. Measured and calculated data of the radiation power agree well. The efficiency of the line radiation at 147 nm has been observed to increase with decreasing xenon pressure.

ETP3 56 Electron transport in rf $E(t) \times B(t)$ fields in argon Z.M. RASPOPOVIĆ, S. SAKADŽIĆ, Z.LJ. PETROVIĆ, *Institute of Physics, Belgrade, Yugoslavia*. * Monte Carlo simulation was applied to study the electron transport in argon in high frequency crossed electric and magnetic fields. The frequencies of 10 and 100 MHz were used in the simulation. The peak E/N value was chosen to be 10 Td, 100 Td and 1000 Td. Peaks of the magnetic field were chosen in the range between 0 and 5000 Hx. The drift velocities and mean energies show similar behaviour to that observed with the Reid's ramp cross section model. Mean energy is modulate more and more at higher E/N leading to significant temporal modulation and localization of the ionization coefficient as B/N increases. The drift velocity perpendicular to the fields $W_{E \times B}$ has sinusoidal shape for small B/N but it changes into triangular form for large B/N . Time dependence of the longitudinal diffusion coefficient is very complex, while $E \times B$ component has a similar shape but without a development of a sharp local minimum at low B/N . Non-conservative effects due to ionization affect transport coefficients significantly at high E/N but the effect is localized in time as B/N increases.

*Supported by MNTRS 01E03 project.

**SESSION ETP4: POSTER SESSION:
HIGH INTENSITY LIGHT SOURCES**
Tuesday evening, 5 October 1999
Poplar Room Sheraton Waterside Hotel at 19:30

ETP4 57 Longitudinal Microhollow Cathode Discharge Arrays A. EL-DAKROURI, A. EL-HABACHI, R.H. STARK, K.H. SCHOENBACH, *Old Dominion University, Norfolk, VA 23529* A novel concept for discharge pumping of DC excimer lasers is explored where the negative glow of microhollow cathode discharges (MHCDs) is used as the active medium. Stacking the discharges -operating them in series - holds the promise for the generation of a laser medium with sufficient length to provide the required threshold gain. In order to explore the coupling between discharges operating in series, two argon discharges have been studied at pressures from 0.1 to 1 atmosphere. With the two anodes facing each other the discharges were found to operate independently down to distances of approximately 50 micrometer at a pressure of 600 Torr and a current of 3 mA. This distance increases when the pressure is decreased. For smaller distances the discharges couple, that means that the anode and cathode currents of the single discharge cease to be identical. Coupling between the two discharges occurs over longer distances when the two cathodes face each other. The results will be used to determine the optimum geometrical and electrical parameters for longitudinal array operation, and to provide guidance for the design of a potential dc excimer laser. This work is supported by the National Science Foundation (NSF).

ETP4 58 Pulsed Operation of Microhollow Cathode Discharge Excimer Sources M. MOSELHY, A. EL-HABACHI, K.H. SCHOENBACH, *Old Dominion University, Norfolk, VA 23529* Spatially resolved measurements on DC microhollow cathode discharges showed that the average radiant emittance of the xenon excimer source increases superlinearly with pressure [1]. At a current of 3 mA and a pressure of 750 Torr, the radiant emittance

is approximately 20 W/cm². For DC operation the current was limited to 8 mA to avoid thermal damage. Pulsed operation at 700 microseconds pulse width allowed us to extend the current range to 80 mA before the discharge became unstable. Pulsing the discharge allowed us also to explore its temporal development and the current dependence of the radiative power at high currents. The results showed that the time to reach a steady-state is about 200 microseconds, independent of pressure and current, in the parameter range of up to 1 atm and 80 mA, respectively. For operation at 80 mA, and 200 V, at 250 Torr the electrical power is 16 W; the optical power, assuming the same efficiency as for DC operation (8%), is 1.25 W. The linear dependence of the intensity on current allows to generate excimer point sources which can easily be controlled electrically over a wide optical power range. This work is supported by the U.S. Department of Energy (DoE), Advanced Energy Division, and the National Science Foundation (NSF). [1] A. El-Habachi, M. Moselhy and K. H. Schoenbach, this conference.

ETP4 59 Influence of the Electrode Geometry on Microhollow Cathode Discharges* O. BILWATSCH, U. ERNST, K. FRANK, *University of Erlangen-Nuremberg, Physics Department I, Erwin-Rommel-Str. 1, 91058 Erlangen, Germany* Recent experiments demonstrated the possibility to operate stable d.c. hollow cathode glow discharges at high gas pressure by reducing the diameter of the cathode opening. The so-called microhollow cathode geometry consists of two thin electrodes separated by an insulator foil with diameters in the sub-millimeter range and an axial hole acting as hollow cathode. In order to optimize the geometry and to examine the validity of the similarity laws, the electrical and optical characteristics of the discharge were investigated by varying electrode thickness (100-800 μm) as well as the dimensions of the electrode hole (200-800 μm). These experiments were performed in argon up to atmospheric pressure with forward voltages around 200V and discharge currents limited to 10mA. Additional experiments were performed using systems with one plane electrode acting as anode or cathode, respectively. Electrical measurements and fast shutter photographs will be presented.

*Funded by DFG FR1273 and DAAD

ETP4 60 Investigation of Plasma Attachment Modes in a Metal Halide High Intensity Discharge Lamp HELMAR G. ADLER, *OSRAM Sylvania Inc., Research and Development, 71 Cherry Hill Drive, Beverly MA 01915* To study the attachment modes of the plasma to the electrode, a metal halide HID-lamp was constructed which allows imaging of the front surface of the lower electrode through a window with good optical quality. Normal lamps provide only a side view of the electrodes, or the tip surface has to be imaged under a steep angle introducing serious optical problems. Measurements are performed with a telescope and video/frame grabber system. Neutral density filters for the reduction of light level and interference filters can be inserted in front of the camera to image at wavelengths of fill species, for example Hg 577/579 or 546 nm. The frame rate is typically fixed to 30 frames per second with selectable shutter speeds down to 1/10000 s. Phase resolution can be achieved by operating the power supply at slightly different frequencies allowing to record changes in cathode and anode operation. Additional measurements with a gateable spectrometer/CCD system will be presented. This system allows phase and spatially resolved spectral measurements to extract plasma information in front of the electrode. Electrode temperature measurements from side and top views will be examined.

ETP4 61 Optical emission spectroscopy of the electrode region in metal halide lamps DOUGLAS DOUGHTY, *Osram Sylvania* Optical emission spectroscopy is used to investigate the plasma characteristics of the near-electrode regions of metal halide high intensity discharge lamps (NaI, ScI₃, and Hg) operated on various ballasts. Spatial resolution of 0.2 mm is obtained by magnifying the region of interest and probing the image plane with a fiber optic coupled to a spectrometer. Temporal resolution of 0.2 msec is obtained by interrupting the emission with a line-synchronized mechanical chopper. Mercury emission dominates the output from the electrode region in both the anode and cathode phases. Ratios of these lines are used to qualitatively picture the variation of the near-electrode electron temperature during an ac cycle. Emission from the metal additives versus electrical phase is significantly different from the mercury emission: during the anode phase the metal emission is nearly absent, whereas the peak of the metal emission is delayed during the cathode phase relative to that from mercury. Variations in optical emission are correlated with various types of electrode structures and with various current waveforms, suggesting how these lamp system design parameters impact plasma parameters.

ETP4 62 Investigation of Temperature and Density Profiles in the Electrode Region of High-Pressure Sodium Lamps MANFRED KETTLITZ, RICO GROSSJOHANN, *Institute of Low-Temperature Plasma Physics, Friedrich-Ludwig-Jahn-Str. 19, D-17489 Greifswald, Germany* A main problem in the operation of high-pressure mercury and sodium discharge lamps is a shortening of lamp life according to a blackening of the lamp wall due to the erosion of the electrodes. The processes in the plasma sheaths near the electrodes are responsible for heating and the undesirable erosion of the electrodes. To describe the energy transport to the cathode the knowledge of the temperature and density distribution of the plasma near the electrode is necessary. Therefore temperature profiles are measured by emission spectroscopy in sodium discharge lamps and electron densities are calculated. The discharges are operated in sapphire tubes with tungsten electrodes. The input power varies between 35 and 100 W and results in temperatures in the arc axis between 3000 and 4500 K and electron densities between 10^{14} and 10^{16} cm⁻³. The arc is constricted towards the electrodes and the point of attachment is diffuse in the cathode phase. In the anode and in the cathode phase there is an increase of the arc temperature towards the electrodes.

ETP4 63 Simulating the Sulphur Lamp with PLASIMO, a plasma simulation model. C.W JOHNSTON, H. VAN DER HEIJDEN, JAN VAN DIJK, VAN DER MULLEN JOOST, *Eindhoven University of Technology, The Netherlands* Several electrodeless lamps are currently available on the market. Examples of these are the Philips QL, Osrams Endura and GE's Genura. While these lamps make use of induction as a means of power coupling, the source of their light, namely mercury, remains the same as in older lamps. Another electrodeless configuration is the microwave powered Sulphur Lamp. Sulphur lighting has several advantages over other lamp systems. Firstly, large fluxes ($\approx 100,000$ lm) of high quality light are obtained with circuit efficiencies of up to 60 percent. Secondly, unlike fluorescent and HID lamps there is no decrease in brightness with time since phosphors and electrodes are not needed. Another significant aspect of the sulphur lamp is that it contains no mercury, lessening environmental hazards associated with disposal. In order to simulate the operation of this light source, PLASIMO, a plasma modeling tool which was developed at the Eindhoven University of Technology, was used. Modules

were included to describe the transport properties and power in-coupling. Results of the simulations will be shown and compared with experiment.

ETP4 64 Theoretical studies of pressure broadening of alkali-metal-rare-gas mixtures. H-K. CHUNG, M. SHURGALIN, J.F. BABB, *Harvard-Smithsonian Center for Astrophysics* Pressure broadening is investigated for alkali-metal atoms perturbed by rare gas atoms at high density. Quasi-molecular vibrational and rotational structures appear in the far-wing spectra. Their importance to understanding energy transport in the gas and also the use of satellite structures as a diagnostic of gas conditions are explored. In the quasi-static limit, the pair-wise interacting alkali-metal atoms and rare gas atoms are treated as quasi-molecules and the far-wings of the broadened spectra are modeled as molecular radiation, calculated quantum-mechanically utilizing critically evaluated molecular data. We also extend our quantum-mechanical approach to a unified theory which can explain not only the far wings but also the core of the broadened lines. Our results are compared with experimental results for sodium-xenon gas mixtures and their relevance to high-pressure sodium lamps will be considered. This research has been carried out in collaboration with OSRAM SYLVANIA Inc. and is supported in part by the NSF.

**SESSION ETP5: POSTER SESSION:
SPARK CHANNEL TEMPORAL VARIATIONS**
Tuesday evening, 5 October 1999
Poplar Room Sheraton Waterside Hotel at 19:30

ETP5 65 Turbulent Cooling of an After-Spark Channel with a Residual Current* MIKHAIL N. SHNEIDER, *Dept. of Mechanical and Aerospace Engineering, Princeton University* A theoretical and computational model describing the cooling and expansion of a post-discharge channel, accounting for generation and dissipation of the turbulent flow, was developed. For the first time, the dependence of the nature of the gas cooling on a relatively weak residual current in the channel was demonstrated. The residual current does not prevent the hydrodynamic instability of the channel boundary. However, Joule heating caused by the residual current suppresses the turbulence development in the channel. For each current pulse, there is a corresponding critical value of the residual current that stabilizes the channel, making it essentially a quasi-stationary arc with relatively high temperature and conductivity. The suggested model can be applied to the development and decay of after-spark channels in a variety of applications: from lightning and long laser-induced sparks to narrow high-current spark gaps, to microwave discharges in dense gases.

*The work was supported by the Plasma Ramparts Program of DoD/AFOSR MURI

ETP5 66 A more correct model for the primary-and-secondary streamer phenomena in short air gap YU.V. SHCHERBAKOV, A.V. SHILOVA, *High Voltage Research Center of All-Russian Electrotechnical Institute, Krasnaya Gorka, Russia* Basic properties of streamer discharges in short air gap is considered. To further analyse two-dimensional structure and dynamics of the streamer, a simplified two-dimensional parametric

model of the primary streamer has been developed. Here, on the base of our previous experimental results obtained in the middle gap space, the behavior of the primary streamer arriving at the cathode is described. Some predicted properties are in qualitative agreement with the available experimental data. An earlier evolution of the cathode zone (fast on-axis propagation of the arriving primary streamer, its fast radial expansion at the cathode surface, motion of the positive-ion beam, reverse phase movement of the boundary ionization zone, reconfiguration and redistribution of the total electric field etc.) has been then shown to yield the physical reason for starting the secondary streamer immediately after an arrival of the primary streamer at the cathode. The well-known Sigmond's theory of the secondary streamer created on the base of the Douglas-Hamilton-Many type attachment instability in one-dimensional approach is thus improved. The primary reason for initiating the secondary streamer is shown to be the electric field lines condensing to an axis, leading to forerunner propagation. So, in the fast stage, the Douglas-Hamilton-Many type attachment instability is primarily initiated in transversal direction. After all fast processes are terminated (that is, in resistive phase), the one-dimensional "longitudinal" classical Sigmond's mechanism prevails.

SESSION ETP6: POSTER SESSION: DUSTY PLASMAS
Tuesday evening, 5 October 1999
Poplar Room Sheraton Waterside Hotel at 19:30

ETP6 67 Control of Strongly-Coupled Fine-Particle Flow in a DC Discharge Plasma GIICHIRO UCHIDA, RYOICHI OZAKI, SATORU IIZUKA, NORIYOSHI SATO, *Department of Electrical Engineering, Tohoku University, Sendai 980-8579, Japan* Fine particles in discharge plasmas have been attracted a strong attention for microelectronics fabrication due to their roles as contamination source. The development of new method to control the motion of fine particles in the processing plasmas is essential to realize the clean process. We have analyzed electrostatic force acting on the particles, and observed dynamic motion of fine-particle clouds. In our experiment, we injected particles into a dc plasma, and controlled the axial and radial potential profiles in particle levitation region [1]. The system is quite simple to analyze the electrostatic force acting on the particles in a dc sheath region. Injected particles are symmetrically levitated above the center of a segmented particle levitation electrode, and construct a lattice-like structure. On the other hand, when the particles levitate in inhomogeneous potential, they are pushed away from stronger electric field region, which results in a vortex formation. The vortex is generated when the density is high enough to satisfy the condition of strong Coulomb interaction among the fine particles. In this way, fine particles under strongly-coupled state interact sensitively with the potential structure confining radially to evolve a remarkable dynamic motion. [1]. G. Uchida *et al.*, in *Proc. International Congress on Plasma Physics*, pp. 2557-2560(1998).

ETP6 68 Behavior of a particle in plasma-wall sheath region Y. WATANABE, M. SHIRATANI, K. KOGA, A. HATAE, A. TOYOZAWA, *Kyushu University, Japan* In processing plasmas, one of particulate contamination sources is flakes of films on reactor wall, electrodes and wafers. To prevent such particles from depositing on the substrate surface, it is important to understand

the trajectory of a particle in the plasma-wall sheath region. Hence, we observed the trajectory of a particle injected from the wall in a He dc glow discharge. A particle $20\ \mu\text{m}$ in size injected, at an injection velocity $v_p = 10\ \text{cm/s}$, from a wall biased by $-200\ \text{V}$ against anode is reflected in the sheath region to return to the wall, while a particle of $v_p > 20\ \text{cm/s}$ passes through the boundary region and goes into the plasma. Particles are charged positively in the sheath region close to the wall as the density of ions is much higher than that of electrons there. Thus when the electrostatic potential energy of the positively charged particle in the sheath region near the wall is larger than its initial kinetic energy, the particle returns to the wall. These results can be explained by a simple simulation of particle trajectory. Behavior of a particle in the sheath region of electro-negative discharges will be presented at the conference.

ETP6 69 Growth suppression of cluster-size particles in silane rf discharges Y. WATANABE, M. SHIRATANI, K. KOGA, S. MAEDA, Y. MATUOKA, K. TANAKA, *Graduate School of Information Science and Electrical Engineering, Kyushu University, Japan* Recently some of cluster-size particles below $10\ \text{nm}$ in size formed in silane rf discharges are recognized to be incorporated into a-Si:H films deposited by the discharges and degrade the film quality. We have found that even under so-called device quality conditions there exist cluster-size particles of about $10^9\ \text{cm}^{-3}$ in density.¹ Effects of pulse discharge modulation, GND electrode heating as well as H_2 dilution on growth of cluster-size particles are studied using novel photon-counting laser-light-scattering and threshold photo-emission methods. While the modulation is effective to reduce considerably particle-density, the GND electrode heating combined with the modulation much enhances the reduction. The enhanced suppression of particle growth by the modulation can be explained by thermophoretic force exerted on particles. High H_2 dilution ($> 80\%$) has been found to suppress effectively growth of particles around the plasma/sheath boundary near the RF electrode. Correlation between particle density and film quality will be presented at the conference.

¹M. Shiratani, T. Fukuzawa and Y. Watanabe, *Jpn. J. Appl. Phys.* Vol. 38, No. 7A(1999).

ETP6 70 Production of Free Electrons from Particulates in a Flowing Gas J. LILLY, A. WHITE, W.C. LEE, W. LEMPERT, V.V. SUBRAMANIAM, *The Ohio State University, Columbus, OH 43210* It is well known that some materials emit electrons thermionically when heated to elevated temperatures. The minimum temperature at which such electron emission occurs is dependent on the work function (ϕ) of the material. This is well known in applications involving high-current electrical discharges where electrodes made of refractory materials are used, and has been revived in recent work. In this paper, two experiments are described in which particles of graphite ($\phi = 4.5\ \text{eV}$) fluidized in flowing air are used as sources of electrons. In one series of experiments, CO_2 laser is used to irradiate the graphite particles while in the other, the fluidized graphite particles are passed through a microwave cavity, resulting in a non-equilibrium plasma. Both sets of experiments rely on heating of the particles in excess of the gas so that unequal gas and particle temperatures result. The presence of electrons is inferred from current drawn by application of a D.C. bias across a pair of electrodes placed transverse to the flow. Experimental measurements of electron densities in these two classes of experiments, and scalability of these schemes for production of volumetric plasmas in atmospheric pressure air are discussed.

SESSION ETP7: POSTER SESSION:
OPTICAL DIAGNOSTICS
Tuesday evening, 5 October 1999
Poplar Room Sheraton Waterside Hotel at 19:30

ETP7 71 Emission Characteristics in a Pulsed Microwave Discharge Containing Hydrogen N. LANG, J. RÖPCKE, *Institut für Niedertemperatur-Plasmaphysik, 17489 Greifswald, Germany* M. KALATCHEV, B.P. LAVROV, *Faculty of Physics, St.-Petersburg State University, 198904 St. Petersburg, Russia* It is well known that the production of H-atoms in discharges plays an important role in many applications of plasmas, e.g. deposition processes or surface treatment. Because of applicability of microwave discharges for that purpose, such processes are investigated in a pulsed hydrogen microwave discharge with time-resolved optical emission spectroscopy (OES). The frequency of the rectangular pulses is $500\ \text{Hz}$ (duty cycle 50%) at a pressure of $55\ \text{Pa}$. The time-resolved evolution of the atomic emission of H and Ar atoms is compared with the emission of the radiative dissociation continuum of the hydrogen molecules and with the emission of Q-branch lines of the Fulcher- α band. The development of the gas temperature is determined and compared to an excitation temperature of atomic hydrogen levels. The experimental results are analysed quantitatively in relation to the dissociation of hydrogen and to excitation and relaxation kinetics in the plasma chemical reactor under the study.

ETP7 72 Spatial and Temporal Monitoring of Active Species in C_7F_{16} Vapor Discharges* C. P. LUNGU, A. M. LUNGU, *Hokkaido Univ., Japan (on leave from Nat. Inst. of Laser, Plasma and Rad. Phys., Romania)* Y. SAKAI, H. SUGAWARA, *Hokkaido Univ.* The decomposition of C_7F_{16} by dc and rf discharges in its vapor was studied as a function of the position from the electrodes and time. The pressure was in the range of $10\sim 100\ \text{Pa}$. The reaction chamber was made of stainless steel cylinder ($\phi = 30\ \text{cm}$ and $h = 40\ \text{cm}$) with optical access ports. In dc mode the discharge voltage was $< 2\ \text{kV}$ and the current was 5 to $50\ \text{mA}$. In the rf ($13.56\ \text{MHz}$) case the power was between $10\sim 100\ \text{W}$. The spatio-temporally behavior of the discharges and the active species produced in decomposition processes were examined by observing optical emission in the visible range (300 to $800\ \text{nm}$) and mass spectrometry. The plasma-induced optical emission was strongly dependent on the discharge properties. The maximum light emission intensity of decomposed species was obtained in the cathode glow in the dc discharge, while the uniform distribution was shown in rf discharges. Electron temperatures and electron densities were estimated from optical emission of rare gases added to fluorocarbon vapor containing plasma.

*Work supported by Grant-in-Aid of The Ministry of Education, Science, Sports and Culture, Japan.

ETP7 73 Three dimensional profiles of a pulsed inductively coupled plasma in Ar and CF_4/Ar K. HIOKI, N. ITAZU, N. NAKANO, T. MAKABE, *Keio University, Japan* Inductively coupled plasma (ICP) has been used as metal etching processes for ULSI circuits fabrications because of its high plasma density at low pressure. Dry etching by using ICP has, however, serious issues, such as low selectivity, local side etching (called as notch), and charge build-up damage. In order to overcome these subjects, the use of time modulated pulse plasma has been proposed. One of the advantages of a pulse plasma is the reduction of charge-up damages and defects by reducing the electron activity and controlling the dissociation of radicals in the plasma. In our previous

studies, we have investigated CW-ICP structures in Ar and mixture CF_4/Ar , driven by one turn current coil at 13.56MHz. In the present study, we have observed CT images of time-averaged and time-resolved net excitation rate of $Ar(3p_5, 2p_1)$ in pure Ar and $CF_4(5\%)/Ar$, as the probes of the plasma structure. These CT images in a pulsed ICP as a function of modulation period and duty ratio (the ratio of the on-time to the total period) are compared with those in a CW-ICP. We discuss the function of the pulsed ICP based on these results, and in particular, as for electron activity during the off phase of the plasma.

ETP7 74 Spectroscopic measurements of electron temperature and density using a collisional radiative model ROGER D. BENTSON, *The University of Texas at Austin* M. L. HUEBSCHMAN, *The University of Texas at Austin* VIVEK BAKSHI, *Sematech* J. TERRY, *MIT* BRUCE LIPSHULTZ, *MIT* KEIJI SAWADA, *Shinshu University* We have used a collisional radiative [CR] model [Sawada & Fujimoto *J. Appl. Phys.* 78 (5) (1995)] which accounts for both collisional and radiative processes along with absolutely calibrated spectroscopic diagnostics to measure electron temperature and density in a low density inductively coupled hydrogen plasma. We have also used the same model to measure the electron temperature and density in a higher density deuterium plasma in the C-Mod divertor. We estimate the electron temperature and density by minimizing the least square deviation of measured populations of upper state densities and the predictions of the CR model. For the RF discharge we will present typical density and temperature profiles and a sensitivity analysis of the technique. The importance of molecular processes in populating the upper state hydrogen levels will be discussed. In the divertor we will compare the densities deduced from Stark broadened line profiles with the density estimates using the Balmer series intensities and the CR model including corrections for plasma opacity.

ETP7 75 Calibration of Electric Field Induced Energy Level Shifts in Argon GREG HEBNER, *Sandia National Laboratories* Argon is a commonly used gas in a number of discharges. As such it is an ideal candidate for spectroscopic based electric field measurements within the sheath and bulk discharge regions. Recently, measurements demonstrated the use of the Stark induced shifts of high lying energy levels in Argon to make spatially and temporally resolved electric field measurements [1]. However, that method relied on the cross calibration of known and calculable shifts in helium discharges to calibrate, in-situ, the energy level shifts in Argon. This poster shows the use of an atomic beam system to calibrate the electric field induced shift of high lying energy levels directly. In addition, data on very high lying argon levels, up to the 20 F manifold, were obtained. Comparison of our electric field induced energy level shift calibration curves with previous work will be shown. The possibility of using this system to calibrate energy level shifts in other gases of technological interest to the microelectronics and lighting industry will be discussed. [1]. J. B. Kim, K. Kawamura, Y. W. Choi, M. D. Bowden, K. Muraoka and V. Helbig, *IEEE Transactions on Plasma Science*, 26(5), 1556 (1998). This work was performed at Sandia National Laboratories and supported by the United States Department of Energy (DE-AC04-94AL85000).

ETP7 76 Studies of a sheath structure in an RF discharge using experimental, analytical and simulation approaches* J. B. KIM, K. KAWAMURA, M. D. BOWDEN, K. MURAOKA, *Kyushu University, Japan* Y. W. CHOI, *Korea Electrotechnology Research Institute, Korea* The electric field distributions in the sheath region were measured using laser-induced fluorescence (LIF) method in capacitively coupled RF glow discharges oper-

ated at different pressures in helium. The measured distributions and sheath thicknesses obtained from the electric field distributions were compared with those obtained from an existing analytical theory¹ and with a numerical simulation². The comparison yielded reasonable agreement, both in general tendency with regard to the pressure dependence and in the absolute magnitude. These results provided evidence of the validity of the analytical sheath theory and the numerical simulation for predicting the sheath properties of an RF glow discharge. 1. M. A. Lieberman and A. J. Lichtenberg, *Principles of Plasma Discharges and Materials Processing*, New York: Wiley, 1994 2. J. P. Verboncoeur, V. Vahedi, M. V. Alves, and C. K. Birdsall, gPDP1, PDC1, PDS1 plasma device 1 dimensional bounded electrostatic codes, Reference manual PDx1 PC version 2.1, 1993

*Laser spectroscopy, Electric field measurement

ETP7 77 Thomson scattering with an ICCD detector for measurements of EEDF in rf discharge plasmas S. MOSHKALYOV, *Queen's University of Belfast, Northern Ireland, UK* C. THOMPSON, T. MORROW, W. GRAHAM, *Queen's University of Belfast, Northern Ireland, UK* Thomson scattering (TS) with high-repetition rate lasers has been recently introduced as a diagnostic of electron parameters in low-temperature gas discharge plasmas. This method has some distinct advantages over other techniques which are commonly used to measure electron parameters in gas discharges. This technique is non-intrusive, and the interpretation of data is straightforward. However, due to the small cross-section of light scattering by free electrons, TS signals are extremely low (20-30 photoelectrons/pulse for an electron density of 10^{11} cm^{-3}). To improve signal-to-noise ratios, measurements are made by accumulating the signals over 10^3 laser pulses. In most TS experiments, photomultiplier tubes are used for the light detection. A further step in the diagnostic development is the use of multichannel detectors (gated intensified CCDs) which record the entire TS spectrum. Here, TS system with 10 Hz YAG laser (0.5 J at 532 nm) and a low-noise high-performance ICCD detector is used for diagnostics of an inductively coupled RF discharge plasma. Experiments were carried out in Ar plasma for low pressures (25-250 mTorr) and relatively low powers (30-70 W). Experiments have shown that EEDF measurements can be performed by accumulating TS signals in 1000-5000 pulses (measurement time of 10-15 minutes).

ETP7 78 Efficient Thomson Scattering Measurement System for the Diagnostics of Processing Plasmas AKIHIRO KONO, KEIGO NAKATANI, *Nagoya University, Nagoya 464-8603, Japan* Optical measurement of electron energy distribution function (EEDF) is desirable for the diagnostics of processing plasmas. In Thomson scattering measurements, EEDF is directly derived from the Doppler broadened profile of the laser light scattered by free electrons, but one must solve the problem of very low signal intensity due to the small scattering cross section. We have constructed an efficient Thomson scattering measurement system for the diagnostics of processing plasmas, which is capable of performing multi-channel measurement of the Doppler broadened profile without suffering from strong interference due to Rayleigh scattering and other stray scattering. The measurement system consists of a specially designed triple monochromator and an ICCD camera. The plasma is irradiated by a frequency-doubled Nd:YAG laser (532 nm). With the aid of a spatial filter between the first and second stage, the triple monochromator outputs the dispersed scattered light with the center wavelength region ($532 \pm 0.5 \text{ nm}$) eliminated, enabling multi-channel measurements with the ICCD camera in the photon-counting mode. Use of a lens

system as the focusing elements in the monochromator enables high transmittance and low aberration, both serving for a high signal collection efficiency. Preliminary Thomson scattering measurements indicated a promising performance of the measurement system.

ETP7 79 Time and Space resolved LIF-Spectroscopy of atomic species in a Dielectric Barrier Discharge CH. LUKAS, M. SPAAN, V. SCHULZ-VON DER GATHEN, H.F. DÖBELE, *Universität GH Essen, Institut für Laser- und Plasmaphysik, 45117 Essen, Germany* Barrier discharges are being used for many applications, such as ozone production, surface modification or VUV lamps. Operating at atmospheric pressure, it is also a candidate for exhaust gas decomposition. The hot electrons of this highly non-thermal discharge with cold background gas can initiate chemical reactions resulting in decomposition of toxic components. Atoms play a keyrole in the ongoing reactions. Knowledge on their properties is therefore an essential prerequisite for the understanding of the decomposition processes. We report on the application of TALIF diagnostics of atomic nitrogen and oxygen for various sets of electrical discharge parameters and different gas compositions. The measurements are performed at a single discharge filament with space and time resolution. One of the main objectives is the identification of effects related to the steepness of the voltage ramps which can be varied between 300 ns and 90 ns (to 15 kV) at repetition rates up to 20 kHz. These measurements are accompanied by a quantitative in-situ analysis of the molecular species by FTIR spectroscopy in the discharge volume and in the exhaust. Funded by the 'Bundesminister für Bildung und Forschung' under project number 13 N 7195.

ETP7 80 Optical Measurements of Atomic and Molecular Species in a Pulsed RF Discharge in Nitrogen S. F. ADAMS, C. A. DEJOSEPH, JR., *Air Force Research Laboratory, Wright-Patterson AFB, OH* T. A. MILLER, *The Ohio State University, Columbus, OH* Emission spectroscopy and LIF have been used to study the heavy particle kinetics in a pulsed, parallel-plate RF discharge in nitrogen. A two-photon LIF technique utilizing 207 nm radiation was used to detect ground state N-atoms, while single-photon LIF was applied to the detection of $N_2(A^3\Sigma_u^+)$ and $N_2(B^3\Pi_g)$ excited molecular states. Emission spectroscopy was used to gain additional information on the molecular states. These optical techniques were used to monitor temporal and spatial changes in the species concentrations. The absolute N atom concentration, determined by titration, allowed an absolute density calibration of each of the molecular species by coupling the temporal LIF and emission measurements with known rate constants of several heavy particle reactions occurring in the post discharge. The measurements, coupled with a simple numerical model, allowed absolute densities of some species, such as $N_2(X^1\Sigma_g^+, v \geq 5)$, to be determined in spite of an inability to detect the species by optical diagnostics. Results will be shown for a variety of pulsed RF discharge conditions.

ETP7 81 The Effect of Electrode Gap on CF_2 Distribution in Fluorocarbon Plasmas KRISTEN L. STEFFENS, *NIST, Gaithersburg, MD* MARK SOBOLEWSKI, *NIST, Gaithersburg, MD* Previous studies on fluorocarbon plasmas in parallel-plate reactors have shown that reactive species density distributions, cleaning rates, and other plasma properties are correlated to the rf current measured at the grounded electrode, I_{ge} . I_{ge} changes with electrode gap, which can be varied to optimize plasma performance. Here, we investigated correlations between electrode gap, electrical parameters, and the spatial distribution of the CF_2 radical in O_2/CF_4 chamber-cleaning plasmas in the capacitively-coupled

GEC Reference Cell. Electrode gaps ranging from 0.5 cm to 2.25 cm were studied at pressures from 0.1 to 1.0 Torr. The spatial distribution of the CF_2 radical was measured by planar laser-induced fluorescence (PLIF). The uniformity and intensity of CF_2 PLIF and broadband optical emission depended on both pressure and gap. The pressure at which the maximum radial uniformity in the CF_2 PLIF was observed correlated well with maximum I_{ge} . Measurements of I_{ge} could be used to optimize the spatial distribution of reactive chemical species in reactors with differing electrode gaps, aiding in the optimization of fluorocarbon plasmas.

ETP7 82 Measurement of atomic hydrogen in silane plasmas used for the deposition of a-Si:H films TOSHINORI KAJIWARA, KIICHIROU UCHINO, KATSUNORI MURAOKA, TATSUO OKADA, MITSUO MAEDA, *Kyushu University, Japan* Atomic hydrogen density and temperature in a silane plasma used for the deposition of a-Si:H films was measured using a two-photon laser-induced fluorescence technique. The plasma was generated by an RF discharge between two parallel electrodes whose diameter was 100 mm and separation was 40 mm using pure silane gas. The gas flow rate was 5 sccm, the pressure was 11 Pa and the RF power was 4 W. In order to suppress the dissociation of gases and radicals due to the absorption of the excitation laser beam and the consequent atomic hydrogen generation, two photon excitation at 243 nm was used. In order to observe fluorescence signals at a visible wavelength, simultaneous excitation at 656 nm also was used. The atomic hydrogen density was found to be $(5 \pm 2) \times 10^{17} \text{ m}^{-3}$ and the temperature was found to be $2200 \pm 600 \text{ K}$. The atomic hydrogen temperature was higher than the gas temperature. The mechanism for this was considered as follows. Hydrogen atoms generated by the dissociation of gas molecules due to electron impact in the plasma have kinetic energy of several eV, which they then lose through collisions with gas molecules. At the same time, they disappear from the plasma due to chemical reactions and diffusion before thermal equilibrium with gas molecules is established. We show experimentally that this model provides a good estimation of atomic hydrogen temperature in the plasma under various conditions of silane and silane-hydrogen mixtures.

ETP7 83 Hydrogen Dissociation in a H_2 - N_2 Pulsed DC Glow Discharge J.M. WILLIAMSON, *Innovative Scientific Solutions Inc., Dayton, OH* B.N. GANGULY, *Air Force Research Laboratory, Wright-Patterson AFB, OH* The relative concentration of hydrogen atoms was measured in the afterglow of a parallel-plate, pulsed DC discharge by two-photon allowed, laser induced fluorescence (TALIF). The TALIF signal was measured, relative to pure H_2 , in H_2 - N_2 gas mixtures at constant pressure (2.5 Torr) and current (250 mA) for different fractions of N_2 (0 to 1). For short pulse durations, $\leq 10 \mu\text{sec}$, the TALIF signal drops off almost linearly with H_2 concentration suggesting H_2 is dissociated primarily by direct electron impact. For longer discharge pulses, $\geq 500 \mu\text{sec}$, there is an enhancement in the fractional dissociation that increases with N_2 concentration in the gas mixture. By varying the discharge pulse duration from 10 μsec to 1.0 msec at constant current and gas pressure, the change in the hydrogen atom production by direct electron impact compared to heavy particle collision induced dissociation has been measured.

ETP7 84 Cavity Ring-Down Spectroscopy of Etching Plasmas JEAN-PAUL BOOTH, *Laboratoire de Spectrometrie Physique, Université J.Fourier-Grenoble, France* GILLES CUNGE, *LSP* LUDOVIC BIENNIER, *LSP* DANIELE ROMANINI, *LSP* ALEXANDER KATACHANOV, *LSP* Many of the reactive species of interest in etching plasmas absorb light in the UV spectral region (200 ~ 300 nm). Measurement of these weak absorbances

($10^{-2} \sim 10^{-4}$ for a single pass) allows their absolute concentration to be determined. Previously, low-resolution spectra have been obtained using broad-band absorption spectroscopy, using a Xe arc lamp as the light source and a small monochromator equipped with a CCD Camera. Here we report high-resolution measurements using the recently developed Cavity Ring-Down Spectroscopy (CRDS) technique. The pulsed tunable output of an excimer pumped doubled dye laser was injected into a high-Q optical cavity in which the plasma is included. The absorbance as a function of wavelength is then deduced from the lifetime of the light pulse in the cavity. This technique offers the possibility of real-time (1 second) absolute concentration measurements. Results have been obtained for the detection of CF, CF₂, AlF and SiF₂ radicals in capacitively-coupled radio-frequency plasmas in fluorocarbon gases. However, the deduction of absolute concentrations from CRDS spectra is complicated by the phenomenon of non-single exponential decays when the line-width of the laser is greater than that of the transition observed.

ETP7 85 Measurement of Atomic Species in High-Density Reactive Plasmas using Vacuum Ultraviolet Absorption Spectroscopy with High Pressure Microdischarge Hollow Cathode Lamp SEIGOU TAKASHIMA, MASARU HORI, AKIHIRO KONO, TOSHIO GOTO, *Nagoya University* MASAFUMI ITO, *Wakayama University* KATSUMI YONEDA, *Nippon Laser & Electronics LAB.* In reactive plasma processes, atomic species such as H and N play important roles. Vacuum ultraviolet absorption spectroscopy (VUVAS) employing a high pressure microdischarge hollow cathode lamp (MHCL) has been developed and applied for the measurements of H and N atoms in high-density plasmas. MHCL is a powerful light source for VUVAS because the discharge volume is very small compared with the conventional hollow cathode lamp and a high current density is obtained. Therefore, a high degree of dissociation of gases in the microdischarge will be attained, resulting in the increase of the emission due to atomic species. Using VUVAS employing MHCL, H and N atom densities have been successfully measured in an inductively coupled plasma (ICP) and in an electron beam excited plasma (EBEP). The N atoms in the N₂-EBEP at a pressure of 0.01 Pa and an accelerating voltage of 50 V were approximately equivalent to those in the N₂-ICP at a pressure of 4.0 Pa and a RF power of 300 W. Therefore, EBEP is expected as the radical source operating at an ultra low pressure of around 0.01 Pa. On the basis of these measured results, the behaviors of H and N atoms in high-density reactive plasmas are discussed.

ETP7 86 Higher Order Diffusion of the Helium Triplet Metastable Measured by Diode Laser Absorption MICHAEL MILLARD, PERRY YANEY, *University of Dayton* BISWA GANGULY, C. A. DEJOSEPH, JR., *Air Force Research Laboratory, Wright-Patterson AFB, OH* We have used an InGaAs Bragg-Reflecting Diode Laser to study the diffusion of the 2^3S_1 metastable of Helium at 1.083 μm by diode laser absorption. A pulsed parallel-plate discharge with 50 mm diameter electrodes with a spacing of 16 mm was used. A glass sleeve with two 2 mm wide slits for optical access was placed over the electrodes to constrain the discharge to the region between the electrodes and to control the exact geometry of the problem. Data were obtained at 2 and 5 torr using a flow-rate of less than 1 sccm. A measured value of $478 \pm 15 \text{ cm}^2/\text{sec}$ was obtained for the diffusion constant after correcting for temperature and pressure. The data also showed the presence of higher order diffusion modes. Analysis of

these modes was performed using a method based on the work of Chantry¹ and by comparison with a 2-dimensional numerical model of the diffusion in the chamber. The results of these analysis and a discussion of the problems imposed by the system will be presented.

¹Chantry, P.J., *J. Appl. Phys.*, **62**, 1141 (1987)

ETP7 87 Laser Absorption Measurement of Atomic Oxygen Concentrations in a dc Corona Discharge* MARIA-ANTOANETA BRATESCU, MITSUYUKI OHKUBO, TAKAHIRO KAMADA, YOSUKE SAKAI, *Hokkaido University, Japan* The atomic oxygen concentrations in both positive and negative corona discharges were measured as functions of the discharge current I , gas pressure p , electrode distance d and fraction k of oxygen in gas mixtures. Two methods of laser absorption spectroscopy, i.e. classical absorption (LA) and plasma modulation (PM) techniques, were used to study the spatial distribution of O($^5S_2^0$) excited state density in the discharge in gas mixtures (He/O₂ and air). LA method was used to calibrate the PM signal. The high sensitivity of PM method allows measuring oxygen density of about 10^6 cm^{-3} . Atomic oxygen transition from O($^5S_2^0$) to O($^5P_{1,2,3}$) at $\lambda = 777.408 \text{ nm}$, 777.631 nm and 777.753 nm can be obtained with commercially available IR laser diodes. The atomic oxygen density in the vicinity of the tip electrode decreases with increasing p (gas pressure) for $d = 1 \text{ cm}$. The density is $3 \times 10^7 \text{ cm}^{-3}$ at 25 Torr · cm and $3.5 \times 10^6 \text{ cm}^{-3}$ at 75 Torr · cm for $I = 3 \text{ mA}$ and $p = 50 \text{ Torr}$. For $k < 0.01 \%$ in He/O₂ the atomic oxygen density between 10^9 cm^{-3} and 10^{10} cm^{-3} was shown to be given by high O₂ dissociation.

*Work in part supported by Grant-in-Aid for Scientific Research (B)

ETP7 88 CF₂ Detection in Radio-Frequency Ar/CHF₃ Plasmas by Fourier Transform Infrared Spectroscopy J. S. KIM,* *NASA-Ames Research Center* M. V. V. S. RAO,[†] *NASA-Ames Research Center* M. A. CAPPELLI,[‡] *NASA-Ames Research Center* S. P. SHARMA, *NASA-Ames Research Center* CF_x radicals, in particular CF₂, are instrumental in anisotropic etching of SiO₂. In order to optimize the CF_x radical population in a given process environment, it is imperative that we understand their production mechanism. Towards this goal, we have conducted a series of quantitative measurements of CF₂ radicals in low pressure RF plasmas similar to those used in SiO₂ etching. In this study, we present preliminary results for Ar/CHF₃ plasmas operating at pressures ranging from 10-50 mTorr and powers ranging from 100-500 W in the GEC reference cell, modified for inductive (transformer) coupling. Fourier transform infrared (FTIR) spectroscopy is used to observe the absorption features of the CF₂ radical in the 1114 cm^{-1} and 1096 cm^{-1} spectral regions. The FTIR spectrometer that is used for these studies is equipped with a high-sensitivity mercury cadmium telluride (MCT) detector and has a fixed resolution of 0.125 cm^{-1} . The CF₂ concentrations are measured for a range of operating pressures and discharge power levels, and are compared to measurements of the relative CF₂ concentrations made by mass spectrometry using the method of appearance potential for radical selectivity.

*Thermosciences Division, Mechanical Engineering Department, Stanford University

[†]Thermosciences Institute, NASA-Ames Research Center

[‡]Thermosciences Division, Mechanical Engineering Department, Stanford University

ETP7 89 Nitrogen CARS Thermometry Within the Outer Jacket of a Metal Halide Lamp LORI R. BROCK, *OSRAM Sylvania Inc.* HELMAR ADLER, *OSRAM Sylvania Inc.* High-resolution coherent anti-Stokes Raman spectroscopy (CARS) was applied to measure axial and radial temperature profiles within the outer jacket of a 360 Watt metal halide lamp. The CARS technique was chosen for this task because its good spatial resolution, coherent signal beam, nonintrusive nature, and selectivity yields spectra with very high signal to noise ratios despite the high level of background radiation from the running lamp. We use nitrogen CARS thermometry here because the outer jacket is filled with 400 torr of nitrogen at room temperature. Rotationally resolved nitrogen CARS spectra are measured at a number of points within the metal halide lamp. A spectral simulation program is utilized to calculate spectra for gas temperatures between 500 and 1000 K. A comparison between these simulations and the measured rotationally resolved nitrogen CARS spectra allows the temperature at each point in the lamp to be accurately determined. In addition, good agreement was achieved between the measured temperature distribution and predicted axial and radial temperature profiles in the outer jacket of the metal halide lamp.

ETP7 90 Raman Measurements of N₂, CO, and O₂ Vibrational State Distributions In Laser-Sustained, High Pressure Non-Equilibrium Discharges W. LEE, I.V. ADAMOVICH, W. LEMPERT, *The Ohio State University, Columbus, OH 43210* It is well known that the CO laser can be used to initiate and sustain electron production in pure CO at low to modest translational temperature. However, in the presence of common diatomic buffer gases such as O₂ or N₂, interspecies vibrational (V-V) energy transfer is known to "quench" the highly excited CO vibrational distribution which is critical for the production of free electrons. Theoretically, V-V exchange rates between CO and typical buffer gases are not well quantified and hence, electron production cannot be accurately predicted. In this paper, we will present new experimental results which quantify the vibrational state distribution functions of the key diatomic plasma species N₂, O₂, and CO in high pressure, laser-sustained non-equilibrium discharges. For the homonuclear diatomics, N₂ and O₂, the measurements will be performed using spontaneous Raman scattering. For CO, measurements will be performed both with Raman scattering, and spontaneous FT-IR emission spectroscopy. The focus of the paper will be two-fold: First, diagnostic issues pertinent to application of Raman spectroscopy to high pressure discharges will be described in some detail. Second, experimental data will be compared to predictions from detailed kinetic "Master Equation" modeling, emphasizing the influence of CO - O₂ and N₂ - O₂ vibrational energy transfer on CO vibrational excitation and, ultimately, free electron production. Measurements will be presented in N₂/CO plasmas, N₂/CO/O₂ plasmas, and Ar/CO/O₂ plasmas.

ETP7 91 Atomic Cu Densities from Optical Absorption by the Curve of Growth Method I. C. ABRAHAM, Y. ANDREW, S. LU, T. G. SNODGRASS, J. H. BOOSKE, A. E. WENDT, *C-PAM, UW-Madison* Discharge characterization of copper ionized metal plasmas (IMP) includes the measurement of gas phase neutral Cu atom density. The IMP system consists of a DC powered 15 cm D Cu sputter source and an RF induction plasma powered by a single turn 36 cm D loop antenna internal to the

vacuum chamber, with an Ar pressure of 50 mTorr. The neutral Cu atom density was measured by two methods. The results of a non-intrusive optical absorption measurement were compared to those of a flux measurement onto a biased quartz crystal microbalance. The application of the curve of growth method, including a full treatment of the hyperfine structure of the 324.754 nm line, to the optical absorption calculations of the ground state Cu atom density was required in order to achieve agreement between the two measurement techniques, even though the apparent fractional absorption levels were quite modest (10-25% from the two measurement methods also allows an inference of the temperature of the Cu atoms, which is shown to increase with applied RF power.

ETP7 92 RF-conductivity method to study Resonance Enhanced Multiphoton Ionization (REMPI) RAINER JOHNSEN, MIROSLAW P. SKRZYPKOWSKI, RICHARD ROSATI, BARUN K. CHATTERJEE, *University of Pittsburgh, Pittsburgh, PA* We have developed a novel technique to detect the weak ionization that is produced by Resonance Enhanced Multiphoton Ionization (REMPI) of a small admixture of nitric oxide (\sim milliTorr) in helium (\sim 200Torr). In the experiment, an unfocused beam from an excimer pumped dye laser (scanned from $\lambda = 226.811$ to 226.955 nm) was used to ionize an NO/He mixture between two plane-parallel condenser plates. The ionization was detected by observing the small phaseshift of a radio-frequency (14.7MHz) signal that is transmitted from one plate to the other. Although the experimental setup is very simple and compact, we were able to obtain the wavelength dependence of REMPI with very high spectral resolution, sufficient to resolve rotational lines. The method may be useful for detecting gaseous impurities, as a means to calibrate the wavelength scale of lasers, and perhaps to study fast kinetic processes in plasma afterglows.

ETP7 93 Optical Diagnostic Characterization of Laser and Electron Beam Ablation Plasma Plumes* R.M. GILGENBACH, S.D. KOVALESKI, M.D. JOHNSTON, *Intense Energy Beam Interaction Laboratory, Nuclear Engineering and Radiological Sciences Department, University of Michigan* Spectroscopic and laser probing diagnostics have been applied to laser and e-beam ablation plasmas, relevant to thin film deposition. Laser ablation experiments utilize a KrF laser generating about 0.8 J per 40 ns pulse. Electron beam ablation is accomplished by a channel-spark with parameters: 15 kV, 1.5 kA, and 200 ns pulselength. Temporally and spatially resolved optical emission spectra have yielded electron temperatures for laser ablated metal targets at fluences up to 20 J/cm². Laser ablation plume temperatures at early times are measured up to 5 eV, decaying to about 1 eV within 600 ns. Electron beam ablation plume electron temperatures start out lower, but persist longer at 1 eV levels. Expansion velocities of ablation plumes have been measured by dye-laser resonance absorption photography in the range of 0.4-1.4 cm/ μ s. Electron beam ablation plume line-averaged electron densities have been measured by nonresonant interferometry from 1.6 to 3.7 $\times 10^{17}$ cm⁻³. Resonant laser interferometry of e-beam ablated fused-silica yielded line integrated densities of silicon neutral atoms of 1.6 $\times 10^{16}$ cm⁻². Measured densities are consistent with thin film deposition rates.

*This research was supported by Sandia National Laboratories and the National Science Foundation.

Invited Paper

8:00

FW1 1 Plasma Issues in Ionized Physical Vapor Deposition Equipment Design.MICHAEL GRAPPERHAUS, *Tokyo Electron Arizona, Inc.*

With the emergence of dual-damascene electroplating as the preferred technique for copper interconnect metal deposition, Ionized Physical Vapor Deposition (IPVD) has become the method of choice for deposition of liners and electroplating seed layers. In the IPVD method, material is sputtered from a dc-cathode, thermalized in the process chamber, ionized by a secondary plasma source, and accelerated through the plasma sheath, giving directional deposition of the material into features on the wafer. Operating pressures of 10's of mTorr are required to allow the sputtered material to thermalize. Two important factors are used to characterize an IPVD deposition process: the uniformity of the deposition, and the fraction of the deposition that is deposited as ions (the ion fraction). Deposition uniformity depends on the erosion of the target, the thermalization distance of the sputtered material, and drift and diffusion of the material in the secondary plasma among other factors. The plasma processing conditions influence all of these factors. For example, the target erosion is altered in the presence of the secondary plasma. The ion fraction depends on the residence time and location of the metal atoms, as well as the secondary plasma density. Residence time is dependent on the background gas density and is influenced by gas rarefaction. RF bias can be applied to the wafer support to impart a more directional ion distribution, but at higher bias voltages, resputtering from the wafer can introduce a large amount of material into the plasma above the wafer. Unless this material is ionized, backscattering and subsequent redeposition of neutral species can adversely affect the ion fraction at the wafer surface. Several plasma phenomena, which must be considered in the development of an IPVD process, will be presented.

Contributed Papers

8:30

FW1 2 Rarefaction in Ionized Physical Vapor Deposition Discharges

Y. ANDREW, I.C. ABRAHAM, J.H. BOOSKE, S. LU, T.G. SNODGRASS, A.E. WENDT, *University of Wisconsin-Madison, Center for Plasma Aided Manufacturing* Ionized physical vapor deposition, I-PVD, is of current interest in semiconductor fabrication for the deposition of thin metal films as diffusion barriers and seed layers in high aspect ratio features. One of the aims of I-PVD is to achieve directionality through high Ionized Metal Flux Fractions (IMFF). A system consisting of a DC powered 15 cm diameter copper sputter source and a RF induction plasma powered by a single turn 36 cm diameter loop antenna internal to the vacuum chamber has been examined. Measurements made with a biased quartz crystal microbalance in an argon background of 10-50 mTorr, demonstrate that at low magnetron sputtering levels of 100 W, IMFFs as high as 90 % are observed. However, measurements of the electron energy distribution function, IMFF and plasma density indicate rarefaction of the background argon gas as the metal flux to the plasma increases. Further results are presented from an experimental investigation of methods to reduce gas rarefaction. These include pulsing the metal flux on the timescale of the process gas residence time and increasing process gas flow through the chamber.

8:45

FW1 3 Development and characterization of an atomic nitrogen source for the epitaxial growth of GaN PHILIPPE MÉRÉL, *INRS-Énergie et Matériaux* MOHAMED CHAKER, *INRS-Énergie et Matériaux* MICHEL MOISAN, *Université de Montréal* An efficient atomic nitrogen source based on a N_2 surface-wave discharge has been developed and was characterized using optical spectroscopy. The production of atomic nitrogen was measured by NO titration as a function of various discharge parameters such as the applied field frequency ($f=13.56, 40.68; 440$ and 2450 MHz)

and the absorbed power ($P_A = 20$ to 200 W). Dissociation rates ($[N]/[N_2]$) as high as 1.7% were obtained at a source pressure of $p_s = 4$ torr, $f = 440$ MHz and $P_A = 100$ W. The N_2 rotational and vibrational temperatures were also measured in the discharge. It was found that the saturation of $[N]/[N_2]$ with increasing P_A at $p_s = 4$ torr occurs at a threshold gas temperature of about 500 K for all values of f . This atomic nitrogen source was used together with a pulsed laser deposition system for the epitaxial growth of GaN on the sapphire(0001) substrate, with a cooled Ga target being used as a gallium source. High quality GaN thin films were deposited by optimizing both the laser intensity and the nitrogen flux. To date, our best GaN films show a FWHM of the GaN(0002) rocking curve peak equal to 200 arcsec. This result was obtained with a substrate temperature of 800°C and under Ga-rich growth conditions.

9:00

FW1 4 Fundamental Studies of In Situ Plasma Chamber Cleaning Chemistries: C2F6/O2, C3F8/O2, and NF3/He.

WILLIAM R. ENTLEY, *Air Products and Chemicals, Inc.* WILLIAM J. HENNESSY, *Air Products and Chemicals, Inc.* JOHN G. LANGAN, *Air Products and Chemicals, Inc.* The plasma etching of SiO_2 and Si_3N_4 in $C_2F_6-O_2$ and $C_3F_8-O_2$ mixtures has been studied as a function of feed gas composition (SiO_2 substrates), pressure (Si_3N_4 substrates), and power (SiO_2 substrates) in a modified-commercial RIE chamber. The chamber has been modified to permit in situ electrical measurements, which allows us to correlate the substrate etch rates and power coupling efficiencies to the discharge impedance. In addition, gas-phase FTIR spectroscopy was used to quantify the PFC emissions for the various gas mixtures investigated. For a fixed rf power, pressure, and total gas flow rate, the maximum etch rate of SiO_2 was found to occur within a relatively narrow range of oxygen concentrations, centered near a gas composition of 33 mol observed for a wider range of oxygen concentrations in C_2F_6 based plasmas. Although the destruction efficiency (the percentage of PFC destroyed in the

plasma) of C2F6 and C3F8 in O2 based mixtures are comparable under similar operating conditions, significantly larger quantities of plasma generated CF4 are formed in C3F8-O2 gas mixtures. Comparisons are made to NF3/He discharges, which show higher etch rates and higher destruction efficiencies for appropriately chosen operating conditions.

9:15

FW1 5 Beam Generated Plasmas for Large Area Materials Processing* R. A. MEGER, *Plasma Physics Division, Naval Research Lab* R. F. FERNSLER, *NRL* M. LAMPE, *NRL* D. LEONHARDT, *NRL* W. M. MANHEIMER, *NRL* D. P. MURPHY, *NRL* R. E. PECHACEK, *SFA, Inc.* S. G. WALTON, *NRC Postdoc* The Naval Research Laboratory is developing a new type of reactor for large area materials processing. This Large Area Plasma Processing System (LAPPS) utilizes a sheet electron beam to ionize a low density (10-500 mTorr) gas mixture. A pulsed or cw sheet beam of electrons is generated by a separate cathode and confined by a magnetic field. A cold (T_e 1 eV, T_i 1/40 eV), $5 \times 10^{12} \text{ cm}^{-3}$ plasma is produced in the channel with areas scalable to square meters. This technique effectively decouples the plasma production from the reactor geometry and provides additional options for process control. Particle fluxes (ions, neutrals, or free radicals) on surfaces can be controlled by beam and substrate geometry, relative densities of constituent gases, and surface bias voltages. Thus far $60 \times 60 \times 1.5 \text{ cm}$ plasmas have been generated using $< 5 \text{ kV}$, 20 mA/cm^2 60-cm wide electron beams in a 200 Gauss magnetic field. The concept and a summary of results including recent processing tests will be presented. Additional oral and poster papers at this conference will provide details.^{1,2} [¹See Fernsler, this conference, ²See papers by Leonhardt, Murphy, and Walton, this conference]

*Work supported by the Office of Naval Research

9:30

FW1 6 Theory of Plasma Production in LAPPS* R. F. FERNSLER, *Plasma Physics Division, Naval Research Laboratory* W. M. MANHEIMER, *NRL* M. LAMPE, *NRL* R. A. MEGER, *NRL* The Naval Research Laboratory is developing a new type of plasma processing reactor called the Large Area Plasma Processing System (LAPPS). This device uses a magnetically confined, sheet electron beam to ionize a background gas. Because energetic electron beams are robust and ionize anything in their path, they offer high control over the plasma being produced through adjustments in the beam current, gas density and composition, magnetic field profile, and distance from the beam to the surface being processed. Moreover, ionization and free radicals are produced efficiently relative to other sources, even though the plasma electron temperature remains low ($< 1 \text{ eV}$). Thus far, uniform planar plasmas have been produced with densities up to $5 \times 10^{12} \text{ cm}^{-3}$ in a volume 1.5 cm thick by 3600 cm^2 in area. Typical operating parameters are gas pressure 10-300 mtorr, beam energy 2-5 keV, beam current density $\sim 20 \text{ mA/cm}^2$, and magnetic field $\sim 200 \text{ G}$. This talk will address the theory underlying LAPPS, while other presentations¹ will provide experimental details.

*Work supported by the Office of Naval Research

¹See papers by R. Meger, D. Leonhardt, D. Murphy and S. Walton at this conference.

SESSION FW2: RF GLOWS

Wednesday morning, 6 October 1999

York Room Sheraton Waterside Hotel at 8:00

S. Popovic, Old Dominion University, presiding

8:00

FW2 1 Simulation of Time Modulated Dual Frequency Capacitively-Coupled Plasmas NOBUHIKO NAKANO, *Keio University* The time modulation technics of plasma source or bias power are reported to improve the problems of anomalous etching in high-aspect-ratio hole and trench, and charging damage in the field of plasma etching in ULSI processing. The two-frequency capacitively coupled plasma(2f-CCP) etching reactor has the remarkable performance for the SiO_2 etching. In this work, time modulated capacitively-coupled plasma in Ar and Ar/ CF_4 are modeled by the two-dimensional relaxation continuum(RCT) model to investigate the effect and function for the charging problem. The low energy ion flux coming into the wafer surface is produced during plasma OFF period. The low energy ion orbits is bended in the microstructure and will decrease charging potential due to the electron shading. The electron flux to the wafer increase during OFF phase also, because positive ion sheath collapse in the phase of bias voltage has positive maximum. These phenomena has advantage to cancel the positively charging in the deep trench or hole on the wafer. Effective time modulation frequency and duty ratio are also discussed.

8:15

FW2 2 Effects of Bias Frequency on 2D Image of Net Production Rate in Two Frequency CCP T. KITAJIMA, *National Defense Academy, Japan* T. FUJITA, T. MANO, T. MAKABE, *Keio University, Japan* Two frequency capacitively-coupled plasma(2f-CCP) is a major processing tool for SiO_2 etching. It is important to optimize the bias frequency for both a control of the ion energy on the wafer and a radial uniformity of 2f-CCP. Effect of bias frequency on 2D(r,z) profiles of axisymmetric 2f-CCP in CF_4/Ar at 25mTorr is investigated by time-resolved OES. Bias frequency in a range of 339kHz \sim 2.71MHz is applied to the 2f-CCP excited at 13.56MHz. For bias frequencies of 339kHz and 678kHz, the radial uniformity of the net excitation rate of probed-Ar($2p_1$) is strongly affected by the bias voltage amplitude due to the excess excitation caused by high energy electrons at the central axis. Radial uniformity is improved for the bias frequency higher than 1.35MHz. The effect of bias frequency is also shown for the temporal variation of the net excitation rate during one bias period. The net rate changes by 50% at 1.35MHz, while it changes by 200% at 678kHz. The effect of secondary electrons from the bias electrode is suppressed in case of 1.35MHz by a temporal trapping. Optimization of the bias frequency above 1MHz becomes a key to enable the bimodal energy distribution of ion on the wafer surface and the radial uniformity of 2f-CCP. Results of VHF(100MHz) excitation and the detail of the sustaining mechanism of 2f-CCP during one RF period are also discussed.

8:30

FW2 3 Modeling of non-local and local behavior of EEDF in argon and silane discharges MIN YAN, *Department of Chemistry, University of Antwerp, Belgium* ANNEMIE BOGAERTS, *Department of Chemistry, University of Antwerp, Belgium* WIM GOEDHEER, *FOM Institute for Plasma Physics "Rijhuizen," The Netherlands* RENAAT GIJBELS, *Department of Chemistry, University of Antwerp, Belgium* Non-local and local behavior of electron energy distribution function (EEDF) has been investigated in electropositive argon discharges and electronegative silane discharges by 1-D PIC/MC modeling, at a frequency of 13.56MHz, pressures varying from 30mTorr to 400mTorr, and at driving voltages of several hundreds volts. The spatial and temporal behavior of the ionization rate has also been studied. It is shown that this rate is strongly influenced by the presence of non-local effects. Silane discharges differ strongly from argon discharges as a result of the large amount of electron impact attachment and the strong electric field in the plasma bulk. This leads to differences in the spatial and temporal behavior of the electron density and average energy profiles, and hence in the ionization rate. The power dissipation has been studied for both kinds of discharges as well.

8:45

FW2 4 Modeling of argon rf glow discharges used for analytical applications ANNEMIE BOGAERTS, *Dept. of Chemistry, University of Antwerp, Belgium* RENAAT GIJBELS, *Dept. of Chemistry, University of Antwerp, Belgium* Beside the more well-known applications of glow discharges (in the semiconductor industry, as lamps, lasers, in plasma displays, etc), they are also used in analytical chemistry as spectroscopic sources for the analysis of solid materials. The material to be analyzed is used as cathode of the discharge, which is sputter-bombarded by plasma species. The atoms of the cathode material arrive in the plasma, where they are subject to collisions (most important are ionization and excitation). The ionization collisions create new ions which can be measured in a mass spectrometer. The excitation collisions create excited atoms, which emit characteristic photons, and the latter can be detected by an optical emission spectrometer. For the analysis of metals, a dc glow discharge is most frequently used. However, in order to analyze also non-conducting materials, rf discharges are becoming more important. In order to improve the analytical results, a hybrid set of models (consisting of Monte Carlo, fluid and collisional-radiative models) has been developed to describe the behavior of electrons, argon ions, fast argon atoms, sputtered atoms and the corresponding ions. Typical calculation results, like densities, energies and fluxes of the various plasma species, the electrical potential distribution, information about collision processes in the plasma and about sputtering, optical emission intensities, etc., will be presented for the rf discharge, and comparison with dc results will be made.

9:00

FW2 5 Three-dimensional particle simulation of low-pressure inductively coupled discharge generated by immersed RF antenna VLADIMIR SERIKOV, *Nippon Sheet Glass Co., Ltd., Japan* SHINJI KAWAMOTO, *Nippon Sheet Glass Co., Ltd., Japan* A particle simulation model for a sub-mTorr ICP reactor with immersed RF antenna has been developed and described. It is based on Monte Carlo approach for simulation of electron motions and collisions combined with the electromagnetic field solver accounting for collisionless electron heating [1]. The electrostatic field due to space charge is approximated from the electron pressure distribution, assuming that the pressure force balances the

electric field force. The sheath is treated as a discontinuity of the electrostatic potential at the wall, the potential jump being a function of the average electron temperature. The results of simulations of a three-dimensional ICP discharge in argon driven by 13.56 MHz RF antenna are to be presented and appropriateness of the model will be discussed. [1] M. M. Turner: *Plasma Sources Sci. Technol.*, 5 (1996), 159; *Rep. Inst. Fluid Science, Tohoku Univ.*, 10 (1997), 21

9:15

FW2 6 A New Quasi-Particle Method for Simulating Steady-State Chemically Reacting Plasmas TIMOTHY BARTEL,* *Sandia National Labs* MICHAEL GALLIS, *Sandia National Labs* SEUNG CHOI, *Sandia National Labs* JUSTINE JOHANNES, *Sandia National Labs* We present a new method for modelling steady-state chemically reacting plasma systems. We have started with a collisional PIC-like particle method for neutrals, ions, and electrons. We then introduce aspects of continuum mechanics in the collision operator and chemistry to greatly simplify and speed-up the convergence to steady-state. We also have redefined the fundamental meaning of the computational particle from a mass quantity to a mass per time quantity ($\rho \cdot V \cdot A$). Now the computational phase space is not simply a stochastic sampling of particles, but rather is deterministic based on the resonance time of each computational particle in a cell. This formulation greatly reduces the statistical noise experienced in pure particle simulations, like Direct Simulation Monte Carlo, for chemically reacting plasma systems. The computational performance is orders of magnitude faster than a traditional particle simulation. This new method solves linear equations instead of a system of PDEs which makes the method inherently stable. We still use a traditional Poisson solver based on the spatial charge density distribution to determine the potential. Also, we use the simpler particle grids which do not require a complex grid generation step. We demonstrate this method by comparing data for inductively coupled manufacturing plasmas systems: pure Cl₂ and C₂F₆. We will also show results from a traditional pure particle simulation and compare their run times. For this comparison, we have assumed quasi-neutrality. We have also applied the method for an ion-optics problem where local charge neutrality is not assumed.

*Plasma & Aerosol Sciences Department

9:30

FW2 7 Explosive Generation of Cold Electrons in Low-Pressure Discharges STANISLAV BEREZHNOI, IGOR KAGANOVICH, LEV TSENDIN, *St. Petersburg State Technical University, ul. Politekhnikeskaya 29, St. Petersburg, 195251 Russia* We have investigated the mechanisms of the formation of two-temperature electron distribution functions (EDF) enriched by slow electrons in low-pressure discharges. Calculations and experiments in argon show that, as the current increases, a radical rearrangement of the EDF can occur, which is accompanied by the formation of cold electron peak in the EDF. As a result, the average electron energy strongly decreases though energy-input increases. For a current density above the critical value, a steady-state solution can be obtained only if the electron-electron collisions are taken into account. The transition mechanism is similar to that for thermal explosion being associated with non-local character of the EDF formation, and that is why it is the general phenomenon for low pressure discharges in various gases.

SESSION GW1: CHEMISTRY AND TRANSPORT PROCESSES

Wednesday morning, 6 October 1999

Stratford Room Sheraton Waterside Hotel at 10:15

Alan Garscadden, Wright Patterson Air Force Base, presiding

10:15

GW1 1 Experimental and theoretical investigations of ionization mechanisms in air plasma discharges at atmospheric pressure* C. LAUX, L. YU, D. PACKAN, L. PIERROT, C. KRUGER, R. ZARE, *Stanford University, Stanford, CA 94305* Investigations are presented of the mechanisms of ionization in two-temperature air plasmas with electron temperatures elevated relative to the gas temperature. We will first present numerical simulations based on vibrational-state specific chemical kinetic mechanisms. These simulations show that the steady-state electron number densities exhibit an S-shaped dependence on the electron temperature for a given constant gas temperature. This behavior is found to be caused by competing ionization reactions and charge transfer between the different species present in the plasma, and thus is a particularity of multicomponent plasmas. The S-shaped curves are then interpreted in terms of macroscopic parameters (electric field and current density) for purposes of comparison with the results of discharge experiments conducted in our laboratory with a controlled discharge in atmospheric pressure air. In these experiments, measurements are made of electron number densities, electric field, and plasma temperature as a function of the discharge current. These results provide a test of the proposed ionization mechanisms, as well as a determination of the volumetric power required to sustain nonequilibrium atmospheric pressure air plasmas with elevated electron number densities.

*This work is supported by the DDR&E Air Plasma Ramparts MURI Program managed by the Air Force Office of Scientific Research

10:30

GW1 2 Detection of CH in an expanding Ar/acetylene plasma using Cavity Ring Down Absorption Spectroscopy RICHARD ENGELN, *CPS, Department of Applied Physics, Eindhoven University of Technology, P.O. Box 513, 5600 MB Eindhoven, The Netherlands* KARINE LETOURNEUR, MAARTEN BOOGAARTS, RICHARD VAN DE SANDEN, DANIEL SCHRAM, CRD ON EXPANDING PLASMAS TEAM, Cavity Ring Down (CRD) absorption spectroscopy is used to measure the methylidyne (CH) radical in an Ar/acetylene plasma. The acetylene is injected in an Ar plasma that expands from a cascaded arc, working at sub-atmospheric pressure, into a low pressure vessel. The rotational spectrum of the $A^2\Delta(v' = 0) \leftarrow X^2\Pi(v'' = 0)$ transition around 430 nm is recorded to determine the total CH groundstate density, both as function of the current through the arc and as function of the injected acetylene flow. Total groundstate densities between $0.5 \cdot 10^{17}$ and $6 \cdot 10^{18} \text{ m}^{-3}$ are detected. A simple plug-down model can qualitatively describe the measured trends in the CH density in both current and flow.

10:45

GW1 3 Temporal Electron Relaxation in Nonisothermal, Collision-Dominated Plasmas Acted Upon by Static Electric and Magnetic Fields DETLEF LOFFHAGEN, ROLF WINKLER, *Institut für Niedertemperatur-Plasmaphysik, 17489 Greifswald, Germany* Studies of the time-dependent behavior of electrons in non-isothermal, collision dominated plasmas have been concentrated on plasmas under the sole action of an electric field so far. In the presence of an external magnetic field e.g. the electron drift and thus the power input are markedly modified when compared with the magnetic field-free case. Thus, the relaxation process can be additionally controlled by the action of a magnetic field. To assess the influence of magnetic fields, an analysis of the temporal relaxation of electrons subjected to electric and magnetic fields has been performed solving the time-dependent electron Boltzmann equation. The new solution technique of this equation is based on the strict time-dependent two-term approximation of the expansion of the velocity distribution function in spherical harmonics. Starting from different initial situations the relaxation process of the electrons towards steady-state is studied for neon plasmas. The analysis of the results points out that the relaxation time with respect to the establishment of the corresponding steady-state can be enlarged by up to some orders of magnitude when increasing the impact of the magnetic force. In particular, this result shows the additional possibility to tune the plasma in its relaxation course by a magnetic field.

11:00

GW1 4 Electron Dynamics in Electric Fields with Spherical and Cylindrical Symmetry HIROYUKI DATE, *College of Medical Technology, Hokkaido University* PETER VENTZEK, *Motorola Inc.* KEI-ICHI KONDO, *Anan College of Technology* MITSUO SHIMOZUMA, *College of Medical Technology, Hokkaido University* HIROAKI TAGASHIRA, *Muroran Institute of Technology* Electric field models in cylindrical and spherical configurations are used to study the electron behavior and contrasted with their behavior in spatially homogeneous electric fields. The cylindrical and spherical fields are typical of those found in discharges about micro-protrusions or gas-filled proportional counters. In this study, we present a formalism for calculating the electron energy distribution function (EEDF) in spherical and cylindrical systems using the Boltzmann equation for the EEDF and demonstrate a Monte Carlo simulation of electron swarms in like conditions for both an Ar-like model gas and Methane. Specifically, an arrival-time spectra (ATS) method treatment of the Boltzmann equation is used to describe the swarm behavior and interpreted using a Monte Carlo experiment. As expected, results of the simulation show a strong dependence of the transport coefficients on the spatial position (i.e., on the field strength) but the EEDF and the spatially averaged swarm parameters converge rapidly to a steady state. Non-equilibrium effects near the thin-wire or point anode will be also discussed.

11:15

GW1 5 Wafer Temperature Calculation with Ion Bombardment Heating Effects HAN-MING WU, *Novellus Systems, Inc.* JACK E MCINERNEY, *Novellus Systems, Inc.* A 2-D numerical study is conducted to explore the effects of the ion bombardment on wafers due to RF bias applied to the pedestal. In the simulation,

the IEDF is calculated based on the collisionless Godyak sheath model. It is found that the ion bombardment power delivered to wafer can be as high as several watts per square centimeter. This can heat the wafer temperature up to a few hundred degrees if high

bias voltage is applied. It is also found that the gap between wafer backside and pedestal is a sensitive parameter to control the wafer temperature profile and wafer heat relaxation time. Some simulation results are compared to the available diagnostic data.

SESSION GW2: WILL ALLIS MEMORIAL SESSION
Wednesday morning, 6 October 1999; York Room Sheraton Waterside Hotel at 10:15
Mark J. Kushner, University of Illinois, presiding

10:15

GW2 1 Introduction to the Session in Honor of Will Allis.

MARK J. KUSHNER, *University of Illinois, Dept. of Electrical and Computer Engr., Urbana, IL, 61801, USA*

Professor Will Allis, co-founder of the Gaseous Electronics Conference and honorary chairman since 1966, died after a brief illness on March 5, 1999. Prof. Allis, in addition to his direct contributions to the GEC, made landmark contributions to the theory of electron and ion transport in low temperature plasmas. This session is being held in his honor. A brief overview of Prof. Allis' academic, technical and administrative accomplishments will be presented.

10:45

GW2 2 Resonance Radiation Transport in Low Pressure Discharges*

J. E. LAWLER, *U. of Wisconsin*

Resonance radiation trapping has a major affect on the power balance and ionization balance of low pressure discharges in atomic gases including Hg-Ar and Na-Ne discharges for lighting applications. The introduction of electrodeless excitation has decreased gas pressures in some lighting products to the sub-Torr region where Partial Frequency Redistribution (PFR) is important. Models of glow discharges and certain types of diagnostic experiments require an accurate treatment of radiation trapping with PFR. The basics of resonance radiation trapping will be reviewed in this presentation. In a recent paper we reported an analytic formula for the fundamental mode decay rate which included the effect of PFR with a lineshape dominated by a combination of radiative, Doppler, and resonance collisional broadening¹. This analytic formula was developed, and its accuracy verified over a vast region of parameter space, using highly realistic Monte Carlo simulations. Extension of this formula to include foreign gas broadening will be described². Recent experimental results³ on the 185 nm resonance of Hg using multi-step laser excitation in a cell, and a comparison of these results to earlier work by Post et al.⁴ using a discharge afterglow, will be described. Highly realistic Monte Carlo simulations including the hyperfine and isotopic structure of the 185 nm line will be presented.

*Supported by OSRAM-Sylvania Inc. and the Electric Power Research Institute

¹J. E. Lawler & J. J. Curry, *J. of Physics D: Applied Physics* 31, 3235-3242 (1998).

²J. E. Lawler, J. J. Curry, & G. G. Lister, to be submitted.

³K. L. Menningen, J. J. Curry, & J. E. Lawler, to be submitted.

⁴H. A. Post, P. van de Weijer, & R. M. M. Cremers, *Phys. Rev.* 33, 2017 (1986).

11:00

GW2 3 Recent Developments in Modeling and Diagnostics of Fluorescent Lamp

GRAEME LISTER, *OSRAM SYLVANIA INC.*

Since the early 1960's, numerical models have been successful in reproducing experimental measurements of discharge parameters (electric field, electron density, radiation efficiency etc.) in conventional fluorescent lamps. These lamps operate with a few micron of mercury vapor in a few torr of buffer gas (usually argon) in a discharge column of 1-2 cm radius, with typical current densities 20-100 mAcm⁽⁻²⁾. Recent developments in the lighting industry have been towards "highly loaded" lamps, with current densities far in excess of these values. Examples are sub-miniature lamps, with discharge radii of order 2 mm and "electrodeless" lamps, in which the absence of electrodes permits standard size lamps to operate at much higher discharge currents. Numerical models have been less succesful in describing these discharges. Since radiation accounts for 60-80% of the power balance, it is natural to question the role of radiation transport in determining the discharge parameters. Recent experimental and numerical work¹ has re-examined this issue, particularly with respect to UV radiation. Further, the cross sections of a number of important electron impact excitation and chemi-ionization processes are poorly known. Finally, most models assume that the electron energy distribution function is "local" and Maxwellian for energies below the first excited state of mercury, with various approximations used regarding the depletion of the high energy tail. This paper will discuss these issues and current activities to improve the quality of data and the theoretical basis for these models.

¹J.E. Lawler, invited paper, this conference

SESSION HW1: BUSINESS MEETING

Wednesday morning, 6 October 1999; York Room Sheraton Waterside Hotel at 11:30
Gerry Hays, Sandia National Laboratory, presiding

**SESSION IWPI1: POSTER SESSION:
TRANSPORT EFFECTS**

Wednesday afternoon, 6 October 1999
Poplar Room Sheraton Waterside Hotel at 13:30

IWPI 1 Effect of Electron Energy Distribution Function on Oxygen Discharges

HAN-MING WU, *Novellus System, Inc.*
GABRIEL FONT, *Novellus Systems, Inc.* A numerical study is conducted to explore the effects of the electron energy distribution function (EEDF) on plasma chemical reactions. In the simulation, the EEDF is assumed to be either a Maxwell-Boltzmann or Druyvesteyn type distribution. The reaction rates, such as ionization, dissociation and attachment rates are all calculated through integration of the EEDF. The simulation results show that the electro-negative species is overestimated for Maxwell-Boltzmann EEDF model. After macroscopic plasma parameters are obtained, some comparisons with experimental data are made.

IWPI 2 Electron Energy Distributions and Rate Coefficients in a N₂ Post-discharge Including Space-charge Field Effects

J. LOUREIRO, V. GUERRA, *CFP-IST, Lisbon Tech. Univ., Portugal*
P.A. SA, *DEEC-FEUP, Oporto Univ., Portugal* The electron energy distribution function (EEDF) in a N₂ microwave (2.45 GHz) post-discharge at low-pressures is obtained by solving the time-dependent Boltzmann equation with a term for electron losses by diffusion assuring the transition from ambipolar to free diffusion regimes. The EEDF at $t=0$ is calculated from the coupled solutions to the stationary Boltzmann equation and a system of rate-balance equations for the N₂(X ¹Σ_g⁺, v) levels, N₂ electronic states, N(⁴S) atoms and N₂⁺ and N₄⁺ ions. It is observed that whereas the high-energy tail of the EEDF is rapidly depopulated in the post-discharge, the electron density and the rate coefficients for some processes induced by electron impact with energy thresholds typically < 2 - 3 eV are practically unchanged up to $t \sim 3 \times 10^{-4}$ s, time at which the electron diffusion starts to deviate from ambipolar diffusion. The rate coefficient for electron stepwise excitation of N₂(B ³Π_g) from N₂(A ³Σ_u⁺) remains almost constant in this time-interval, while the rate coefficients for vibrational excitation can even increase due to a concentration of electrons in the low-energy part of the EEDF. The N₂(X, v) states continue to be strongly populated in the beginning of the afterglow not only as a result of the e - V processes but also due to the pumping up effect originated by V - V energy exchanges.

IWPI 3 Mobility of CF₃⁺ in CF₄ and CHF₂⁺ in CHF₃

E. BASURTO, J. DE URQUIJO, C. CISNEROS, I. ALVAREZ, *Centro de Ciencias Físicas, UNAM México.* * The mobilities of the above ions have been measured in their respective parent gas with a drift tube-double mass spectrometer apparatus. The density-reduced electric field strength, E/N, was varied over the combined range 300 - 700 × 10⁻¹⁷ Vcm². The density-reduced mobility, K₀, of CF₃⁺ in CF₄ shows a pronounced peak between 200 and 300 × 10⁻¹⁷ Vcm², followed by sudden decrease at higher E/N values. At low E/N, K₀ tends to a rather constant value of 0.92 cm² V⁻¹ s⁻¹. On the other hand, the reduced mobility of

CHF₂⁺ in CHF₃ remains essentially constant up to E/N = 120 × 10⁻¹⁷ Vcm², with K₀ = 0.52 cm² V⁻¹ s⁻¹, peaking at a value of E/N in the neighborhood of 340 × 10⁻¹⁷ Vcm². An Abundance study of other ions produced in the source revealed that these were the predominant species, and the only ones for which their mobility could be measured.

*Work supported by DGAPA, IN 113898, and by CONACyT.

IWPI 4 Drift Velocity of Electrons in Hot and Moist Air mixtures

DOUGLAS ABNER, *Air Force Research Laboratory, Wight-Patterson AFB, OH* The drift velocity of electrons in hot and moist air is presented. The apparatus consisted of a pulsed Townsend-type drift tube with an oil-free vacuum system and employed a temperature controller and heating system to regulate the temperature of the gas mixture and chamber to within 0.1 deg. C. over a range of ambient to 200 deg C. The drift tube is equipped with a movable anode allowing the anode-cathode separation to be varied from 0.8 to 7.4 cm. Water vapor concentration in the air mixture ranged from 0.7510.0. Temperature was varied from ambient to 150 deg C. E/N (electric field normalized to gas density) ranged from 1.0 to 16 Td (1 Td = 10⁻¹⁷ V-cm²). Comparisons of data collected at elevated temperature, data collected at ambient temperature, and Boltzmann transport equation calculations show the effects of enhanced rotational and vibrational populations on the drift velocity.

IWPI 5 A self consistent kinetic scheme for ions in complex geometry

W.N.G. HITCHON, *Center for Plasma Aided Manufacturing; Univeristy of Wisconsin Madison*
A.J. CHRISTLIEB, *Center for Plasma Aided Manufacturing; Univeristy of Wisconsin Madison* In this work a two dimensional self consistent kinetic simulation for ions was developed. The ion simulation is based on the Convected Scheme (CS) method. This CS simulation makes use of an irregular mesh to allow for the description of complex geometry and for the possibility of simultaneously resolving both the bulk and sheath regions of a discharge. The concept of 'trains of moving cells' (TMC) in combination with 'long lived moving cells' (LLMC) was developed to help reduce numerical diffusion in physical space. TMC and LLMC allow for the possible optimization of the phase space coordinates which would have otherwise resulted in significant numerical diffusion. Moving cells (MC) are easily mapped back onto an irregular fixed mesh through quick sorting and chopping algorithms. The sorting is done by use of a fine regular mesh, which the irregular mesh is mapped onto prior to the start of the simulation. The mapping of MC onto the fixed mesh is done using a chopping algorithm which uses the faces of the fixed elements to divide up the MC. MC are launched in contiguous sheets such that the corners of neighboring cells stay in contact for the entire life of the MC. This kinetic method was developed and run on low cost work stations. The method was determined to converge in a reasonable amount of time.

IWPI 6 Monte Carlo simulation of electron back diffusion in argon

M. RADMILOVIĆ, V. STOJANOVIĆ, Z.LJ. PETROVIĆ, *Institute of Physics, Belgrade, Yugoslavia.* * Monte Carlo simulation was applied to study the back-diffusion of electrons in argon at low and moderate values of E/N from 10Td to 10 kTd. Simula-

tions were performed for gaps of 1 cm and for pressures corresponding to the breakdown voltages taken from experimental Paschen curves. Effects of inelastic collisions, ionization, reflection of electrons and anisotropic scattering as well as anisotropic initial and reflected angular distributions of electrons were included. A complete and detailed set of electron scattering cross sections that describes well electron transport in argon was used. We found a very good agreement of the results of simulations with the experimental data for well defined initial conditions, and with several models available in the literature.¹ While effect of reflection may be large, for realistic values of reflection coefficient and for realistic secondary electron productions the effect may be neglected for the accuracy required in gas discharge modeling.

*Supported by MNTRS 01E03 project.

¹A.V. Phelps and Z.L.J. Petrović, *Plasma Sources Sci. Technol.* **8**, R21 (1999).

**SESSION IWP2: POSTER SESSION:
GAS PHASE CHEMISTRY
Wednesday afternoon, 6 October 1999
Poplar Room Sheraton Waterside Hotel at 13:30**

IWP2 7 Particle Nucleation in Acetylene RF Plasmas SVETO-SLAV STOYKOV, CHRISTOPH EGGS, UWE KORTSHAGEN, *Mechanical Engineering, University of Minnesota, MN 55455* The formation, growth and transport of sub-micron particles are critical issues in many plasma processes. The theory of gas phase nucleation of particles in plasmas is still in an early stage. It is commonly assumed that clustering in plasmas occurs through addition of growth species and formation of linear molecules. However, we believe that the formation of cyclic structures is an underlying theme of particle generation in plasmas. A chemical model describing the clustering kinetics in a low pressure acetylene RF discharge has been developed. The gas-phase chemistry includes neutral-neutral reactions and electron-induced H-abstraction. In addition, diffusion losses to the reactor walls are considered. The model predicts the time evolution of species concentrations and chemical reaction rates, and gives the preferred clustering pathways. Even at room temperature the amount of produced polycyclic aromatic hydrocarbons (PAH) in the gas-phase is considerable and strongly temperature dependent. Keeping the acetylene concentration constant, a balance between the species production by acetylene decomposition and diffusion losses is reached. The current chemical model will be extended by including negative ions, which have a long residence time in the plasma.

IWP2 8 On the Hydrocarbon Chemistry in H₂-Ar-O₂ Microwave Plasmas L. MECHOLD, J. RÖPCKE, D. LOFFHAGEN, *Institut für Niedertemperatur-Plasmaphysik, 17489 Greifswald, Germany* P.B. DAVIES, *Department of Chemistry, University of Cambridge, Cambridge CB2 1EW, U.K.* Low pressure, non-equilibrium, molecular plasmas are of great interest in the field of plasma processing and technology because of their high chemical reactivity. To extend the understanding of the main chemical processes in H₂-Ar-O₂ plasmas containing small amounts of methane or methanol, tuneable infrared diode laser absorption spectroscopy has been used. The experimental arrangement consists of a diode laser spectrometer and a planar microwave discharge reactor (P

=1.5 kW and p=1.5 mbar). The ground state concentrations of various species have been measured for different H₂/O₂ ratios. These include the methyl radical, related hydrocarbons, and small molecules containing oxygen. The degree of dissociation of methane or methanol was between 62 and 93%. Absolute concentrations of the methyl radical were between 10¹⁰ and 10¹¹ cm⁻³. For plasmas studied in the absence of oxygen the experimental results were compared with results obtained by model calculations of the plasma chemistry. The model takes into account 12 molecular species and 57 reactions, where improved rate coefficients for the relevant electron collision processes were used. Good agreement is found between measured and calculated concentrations.

IWP2 9 Chemical Nucleation of Silicon Hydride Particles in Silane Plasmas UPENDRA BHANDARKAR, STEVEN L. GIRSHICK, UWE KORTSHAGEN, *Mechanical Engineering, University of Minnesota, MN 55455* MARK T. SWIHART, *Chemical Engineering, University at Buffalo (SUNY)** Particles generated in plasmas can have "good" or "bad" properties. "Good" nanoparticles embedded in thin films can increase the efficiency of solar cells or show photo-luminescence. "Bad" particles can lead to fatal defects of electronic devices during manufacturing. The theory of gas phase nucleation of particles in plasmas is still in its infancy. We are currently developing a model which will describe the chemical nucleation of particles, their growth due to surface deposition and coagulation, and their transport. Here we describe progress made on the nucleation model. Nucleation is described as a sequence of reversible chemical reactions. The reaction mechanism currently comprises both neutral and anionic silicon hydride clusters with up to ten silicon atoms. A total of 340 species and about 2000 reactions is considered. A thermochemical database for these reactions has been developed using group additivity rules. Reaction rules for certain reaction classes were defined by extrapolation from known reaction rates. The clustering kinetics will be studied and the importance of neutral and anionic pathways will be discussed.

*Supported by the NSF under grant ECS 97-31568 and the Univ. of Minnesota Supercomputing Center

IWP2 10 Decomposition of Hydrogen Sulfide in a Dielectric-Barrier Discharge ULRICH KOGELSCHATZ, *ABB Corporate Research Ltd, Baden, Switzerland* ERIC KILLER, *ABB Corporate Research Ltd, Baden, Switzerland* BALDUR ELIASSON, *ABB Corporate Research Ltd, Baden, Switzerland* Hydrogen sulfide is not only an unwanted compound that has to be efficiently removed in many industrial processes but it is also an abundant source for potentially cheap hydrogen. Many natural gas reserves contain large amounts of hydrogen sulfide mixed with the natural gas. In the past plasma processing of H₂S has been extensively investigated in low-pressure microwave discharges. Some laboratory experiments have also been performed in dielectric-barrier discharges (DBDs). We report on complete decomposition of atmospheric pressure H₂S into hydrogen and solid sulfur in a small laboratory through-flow DBD reactor made of two coaxial cylindrical quartz tubes with external coaxial electrodes. The discharge is confined to an annular gap of 2 mm radial width and 110 mm length. It can be observed through a wire mesh electrode. In some of the experiments helium was used as a carrier gas. The concentrations of H₂ and H₂S were measured with a gas chromatograph equipped with a PorAPlot Q column and a molecular sieve column. The dielectric-barrier discharge was operated in the frequency range 20-25 kHz or in the range 180-215 kHz. The amount of hydrogen generated was related to the amount of energy put into the discharge.

IWP2 11 Thermal Gas Phase Electron Attachment Reactions of Sulfuryl- and Thionyl-halides at 300 K JANE M. VAN DOREN, *College of the Holy Cross* MATTHEW S. THOMPSON, *College of the Holy Cross* ELIZABETH M. MONACO, *College of the Holy Cross* MATTHEW F. WSZOLEK, *College of the Holy Cross* The reactions of the sulfuryl-halides SO_2Cl_2 , SO_2ClF , and SO_2F_2 , and thionyl-halides SOCl_2 and SOF_2 were studied in the gas phase under thermal conditions at 300K with a Flowing Afterglow Langmuir Probe with mass spectrometric detection. The chloride-containing species react efficiently with electrons while the fluoride analogues react relatively inefficiently. All of these species react with electrons through cleavage of the sulfur-halide bond. Non-dissociative attachment is also observed in the reaction with sulfuryl fluoride. In the reactions of both thionyl halides as well as that of sulfuryl chloride, the only observed product ion is the atomic halogen anion. In the reaction of sulfuryl fluoride, cleavage of the sulfur-fluorine bond leads to the formation of $\text{SO}_2\text{F}^- + \text{F}$. Both possible primary product anions are observed for the mixed sulfuryl halide (SO_2ClF), Cl^- and SO_2F^- . Efficient secondary ion-molecule reactions were also identified and their products were characterized.

**SESSION IWP3: POSTER SESSION:
ELECTRON-ATOM COLLISIONS**
Wednesday afternoon, 6 October 1999
Poplar Room Sheraton Waterside Hotel at 13:30

IWP3 12 Measurement of Electron-Impact Cross Sections using Trapped Rb atoms* M. L. KEELER, TODD A. ZIMMERMAN, JOHN B. BOFFARD, THAD WALKER, L. W., CHUN C. LIN, *University of Wisconsin-Madison* A magneto-optical trap (MOT) can act as a compact, high number density, source of low velocity atoms for use in electron-impact cross section work. The low initial velocity of the trapped atoms, allows the measurement of electron total scattering cross sections by determining the loss rate of recoiled atoms from the trap. Electron-impact ionization cross sections can also be measured in an analogous manner, since the resulting ions are also lost from the trap. When the trapping lasers are 'on', a substantial fraction of atoms in the trap are in the excited $5^2P_{3/2}$ level. This allows the trap to serve as a source for measurement of excitation and ionization measurements from the laser excited $5^2P_{3/2}$ level. Sample results from these various measurements will be presented.

*This work supported by the National Science Foundation and the Air Force Office of Scientific Research.

IWP3 13 Electron Excitation out of the Metastable Levels of Neon* JOHN B. BOFFARD, M. L. KEELER, L. W. ANDERSON, CHUN C. LIN, *University of Wisconsin-Madison* The $2p^53s$ configuration of neon has two metastable levels the 3P_0 ($1s_3$ in Paschen's notation) and 3P_2 ($1s_5$) levels. Due to low energy threshold for excitation of these long-lived levels, the low number density of metastable atoms can have a substantial effect on many plasma properties. We have measured cross sections for electron-impact excitation into the ten levels of the $2p^53p$ configuration. For the $J = 1, 2, 3$ levels, the cross sections for excitation from the metastable levels are two to three orders of magnitude larger than the corresponding excitation cross sections from

the ground state. For the two $J = 0$ levels, however, the metastable excitation cross sections are less than an order of magnitude larger.

*This work supported by the National Science Foundation and the Air Force Office of Scientific Research.

IWP3 14 Electron-impact excitation of Kr atoms* J. ETHAN CHILTON, CHUN C. LIN, *University of Wisconsin-Madison* Previous work in our lab has involved the study of electron impact excitation of the $2p$ (Paschen's notation) levels of Ne, Ar, and Xe, using the optical method. The Xe atom differs from Ar and Ne in that it is close to the $ij-1$ coupling scheme in which the $5p^5 2p_j$ core angular momentum j ($1/2$ or $3/2$) first couples with the orbital angular momentum l and then with the spin of the outer electron. For Xe, the ten $2p$ levels ($5p^56p$) separate into an upper group of four levels and a lower group of six, corresponding to the $j = 1/2$ and $j = 3/2$ cores, respectively. The lower group has much larger cross sections than the upper group. Such two-group patterns are not found in the $2p$ cross sections for Ar and Ne. We now report preliminary measurements of Kr, whose excited level structure more closely resembles Xe. Most of the $2p \rightarrow 1s$ transitions lie in the visible region (0.5 to $0.9 \mu\text{m}$), easily accessible with a monochromator/PMT apparatus. The remaining $2p \rightarrow 1s$ transitions as well as the cascade into the $2p$ manifold, however, lie in the infrared region ($0.9 - 2.6 \mu\text{m}$), and are measured with our Fourier-transform spectrometer.

*Supported by the United States Air Force Office of Scientific Research.

IWP3 15 Electron Excitation of Argon: $4s'[1/2]_1$, $4p[1/2]_1$, and $4p'[1/2]_0$ D. V. FILIPOVIC, V. PEJCEV, B. MARINKOVIĆ, *Institute of Physics, P. O. Box 57, 11001 Belgrade, YU* L. VUSKOVIĆ, *Old Dominion U., Norfolk, VA* A broad interest in low-energy electron collisions with argon has recently led to very sophisticated calculations.^{1,2,3} The agreement between theoretical results and the only existing full set of experimentally obtained absolute differential cross sections⁴ is not satisfactory. We have performed a set of experiments to resolve existing discrepancies between available data. At the conference we will present absolute differential cross sections for argon excited in $4s'[1/2]_1$, $4p[1/2]_1$, and $4p'[1/2]_0$ states by electron collision. The incident electron energies were in the range of 16 to 80 eV and overall energy resolution was 40 meV. The angular range covered in our experiments was 5° to 150° . Data were extrapolated to 0° and to 180° and numerically integrated to yield integral, momentum transfer, and viscosity cross sections.

¹D. H. Madison, C. M. Maloney, and J. B. Wang, *J. Phys. B* **31**, 873 (1998).

²S. Kaur, R. Srivastava, R. P. McEachran, and A. Stauffer, *J. Phys. B* **31**, 4833 (1998).

³V. Zeman, K. Bartschat, C. Noren, and J. W. McConkey, *Phys. Rev. A* **58**, 1275 (1998).

⁴A. Chutjian and D. C. Cartwright, *Phys. Rev. A* **23**, 2178 (1981).

IWP3 16 Electron Impact Excitation of Krypton X. GUO, *Dept of Physics, California State University, Fullerton, CA* G. MIKAE-LIAN, *Dept of Physics, California State University, Fullerton, CA* D.F. MATHEWS, *Dept of Physics, California State University, Fullerton, CA* M.A. KHAKOO, *Dept of Physics, California State University, Fullerton, CA* A. CROWE, *Dept of Physics, University of Newcastle, Newcastle, UK* V. ZEMAN, *Maths Department, University of Nottingham, Nottingham, UK* K. BARTSCHAT, *Dept Of Physics and Astronomy, Drake University, Des Moines, IA* C. J. FONTES, *Applied Theoretical and Experimental Computational Physics Division, Los Alamos National Laboratory, Los*

Alamos, NM I. KANIK, *Jet Propulsion Laboratory, Caltech, Pasadena, CA* S. TRAJMAR, *Jet Propulsion Laboratory, Caltech, Pasadena, CA* We present new differential cross section (DCS) measurements of the electron impact excitation of ground-state krypton at 20.0eV, 15.0eV, 13.5eV and 12.0eV incident electron energies, to the first four excited electron configurations. We also present calculations of these DCSs using the Unitarized First-Order Many-Body Theory and a 31-state R-Matrix method. Comparisons with existing measurements and theories will also be made.

IWP3 17 Balmer- α Excitation and Polarization in e-H Collisions W KEDZIERSKI, *University of Windsor, Ontario, Canada N9B 3P4* J W McCONKEY, *University of Windsor, Ontario, Canada N9B 3P4* We have used an apparatus in which electron and atomic hydrogen beams intersect at right angles, to study the excitation and polarization of the resultant Balmer- α radiation. A special microwave source is operated in a pulsed mode and the detection system is gated on when the discharge is off thus eliminating problems arising from background light from the discharge. Particular attention is paid to the low energy region below the threshold energy for dissociative excitation of H₂. Here Balmer- α can only be excited by electron impact on H. At higher energies corrections are applied for the background contribution from H₂ in the interaction region. We compare our polarization data with recent calculations. Research supported by the Natural Sciences and Engineering Research Council of Canada.

IWP3 18 Calculated Cross Sections for the Electron-Impact Ionization of Metastable Atoms H. DEUTSCH, *Univ. Greifswald, Germany* K. BECKER, *Stevens Institute of Technology, Hoboken, USA* S. MATT, T.D. MAERK, *Univ. Innsbruck, Austria* We used the semi-classical Deutsch-Maerk (DM) formalism to calculate absolute cross sections for the electron-impact ionization of atoms such as the meta-stable rare gas atoms Ne, Ar, Kr, and Xe and metastable Hg and Cd atoms from threshold to 200 eV. Systematic trends in the calculated data are discussed and a comparison is made with available experimental cross sections and with other calculated cross sections. Specifically, our calculation allows us to determine separately the contributions to the ionization cross section arising from the removal of the single excited electron in the outermost shell and the removal of one of the lower-lying innershell electrons. *Work supported by OEAWEURATOM Assoc., FWF, OENB, BMWV, and the US DOE.

IWP3 19 Dielectronic recombination rate coefficients to excited states of He from He⁺ J. G. WANG, T. KATO, I. MURAKAMI, *National Institute for Fusion Science, Japan* A Simplified Relativistic Configuration Interaction (SRCI) method is used to calculate the dielectronic recombination rate coefficients to the excited states of He from He⁺. In this method, the infinite resonant doubly excited states involving high Rydberg states are treated conveniently in a unified manner by interpolation. The dielectronic recombination processes for $\Delta N = 1$ and $\Delta N = 2$ transitions are included in our calculations, and the cross sections are in agreements with the experimental measurements. The rate coefficients to the excited states are fitted to an analytical formula and the n-dependences of the fitting parameters are discussed.

IWP3 20 Normalization of Electron Impact Ionization Differential Cross Sections.* ZINEB FELFLI, *CTSPS/Clark Atlanta University* NINA AVDONINA, *U. of Pittsburgh* ALFRED MSEZANE, *CTSPS/Clark Atlanta University* In electron-atom scattering, absolute differential cross sections (DCSs) are difficult to obtain from relative measurements [1]. In the present work, a new

normalization procedure is proposed that brings relative experimental ionization scattering data on an absolute scale. The theoretical absolute noermalization scale is found beyond the First Born Approximation [2] and avoids entirely the non-physical region. This is achieved by simultaneously increasing the incident energy and decreasing the momentum transfer. The method is general and is not restricted to electron impact ionization transitions but can be applied to electron impact excitation as well, over a wide range of scattering angles and electron impact energies. It can also be readily adapted, with little modification, for application to optically forbidden transitions. [1]T. Ester and J. Kessler, *J. Phys. B* 27 4295 (1994) [2] A. Saenz, W. Weyrich and P. Froelich, *J. Phys. B* 29, 97 (1996)

*Work at CTSPS supported by NSF and DoE Division of Chemical Sciences, Office of Basic Energy Sciences, Office of Energy Research.

IWP3 21 Low-lying resonances in Rb⁻, Cs⁻, and Fr⁻* U. THUMM, C. BAHRIM, *J.R. Macdonald Laboratory, Kansas State University* I.I. FABRIKANT, *Department of Physics and Astronomy, University of Nebraska, Lincoln* Based on the Dirac R-matrix method¹, new electron scattering calculations in the energy range up to 2.8 eV for Rb, Cs, and Fr targets are reported. The low-lying ³P^o, ³P^e, and ³F^o shape resonances and the ¹P^o window resonance (located below the first excitation threshold) are identified in the partial and converged total cross sections. Our results suggest that none of the Rb⁻, Cs⁻, and Fr⁻ negative ions has an excited bound state and are in excellent agreement with both scattering² and photodetachment³ experiments. We also propose a new value for the electron affinity of Fr, provide the scattering length for electronic collisions with Rb, Cs, and Fr, and discuss the nuclear charge-dependence of relativistic effects in the resonance profiles. For collision energies below 0.1 eV, we compare our relativistic quantum calculations with semi-empirical results based on the modified effective range potential⁴.

*Supported by the Office of Fusion Energy Sciences, Office of Energy Research, U.S. DOE.

¹U. Thumm and D.W. Norcross *Phys.Rev.* **A45**, 6349, 1992

²W. Gerhenn and E. Reichert *J.Phys.B: At.Mol.Phys.* **10**, 3105, 1977; A.R. Johnson and P.D. Burrow *J.Phys.B: At.Mol.Phys.* **15**, L745, 1982.

³M. Scheer *et al.* *Phys.Rev.Lett.* **80**, 684, 1998.

⁴I.I. Fabrikant *Comments At.Mol.Phys.* **32**, No.5, 267, 1996.

IWP3 22 An enhanced database of atomic data for numerical simulations of plasma discharges.* YU. SOSOV, J.M. TRUXON, D. HOJNACKI, C.E. THEODOSIOU, *University of Toledo* W. WILLIAMSON, JR., *Embry-Riddle Aeronautical University* As part of our simulations of Plasma Display Panel pixel discharges, we have undertaken the task of a systematic analysis and consequent enhancement of the available databases of the relevant and necessary atomic data: electron impact cross sections for ground and excited initial states, lifetimes, transition rates and branching ratios, ion-atom and atom-atom cross sections, etc. Our objective is to create a relatively complete set of data by (i) evaluating the available experimental and theoretical data, (ii) performing calculations to obtain unavailable data, and (iii) producing a set of "recommended" values available to the broader plasma community. We will present the status of our work with examples from the database and the progress towards "filling all the gaps" in the needed information.

*Work supported by NSF, Grant ECS-9896103

IWP3 23 Electron excitation coefficients in xenon A. STRINIĆ, G. MALOVIĆ, J. BOŽIN, Z.LJ. PETROVIĆ, *Institute of Physics, Belgrade, Yugoslavia*. * We have performed measurements of excitation coefficients for electron swarms in xenon for the range of E/N from 90 Td to 10 kTd. The measurements were performed for $2p_1, 2p_2, 2p_3, 2p_4, 2p_5, 2p_6, 3p_5, 3p_6, 3p_7, 3p_8,$ and $3p_{10}$ levels of neutral xenon and for $6p^4D^0$ and $6p^4P^0$ of xenon ion. The results were obtained in self-sustained low current diffuse discharge for currents of up to $2 \mu A$ and pressures ranging from 0.09 Torr to 6 Torr. Available excited state quenching data were used to take into account the quenching of neutral atoms while quenching was neglected for ionic lines. Spatial emission profiles obtained up to 10 kTd showed no indication of significant heavy particle excitation.

*Supported by MNTRS 01E03 project.

**SESSION IWP4: POSTER SESSION:
GLOWS II**

Wednesday afternoon, 6 October 1999
Poplar Room Sheraton Waterside Hotel at 13:30

IWP4 24 1D Simulations of Series Resonant Discharges with Asymmetric Electrodes* H.B. SMITH, *UC Berkeley* C.K. BIRD-SALL, *UC Berkeley* The series resonance frequency is a natural resonance, on the order of but less than the plasma frequency, which occurs in bounded plasmas. When the discharge is driven at the series resonance frequency the plasma impedance approaches a purely resistive state, allowing the discharge to be sustained at voltages of only a few times the electron temperature. This work uses 1D Particle-in-cell simulations with concentric cylindrical and spherical electrodes to study series resonant discharges in asymmetric systems. We determine scaling laws for the resonant frequency as a function of electron temperature, density and electrode radii, and compare the simulation results with theoretical calculations. Differences between cylindrical, spherical and planar systems are discussed. Choosing an appropriate driving frequency, voltage and initial plasma density, we show how the discharge "locks on" to the resonant mode to produce a self-sustained discharge which is very different from a traditional rf-driven system. The transition is marked by a change from an almost purely capacitive discharge impedance, to an impedance with a substantial resistive component.

*Support is acknowledged from DOE contract DE-FG03-97ER54446, and ONR contract N00014-97-1-0241.

IWP4 25 Massively Parallel, Atmospheric-Pressure Microdischarges* T. ISLAM, N.J. IANNO, P.F. WILLIAMS, *Department of Electrical Engineering, University of Nebraska-Lincoln* Several workers have reported the production of glow-like discharges in near-atmospheric pressure gases by constricting the discharge to one or more small diameter channels. Schoenbach et al. and Frame et al. use one or more small diameter holes in the cathode material to form "microhollow-cathode" discharges, whereas Kunhardt forces the discharge to pass through a thin,

insulating disk with numerous small-diameter holes. We have used conventional plasma-processing techniques (TCP reactor, CF_4 feedgas) to etch a dense array of $10 \mu m$ diameter holes in a $100 \mu m$ thick silicon wafer. In this paper we discuss our results.

*Work supported by AFOSR F49620-98-0454

IWP4 26 Optical Emission Spectroscopy of the Laser Ablation Plume Controlled by RF Plasma* YOSHIYUKI SUDA, TAKUMA NISHIMURA, MANABU MIZUNO, MARIA ANTOANETA BRATESCU, YOSUKE SAKAI, *Hokkaido University, Japan* Recently, film deposition has been investigated using laser ablation methods which have a lot of advantages. For the purpose of control of the laser ablation plume, we introduced a radio frequency (RF) plasma. In this report we present position resolved optical emission spectra of the plume observed by an OMA (optical multichannel analyzer). The plume current is also measured. The RF plasma is generated in a helical coil installed between the substrate and the target. An ArF excimer laser (wavelength 193 nm, pulse duration time 20 ns) is used as a light source, and the target material is sintered carbon graphite. The laser fluence on the target surface is changed in a range from 1.2 to $6.4 J/cm^2$. Ar gas is introduced to sustain the RF plasma. When the plume goes through the RF plasma, interaction of the plume with the plasma is expected. The possibility of control of the plume behavior is discussed.

*Work in part supported by Grant-in-Aid 11750245 of The Ministry of Education, Science, Sports and Culture, Japan.

IWP4 27 Laser-Induced Vibrational Excitation of Molecules as a Tool of Ionization Enhancement in Air Plasmas SERGEY O. MACHERET, RICHARD B. MILES, *Dept. of Mechanical and Aerospace Engineering, Princeton University* The paper analyzes mechanisms of increasing ionization rate in air plasmas by vibrationally exciting nitrogen and oxygen. The analysis is focused on mechanisms that do not require high levels of vibrational excitation. One such mechanism is detachment of electrons from molecular negative ions of oxygen, requiring vibrational level $v=4$ to be populated. Another mechanism is increasing Frank-Condon factors for electron-impact excitation and ionization; highly excited triplet metastable state of nitrogen can be produced a few orders of magnitude faster with this mechanism. Perhaps the most important mechanism involves superelastic collisions of electrons with vibrationally excited molecules, rising the high-energy tail of electron energy distribution function, and enhancing ionization and dissociation. Theoretical estimates give vibrational temperatures and excitation rates needed to substantially enhance ionization in air. Scenarios involving a weakly ionized background plasmas sustained by a weak d.c. or RF field, and an IR laser excitation of vibrational states, are given as examples.

IWP4 28 Simple Model of a Capacitive Discharge with a Bi-Maxwellian Electron Distribution F.A. HAAS, *Oxford Research Unit, The Open University* N.ST.J. BRAITHWAITE, *Oxford Research Unit, The Open University* Particle and energy conservation equations are used to establish a simple model of a capacitive discharge with a bi-Maxwellian distribution. Denoting the properties of the hot and cold distributions by T_h, n_h and T_c, n_c , and given $T_h \gg T_c$ and $n_c \gg n_h$, then the Bohm velocity is essentially due to T_c . The cold electrons satisfy the Boltzmann distribution and follow the Godyak and Maximov⁽¹⁾ prescription for the ratio of electron density at the boundary to the centre. Neglecting ohmic

heating the hot electrons are stochastically heated and lose energy to the electrodes. T_c is maintained by Coulomb collisions with the hot electrons, and energy loss to the sheaths. The latter is not to the electrodes but through stochastic heating of cold electrons which join the hot distribution. Together with particle conservation, there are three equations for T_h , T_c , n_h . Prescribing n_c and comparing with data from a 100 mTorr argon plasma, T_h and n_h are in good agreement, while T_c agrees to considerably better than a factor of two. (1) Godyak, V.A., Soviet Radio Frequency Discharge Research, Delphic Associates, Falls Church, VA (1986).

IWP4 29 Self-Consistent Simulation of Transient Argon Glow Discharges ZOLTÁN DONKÓ, *Research Institute for Solid State Physics and Optics, Budapest, Hungary** Recent experiments¹ on the transition between low-current diffuse (Townsend) discharge and moderately high-current diffuse (abnormal glow) discharge are simulated using a self-consistent hybrid model. In the model the Monte Carlo treatment of fast electrons is combined with the fluid description of slow electrons and positive ions. The fluid equations are solved in the model together with the Poisson equation and the equations for the external electrical circuit. The model provides the spatio-temporal variations of the electric field, the fluxes and the density of charged particles, and makes it possible to trace the formation and decay of the cathode sheath in the transition period between the two (steady-state) discharge modes.

*Supported by the Hungarian Science Foundation OKTA, Grant # T-25989

¹B. M. Jelenković and A. V. Phelps, *J. Appl. Phys.* **85**, 7089 (1999).

IWP4 30 VUV Spectroscopy of High-Pressure Discharge Plasmas P. KURUNCZI, K. BECKER, *iStevens Institute of Technology, Hoboken, USA* Hollow cathode discharges with hole sizes in the range of about 100 micro-meters (microhollow cathode discharges, MHCDs) are simple, compact, and convenient sources of high-pressure (up to atmospheric pressure) discharge plasmas. Among other things, MHCDs can be used as efficient excimer light sources or sources of other vacuum ultraviolet radiation such as rare gas ion emissions, e.g. the NeII emissions at 46 nm or the HeII emission at 30.4 nm. We have started a comprehensive series of spectroscopic studies of vacuum ultraviolet emissions from MHCDs operated in Ne, He, and N₂. These studies are aimed at obtaining a rudimentary understanding of the electron, ion, and neutral temperatures in MHCDs under various operating conditions. Specifically, in Ne we want to quantify the conditions under which NeII emissions are favored vs. the conditions under which Ne2 excimer emissions are favored. Our experimental set-up uses a calibrated VUV monochromator/detection system with the MHCD mounted directly on the entrance slit of the monochromator. *Work supported by the NSF.

IWP4 31 Finite element modeling of multipolar buckets with permanent magnets MIRKO VUKOVIC, *Tokyo Electron Arizona, Inc.* The efficiency of the multipolar bucket is determined largely by the trapping of energetic electrons in the magnetic field. The calculation of fields generated by permanent magnets is not trivial, as the field strength depends on the energy stored in the magnetic field and the demagnetization curve of the permanent magnets. The magnetic field properties of multipolar buckets are

modeled for a variety of magnet dimensions and number of columns using a finite element modeling software package. The energy of the magnetic field is combined with demagnetization curves for permanent magnets to predict the magnetic field strength. Field strength, decay length, and leak width are determined for a variety of chamber sizes, magnet dimensions and strengths. These parameters are also computed for experiments on optimization of multipolar bucket plasma confinement¹. Criteria for optimizing the magnetic bucket configuration are proposed.

¹Leung, K. N. et al., *Phys.Lett.* 51A(1975)490

IWP4 32 Breakdown Simulation of Microwave Pulsed Discharges in Hydrogen A. LACOSTE, *LEMD, Univ. Joseph Fourier (France)* L.L. ALVES, *CFP, IST (Portugal)* G. GOUSSET, *LPGP, Univ. Paris-Sud (France)* C.M. FERREIRA, *CFP, IST (Portugal)* In this work we simulate the breakdown of high-power, short-pulse microwave discharges in hydrogen, produced when an electric field of the form $\vec{E}(\vec{r}, t) = \vec{E}_0(\vec{r})(1 - e^{-t/\tau})\sin(\omega t)$ is applied to a cylindrical resonant cavity of 25.71 cm in diameter. Typical discharge operating conditions correspond to input powers between 1-15 kW, gas pressures in the range 0.5-40 Torr, tube radius of 0.8 cm, oscillating frequency $\omega/2\pi = 1.1$ GHz, rising time $\tau \approx 2$ μ s, pulse width $\Delta t \approx 10$ μ s, and time gap between pulses of 10 ms. Under these conditions, discharge breakdown occurs before the electric field reaches its maximum value E_0 . The simulation uses a Monte-Carlo model to calculate the breakdown time, t_b , and field, E_b , for different field slopes $E_0/\tau \approx 10^{-1} - 10^3$ Vcm⁻¹ns⁻¹. A breakdown criterium based on the electron energy balance ($\epsilon_{\text{gain}} > \epsilon_{\text{loss}}$) has been adopted instead of the classical particle balance criterium ($\nu_{\text{gain}} > \nu_{\text{loss}}$)¹. The adopted criterium yields excellent agreement between calculated and measured values of t_b and E_b , while the classical one is well satisfied only at pressures below 0.5 Torr.

¹A.D. MacDonald and S.C. Brown, *Phys. Rev.* **76**, 1634 (1949)

IWP4 33 Time-resolved measurements of ion energy distributions and optical emissions in pulsed rf discharges YICHENG WANG, *NIST* ERIC BENCK, *NIST* MARTIN MISAKIAN, *NIST* MANABU EDAMURA, *NIST* JAMES OLTHOFF, *NIST* In pulse-modulated inductively coupled plasmas generated in CF₄:Ar and O₂:Ar mixtures, a transition between a capacitive coupling mode (E mode) and an inductive coupling mode (H mode) was observed. The E→H mode transition observed for a pulsed plasma in a 50%CF₄:50%Ar volume mixture with the peak rf power of 300W at 13.56 MHz and the modulation frequency at 500 Hz with a duty cycle of 95% occurs repetitively 0.75 ms after each rf pulse is applied. This long delay in the mode transition allows us to perform not only time-resolved measurements of optical emission and electrical characteristics but also time-resolved measurements of ion energy distributions at the grounded electrode. Relative abundance of ionic species were observed to vary dramatically with time and their implications are discussed.

IWP4 34 Shock Propagation through a Thomson Discharge A. WHITE, W.C. LEE, I.V. ADAMOVICH, V. V. SUBRAMANIAM, W. LEMPERT, J.W. RICH, *The Ohio State University, Columbus, OH 43210* The characteristics of shock propagation through and downstream of an externally sustained) optically pumped Thomson discharge are explored in this paper. Such discharges have been shown earlier to produce ionization by an associative process involving pooling of energy among vibrationally excited CO molecules immersed in an Argon bath. The vibra-

tionally excited CO is produced by optical pumping using irradiation from a CO laser, and the shock is generated using a capacitive discharge. Additionally, current (primarily due to electrons) may be drawn from the optically pumped discharge using a pair of electrodes placed in the transverse direction. Passage of the shock waves through the Thomson discharge and in the discharge afterglow is detected using photo-acoustic deflection. Measurements of shock speed and recovery of the photo-acoustic deflection signal are performed both in the presence of current flow as well as in its absence, and raise the possibility of altering shock structure and shock propagation characteristics in the presence of ionization and externally applied electric fields. This possibility of mitigating the strength of propagating shocks produced by detonations and explosions by application of electric fields, was suggested by J. J. Thomson as early as 1910, but is yet to be unequivocally demonstrated experimentally.

**SESSION IWP5: POSTER SESSION:
LASER MEDIA AND THERMAL PLASMAS
Wednesday afternoon, 6 October 1999
Poplar Room Sheraton Waterside Hotel at 13:30**

IWP5 35 Properties of Laser Produced TMAE Plasma Admixed with Air Constituents, Nitrogen and Noble Gases*
GUOWEN DING, JOHN SCHARER, KURT KELLY, *Electrical and Computer Engineering Department, University of Wisconsin, Madison 53706* A high initial density ($> 10^{13} \text{ cm}^{-3}$) and a large volume (hundreds of cm^3) plasma is created by a 193 nm laser ionization of an organic molecule, tetrakis(dimethyl-amino)ethylene (TMAE). The properties of this plasma mixed with nitrogen and noble gases are studied. Fast probe measurements which include a detailed considerations of probe structure, probe surface cleaning, shielding, probe perturbation, frequency response, temporal and spatial resolutions, dummy probe corrections and noise analysis will be described. Electron densities obtained by this method are independent on the ion species mixture. A plasma emission diagnostic is used to estimate plasma densities for the higher admixture pressures. Electron density and temperature vs. time for various TMAE, nitrogen and noble gas pressures and laser power will be presented. The role of super-excited and metastable states in the decay process will also be discussed.

*Supported by Air Force Office of Scientific Research grant (F49620-97-1-0262) in cooperation with the Defense Department Research and Engineering Air Plasma Ramparts Multi-University Research Initiative.

IWP5 36 Mass Spectrometric Investigations of a Plasma Jet Chemical Vapor Deposition Reactor ALAN KULL, *Stanford University* MARK CAPPELLI, *Stanford University* Direct current plasma jets (arcjets) are plasma sources that produce a high velocity (5-10 km/sec) plasma stream (.20-.30 dissociation fraction, $n_e 10^{13} \text{ cm}^{-3}$). The plasma jet provides large convective fluxes of chemically reactive radical species that are stagnated on a substrate on which film deposition occurs. Films such as diamond, cubic boron nitride, aluminum nitride, and gallium nitride have been grown by this method. To determine the concentrations of the important gas phase species and thus elucidate the growth kinetics of the deposited films, molecular beam mass spectrometry is employed. A small amount of the plasma is sampled through a

hole in the substrate into a nearly collisionless environment provided by differential pumping. The sampled plasma is analyzed by a mass spectrometer to determine the constituency of the plasma and by an ion energy analyzer to determine the energy distribution of the ions present. Radical and stable species concentrations and ion energy distributions are presented for a range of reactor operating conditions involved in III-nitride film growth. The roles of different species in film growth mechanisms are compared.

IWP5 37 Localized Electronic Excitation Temperature Measurements in an Air Microwave Plasma Torch at Atmospheric Pressure* K.M. GREEN, G.J. FLORES III, P.P. WOSKOV, K. HADIDI, P. THOMAS, *MIT Plasma Science and Fusion Center* The Microwave Plasma Continuous Emissions Monitor, currently under development, uses atomic emission spectroscopy for trace metals pollution monitoring of stack exhaust. Operating at 2.45 GHz, the 1.5 kW magnetron sustains the plasma in a shorted WR-284 waveguide. Air flows through a 25.4 mm i.d. fused quartz tube traversing the waveguide. A pneumatic nebulizer introduces an iron nitrate solution into the axial gas flow. Radial profile measurements of atomic excitation temperature inside the waveguide have been obtained by Abel inversion of Fe I emission lines in the 367 nm to 377 nm range. An optical system with image magnification lenses and a fiber optic cable on a translation stage scans the radial intensity profile along 66 chords. Intensity and temperature profiles show peaked values on axis with a FWHM of 11 mm. An electronic excitation temperature of $6551 \text{ K} \pm 349 \text{ K}$ is measured with an axial flow of 12 l/min and a swirl flow of 10 l/min.

*Supported by the Mixed Waste Focus Area, Office of Science and Technology, U.S. DOE

**SESSION IWP6: POSTER SESSION
MAGNETICALLY-ENHANCED PLASMAS
Wednesday afternoon, 6 October 1999
Poplar Room Sheraton Waterside Hotel at 13:30**

IWP6 38 A TE_{01}° Mode Permanent Magnets ECR Discharge K.C. LEOU, *National Tsing Hua University* T.Y. LO, *National Tsing Hua University* T.L. LIN, *National Tsing Hua University* C.H. TSAI, *National Tsing Hua University* We report the results of experimental studies of an ECR plasma source which employs the TE_{01} circular waveguide mode and permanent magnets. The 2.45 GHz microwave power is sent into the plasma chamber through a Flower-Padel mode converter which transforms the wave from the TE_{10}^{\square} mode to the TE_{01}° mode. The converter design has been simulated by a finite element code, HFSS, and a conversion efficiency of 96% has been achieved. The magnetic field is provided by a permanent magnets structure formed by two ring shaped magnets, which results in a divergent profile of the magnetic fields. Plasma parameters such as density and electron temperature were obtained by Langmuir probe measurements. In addition, a CCD camera was also employed to image the plasma induced optical emission from the bottom of the chamber in order to quickly examine the azimuthal uniformity of the plasma. Initial results showed that at low power levels the plasma seems fairly uniform in the azimuth direction which basically reflects the characteristics of the TE_{01}° mode. However, various mode patterns

appeared for high power levels indicating the excitation for high order azimuthal mode in the circular waveguide. Efforts are being made to modify the structure of the TE_{01}^o to eliminate those unwanted cavity modes. Detailed experimental results will be presented.

IWP6 39 Electron Boltzmann Kinetic Equation Averaged over Fast Electron Bouncing and Pitch-Angle Scattering for Fast Modeling of Electron Cyclotron Resonance Discharge IGOR KAGANOVICH, *Department of Chemical Engineering, University of Houston, 4800 Calhoun Rd., Houston, TX 77204-4792* MARTIN MISINA, *Institute of Physics Academy of Sciences of the Czech Republic Na Slovance 2 182 21 Prague 8 Czech Republic* STANISLAV BEREZHNOI, *Physical Technical Department, St. Petersburg State Technical University, 195251, Russia* RENAAT GIJBELS, *Department of Chemistry, University of Antwerp, Universiteitsplein 1,B-2610 Wilrijk, Belgium* The electron distribution function (EDF) in an electron cyclotron resonance (ECR) discharge is far from Maxwellian. The self-consistent simulation of ECR discharges requires calculation of the EDF on every magnetic line for various ion density profiles. The straight-forward self-consistent simulation of ECR discharges using the Monte-Carlo technique for the EDF calculation is very computer-time expensive, since the electron and ion time scales are very different. An electron Boltzmann kinetic equation averaged over the fast electron bouncing and pitch-angle scattering was derived in order to develop an effective and operative tool for the fast modeling (FM) of low pressure ECR discharges. A new analytical solution for the EDF in a loss-cone was derived. To check the validity of the FM, a 1D (in co-ordinate) 2D (in velocity) Monte-Carlo simulation code was developed. The validity of the fast modeling method is proved by comparison with the Monte-Carlo simulations. The complete system of equations is presented for FM. The results of the self-consistent simulation are discussed.

IWP6 40 Effects of antenna geometry on helicon plasma sources EARL SCIME, MATTHEW BALKEY, ROBERT BOIVIN, PAUL KEITER, JOHN KLINE, *Department of Physics, West Virginia University* Helicon plasma sources have been constructed with a variety of antenna geometries. The Nagoya III, double-saddle, and $m=1$ are the most common antenna designs. In the large volume helicon plasma source at West Virginia University, all three of these antenna geometries have been employed. We will present the results of investigations into the optimum antenna aspect ratio (length/radius) for coupling RF power to the plasma. Measurements of plasma density and ion temperature are used to quantify the antenna coupling efficiency. The $1/f$ dependence of the plasma density predicted by the helicon dispersion is found to exist only at moderate fill pressures, suggesting that at low pressure the discharge is under-fueled.

IWP6 41 Microwave Reflectometry Measurements of Mode Transitions in Helicon Plasmas ROBERT SPANGLER, ROBERT BOIVIN, MATTHEW BALKEY, EARL SCIME, *Department of Physics, West Virginia University* Considerable research effort has been devoted to developing probe techniques for measurements of electron temperatures and densities in rf plasmas. However, the densities ($n > 10E13 \text{ cm}^{-3}$) and electron temperatures ($T > 3 \text{ eV}$) found in steady-state helicon plasmas make probe measurements problematic, particularly in helium plasmas as they have significantly higher electron temperatures. We have designed and built a microwave density diagnostic for a steady-state helicon plasma. The cornerstone of the diagnostic is a 20 - 40

GHz variable frequency microwave source. The microwave horns located inside the vacuum chamber are configured so that the system operates in the far-field diffraction regime. The diagnostic can be operated in two different configurations: 1) Simple interferometry, where at a fixed microwave frequency the average electron density is obtained by measuring either the phase shift of the attenuation of the microwave beam; 2) Differential interferometry where the Fourier transform of the plasma phase shift response to a slightly non-linear frequency ramp yields the average density. The change in peak plasma density is reported for transitions into the helicon mode for both helium and argon plasmas. The transitions occur as a function of rf power, magnetic field, and rf frequency.

IWP6 42 Electron Temperature Measurement by a Helium Line Intensity Ratio Method in Helicon Plasmas R. F. BOIVIN, M. M. BALKEY, M. A. BLACKBURN, P. A. KEITER, J. L. KLINE, E. E. SCIME, R. SPANGLER, *West Virginia University, Morgantown, WV 26506* T_e measurements in helicon plasmas are not an easy task. The presence of intense RF fields complicates the interpretation of the Langmuir probe curves. A spectroscopy technique based on the relative intensities of He I lines is used to measure T_e in the HELIX plasmas. This non-intrusive diagnostic is based on the fact that the dependence on the electron energy of the excitation rate differs between singlet and triplet lines of the He atom. This method has been applied to measure T_e in many plasma conditions and, lately has been extended to high-density, fusion edge plasmas. The validity of this technique to measure T_e in RF plasmas has not yet been established. The wide range in density that can be generated by HELIX (10^{10} to 10^{13} cm^{-3}) makes it an ideal source to verify if this diagnostic can be used in such RF plasmas. At low density, this diagnostic is believed to be very reliable since the population of the emitting levels can be accurately estimated by assuming that all excitation originate from the ground state. At higher density, secondary processes become important and can seriously affect the validity of the diagnostic. We measured the excitation rate for many He lines and compared them to the excitation rate from ground state previously published. The validity density range for the diagnostic is presented together with the apparent excitation rate observed for the different transitions.

IWP6 43 Auburn Large-area Plasma Helicon Array CHRISTOPHER WATTS, *Auburn University* JEREMY HANNA, *Auburn University* Auburn University is constructing research facility for basic plasma studies incorporating a multi-helicon array for creating large-area high-density plasmas. The Auburn Large-area Plasma Helicon Array (ALPHA) consists of a 4m vacuum chamber with 13 magnetic field coils to create a maximum field of 0.2T on axis. The helicon array uses seven helical twist type helicon antenna surrounding quartz tubes of 10cm diameter, for a total diameter of about 30cm. We anticipate peak densities of order 10^{20} m^{-3} . Results from a single helicon source in a 2m facility will be presented, as well as initial results from ALPHA.

IWP6 44 Characteristics of DC Magnetron Sputtering Discharge Assisted by Microwave Plasma AKIRA YONESU, HIROKI TAKEMOTO, NAOKI NISHIMURA, SHOICHI SATO, YASUMASA YAMASHIRO, *Faculty of Engineering, Ryukyu University, Japan* We have developed a DC magnetron sputtering apparatus assisted by microwave plasma to achieve high sputter deposition rates at low gas pressures. Conventional configuration of the cylindrical multipolar magnetron was employed in this apparatus. But magnets placed in a cathode electrode (target) have higher magnetic flux density than that of the magnets used in the

conventional magnetron system, so that they provide resonant magnetic surface for electron cyclotron resonance (ECR) absorption of the microwave power. When the microwave is introduced into the chamber, ECR microwave plasma is produced around the electrode and utilized for DC magnetron sputtering. With the assistance of the microwave plasma, operation of the DC magnetron sputtering discharge has been achieved at pressures on the order of 10^{-4} Torr. Furthermore the target current is high, about 1.5A, at low gas pressure of 0.2mTorr. Also a jump was observed in the target voltage dependence of the target current at gas pressures below 1mTorr. This result suggests that the transition between the magnetron discharge mode and ECR microwave discharge mode occurred in the plasma.

**SESSION IWP7: POSTER SESSION:
PLASMA-SURFACE INTERACTIONS**
Wednesday afternoon, 6 October 1999
Poplar Room Sheraton Waterside Hotel at 13:30

IWP7 45 Interaction of Multiple Frequency Sources in Plasma

Sheaths S. RAUF, P. L. G. VENTZEK, *Motorola Inc.* Sheaths are crucial to the operation of many plasma materials-processing tools. Sheaths at all surfaces inside the reactor are coupled and, because of their inherent nonlinearity, multiple frequency sources can interact in sheaths. Plasma sources with multiple dc and rf sources (at different frequencies) are rapidly becoming prevalent in the microelectronics manufacturing industry and it is important to understand the behavior of intercoupled sheaths being excited at multiple frequencies. This paper investigates this issue, specifically in the context of electronegative discharges. The model used in this study includes the coupled set of continuity and momentum equations for all charged species in (collisionless) sheaths, Poisson's equation and equations describing the behavior of external electrical components. The plasma conditions at the sheath-presheath interface are obtained from a detailed plasma equipment simulation using the Hybrid Plasma Equipment Model (HPEM). It is found that dc sources significantly alter the sheath dynamics and low frequency sources generally have a greater influence on the sheath voltage. The effects of plasma conditions and source frequencies on the sheath dynamics are investigated in detail.

IWP7 46 Sheath Model for High-Density Plasmas at Arbitrary RF Bias Frequency

MARK SOBOLEWSKI, *NIST, Gaithersburg, MD 20899-8362* Particle dynamics in the narrow sheaths of high-density plasmas, especially in sheaths biased by radio-frequency (rf) voltages, are complicated and nonlinear. Models of such high-density, rf sheaths are needed to predict ion bombardment energies and discharge electrical characteristics. Here, we report results from a new sheath model designed to span the entire range of rf bias frequency in high-density, low-pressure discharges. Ions are treated using the hydrodynamic fluid equations, including all time-dependent terms. Electrons are treated using the "oscillating step sheath" formalism. The model equations are solved numerically. Current and voltage waveforms predicted by the model are in agreement with waveforms measured in a high-density plasma reactor. Predictions for the time-dependent sheath width obtained from the model are in agreement with time-

resolved optical emission measurements. Ion kinetic energy distributions predicted by the model will also be presented. In addition, the model provides intuitive insight into ion dynamics in the sheath and suggests new methods of plasma process monitoring and control.

IWP7 47 Diffusive Plasma with Negative Plasma Potentials*

LUTFI OKSUZ, *University of Wisconsin -Madison* NOAH HER-SHKOWITZ, *University of Wisconsin Madison* Negative plasma potentials were obtained in dc hot filament multi-dipole argon plasmas. Plasma properties were determined using emissive probes and Langmuir probes. It is argued that a fraction of the primary electrons emitted across the filament/plasma sheath lose energy by ionization and/or inelastic collisions and become trapped in the plasma. The plasma potential then becomes more negative to allow some of these trapped electrons to help balance the ion loss current. For sufficiently low bias voltage, the bulk plasma potential becomes negative with respect to the grounded wall. A grounded plate was mounted inside the plasma and a potential dip was found around the conductor, for both positive and negative bulk plasma potentials. Experiments which employed a second filament biased between ground and -15V achieved bulk plasma potentials as low as -15V. Ion losses were to the filament supports and to the chamber windows. Curiously, the potential profiles from the center of the plasma to the potential minimum are quite similar in shape indicating the diffusive nature of the plasma.

*Work supported by DOE grant no. DE-FG02-97ER54437

IWP7 48 Secondary electron energy spectra and current density levels emitted from rf biased plasma electrodes in He, Ar, H₂, and N₂ feedstock gases

D. M. SHAW, M. WATANABE, H. UCHIYAMA, G. J. COLLINS, *Dept. of Electrical Engineering, Colorado State University, Fort Collins, CO 80523* Ion-induced secondary electron energy spectra $I(E)$ are studied both experimentally and theoretically. The results are based on a radio frequency (rf) biased (13.56 MHz) electrically insulating (Al₂O₃) plasma electrode surface immersed in a separately powered inductively coupled plasma. Electrode rf bias voltages of 140, 285 and 425 V (peak to ground) are employed and the emitted $I(E)$ spectra are measured 14 cm from the rf biased electrode using a differentially pumped retarding potential analyzer. Plasma feedstock gases employed are H₂, N₂, Ar, and He in the pressure range of 1 to 20 mTorr. Although generally ignored in the literature, the total measured secondary electron current density j_e in a 10 mTorr Ar ICP with plasma electron density $n_e = 10^{12}$ cm⁻³ is $j_e = 2$ mA/cm², which is comparable to the ion current density from the ICP. Such $I(E)$ spectra may play roles in rf discharge mode changes and other phenomena. A crude collisionless rf Child-Langmuir sheath model is used to explain the experimentally measured electron energy spectra.

IWP7 49 Transport of particle sputtered from Si and SiO₂ in oxide etching in CCP

K. MAESHIGE, N. NAKANO, T. MAKABE, *Keio University at Yokohama, Japan* Spatiotemporal behavior of by-products sputtered from the active etching surface is one of the interesting issues under the recent trend of a high rate and large area plasma processing of semiconductor device fabrications. Nonvolatile neutral particles sputtered from the substrate will be the origin of an absorbed layer on the substrate as well as the particle growth in the plasma due to the non-negligible density. Design of the transport of neutral particles ejected with high energy from the substrate under the presence of a feed gas flow and an active plasma will be of importance. We have investigated the

particle production on Si and SiO₂ wafers and the transport in a self-consistent model of CCP, including background gas flow by using 2D-RCT/Boltzmann equation models. The plasma structure and the 2D ion velocity distribution are first computed as a function of external plasma parameters. We discuss the effect of reactor geometry and the wafer size in Ar CCP maintained at 13.56MHz and 100MHz with amplitude of 300V. Due to the difference of sputtering yield $Y(\epsilon)$ between Si and SiO₂, the spatial density of sputtered Si changes. The effect of ejected initial energy of particles on the spatial steady state distribution in the reactor is critically dependent on the dissipated power into CCP.

IWP7 50 Competitive Low Pressure Oxygen Plasma Interactions with Different Carbon-Carbon Double Bonds P. PATIÑO, A. SIFONTES, G. GAMBÚS, *Escuela de Química, Facultad de Ciencias, Universidad Central de Venezuela* Recently we have shown advances from reactions of O(³P) with both, 1 on-chain hydrocarbons and refinery residuum. The oxidation products of the process, a mixture of alcohols, epoxides and carbonyl compounds, might have potential properties as additives in formulating fuels. This work shows the results of the interactions of an oxygen plasma with double bonds, both olefin and aromatic, in the same compound. The reactions have been carried out by making the plasma, created by a high voltage glow discharge, reach the low vapor pressure surface of liquid 4-phenyl-1-butene. This (3 mL) was cooled down to -45 °C in a glass reactor, applied power was 24 W, at an oxygen pressure of 20 Pa. Products were analyzed by IR, NMR and mass spectroscopies. Conversions were studied as a function of the reaction time, this ranging from 5 to 120 minutes. At short times the O(³P) atoms produced in the discharge only reacted with the alkene fraction of the hydrocarbon, 4-phenyl-1,2-epoxibutane (52%) and 4-phenylbutanal (48%) being the products. Reactions on the benzene ring were observed from about 30 minutes on, the corresponding phenols having been produced at ratios *ortho:para:meta* :: 4:1:0.7. At 120 minutes, the olefin have been completely oxidized and a low fraction of the non-equivalent two methylene groups have reacted to produce alcohols and ketones.

IWP7 51 Plasma Chemistry of C₃F₆ and C₅F₈ Gases as PFC Alternatives in an ICP Source for SiO₂ Etching K. TACHIBANA, H. MOTOMURA, *Kyoto University* S. IMAI, *Matsushita Electronics Corp.* Unsaturated fluorocarbon gases such as C₃F₆ and C₅F₈ are potential candidates of PFC (perfluorocompound) alternatives for diminishing the global warming effect. We have studied gas-phase and surface reactions in plasmas of these gases as well as etching characteristics in comparison with the data taken in C₂F₆ and C₄F₈ plasmas. In the diagnostics of gas-phase species, polymerized species, which contain carbon atoms more than the numbers in parent molecules, are detected by electron attachment mass spectrometry (EAMS), and this tendency becomes the largest in C₅F₈. The polymer deposition rates measured by *in situ* FT-IR ellipsometry are in the following order: C₅F₈ > C₄F₈ > C₃F₆ > C₂F₆. This suggests that polymerized species are involved largely in the deposition. This result is consistent with the higher etching selectivity of SiO₂ to photo-resist attained in C₃F₆. Performance in the contact hole etching, however, is not deteriorated by using C₅F₈ if the flow rate is controlled appropriately.

IWP7 52 Atomic Oxygen Density Measurements in a Low Pressure Textile Processing Plasma* S. GOMEZ, *The Queen's University of Belfast* P.G. STEEN, W.G. GRAHAM, *The Queen's University of Belfast* There is increasing interest in plasma processing of textile materials. Here the effect of textile materials on low pressure oxygen plasmas has been investigated. In particular laser induced fluorescence (LIF) measurements of the atomic oxygen density with and without textile samples are presented. Polypropylene and polyester samples were placed on the lower electrode of an inductively coupled Gaseous Electronic Conference (GEC) reactor. This had to be operated at low power and hence in the capacitive mode to avoid toasting the material. Operation with a bare stainless steel electrode and one loaded with the sample materials is contrasted by comparing spatially resolved LIF measurements of atomic oxygen under a wide range of pressures and powers, from a few Pa to 133 Pa, and from 10 to 300 W. Atomic oxygen densities with samples present are around one third lower than those without samples, and in both cases the atomic oxygen density increases linearly with gas pressure. Previous optical emission spectroscopy (OES) measurements indicate that plasma interaction with the substrate commences a few seconds after plasma turn on. Similar trends are observed with time resolved LIF measurements of the atomic oxygen.

*Supported by the EU BRITE programme, grant EURAMCT 960365

IWP7 53 Surface recombination of atomic nitrogen in a parallel plate rf discharge S.F. ADAMS, *Air Force Research Laboratory, Wright-Patterson AFB, OH* T.A. MILLER, *The Ohio State University, Columbus, OH* The loss of atomic nitrogen due to surface reaction in a parallel plate rf reactor was investigated using a pulse N₂ discharge and two-photon LIF detection of ground state atomic nitrogen. Metal electrode surfaces as well as various substrate materials and other reactor surface materials were investigated for their reactivity with atomic nitrogen within the pulsed discharge environment. A two-dimensional numerical code was developed to model N atom diffusion and wall loss. This model determines the surface recombination coefficient, γ , from the N atom density decay measured near the surface. The values of γ for the materials tested ranged from 0.5% to 0.02%. Stainless steel, aluminum, silicon and boron nitride were all found to have N atom recombination rates that had an inverse pressure dependence in the pressure range of 1 to 5 Torr. Theories behind this inverse pressure dependence will be discussed. It was also found that aluminum had a surface loss rate of 3 to 5 times less than that of stainless steel. Boron nitride was found to have the lowest N atom recombination rate of the materials studied under each discharge condition.

IWP7 54 Sputtered Atoms Transport in a Cylindrical Hollow Cathode I. M. RUSINOV, A. B. BLAGOEV, *Sofia University, Faculty of Physics, 5 James Bourchier Blvd., 1164 Sofia, Bulgaria* A pulsed hollow cathode discharge in Ar and Ne is used to investigate the temporal evolution of sputtered Mg density in the afterglow phase. A diffusion model of this transport is assumed, including the process of reflection by the wall through a boundary condition of the third kind.¹² Decays of ground-state Mg atom densities are recorded using an optical absorption technique. The observed decay rates reveal an essential temporal dependence. This behavior is supposed to be due to changes in the wall loss probability with time during the afterglow. The influence of ad-

sorbed hydrogen on the properties of the wall surface is investigated. Suppression of Mg atoms sputtering and change in the wall sticking probability value for these atoms is observed in the presence of hydrogen. The typical experimental conditions are: cathode radius and length 1.3 cm and 28 cm respectively, pulse duration 1-3 ms, pulse period 20-70 ms, and pulse current 50-200 mA.

¹S. Suzuki, H. Itoh, N. Ikuta, and H. Sekizawa *J. Phys. D: Appl. Phys.* **25**, 1568 (1992).

²I. M. Rusinov, G. W. Paeva, and A. B. Blagoev *J. Phys. D: Appl. Phys.* **30**, 1878 (1997).

IWP7 55 Study on the Secondary Electron Yield γ of Insulator for PDP Cathode Y. MOTOYAMA, M. USHIROZAWA, H. MATSUZAKI, Y. TAKANO, M. SEKI, *NHK Sci. Tech. Res. Labs., Tokyo 157-8510, Japan* The secondary electron yield γ of the Plasma Display Panel (PDP) cathode is an important research object because it is closely related to the discharge voltages etc. For metal cathodes, we made a comprehensive examination¹ of γ for all rare gas ions and metastables according to Hagstrum's theory.² For γ of MgO, which is the useful insulator cathode, Aboelfotoh et al.³ calculated the values for Ne and Ar ions supposing a monochrome PDP. However, the values of γ for other rare gas ions and their metastables necessary for a full color PDP have not yet been calculated. These values are calculated in the present study after them. The results are as follows: For ions, He:0.481 and Kr,Xe:0, assuming that there are no impurity levels in MgO; For metastables, He:0.491, Ne:0.489, Ar:0.428, Kr:0.381, and Xe:0.214. These results should serve as useful parameters in discharge simulation for the PDP.

¹H. Matsuzaki: *Trans. IEE Jpn.*, **111-A**, 971 (1991).

²H.D. Hagstrum: *Phys. Rev.*, **96**, 336 (1954), *ibid.*, **122**, 83 (1961).

³M.O. Aboelfotoh and J.A. Lorenzen: *J. Appl. Phys.*, **48**, 4754 (1977).

IWP7 56 A model of hydrocarbon reactions and surface interactions in low temperature hydrogen plasmas DARREN A. ALMAN, *University of Illinois* DAVID N. RUZIC, *University of Illinois* A model of collisional processes and surface interactions of hydrocarbons in hydrogen plasmas has been developed to aid in computer modeling efforts relevant to plasma-surface interactions. It includes 16 molecules (CH up to CH₄, C₂H to C₂H₆, and C₃H to C₃H₆) and four reaction types (electron impact ionization/dissociative ionization, electron impact dissociation, proton impact charge exchange, and dissociative recombination). Experimental reaction rates or cross sections have been compiled, and estimates have been made for cases where these are not available. The surface model incorporates experimental data on chemical sputtering of graphite due to hydrogen ions to help predict the effects of hydrocarbon bombardment at varying energies and surface temperatures. The experimental data for hydrogen ions is used to determine the composition of the surface. A set of rules is then followed to determine what species are given off, and with what probabilities, when any of 16 hydrocarbons are incident on the surface. Potential uses of this surface model include modeling the growth of high-density polycrystalline diamond films and low-density (porous) low-k organic polymers for semiconductor dielectrics.

IWP7 57 Deviation from the uniform field in low current diffuse discharges S. ZIVANOV, J. ZIVANOVIC, S. VRHOVAC, Z.LJ. PETROVIC, *Institute of Physics, Belgrade, Yugoslavia*.^{*} We have recorded axial distribution and radial distribution of emission in low current discharges at low pressures between 0.5 and 3 Torr in argon. The axial profile of emission was shown to

depend on the current density and to deviate from the single exponential distribution expected for the uniform electric field. Assuming equilibrium between electron swarm and the local field it was possible to determine the local field from the slope of emission and obtain the distribution of the field in the region where assumption of equilibrium may be made. The field distribution proved to be in good agreement with the calculations based on the theory of Phelps and coworkers.¹ Even below the onset of constriction the field may change by as much as a factor of 2 between the anode and the cathode. These results were obtained in stationary discharges and indicate that under special circumstances the transition to constriction may be gradual and may be studied on the bases of theories for diffuse low current discharges.

^{*}Supported by MNTRS 01E03 project.

¹A.V. Phelps *et al.*, *Phys. Rev. E* **47**, 2825 (1993).

**SESSION IWP8: POSTER SESSION:
LIGHTING-RELATED DISCHARGES
Wednesday afternoon, 6 October 1999
Poplar Room Sheraton Waterside Hotel at 13:30**

IWP8 58 Pressure Dependence of Xe₂^{*} Excimer Emission in AC Dielectric Barrier Discharges HARUAKI AKASHI, NOBUAKI TAKAHASHI, TAI SASAKI, *National Defense Academy, Japan* AKINORI ODA, YOSUKE SAKAI, *Hokkaido University, Japan* Excimer lamps have been developed using dielectric barrier discharge (DBD) as an important VUV light source, however the physics of DBD is not understood well. For further development of efficient DBD excimer lamps, understanding of the characteristics of DBD is necessary. In this paper, we investigate the light intensity and efficiency in atmospheric Xe gas by a computational method. DBDs are calculated using a 1D fluid model coupled with Poisson's equation considering microdischarge radius under the condition of a gas pressure of 100 ~ 600 Torr, an electrode distance of 1 cm and a dielectric barrier ($\epsilon_r=4$) width of 2 mm. Both electrodes are covered with dielectric barrier and 10 kV amplitude AC voltage (100 kHz) is applied to the electrodes. 173 nm intensity increases with increasing the pressure. The maximum intensity is obtained at 200 Torr, then decreases with increasing the pressure. The tendency of input power is similar to that of light intensity. However, at 500 Torr, input power has a little peak. Here, the sustaining system of the discharge is changed from direct ionization to step-wise ionization. The tendency of efficiency is also similar to that of light intensity. Contrary to the input power, in the efficiency curve, a steep depletion appears at 500 Torr. The maximum efficiency is obtained at 200 Torr to be 16.8% (output light power/input discharge power).

IWP8 59 A Monte-Carlo Model of Partially Trapped UV Radiation in a Plasma Display Panel Cell^{*} TRUDY VAN DER STRAATEN, MARK J. KUSHNER, *University of Illinois, Dept. of Electrical and Computer Engr., Urbana, IL, 61801, USA* Plasma Display Panels (PDPs) are being developed for large-area high-brightness flat panel displays. Color PDP cells generally use xenon gas mixtures to generate UV photons that are converted to visible light by phosphors. While the UV photons produced by Xe(6s¹-5s5p6, 6s-5s5p6) are only in a quasi-optically thick regime due to the small dimensions (100s μ m) of PDP cells, current

models of PDPs do not explicitly address UV radiation transport other than by using radiation trapping factors. In this paper we report on results from a two-dimensional hybrid simulation of a PDP cell which models radiation transport using Monte Carlo (MC) photon transport and frequency redistribution algorithms. We examine the spectrum of UV photons incident on the phosphor and their escape probability. For typical operating conditions (400 Torr, 1-4% Xe mole fraction) there is significant frequency redistribution of resonance radiation due to absorption and subsequent re-emission at a different frequency within the lineshape. Significant line reversal occurs at Xe mole fractions of a few percent, the degree of which depends on PDP cell dimensions. The escape probability generally decreases during the current pulse due to additional quenching by electron impact processes.

*Work was supported by LG Electronics

IWP8 60 1S₂ and 1S₅ Level Densities in a Neon Discharge via Laser Spectroscopy PHIL MOSKOWITZ, OSRAM SYLVANIA GRAEME LISTER, OSRAM SYLVANIA The low pressure neon gas discharge in small diameter (5mm) tubes found, for example, in automotive signal lighting, is the subject of this experimental study. We examine the population density of a neon resonance (1S₂) and metastable (1S₅) level for d.c. and pulsed operation over a range of pressure (10 - 200 Torr) and current (10 - 200 mA). A single mode dye laser is used to measure the absorption profiles of the 585nm and 588nm spectral lines to access these levels respectively. Density and gas temperature as a function of discharge radius are also presented. Positive column electric fields are measured using capacitively coupled external probes. Density and electric field data are compared with a d.c. positive column discharge model developed here.

IWP8 61 Plasimo — A General Purpose Plasma Modelling Toolkit JAN VAN DIJK, BART HARTGERS, HARM VAN DER HEIJDEN, GER JANSSEN, COLIN JOHNSTON, JOOST VAN DER MULLEN, *Department of Applied Physics, Eindhoven University of Technology, The Netherlands* In recent years the plasma simulation model, Plasimo, has been developed at Eindhoven University of Technology. Initially intended as a program dedicated to the modelling of thermal argon ICP's, it has developed into a fully-fledged code capable of handling a variety of equilibrium and non-equilibrium plasmas. In this contribution we shall give an overview of the assumptions which form the basis of Plasimo. The design of the most important modules will be discussed and their capabilities shown. These are the modules for electromagnetic incoupling, diffusive and convective mass, momentum and energy transport, transport coefficients and transfer of radiation. Some results of the application of Plasimo to inductive light sources and the expansion chamber of a cascaded arc plasma will be shown. Please note three other contributions in which some aspects are dealt with in more detail.

IWP8 62 Collisional Radiative Models for non-Maxwellian plasmas BART HARTGERS, JAN VAN DIJK, JOOST VAN DER MULLEN, *Department of Applied Physics, Eindhoven University of Technology, The Netherlands* Collisional Radiative models are a useful tool for studying plasmas. In their simplest form, they are used to calculate an atomic state distribution function (ASDF) from given electron and neutral densities and an electron temperature. Additionally, global ionization and recom-

bination coefficients can be calculated as a function of electron density and temperature. In turn, these coefficients are used as input for the general plasma model Plasimo. Simulations of conventional fluorescent lamps are more difficult, since assumptions about a Maxwellian energy distribution of the electrons no longer hold, due to the low electron densities in such lamps ($< 10^{18} \text{ m}^{-3}$). One way of handling this problem is to use the two electron group model, in which the electron distribution function is divided into two parts with distinct temperatures.

**SESSION IWP9: POSTER SESSION:
PLASMA DISPLAYS**

Wednesday afternoon, 6 October 1999

Poplar Room Sheraton Waterside Hotel at 13:30

IWP9 63 Time-resolved VUV emission from a model PDP with in situ deposited MgO* J. R. GOTTSCHALK, *Dept. Physics & Astronomy University of Toledo* A. D. COMPAAN, *Dept. Physics & Astronomy University of Toledo* M. SHAO, *ElectroPlasma, Inc.* J. D. SCHERMERHORN, *ElectroPlasma, Inc.* We have studied the performance of a model PDP cell in a specially constructed deposition/test chamber. The deposition system permits either pulsed laser deposition (PLD) or sputter deposition and provides for transfer of the electrode structure under high vacuum conditions into a discharge test configuration. With nanosecond time resolution, we have studied the voltage and current waveform as well as the vacuum ultraviolet (VUV) and visible light emission from the planar electrode structure. Changes in the integrated atomic (Xe) vs. excimer (Xe₂) emission will be presented as a function of the gas mixture ranging from 0.1 to above 30 and sputter-deposited films will be given as well as the effects of air exposure on the VUV

*Work supported in part by Electroplasma, Inc.

IWP9 64 VUV spectroscopy and VUV and IR space and time resolved emission of AC-PDP micro discharges R.J.M.M. SNIJKERS, M. KLEIN, *Philips Research Laboratories, Weisshausstrasse 2, 52066 Aachen, Germany* Plasma Display Panels (PDP) consist of a matrix of micro discharge cavities. The micro discharges produce VUV radiation to excite the phosphors in the cavities. The low discharge efficiency is one of the drawbacks of PDPs. To optimize the discharge efficiency, to improve the overall panel efficacy, the energy loss channels of the micro discharges have to be understood. Therefore, experiments and modeling activities have been developed to characterize the discharge as function of the parameters that influence the discharge efficiency. VUV spectroscopy has been used to analyze the VUV resonance and dimer radiation in Ne-Xe discharges as function of the Xe content. For these experiments an experimental set-up is used in which discharges are generated that equal the discharges in PDPs. Space and time resolved emission spectroscopy in VUV and IR has been obtained to analyze the discharge development as function of several electrode geometries. A clear difference has been observed between striped and T-shaped electrodes.

IWP9 65 Parametric Study of Rare Gas Mixtures Containing Ar and Kr on the Performance of Plasma Display Panel Cells* DANIEL CRONIN, TRUDY VAN DER STRAATEN, MARK J. KUSHNER, *University of Illinois, Dept. of Electrical and Computer Engr., Urbana, IL, 61801, USA* Plasma display panels (PDPs) are being developed for use as a large area, high luminosity, flat panel displays. Conventional PDP cells use He/Ne/Xe gas mixtures with the goal of maximizing the power efficiency of producing UV radiation from Xe resonance states and from xenon dimers. Alternate gas mixtures may, however, have advantages with respect to power efficiency and cell lifetime. In this paper, a 2-dimensional fluid model will be used to assess the performance and efficiency of PDP cells using gas mixtures composed of He/Ne/Ar/Kr/Xe. The model consists of fluid continuity and momentum equations for all neutral and charged species and Poisson's equation for the electric potential. The electron energy equation is solved to obtain electron temperatures and electron impact rate coefficients. A reaction mechanism was formulated consisting of the rare gas monomer and dimer excited states and ions, as well as heterogeneous dimers (e.g., HeXe*). Typical conditions are gas pressures of 400-500 Torr and cell height of 150-200 μm . Initial results show significantly degraded performance in gas mixtures containing Kr.

*Work was supported by LG Electronics

IWP9 66 Simulations of Cell Geometry Effects of ac Plasma Display Panel with Fluid and Hybrid codes SHON CHAE HWA, *POSTECH* SHIN YOUNG KYO, KIM WOONG, KANG JIN HO, LEE JAE KOO, *POSTECH* The simulation of new Plasma Display Panel (PDP) cell geometry was carried out by two different codes. One is a fluid-type code[1] and the other is a hybrid type which uses fluid equation for ions and particle-in-cell, Monte-Carlo collision model[2] for electrons. Self consistent electron energy distribution function (EEDF) can be obtained from the hybrid code instead of assumed one as in the fluid code. We obtain various plasma characteristics (density, potential, power consumption, electron temperature, and others) of PDP cell using these codes. We also implemented a simple radiation transport model in these codes to calculate the amount of visible light at the front window. The new cells, hollow cathode and ditched surface discharges, are simulated with these codes. These cells show somewhat different characteristics compared with coplanar-type PDP cells. The plasma distributions of these cells are broader than the usual coplanar-type PDP cells.

[1] Y.K. Shin, J.K. Lee, and W. Kim, *Jpn. J. Appl. Phys.*, 38(1999) pp. L174-177.

[2] Y.K. Shin, C.H. Shon, H.S. Lee, W. Kim, and J.K. Lee, *Proc. 18th Int. Display Research Conf. Asia '98*, p. 609 (1998); Vahidi Vahedi and G. DiPeso, *J. Comp. Phys.* 131, p149-163 (1997).

IWP9 67 The Breakdown and Vacuum Emission Characteristics of a High Surface Area to Volume Ratio Discharge OLIVIER B. POSTEL, MARK A. CAPPELLI, *Stanford University, Mechanical Engineering Department, Thermosciences Division* Commercially available flat panel displays operate with various gas compositions over a broad range of pressure. Few experimental studies have addressed the question of optimum gas mixture and total pressure for maximum luminance as well as discharge control for the minimization of sputtering damage. In

this study, the vacuum emission and breakdown characteristics of a high surface area to volume ratio direct-current discharge have been measured for various xenon and xenon/helium gas mixtures. The breakdown characteristics in pure helium are consistent with previous studies. A database of the breakdown characteristics for a range of gas mixtures is collected and compared to the pure gas reference cases. Steady-state operation of the discharge at high pressures (>200 Torr) gives rise to operating discharge voltages that are relatively insensitive to discharge current densities. Vacuum emission spectra are obtained over the spectral range from 110 nm to 200 nm, pressure range from 100 Torr to 400 Torr, voltage range from 200 V to 500 V, and electrode gap from 50 microns to 500 microns. These experimental measurements will provide the basis for collisional-radiative model development and insight on the discharge physics that controls the population of excited ultraviolet-emitting states.

**SESSION IWP10: POSTER SESSION:
PLASMA PROCESSING
AND SURFACE MODIFICATIONS
Wednesday afternoon, 6 October 1999
Poplar Room Sheraton Waterside Hotel at 13:30**

IWP10 68 On the Electron Kinetics in the H₂/Ar/N₂ DC Discharge* MARIO HANNEMANN, PETER HARDT, DETLEF LOFFHAGEN, MARTIN SCHMIDT, ROLF WINKLER, *Institut für Niedertemperatur-Plasmaphysik, 17489 Greifswald, Germany* The TiN deposition on the basis of TiCl₄ in H₂/Ar/N₂ discharges is successfully used for hard coatings of metals at lower temperatures. As a first step to a deeper understanding of such complex chemically reactive plasmas experimental and theoretical studies of dc discharge plasmas have been performed for H₂/Ar/N₂ mixtures with a composition of about 72/15/13 at pressures around 200 Pa and current densities around 0.3 mA/cm². By means of Langmuir probes the space potential and the energy distribution function, density and mean energy of the electrons have been measured in the Faraday dark space and the negative glow of discharges with an electrode separation of 5.5 cm. The experimental results are discussed and compared with corresponding results obtained by solving the space-dependent electron Boltzmann equation using a recently developed multi-term approach. Good agreement between measured and calculated results for the mean energy and satisfactory agreement for the energy distribution function and the density are found. Remaining discrepancies are evaluated with regard to possible reasons.

*Supported in part by the Volkswagen-Stiftung.

IWP10 69 Diagnostics of ultra high frequency SiH₄/H₂ plasmas for synthesizing polycrystalline silicon thin film at low substrate temperatures MASAFUMI ITO, SHIGEAKI SUMIYA, YUKO MIZUTANI, MASARU HORI, TOSHIO GOTO, *Nagoya University* SEIJI SAMUKAWA, *NEC Corp.* TSUTOMU TSUKADA, *ANELVA Corp.* A 500MHz - ultra high frequency (UHF) plasma has attracted the scientific and practical attention because of excellent properties, e.g. low electron temperature and uniform high density plasma at wide area. The UHF plasma was successfully applied to ULSI fabrication processes. Recently, we applied the UHF plasma to the process for synthesizing polycrystalline silicon thin films at low substrate temperatures below 300

degree C. The high deposition rate of 1nm/s and the crystalline fraction of > 60% were obtained even at a low substrate temperature of 100 degree C. In this study, we have investigated the mechanism for obtaining better-quality polycrystalline silicon thin film at the substrate temperatures in the ultra high frequency plasma. The mechanism was analyzed by using an ultraviolet absorption spectroscopy, a microwave interferometer, a photo-emission spectroscopy and a Langmuir probe for plasma diagnostics. The analyses of deposited films were carried out by using a Raman spectroscopy and a spectroscopic ellipsometry. From these results, the reduction of ion-bombardment energy and the increase of H atoms were found to be essential to form the polycrystalline silicon thin films with high quality.

IWP10 70 Polycrystalline diamond films deposited at high microwave power densities CELINE CAMPILLO, SAMIR ILIAS, MICHEL MOISAN, *Universite de Montreal, Montreal, Quebec* Polycrystalline diamond films have been deposited using a surface-wave sustained discharge in a non-conventional system¹. In such a system, the microwaves are totally absorbed in the discharge and, consequently, the substrate temperature does not increase much as the input microwave power is increased. This characteristic enables us to reach higher power densities (> 150 W/cm³) than in conventional systems, while maintaining the substrate temperature at the required temperature for deposition, say 800°C. The effect of microwave power density on diamond nucleation density, grain size, growth rate and crystalline purity was studied using Raman spectroscopy and scanning electron microscopy (SEM). Varying the methane percentage in the CH₄/H₂ mixture from 0.5 to 3% does not affect the diamond film crystallinity, while the growth rate is observed to increase.

¹S. Schelz, C. Campillo, M. Moisan, Diamond and related materials, 7 (1998) 1675-1683.

IWP10 71 Plasma emission spectroscopic study of CVD diamond growth WEIHAI FU, *Microelectronics & Photonics Research Laboratory, Department of Electrical & Computer Engineering, Old Dominion University, Norfolk, Virginia 23529* ARNEL LAVARIAS, *Microelectronics & Photonics Research Laboratory, Department of Electrical & Computer Engineering, Old Dominion University, Norfolk, Virginia 23529* SACHARIA ALBIN, *Microelectronics & Photonics Research Laboratory, Department of Electrical & Computer Engineering, Old Dominion University, Norfolk, Virginia 23529* Diamond film has been grown for field emission device applications using microwave enhanced chemical vapor deposition process. Conformal coating of sharp silicon tips has been achieved to obtain low turn-on voltage and stable emission from diamond emitter arrays. A high nucleation density required for continuous film growth is achieved by bias enhanced nucleation. The emission spectra of the reactive species in the plasma of hydrogen and methane gas mixture have been monitored using a fiber optic spectroscopy system. As the methane concentration was changed from 0 to 2% were found to increase and correlate with an increase in uniformity and quality of the diamond film. The application of a negative or positive substrate bias voltage up to 150 V had no measurable change in CH and C₂ emission line intensities; however, bias assisted diamond growth resulted in better conformal coating of the silicon tips. Field emission properties of diamond coated silicon emitter arrays will be discussed in relation to the plasma emission spectra.

IWP10 72 Modeling of a Two Stage RF Plasma Reactor for SiC Deposition* J. L. GIULIANI, *Plasma Physics Division, Naval Research Laboratory* J. W. THORNHILL, *Plasma Physics Division, Naval Research Laboratory* Chemical Vapor Deposition (CVD) is often used for the growth of Silicon Carbide (SiC) films. The precursor gases, silane and methane, flow through a quartz tube at atmospheric pressure with a graphite susceptor located downstream of the inlet. The susceptor is heated by low frequency (kHz) RF which in turn heats the gas by thermal transfer to several thousand K and forms reactive species near the growth substrate. The high temperature and pressure of the gas may be the cause of micropipes, i.e., film defects, found in CVD SiC. An alternative approach is plasma-enhanced CVD wherein a plasma is used to dissociate the precursor gases in non-equilibrium conditions. Consequently the neutral gas temperature and pressure can be substantially reduced. The present research focuses on the design of a two stage RF reactor in which a high frequency RF (MHz) antenna is added upstream of the substrate to form the plasma. We have developed a 1-D flow code to investigate various design options for the reactor. The model includes electromagnetic coupling, electron heating, plasma chemistry for silane and propane reactions and products, neutral and ambipolar diffusion. We will report on the impact of the design parameters: pressure, RF frequency, flow rate, and tube diameter. In particular, the optimal separation of the plasma region from the growth substrate results from a trade-off between radical concentration and minimal ion induced damage.

*Supported by BMDO.

IWP10 73 CW and pulsed inductively coupled chlorine plasma diagnostics for polysilicon etch MARWAN KHATER, LAWRENCE OVERZET, *University of Texas at Dallas* We will present plasma parameters and etch results for CW and pulsed ICP chlorine discharges. Plasma parameters were measured with Langmuir probes for ICP powers up to 900 W at pressures from 1 to 25 mTorr. In CW mode, the positive ion density (n_+) was on the order of 10^{11} cm^{-3} and increased monotonically with ICP power. However, n_+ peaked at 5 mTorr as the pressure was varied. The electron temperature decreased with pressure from 3.5 eV at 1 mTorr to 2.2 eV at 25 mTorr. Blank 150 mm polysilicon coated wafers were etched in CW chlorine plasmas at 3 mTorr. The etch rate increased with both ICP and bias powers to 0.5 $\mu\text{m}/\text{min}$ at 900W ICP power and 200 W bias power with overall nonuniformity of 3%. Preliminary etch results in pulsed plasma showed an increase in polysilicon etch rate compared to CW plasma. Furthermore, increasing the pulse period from 20 to 100 μsec caused a slight increase in the polysilicon etch rate. CW and pulsed Chlorine plasmas were used to etch feature sizes as small as 0.7 μm . The effects of pulse period on plasma parameters, etch rates and nonuniformities are under further investigation. The possibility of negative ion assisted etch will also be examined. This material is based upon work supported by NSF grant # CTS-9713262

IWP10 74 Emissions and Mass Analysis of Fluorocarbon Processing Discharges During Oxide Etch* ESHWAR DANDA-PANI, *Electronic Materials Processing Research Laboratory, Penn State University* RAVIPRAKASH JAYARAMAN, ROBERT MCGRATH, *Electronic Materials Processing Research Laboratory, Penn State University* A number of groups are developing computer models for simulation of reactive chemistry fluorocarbon discharges to aid process optimization and new process development. In order to provide additional experimental data for validation of computer simulations, we have used optical emission

spectroscopy, un-collided beam neutral gas mass spectroscopy, and ion extraction mass spectroscopy to monitor the relative concentrations of discharge species present during reactive ion etching of silicon dioxide. Wafers were etched and measurements were made in two commercial reactive ion etchers, an AMAT MERIE Chamber and a PlasmaTherm RIE Chamber. Measurements were made using various lithographic patterns, which allowed variation of the surface fraction covered by resist and by the exposed oxide to be etched. In addition, photolithography has been used to define trench features with widths varying from 2 mm to 0.5 mm, and electron beam lithography has been used to define trench features with widths as small as 50 nm. We will report on variations in optical emissions and discharge species concentrations as etch process conditions and wafer materials in contact with the discharge are varied. These observations will be correlated to profilometer and SEM measurements of etch rate, selectivity and trench profile.

*Work supported by the Pennsylvania Semiconductor Manufacturing Initiative

IWP10 75 Effect of pressure gradients on plasma characteristics KEITH THOMPSON, LAWRENCE OVERZET, *University of Texas at Dallas* Plasma technology has come under great strains to conform to tight uniformity standards. Fundamental to this issue is gas distribution, and while work has been done with numerical simulations, few complete experimental data sets have been gathered showing gas distribution in industrial chambers. The goal of this project is to create detailed maps of the pressure, both at the inlet and at the wafer levels, with and without the plasma for various pressures and flow rates of Ar, SF_6 , Cl_2 , and Ar/ SF_6 using different gas distribution techniques. Once completed, these maps, along with langmuir probe measurements, will be used to study differential pressure effects on plasma characteristics. Recent results have shown, at the top of the chamber, the expected difference between a gas distribution ring and a single inlet, but at the wafer surface both setups yield very good pressure uniformity. This contradicts test wafer etches, showing 3% variation with the ring and greater than 20% with the single inlet. Striking a plasma illustrates the difference. Since power deposition occurs at the top of the chamber, near the gas non-uniformity, ion and radical formation will reflect this. As the ions move down to the wafer, this non-uniformity may not have the chance to even out; resulting in a non-uniform etch. Continued study will focus on extracting plasma characteristics to illustrate this phenomenon.

IWP10 76 Interaction of low energy electrons and ion beam during ion beam implantation SVETLANA B. RADOVANOV, JIM BUFF, GORDON ANGEL, *Varian Semiconductor Equipment Associates, 35 Dory Road, Gloucester, MA 01930*. When glow discharge plasma is introduced into an ion beam low energy electrons from the plasma efficiently neutralize an ion beam. There appears to be a drastic decrease in beam-plasma potential, accompanied by a production of beam-plasma neutrals. The knowledge of Electron Energy Distribution Function (EEDF) and plasma density of a glow discharge plasma that interacts with an ion beam is of fundamental interest for determining the efficiency of the charge neutralization. In this study we have measured EEDF of a xenon low-pressure discharge using a tuned Langmuir probe. Additionally a new source geometry was proposed to enhance the electron density and maintain the low electron temperature. A two-dimensional (2D) model of plasma interaction with a high current ion beam was developed. Calculations in which a one-dimensional electron trajectory was assumed were coupled to an ion trajectory simulation for a 2D process chamber transport model. A 2D beam-plasma potential distribution was compared to the experimental data.

IWP10 78 Direct Measurement of Surface Charge Distribution During Ion Implantation S. RADOVANOV, G. ANGEL, J. BUFF, J. CUMMINGS, D. BROWN, *Varian Semiconductor Equipment Associates, 35 Dory Road, Gloucester, MA 01930*. A knowledge of the surface charging potential distribution at the wafer plane during beam ion implantation is necessary for better understanding of the charge neutralization nonuniformity. In this paper the surface charging potential was measured using an in situ monitor wafer with a two-dimensional array of probes. The probes could measure the potential difference between the different aluminum (Al) sites and/or Al-sites and system ground. The actual device consisted of 64 probes that were uniformly distributed on the wafer surface. In this way the potential variation could be detected from the area under the ribbon beam used as well as from the area where the beam did not strike the wafer. The probes were connected through a vacuum feed-through to a storage oscilloscope and/or data acquisition board plane beam potential variations during the implant. In a steady state, charge neutralization occurs in a direction to reduce local imbalance between the ion and electron current. In the region where beam-plasma potential and current density is higher the electron current is reduced by the large potential barrier in the plasma sheath and positive current is present in excess. In the region where there is no direct ion beam surface interaction, primary electrons coming from the plasma neutralization system and secondary electrons cause negative charging. If the local charging becomes significant it can cause surface potential nonuniformity across the wafer and possibly oxide degradation. The charging potential nonuniformity was measured and related to the ion beam plasma nonuniformity and presence of the stray magnetic field in the process chamber. The effect of stray magnetic field on the surface charging distribution was evaluated.

SESSION IWP11: POSTER SESSION:
ENVIRONMENTAL APPLICATIONS
Wednesday afternoon, 6 October 1999
Poplar Room Sheraton Waterside Hotel at 13:30

IWP11 79 Dissociation of Benzene in a Pulsed Glow Discharge* WEIXING DING, ORNL DENNIS MCCORKLE, UT/ORNL CHENG-YU MA, ORNL LAL PINNADUWAGE, ORNL/UT Destruction of benzene in a benzene/Ar mixture subjected to a pulsed glow discharge was studied. The destruction efficiency was much improved compared to that of a DC glow discharge,¹ and the destruction efficiency increased with decreasing pulse width at a constant pulse frequency. There were no gaseous byproducts (other than Ar) at the reactor output. Instead benzene was converted to dust particles in the reactor. Diagnostic experiments, including spectroscopic measurements, were conducted to elucidate the destruction mechanisms involved. These diagnostics – together with the fact that negative ions have been shown to be the precursors for dust formation – indicate that dissociative electron attachment to high-Rydberg states of benzene produced primarily by excitation transfer from the metastable states of Ar was responsible for the observed dissociation of benzene. The effects of oxygen on the formation of dust particles and the details on the by-product analysis will be discussed.

*Research Supported by DOE-EMSP Program. The ORNL is managed by Lockheed Martin Energy Research Corp. for the U.S. Department of Energy under contract number DE-AC05-96OR22464.

¹D.L. McCorkle, W. Ding, C.Y. Ma, and L.A. Pinnaduwege, J. Phys. D, 32, 46 (1999).

IWP11 80 Ion-Molecule Reactions in a Nitrogen-Benzene Plasma: Implications for the Destruction of Aromatic Compounds

SKIP WILLIAMS, *Air Force Research Laboratory/Space Vehicles Directorate (AFRL/VS)* SUSAN ARNOLD,* *AFRL/VS* A. A. VIGGIANO, *AFRL/VS* ROBERT MORRIS, *AFRL/VS* RAJESH DORAI, *University of Illinois, Urbana* MARK KUSHNER, *University of Illinois, Urbana* The destruction of aromatic compounds in low temperature plasmas is problematic due to the low rate of ring-cleaving reactions by plasma generated oxidizing radicals at ambient gas temperatures. We report on a combination of laboratory flow tube kinetics measurements and computational modeling to investigate the question of whether a nitrogen plasma can be used for the destruction of waste aromatic compounds based on ion-molecule reactions. N_2^+ reacted rapidly with benzene by pathways which cleave the benzene ring in more than 50% entirely by non-dissociative charge transfer. A global kinetics model of a dielectric barrier discharge sustained in nitrogen containing mixtures was used to assess the destruction efficiency of benzene while incorporating both these mechanisms and dissociative recombination of benzene ions. This work was supported in part by AFOSR and NSF.

*On contract to Wentworth Institute of Technology

IWP11 81 Influence of Discharge Properties on CF_x Polymer Thin Films Deposited in Fluorocarbon Vapor Discharges*

Y. SAKAI, *Hokkaido Univ., Japan* C. P. LUNGU, A. M. LUNGU, *Hokkaido Univ. (on leave from Nat. Inst. of Laser, Plasma and Rad. Phys., Romania)* H. SUGAWARA, *Hokkaido Univ.* M. MIYAMOTO, *Fuji Electric Corp. R&D Ltd.* Polymer $(CF_x)_n$ film has been deposited in dc and rf C_7F_{16} and C_8F_8 vapor discharges. The film properties made in the dc and rf discharges were compared. The discharges were examined by optical emission spectroscopy and the gas composition was monitored by a quadrupole mass spectrometer. The film were deposited at room temperature, with pressures between 10~ 100 Pa. The substrates were stainless steel, glass and [111] Si wafers. The composition and characteristics of the film was determined by Fourier transform infrared and X-ray photo-electron spectroscopy techniques, scanning electron microscope and electron spin resonance spectroscopy. The dielectric strength was also measured. It was shown that the surface of film deposited in dc discharge contained particles of 5 to 10 μm size, while the film deposited in rf discharge were smooth and free of particles structure. A CF molecular fragment was found in the film composition.

*Work supported by Grant-in-Aid of The Ministry of Education, Science, Sports and Culture, Japan.

IWP11 82 Time Resolved Investigations of NO removal in a Homogeneous Pulsed Discharge*

F. FRESNET, G. BARAVIAN, L. MAGNE, S. PASQUIERS, C. POSTEL, V. PUECH, A. ROUSSEAU, M. ROZOY, *LPGP, Universit Paris-Sud / CNRS, France* A pulsed homogeneous discharge has been obtained in air-like mixtures at high pressure using the photo-triggering technique, and has been demonstrated to be very efficient for NO

removal¹. It allows efficient comparison between time resolved measurements of pollutant density, [NO], and predictions of kinetics models. We use the LIF diagnostic at 226 nm to measure [NO] during the post-discharge, after a 75 ns-duration current pulse. The influence of the deposited electrical energy, up to 200 J/l, and of the applied electric field, up to 225 Td, on the NO removal efficiency are discussed. Experiment shows that almost 100 per cent of the initial NO population can be removed with a single shot in N_2/NO , depending on parameters values. It will be compared to results of a self-consistent 0D-model.

*Work supported by PSA-Renault, ECODEV-CNRS, and ADEME

¹M.Rozoy, C.Postel, V.Puech, to appear in Plasma Sources Sci. Technol. (1999)

SESSION IWP12: POSTER SESSION: ELECTRICAL DIAGNOSTICS AND MASS SPECTROMETRY

Wednesday afternoon, 6 October 1999

Poplar Room Sheraton Waterside Hotel at 13:30

IWP12 83 Comparison of three rf plasma impedance monitors on a high phase angle planar inductively coupled plasma source

H. UCHIYAMA, M. WATANABE, D. M. SHAW, J. E. BAHIA, G. J. COLLINS, *Dept. of Electrical Engineering, Colorado State University, Fort Collins, CO 80523* Accurate measurement of plasma source impedance is important for verification of plasma circuit models, as well as for plasma process characterization and endpoint detection. Most impedance measurement techniques depend in some manner on the cosine of the phase angle to determine the impedance of the plasma load. Inductively coupled plasmas are generally highly inductive, with the phase angle between the applied rf voltage and the rf current in the range of 88 to near 90 degrees. A small measurement error in this phase angle range results in a large error in the calculated cosine of the angle, introducing large impedance measurement variations. In this work, we have compared the measured impedance of a planar inductively coupled plasma using three commercial plasma impedance monitors (ENI V/I probe, Advanced Energy RFZ60 and Advanced Energy Z-Scan). The plasma impedance is independently verified using a specially designed match network and a calibrated load, representing the plasma, to provide a measurement standard.

IWP12 84 Langmuir Probe Distortions and Probe Compensation in an Inductively Coupled Plasma

J. S. JI,* *NASA-Ames Research Center* M. A. CAPPELLI,[†] *NASA-Ames Research Center* J. S. KIM,[‡] *NASA-Ames Research Center* M. V. V. S. RAO,[§] *NASA-Ames Research Center* S. P. SHARMA, *NASA-Ames Research Center* In many RF discharges, Langmuir probe measurements are usually made against a background of sinusoidal (and not so sinusoidal) fluctuations in the plasma parameters such as the plasma potential (V_p), the electron number density (n_e), and the electron temperature (T_e). The compensation of sinusoidal fluctuations in V_p has been extensively studied and is relatively well understood. Less attention has been paid to the possible distortions introduced by small fluctuations in plasma density and/or plasma temperature, which may arise in the sheath and pre-sheath regions

of RF discharges. Here, we present the results of a model simulation of probe characteristics subject to fluctuations in both V_p and n_e . The modeling of probe distortion due to possible fluctuations in T_e is less straightforward. A comparison is presented of calculations with experimental measurements using a compensated and uncompensated Langmuir probe in an inductively coupled GEC reference cell plasma, operating on Ar and Ar/CF₄ mixtures. The plasma parameters determined from the compensated probe characteristics are compared to previous measurements of others made in similar discharges, and to our own measurements of the average electron density derived from electrical impedance measurements.

*Thermosciences Division, Mechanical Engineering Department, Stanford University

†Thermosciences Division, Mechanical Engineering Department, Stanford University

‡Thermosciences Division, Mechanical Engineering Department, Stanford University

§Thermosciences Institute, NASA-Ames Research Center

IWP12 85 Langmuir Probe and Ion Acoustic Wave Velocity Measurement of the Concentration of Two Species in a Multi-Dipole Plasma*

AHMED HALA, *University of Wisconsin-Madison* NOAH HERSHKOWITZ, *University of Wisconsin-Madison* The concentrations of Argon and Xenon ions vs. the Ar/Xe pressure mixture ratios were measured in a multi-dipole DC-filament plasma. Typical parameters of the plasma are electron temperature of 1 eV and plasma density of 10^{10} cm⁻³. The pressure was varied in a range of 1 to 2 mTorr and measured using a capacitance manometer. Two techniques were used to measure the ion concentrations. The first method found the concentration of the species by measuring the ratio of the ion saturation current to the electron saturation current to a two-sided inch planar Langmuir probe assuming that each species are collected with their respective Bohm velocities. The second method found the concentration of one species by directly measuring the phase velocity of the two-component plasma ion acoustic wave through launching ion sound waves from a grid. For an equal neutral pressure mixture of the two gases, the plasma was found to consist mainly of Xenon. Comparison between the two techniques are discussed and results for other species mixture are presented.

*Work is supported by USDOE grant DE-FG02-97ER54437

IWP12 86 Gas Phase Diagnostics in LAPPS D. LEONHARDT, S.G. WALTON,*D.P. MURPHY, W.E. AMATUCCI, R.A. MEGER, R.F. FERNSLER, *Plasma Physics Division, Naval Research Laboratory* NRL is developing a scalable Large Area Plasma Processing System for materials processing applications.^a Using a magnetically collimated sheet of high energy electrons (2-5kV, 10 mA/cm²) to ionize a neutral background gas, a high density plasma of comparable size with cold electrons and ions is produced independent of chamber configuration. This beam ionization process is readily scalable (to meters²) with the limiting factor being the range of the electron beam in the background gas (~ 10 eV/cm). Presently, operating pressures range from 10-500 mtorr with 0-300 Gauss magnetic fields, using a hollow cathode as an electron beam source. Temporally and spatially resolved data from Langmuir probes, optical emission, microwave absorption/

transmission and electron beam analysis of the plasma sheet in recent pulsed operation studies (10-1000 μ s pulse length, < 10 kHz pulse repetition frequency) will be presented for various gas mixtures. Ion densities from 10^9 to 5×10^{12} cm⁻³ are obtained in plasma volumes of $1 \times 30 \times 30$ cm³ in mixtures of oxygen, nitrogen, argon and neon. Overviews and additional details of the LAPPS process will be presented by co-authors.¹

*NRC/NRL Postdoctoral Research Associate

¹See presentations by R. A. Meger, R. F. Fernsler, S. G. Walton and D. P. Murphy at this conference.

IWP12 87 Plasma-Surface Interactions in LAPPS

S.G. WALTON,*D. LEONHARDT, D.P. MURPHY, R.A. MEGER, R.F. FERNSLER, *Plasma Physics Division, Naval Research Laboratory* NRL's Large Area Plasma Processing System (LAPPS) utilizes an electron beam generated plasma for large scale materials processing applications.^a Since the plasma source is independent of the reactor geometry, LAPPS possesses unique processing capabilities including scalability, continuous or pulsed operation, and electrode positioning/biasing options. Investigations of plasma-surface interactions, via in situ measurements of species fluxes to conducting and non-conducting surfaces, are presented for various processing conditions. Incident ion and neutral species are mass and energy analyzed and the relative fluxes are determined for plasmas generated in argon, oxygen, nitrogen, and noble gas mixtures. The dependence of these fluxes on surface location and biasing conditions is also presented. Recent results for oxygen ashing of a photoresist is correlated to the surface fluxes to identify the optimum processing conditions for ideal (isotropic vs. anisotropic) etching. Additional details about LAPPS are presented by co-authors.^a [^a See presentations by D. Leonhardt, D.P. Murphy, R.A. Meger, and R.F. Fernsler at this conference.]

*NRC/NRL Postdoctoral Research Associate

IWP12 88 Cathode Development for LAPPS*

D. P. MURPHY, W. E. AMATUCCI, D. LEONHARDT, S. G. WALTON,†R. A. MEGER, R. F. FERNSLER, *Plasma Physics Division, Naval Research Laboratory* NRL is developing a Large Area Plasma Processing System^a. The plasma generation technique utilizes a sheet electron beam to ionize a low density gas mixture. The beam electrons are confined to a narrow channel by a solenoidal magnetic field. The beam source can be operated in either pulsed or continuous modes. Pulsed beams have been produced at up to 5 keV and 20 mA/cm² using a 60 cm long by 1 cm wide cylindrical, hollow cathode. Continuous electron beam sources using heated filaments are being developed also. The electron beam will enter the reactor from a differentially pumped source either through a narrow slit or through a thin pressure window. Various window materials are being evaluated. 5 keV electrons have a propagation range of several hundred cm in either oxygen or argon/chlorine gas mixtures within the operating pressure range of the reactor. Results of pulsed and cw cathode development will be presented. ^aSee presentations by Meger, Fernsler, Leonhardt and Walton at this conference.

*Work supported by Office of Naval Research

†NRC/NRL Postdoctoral Research Associate

IWPI3 89 Laser Control of Microwave-Driven Filamentary Discharges* RICHARD MILES, PETER BARKER, JIZOU ZOU, SERGEY MACHERET, *Dept. of Mechanical and Aerospace Engineering, Princeton University, Princeton, NJ* Microwave-driven, atmospheric pressure discharges have been shown to consist of numerous sequentially-formed plasma filaments. These filaments occur at random locations and tend to grow to a length corresponding to the half wavelength of the microwave field. After achieving that length, they act as tuned dipole antennas and strongly absorb the microwave radiation. With the use of a focused argon-fluoride laser, it is now possible to control the timing, location, and structure of these filaments. The argon-fluoride laser focused into atmospheric pressure air leads to a filament which forms at the focal region and grows along the laser beam path in a highly repeatable fashion. This growth occurs well after the laser has turned off. Filament growth is driven by the microwave field and a large fraction of the microwave energy is coupled into the filament in the final growth stages. Such filaments may be applicable as high brightness ultraviolet and X-ray light sources.

*Work supported by the AFOSR Plasma Ramparts MURI program

IWPI3 90 Mass Spectrometry of Active Species Convected from an Atmospheric Air Plasma in a Remote Exposure Reactor* D. M. SHEMAN, F. KARAKAYA, Z. CHEN, J.R. ROTH, UNIVERSITY OF TENNESSEE TEAM, The Remote Exposure Reactor (RER)[1] utilizes multiple panels covered with a surface layer of One Atmosphere Uniform Glow Discharge Plasma (OAUGDP) to generate active species from air. These active species are capable of sterilizing the surfaces and increasing the surface energy of materials [1]. Our investigations have shown that the energizing voltage, the RF frequency, the RF power input, the number of panels generating the surface layers of the OAUGDP, and the distance active species are convected from the plasma panels to the workpiece all affect the killing times of microorganisms and other plasma processing effects. The relative concentration of active species will be determined by mass spectrometry and reported as a function of the above plasma parameters and the distance from the last plasma generating panel. Such information will be correlated with the plasma sterilization and surface energy data from the RER in an attempt to determine the agents responsible for sterilization and other effects. 1.) Roth, J. R. et al., "A (RER) for sterilization by plasma active species at one atmosphere." Abstracts, ElectroMed 99, April 12-14, Norfolk, Va., 1999.

*Supported by EEC of Baltimore, MD, under AFOSR contract 98-C-0069, and by the Univ. of TN CMP and TANDEC

IWPI3 91 Formation of Ion-Ion Plasmas SIVANANDA K. KANAKASABAPATHY, L. J. OVERZET, *University of Texas at Dallas* Ion-ion plasmas are almost electron free plasmas, with only positive and negative ions. Ion-ion plasmas are formed in the late afterglow of electronegative discharges and under certain conditions in CW plasmas. Negative ions that can be extracted from ion-ion plasmas have been claimed to reduce charging-induced etch damage. We use a Langmuir probe to study the spatio-

temporal decay of weakly (O_2) and strongly (Cl_2) electronegative afterglows. A modified probe theory that accounts for Bohm flux reduction due to negative ions is used in the early afterglow and OML theory beyond the ion-ion transition. Preliminary results indicate how the lack of sufficient ground reference can lead to an incorrect inference of an ion-ion plasma. We also correlate the incipience of negative wall fluxes to the ion-ion transition using a Quadrupole Mass Spectrometer. This work is based upon work supported by the NSF Grant No. CTS-9713262.

IWPI3 92 Mass spectrometry of atomic and molecular anions from a hot-cathode plasma STEPHEN E. MITCHELL, *Dept. of Physics, Univ. Nevada, Las Vegas* JOHN W. FARLEY, *Dept. of Physics, Univ. Nevada, Las Vegas* Atomic and molecular anions are produced in a hot-cathode discharge, anions are extracted through an aperture in the anode, and negative ion mass spectrometry is employed as a plasma diagnostic. The mass spectrometer samples the volume density of anions in the discharge near the anode. The discharge has a typical pressure of 0.1 Torr, a typical electron emission current of 5 mA, and a bombarding voltage of 75-150 V. The 2-keV beam of anions is mass-filtered by a Wien filter and detected in a Faraday cup. Typical mass-selected ion currents range from pA to tens of nA. The mass spectrometer has a section which allows interrogation of the mass-selected ion beam by a coaxial laser beam for laser photodetachment studies. Our laboratory can handle toxic and explosive source gases, e.g., hydrogen azide (HN_3) or diazomethane (CH_2N_2). Chloride (Cl^-) is readily detected; indeed, trace amounts of $^{35}Cl^-$ and $^{37}Cl^-$ are almost always present, and serve as convenient calibrating ions in the mass spectrum. Supported by DOE EPSCoR

IWPI3 93 Anomalous Transport in Closed and Open-Drift Hall Discharges* MARK CAPPELLI, *Mechanical Engineering Department, Stanford University* NATHAN MEEZAN, *Mechanical Engineering Department, Stanford University* DAN SCHMIDT, *Mechanical Engineering Department, Stanford University* Hall discharges are presently under development for use in space propulsion applications. These discharges exhibit characteristic cross-field transport, which is enhanced by fluctuations in the electric field and plasma density. Our recent electrostatic probe and laser-induced fluorescence measurements in closed-drift coaxial geometry discharges indicate that the effective Hall parameter ranges from 1 - 20. This value is much less than that based on classical electron transport, and while it brackets the value typical of anomalous Bohm transport, it is found to vary significantly along the axial direction of the discharge, increasing to unusually low values near the anode. This high anomalous transport explains in part why we have been able to successfully operate Hall discharges of a linear geometry (with an open Hall current). In this paper, we shall also present recent measurements of time-resolved emission along the anode from which fluctuations in electron density and average electron energy are characterized. The emission measurements are found to be in qualitative agreement with time-averaged measurements of the Hall parameter, indicating that in some operating regimes, there are intense fluctuations in the near-anode plasma regions.

*This research is supported by the Air Force Office of Scientific Research

IWPI3 94 Comparative Study of Ion Sources for Proton Transfer Reactions* G. M. BROOKE, S. POPOVIC, L. VUSKOVIC, *Old Dominion U., Norfolk, VA* Two types of electrical discharges were compared with respect to the efficiency of producing molecular ions for proton transfer reactions in the selective

ion flow tube.¹ The hollow cathode (HC) discharge is capable of producing an intense flux of molecular ions,² but it suffers from dual mode operation and from the contamination from sputtered cathode ions. Inductively coupled plasma (ICP) sources produce an ion flux of lower intensity,³ but they are not contaminated by sputtering and they operate in a single mode. Density profiles and ion flux intensities were measured using a solenoidal ICP source and an HC source containing an argon-water mixture. Data were compared with a kinetic model, and used to optimize the ion production. Preliminary data on proton transfer reactions will be presented.

*Supported by Jeffress Foundation.

¹D. Smith and N. G. Adams, *Adv. Atom. Mol. Phys.* **24**, 1 (1987).

²G. Brooke, S. Popović, and L. Vušković, *Bull. Am. Phys. Soc.* **42**, 1714 (1997).

³G. Brooke, S. Popović, and L. Vušković, *Bull. Am. Phys. Soc.* **43**, 1435 (1998).

IWP13 95 Investigation of the Effect of Different Parameters Governing the Generation of Ozone by Silent Discharge

A.A. GARAMOON, F.F. ELAKSHAR, *Center of Plasma Technology, Faculty of Science, AL-Azhar U., Nasr City, Cairo, Egypt* A.M. NOSSAIR, E.F. KOTP, *Physics Dep., Faculty of Science, AL-Azhar U., Assuit Branch, Assuit, Egypt* Although ozone applications in environment and industry are very important, only little data has been published in the literature on the effect of the different parameters governing the ozone generation. A modification for the ozone generator has been proposed in order to study such effects. A silent discharge ozonizer has been used whereas its design enables the study of concentration improvement. The concentration enhanced by three folds whenever gas pressure is reduced by a factor of two. The concentration increased sharply by increasing the used electrical power at the first stage of the discharge, and then it tends to saturate. This may be related to ozone dissociation at high power. The concentration is optimized at atmospheric pressure using 18 kV-applied voltage. The concentration is doubled also by increasing the gap space by four times. The length, the thickness and the dielectric constant of the insulating materials are found to have a considerable effect on the generated ozone concentration.

IWP13 96 Energetic Negative Ion Production on a W Surface due to Low Energy Incident H^- , H^+ , H_2^+ and H_3^+

B. L. PEKO, *University of Denver* T. M. STEPHEN, *University of Denver* In an attempt to understand the role of incident ion charge state on surfaces resulting in the production of negative species, specularly reflected negative ion production has been investigated for H^+ , H_2^+ , H_3^+ and H^- incident upon a polished polycrystalline W surface. The ions impacted at 72° from the normal at energies ranging from 50 to 500 eV. The experiments were conducted in a cryopumped vacuum system maintained at 10^{-8} mbar. Energy distributions of the secondary species were measured using retarding potential analysis. These distributions are strongly peaked at lower energy and fall off monotonically with increasing energy. Thanks to NASA/Goddard Space Flight Center NAG5-3386 and the William F. Marlar Foundation

IWP13 97 Measurements on the Parameters of Neutron by the DPF Device GUO HONGSHENG, *Southwest Institute of Fluid Physics, P. O. Box 523-51, Chengdu, Sichuan China* We have measured the yield and FWHM of neutron produced by the Dense Plasma Focus (DPF) device. The energy of the capacitance bank is 12.5 kJ. The operating voltage is 25 kV. The measurements are performed by the silver activate counters and scintillant-photomultiplier (ST-PMT) system. At the end of this paper, the error of measurements is also given.

IWP13 98 Vacuum Multipactor Electron Generation

D. M. SHAW, Z. YU, G. J. COLLINS, *Dept. of Electrical Engineering, Colorado State University, Fort Collins, Colorado, 80523* The multipactor effect is a well-known phenomena in rf amplifier vacuum tubes and waveguides, where, under certain resonant conditions, secondary electron emission may multiply and destroy the rf devices. Multipactor effects have been studied for decades in an attempt eliminate this undesired phenomena. Herein, we show that the multipactor effect may be used as a low pressure ($p < 1$ mTorr) vacuum electron source. A multipactor "discharge" is created by applying radio frequency (rf) voltage to one of two parallel 32.8 mm diameter copper disk electrodes spaced 12.5 mm apart. The second electrode is electrically grounded. Around 5 mA of electron current is extracted from the discharge region via a 1 mm diameter sampling hole in the grounded electrode. The measured electron current is unchanged over the pressure range from high vacuum (pressure below 2×10^{-7} Torr) up to 4×10^{-4} Torr air. The energy spectra of electrons emitted from the parallel plate device have been measured over a range of applied rf amplitudes (100 - 400 V) and frequencies (100 - 180 MHz). The emitted electrons typically fall into two energy groups, one at higher energy range, corresponding to the applied rf frequency and amplitude, and the second at energies below 10 eV. Total measured electron current is increased to 0.3 mA using multiple extraction holes in the grounded 8 cm² electrode of the parallel plate experimental configuration.

IWP13 99 Application of rf plasma for treatment of wool*

M. RADETIĆ, D. JOVIĆ, P. JOVANČIĆ, *Faculty of Technology and Metallurgy, University of Belgrade* Z.LJ. PETROVIĆ, *Institute of Physics, Belgrade, Yugoslavia* Capacitively coupled rf plasma was used to treat wool fabrics. We have used pressures in the range of 0.25-0.75 mbar and powers of the order of 100 W. The rf plasma chamber was cylindrical and the central electrode was powered making it a very asymmetric system. The wool fibers were placed on the outer chamber walls which have the radius of 35 cm and which were grounded. The treatment lasted between 0 and 10 minutes in air, oxygen and argon 13.56 MHz plasmas. Even after 2 minutes the properties of the wool have changed sufficiently to match the treatment by chlorination as far as the quality of printing and dyeing goes. In addition fiber swelling, pilling and wettability were also considerably improved. Extended treatment by plasma reduces mechanical properties of wool fibers so limited duration of treatment of 2-5 minutes in oxygen was found to give optimum results. Topography of the fibers was analyzed by using atomic force microscopy and scanning electron microscopy. It was discovered that the improvement was brought about by superficial modification of the fiber through replacement of the fatty layer and partial destruction of the epicuticle.

*Supported by MNTRS 01E03 project.

Invited Papers

16:00

JW1 1 Electron-Impact Excitation out of the Metastable Levels of Rare Gas Atoms.*

CHUN C. LIN, *University of Wisconsin-Madison*

Recent experiments on electron-impact excitation out of the metastable levels of rare gas atoms have revealed many interesting features that are important for understanding the basic nature of the excitation process and for applications. For the case of argon two kinds of metastable atom targets, $1s_3$ ($3p^5 4s, J = 0$) and $1s_5$ ($3p^5 4s, J = 2$), were generated and cross sections for excitation out of each metastable level into various levels of the $3p^5 4p$ configuration ($2p_x$ in Paschen's notation) were measured. The gross features of the magnitude of the cross sections and the shape of the excitation functions are discussed in terms of a multipole field picture and in terms of the vector coupling schemes with special reference to the variations of the results with respect to the total angular momentum J . These features show interesting contrasts to the cross sections for excitation into the $3p^5 4p$ levels out of the ground level, and the results are of particular relevance to the analysis of optical emissions from the $3p^5 4p$ levels in a plasma. Experiments on excitation out of the metastable levels of neon into the $2p^5 3p$ levels have also been performed. The cross sections vary with the individual levels in the same general pattern as the argon data.

*Supported by the National Science Foundation and the Air Force Office of Scientific Research.

16:30

JW1 2 Coincident Electron-Energy-Loss Study of Highly Excited Molecules.

N. KOUCHI, *Tokyo Institute of Technology*

The dynamics and spectroscopy of highly excited molecules have been subjects of current interest since they play an important role as intermediate states in a wide range of atomic and molecular processes, many of which are important in plasmas. Our group has recently developed a new experimental method to investigate this subject, i.e. *the coincident electron-energy-loss spectroscopy*. We measure the electron energy-loss spectra of molecules with the coincidence detection of the atomic fragments ascribed to the neutral dissociation of highly excited molecules, i.e. *the coincident electron-energy-loss spectra*. The coincident energy-loss spectra show rich structures due to the highly excited states of molecules, e.g. superexcited states. We have extensively applied this new method to the study of the highly excited states of molecular hydrogen and nitrogen. It has been clearly shown that the contribution of the forbidden highly-excited states is remarkable, while they are not accessible in the photoexcitation. The dynamics and spectroscopy of these highly excited molecules will be discussed in detail, in particular the competition between the neutral dissociation and auto-ionization.

17:00

JW1 3 Elastic and inelastic electron scattering by laser-excited $^{138}\text{Ba}(\dots 6s6p\ 1P1)$ atoms.*

M.A. KHAKOO, *California State University, Department of Physics, Fullerton, CA 92834, USA*

We present a review of elastic and inelastic electron scattering from laser-excited Barium.¹ The talk will however concentrate on the results of a joint experimental and theoretical study concerning elastic electron scattering by laser-excited $^{138}\text{Ba}(\dots 6s6p\ 1P1)$ atoms are described. These (first such) studies demonstrate several important aspects of elastic electron collisions with coherently excited atoms. From the measurements, collision and coherence parameters, as well as cross sections associated with an atomic ensemble prepared with an arbitrary in-plane laser geometry and linear polarization (with respect to the collision frame), or equivalently with any magnetic sublevel superposition, have been obtained at 20 eV impact energy and at 10° , 15° and 20° scattering angles. The convergent close-coupling (CCC) method was used within the non-relativistic LS-coupling framework to calculate the magnetic sublevel scattering amplitudes. From these amplitudes all the coherence parameters and cross sections at 20 eV impact energy were extracted in the full angular range in 1° steps. The experimental and theoretical results were found to be in good agreement, indicating that the CCC method can be reliably applied to elastic scattering by $^{138}\text{Ba}(\dots 6s6p\ 1P1)$ atoms, and possibly to other heavy elements when spin-orbit coupling effects are negligible. Small but significant asymmetry was observed in the cross sections for scattering to the left and to the right. We also find, thus, that elastic electron scattering by the initially isotropic atomic ensemble resulted in the creation of significant alignment. As a by-product of the present studies, elastic scattering cross sections for metastable ^{138}Ba atoms were also obtained.

*This work was carried out in collaboration with: S. Trajmar, California Institute of Technology, Jet Propulsion Laboratory, Pasadena, CA 91109 and California Institute of Technology, Division of Chemistry and Chemical Engineering, Pasadena, CA 91109, USA; I. Kanik, California Institute of Technology, Jet Propulsion Laboratory, Pasadena, CA 91109, USA; I. Bray, Electronic Structure of Materials Centre, The Flinders University of South Australia, GPO Box 2100, Adelaide 5001, Australia; D. Fursa, Electronic Structure of Materials Centre, The Flinders University of South Australia, GPO Box 2100, Adelaide 5001, Australia; and G. Csanak, University of California, Los Alamos National Laboratory, Los Alamos, NM 87544.

¹S. Trajmar et al. *J. Phys. B: Atom. Molec. Opt. Phys.* **31**, L393-400 (1998).

Contributed Papers

17:30

JW1 4 Electron Interactions with Excited Atoms LOUCAS CHRISTOPHOROU, *NIST* JAMES OLTHOFF, *NIST* The results of a comprehensive review of published experimental and theoretical results on elastic, inelastic, superelastic, total, and differential scattering of electrons by, and electron-impact ionization of, excited atoms will be presented and discussed. The cross sections for low-energy electron interactions with excited atoms are generally much larger than the cross sections for the ground-state atoms. The enhancement depends on the species itself, the excited state, the electron energy, and for differential scattering cross sections on the scattering angle. Experimental data show the dominant role of the electric dipole polarizability in determining the magnitude of the total electron scattering cross section from excited atoms, and Born-calculations show that the cross section for superelastic electron scattering increases as the energy gain in the collision decreases. The large polarizability of excited rare-gas atoms also accounts for the absence of the Ramsauer-Townsend minimum in the electron scattering cross sections of the excited rare-gas atoms.

17:45

JW1 5 Electron Interactions with Excited Molecules LOUCAS CHRISTOPHOROU, *NIST* JAMES OLTHOFF, *NIST* Existing knowledge on the scattering of slow electrons from rovibrationally and electronically excited molecules, and on excitation and ionization by electron impact of electronically excited molecules will be summarized and discussed. The meager data on electron scattering from excited molecules indicate that the cross sections are generally larger than for the ground states. The more abundant data on dissociative electron attachment to rovibrationally excited molecules show large increases in the cross section with increasing total molecular internal energy and vary with the negative ion states involved and their location. Data on nondissociative electron attachment to rovibrationally excited molecules show an enhancement in the thermally induced detachment as the total internal energy is increased. The reported large increases in dissociative electron attachment to electronically excited molecules may in part be due to the higher polarizability of the excited states and the lower energies of the captured electrons, but more reliable methods are needed to quantify the data.

18:00

JW1 6 Polarized Electron Impact Excitation of ArII** H.M. AL-KHATEEB, *University of Nebraska* B.G. BIRDSEY, *University of Nebraska* T.J. GAY, *University of Nebraska* Using beams of transversely polarized electrons, we have studied the simultaneous excitation and ionization of Ar. Both the excitation functions and the Stokes parameters of light emitted by the ArII ($3p^4 4p$)²F_{7/2} and ²F_{5/2} states were measured without detection of the scattered electrons. We find the excitation functions to have a significantly different shape than those measured in earlier studies [1,2], and attribute this difference to strong target pressure dependence. Because the ($3p^4 4p$) manifold is well-LS coupled, we can use Stokes parameter measurements of four different excited states to deduce the quadrupole and hexadecapole moments of the excited $3p^4$ core, as well as the spin orientation of the $4p$ electron. *Work supported by NSF Grant PHY-9732258 [1] P.V.Feltsan and M.M.Pova, *Opt. Spectrosc.* **28**, 199 (1970). [2] P.N.Clout and D.W.Heddle, *J.Phys.B* **4**, 483 (1971).

*Work supported by NSF Grant PHY-9732258

18:15

JW1 7 Dissociative electron attachment to vibrationally and rotationally excited H₂ molecule* Y. XU, I.I. FABRIKANT, *University of Nebraska* Vibrational and rotational state dependence of dissociative attachment in low-energy e-H₂ collisions is studied within the framework of the nonlocal resonance theory. The dynamics of nuclear motion in the nonlocal complex potential is treated by the quasiclassical approach¹, the resonance energy, the width function and the level-shift function are taken from calculations based on the projection operator formalism². Our results for attachment to vibrationally and rotationally excited states are different from previous non-local or local results. In particular, our dissociative attachment cross section exhibits a plateau structure in the energy region above the dissociation threshold, and this structure gets more pronounced with higher v or J . We attribute this behavior to the effect of the vibrational continuum in the dissociative attachment channel which becomes stronger above the dissociation threshold.

*Supported by the National Science Foundation

¹S. A. Kalin and A. K. Kazansky, *J. Phys. B* **23**, 4377 (1990)

²G.A. Gallup, Y. Xu, and I.I. Fabrikant, *Phys. Rev. A* **57**, 2596(1998)

Invited Papers

16:00

JW2 1 Pulsed Power Excitation and Instabilities in Low Pressure Electronegative Discharges.*MICHAEL A. LIEBERMAN, *University of California, Berkeley*[†]

Global (volume-averaged) models of high density, low pressure discharges in attaching (electronegative) gases can provide considerable insight into the time-varying dynamics for both pulsed-power excitation and instabilities. Pulsed-power modulated discharges are under active consideration for materials processing applications. The particle and energy balance equations can be applied to determine the charged particle and neutral dynamics. The time-average electron density can be considerably higher and the electron temperature can be considerably lower than for continuous discharges for the same time-average power. Dissociation rates for production of neutral radicals can be higher or lower depending on the dissociation energies. A pulsed discharge can have the same neutral radical flux to the walls for a reduced average power, and the plasma potential can collapse during the power-off phase, leading to a flow of negative ions to the walls. Inductively driven low pressure discharges are widely used for materials processing. Plasma instabilities at frequencies 2 Hz–200 kHz have been observed in these discharges in attaching gases using time-resolved optical emission, Langmuir probes, and videotape imaging. Instability windows in pressure and driving power are found. A global model of the instability is developed considering negative and positive ion particle balance, electron energy balance, charge conservation, and idealized inductive and capacitive energy deposition. As pressure or rf power is varied to cross a threshold, the instability is born at a Hopf bifurcation, such that oscillations occur having weak modulations of charged particle densities, electron temperature, and plasma potential. Further into the instability zone, strong relaxation oscillations develop between inductive and capacitive modes. The oscillations can be so strong that the potential collapses and negative ions flow to the walls.

*Work supported by NSF Grant ECS-9529658, the Lam Research Corporation, California Industries, the State of California UC-SMART Program under Contract 97-01, and the ANU Space Plasma and Plasma Physics Group.

[†]July – December 1999 at the Research School of Physical Sciences and Engineering, The Australian National University, Canberra ACT 0200.

16:30

JW2 2 Approximation Methods for Plasma-Surface Processes.DAVID GRAVES, *University of California at Berkeley*

Most reactive plasma applications involve some type of surface modification. The largest single application currently is semiconductor manufacturing, where plasmas are used extensively for etching, deposition, stripping, cleaning and other surface processes. There is a continuing interest in developing accurate models and simulations of these low pressure reactive plasma processes. In models of low pressure reactive plasmas, surface interactions appear as boundary conditions. Commonly, the least accurate part of the plasma model is the treatment of surface interactions. Plasma often strongly interact with surfaces that bound it. For example, in semiconductor etching applications, the highly reactive nature of the plasma chemistry results in considerable erosion of the chamber materials, in addition to materials deliberately etched from wafers. The plasma composition, structure and dynamics are substantially changed because of material entering the plasma from surfaces. Furthermore, a common objective in modeling plasmas for semiconductor manufacturing applications is to include predictions of microfeature shape evolution. Within these submicron features, only surface interactions occur since the gas phase collisional free paths greatly exceed feature dimensions. The modeling challenge is to develop rate expressions for surface processes that are sufficiently accurate to match the model objectives. In this talk, I will discuss the challenges of developing self-consistent, physically-based rate expressions for surface processes that can be used as plasma model boundary conditions and in feature profile evolution simulations. I will review the various approximation methods that have been developed to treat plasma-surface interactions, including the concept of a 'sticking coefficient', the modified site-balance approach, and more elaborate models of plasma-surface interactions. Recent results using molecular dynamics and vacuum beam experiments will be used to suggest better approximations for plasma-surface interactions.

17:00

JW2 3 Strategies for Rapidly Developing Plasma Chemistry Models.*MARK J. KUSHNER, *University of Illinois, Dept. of Elect. and Comp. Engr., Urbana, IL 61801 USA*

The development of plasma chemistry models for microelectronics fabrication, lasers, toxic gas remediation and lighting sources has significantly progressed over the past decade. With increasing sophistication in algorithms and increasing access to high performance computing, the use of 2-dimensional and 3-d models for design of equipment and processes is now common. Unfortunately, in many cases, the lack of fundamental data (e.g., electron impact cross sections,

chemical reaction mechanisms) for the systems of interest has resulted in the capability of the computational infrastructure exceeding that of the quality of the database. Given that the timescale required to assemble databases for new chemistries is years whereas the result may be required in months, methodologies are required for assembling reaction mechanisms and databases from what are often fragmentary resources. In this presentation, strategies are discussed for rapidly developing such models and reaction mechanisms using examples from etching and deposition systems.

*Work supported by NSF, SRC and DARPA/AFOSR

17:30

JW2 4 Electron-Impact Ionization Cross Sections for Polyatomic Molecules, Radicals, and Ions.*

YONG-KI KIM, *NIST*

Recent progress in the theory for electron-impact total ionization cross sections of large molecules will be reviewed with emphasis on electron correlation effect and applications to radicals and molecular ions. With the binary-encounter-Bethe (BEB) theory,¹ we found that the electron correlation effect on large molecules, such as C_3F_8 , can be as much as 20%,² while multiple ionization resulting from the creation of deep inner-shell holes contributes 5–10% in SF_6 .³ The BEB cross sections on hydrocarbon radicals are in excellent agreement with available experimental data. However, experimental ionization cross sections for fluorocarbon radicals⁴ are a factor of two lower than the BEB cross sections. The original BEB theory must slightly be modified to apply the theory to molecules with heavy atoms and to molecular ions. These modifications will be illustrated with examples.

*Work supported in part by DOE's Office of Fusion Energy Sciences and NIST's Advanced Technology Program.

¹Y.-K. Kim and M. E. Rudd, *Phys. Rev. A* **50**, 3954 (1994)

²H. Nishimura, W. M. Huo, M. A. Ali, and Y.-K. Kim, *J. Chem. Phys.* **110**, 3811 (1999).

³Y.-K. Kim and M. E. Rudd, *Comments At. Mol. Phys.* **34**, 309 (1999).

⁴V. Tarnovsky and K. Becker, *J. Chem. Phys.* **98**, 7686 (1993)

Contributed Papers

18:00

JW2 5 Numerical Simulation of a Constant Current Density Discharge in a Flowing Plasma GRAHAM CANDLER, MANOJ NAGULAPALLY, *University of Minnesota* CHRISTOPHE LAUX, CHARLES KRUGER, *Stanford University** We will

present numerical simulations of a series of experiments at Stanford University. In these experiments a controlled current density discharge is applied to a 2000 K, atmospheric-pressure flowing nitrogen or air plasma. The resulting electric field, electron concentration, and temperature are measured. We simulate the non-equilibrium plasma by solving the Navier-Stokes equations that have been extended to account for the effect of finite-rate chemical reactions, thermal non-equilibrium, and internal and collisional energy relaxation. The electron energy conservation equation is included, and the energy deposition rate due to the discharge is modeled. This allows the volumetric energy addition rate to be calculated from the local current density and the known applied field. The 2D simulations will be used to determine spatial profiles of electron concentrations as a function of the discharge conditions in the flowing gas. The results will be used to analyze the experimental results and test the reaction kinetics. Additionally, this will help determine if elevating the electron temperature in an atmo-

spheric pressure plasma is a possible means for generating high electron concentrations with low energy input.

*This work is supported by the Air Plasma Ramparts MURI Program managed by the Air Force Office of Scientific Research.

18:15

JW2 6 An effort at parallelizing numerical simulations of plasma discharges.* J.M. TRUXON, YU. SOSOV, J.R. GOTTSCHALK, C.E. THEODOSIOU, *University of Toledo* W. WILLIAMSON, JR., *Embry-Riddle Aeronautical University* We have studied current approaches to numerical simulation of the plasma discharge associated with the firing of a single pixel in a plasma display panel of opposing and co-planar electrode structures. We found that in all methods studied, the adoption of a suitable 3-dimensional model as a basis from which to simulate the pixel results in a prohibitively large number of calculations, which in turn reduces the effectiveness of these methods from an industrial development standpoint. Consequently, we have undertaken the task to pinpoint which areas of a 3-dimensional simulation might be parallelized, with the preliminary goal of reducing the run time of the simulation by fifty to seventy percent. We will present results of our efforts and their implementation in "JSimulator," a particle simulator package.

*Work supported by NSF, Grant ECS-9896103

SESSION KW1: LABORATORY TOURS

Wednesday evening, 6 October 1999; Old Dominion University Campus at 20:00

Invited Paper

8:00

LR1 1 Mechanisms for Dissociative Recombination.

STEVEN GUBERMAN, *Institute for Scientific Research**

Dissociative recombination of molecular ion AB^+ with an electron, e^- is described by $AB^+ + e^- \rightarrow A + B$. To date, dissociative recombination cross sections and rate constants have been determined by theoretical methods for seven molecular ions and their isotopomers. These calculations have shown that dissociative recombination is rich in distinct mechanisms which complement the original direct and indirect mechanisms of Bates¹ and Bardsley², respectively. Each of the new mechanisms will be described with examples from recent calculations. note

*This research is supported by NASA and NSF.

¹D. R. Bates, Phys. Rev. 78, 492 (1950)

²J. N. Bardsley, J. Phys. B 1, 365 (1968)

8:30

LR1 2 Dissociative Recombination of Complex Ions.

J. BRIAN A. MITCHELL, *P.A.L.M.S., U.M.R. du C.N.R.S. No. 6627, University of Rennes I, 35042 Rennes, France*

The FALP-MS apparatus at the University of Rennes allows the measurement of rate coefficients for the recombination of molecular ions to be made (at 300K) even though several ions may be present in the afterglow. The recombination of a number of hydrocarbon ions derived from alkane¹, alkene² and aromatic³ parent molecules has been studied. Despite the wide range of complexity of these compounds, the measured recombination rates are remarkably similar having values in the range of $4 \cdot 10^{-7} \text{ cm}^3 \cdot \text{s}^{-1}$. Plans are being laid for a new version of this apparatus that will allow pre-prepared ions to be injected into the inert buffer gas flow. This will allow reactive ions to be studied as well as halogen containing ions whose recombination rates would normally be masked by electron attachment to their parent gases in a conventional flowing afterglow apparatus. A high temperature modification to the CRESU supersonic flow apparatus⁴ in our laboratory will allow electron attachment to radicals to be studied by means of the mass spectrometric detection of products, Langmuir probe measurement of the electron density in the flow and Laser Induced Fluorescent identification of the radical species. Such measurements are needed for the modeling of semiconductor processing plasmas.

¹Lehfaoui et al. J. Chem. Phys. 106, 5406, 1997.

²Rebrion-Rowe et al. J. Chem. Phys. 108, 7185, 1998.

³Rebrion-Rowe et al. (Submitted to J. Chem. Phys.)

⁴J.L. Le Garrec et al. J. Chem. Phys. 107, 54, 1997.

Contributed Papers

9:00

LR1 3 Collisional Decomposition of SF_6^- by N_2 ILYA DYA-

KOV, BRIAN PEKO, ROY CHAMPION, *College of William and Mary* The widely used gaseous dielectric SF_6 is a potentially potent greenhouse gas. It has been suggested that N_2/SF_6 mixtures might, in some applications, serve as a replacement for pure SF_6 . In order to improve the understanding of dielectric properties of N_2/SF_6 mixtures, total cross sections for electron detachment and collision induced dissociation (CID) have been measured for $\text{SF}_6^- + \text{N}_2$ for relative collision energies $2 < E < 80 \text{ eV}$. Within this energy range, cross sections for electron detachment are small, and CID is the dominant destruction mechanism for SF_6^- . These experimental results are remarkably similar to those obtained earlier for inert gas targets, suggesting that the processes are largely independent of target's structure. Hence, collisional decomposition has been modeled with a two-step mechanism in which collisional excitation of SF_6^- to SF_6^-* is followed by unimolecular decomposition of SF_6^* . Unimolecular decomposition rates are based upon recent thermochemical data and a statistical theory first proposed

by Klots¹. The model results are in qualitative agreement with the experimental observations.¹ C. E. Klots, Chem. Phys. Lett. 38, 61 (1976) This work was supported in part by the U.S. DOE, Basic Energy Sciences, Div of Chem. Sciences

9:15

LR1 4 Collision-induced dissociation dynamics of Ar_2^+ at high levels of vibrational excitation R. A. DRESSLER,* *Air Force*

Research Laboratory, Hanscom AFB, MA 01731Y. -H. CHIU, *Boston College, Newton, MA 02159-1164* D. J. LEVANDIER, *Boston College, Newton, MA 02159-1164* S. PULLINS, *Air Force Research Laboratory, Hanscom AFB, MA 01731* Nonequilibrium plasmas in rarefied flows are highly challenging to model. A key difficulty is the correct implementation of the vibrational energy dependence of collision-induced dissociation (CID) cross sections of diatomic ions at high levels of excitation. We report guided-ion beam measurements of the translational energy dependence of cross sections for the reaction $\text{Ar}_2^+ + \text{Ar} = \text{Ar}^+ + 2 \text{Ar}$. The Ar_2^+ ions are produced in a supersonic jet ion source. Varying the intersection point between the ionizing electron beam and the supersonic Ar jet controls the degree of internal excitation. Photo-

dissociation recoil velocity analysis² is used to determine the vibrational energy distribution of the dimer ions. Model cross sections functions are fit to the experimental CID curves observed for different vibrational energy distributions. The results are compared with currently applied vibrational dissociation models. [2]S. Williams, Y.-H. Chiu, D. J. Levandier, and R. A. Dressler, *J. Chem. Phys.* 109, 7450 (1999)

*Presenting Author

9:30

LR1 5 Production of OH(A) in fast collisions of O with H₂O
DEBBIE LEVIN, *Dept of Chemistry, George Washington University* JAMES DRAKES, *Sverdrup Technology, Inc. / AEDC Group, Arnold AFB* For spacecraft flying in low-earth orbit of 250 to 250 km altitude, typical vehicle velocities with respect to the ambient atmosphere can exceed 7 km/sec. The atmospheric composition is also almost solely atomic oxygen at translational temperatures near 1000K. When the spacecraft thrusters operate, the effluent can attain speeds over 10 km/sec in the lab frame with respect to the atomic oxygen, depending upon the thruster orientation. Reactions between the fast exhaust effluent species, dominated by H₂O, and the atmospheric atomic oxygen can result in the direct generation of product molecules, such as OH, in electronically excited states. A study has been undertaken to examine the product reaction channels for the generation of OH excited states in fast collisions of atomic oxygen with H₂O. A potential hypersurface for H₂O has been used to compute the branching fractions of the collision exit channels using monte carlo molecular dynamics techniques. The results of the computation are compared to the

literature extrapolation of the OH(A) excitation rate. These rates are based upon thermal measurements of the ground state products of O with H₂O, with adjustment to the activation energy to accommodate the increased endothermicity of the electronically excited A₂PI state. The trajectory calculations presented herein will be used to derive a more appropriate rate expression.

9:45

LR1 6 Excitation and Ionization in H(1s)-H(1s) Collisions*
MERLE E. RILEY, *Sandia National Laboratories, Albuquerque, NM 87185* BURKE RITCHIE, *Lawrence Livermore National Laboratory, Livermore, CA 94550* Hydrogen atom - hydrogen atom scattering is a prototype for many of the fundamental principles of atomic collisions. In this work we present approximations to the H+H system for scattering in the intermediate energy regime of 1 to 100 keV. The first approximation ignores electron exchange and two-electron excitation by assuming that one of the atoms is frozen in the 1s state. We allow for the evolution of the active electron by numerically solving the 3D Schroedinger equation. The results capture many features of the problem and are in harmony with recent theoretical studies. Excitation and ionization cross sections are computed and compared to other theory and experiment. New insight into the mechanism of excitation and ionization is inferred from the solutions. The second approximation for H+H consists of a two electron, 3D, exchange, time-dependent, self-consistent field (SCF) approximation. These novel SCF equations will be described along with ongoing results.

*Supported by US DoE under contracts DE-AC04-94AL85000 and W-7405-ENG-48

SESSION LR2: HIGH PRESSURE LIGHTING PLASMAS

Thursday morning, 7 October 1999; York Room Sheraton Waterside Hotel at 8:00

Gerrit Kroesen, Eindhoven University of Technology, presiding

Invited Paper

8:00

LR2 1 Microhollow Cathode Discharge Excimer Lamps.

KARL H. SCHOENBACH, *Physical Electronics Research Institute, Old Dominion University, Norfolk, VA*

Reducing the diameter of the cathode hole in hollow cathode discharge geometry to values on the order of 100 μm has allowed us to extend the pressure range of stable, direct current hollow cathode discharges up to atmospheric pressure. The large concentration of high-energy electrons in the nonthermal discharge, in combination with the high neutral gas density favors three-body processes such as rare gas excimer formation. Excimer emission in argon and xenon discharges peaking at 130 nm and 172 nm, respectively, was observed with an efficiency for xenon excimer emission between 6% and 9% in a pressure range from 250 Torr and 450 Torr. Typical forward voltages are 200 V at dc currents of up to 8 mA. Pulsed operation allowed us to extend the current range in xenon discharges to 80 mA. At pressures in the hundreds of Torr range the source of the excimer radiation extends over an area of several times the cathode opening. With increasing pressure the source is reduced in size and eventually, at pressures exceeding atmospheric becomes confined to the cathode opening. For a specific pressure the radiative power increases linearly with current at constant radiant emittance. For atmospheric pressure discharges in xenon the radiative emittance is approximately 20 W/cm². In addition to operating the discharge in rare gases, we have also explored its use as rare gas-halide excimer source. In a gas mixture containing 1% ArF we were able to generate stable dc discharges in flowing gas at pressures ranging from 100 Torr to atmospheric pressure. The spectra of the high-pressure ArF discharges are dominated by excimer radiation peaking at 193 nm. The excimer emission of an ArF discharge at 700 Torr was measured as 150 mW. With a discharge voltage of 500 V, and a current of 10 mA the efficiency is 3%. Parallel operation of the micro-discharges by means of a resistive anode offers the possibility to use microhollow cathode discharge arrays as dc-excimer lamps, with estimated power densities exceeding 10 W/cm². -This work is funded by the Department of Energy, Advanced Energy Division, and by the National Science Foundation.

8:30

LR2 2 Spatial Distribution of the Excimer Emission from Microhollow Cathode Discharges A. EL-HABACHI, M. MOSELHY, K.H. SCHOENBACH, *Old Dominion University, Norfolk, VA 23529* Microhollow cathode discharges in xenon and argon are intense sources of excimer radiation [1]. Its efficiency peaks at 400 Torr (xenon). The discrepancy between the results of spatially integrated measurement and a zero-dimensional model [1], which predicts a monotonous increase in radiant power with pressure, is assumed to be due to finite area of the source. The spatial distribution of the excimer source was studied by means of a VUV imaging system. At low current (resistive discharge mode) the radiation is emitted from a well-defined area at the circumference of the cathode hole. At a threshold current the discharge switches into a negative differential resistivity mode and the plasma expands into the area outside the cathode hole. The radius of the emitting area outside the hole increases with current and decreases with pressure. The average radiant emittance increases monotonously with pressure up to 20 W/cm² at atmospheric pressure, confirming the results of the zero-dimensional model. This work is supported by DoE and NSF. [1] A. El-Habachi and K. H. Schoenbach, *Appl. Phys. Lett.* 73, 885 (1998).

Invited Paper

9:00

LR2 4 Characteristic Curves of a coupled Power Supply and Gas Discharge.
KLAUS GUENTHER, *OSRAM GMBH, Berlin, Germany*

The electric characteristics of conventional and electronic power supplies is discussed for the most important types of electrical output circuits and the size of their components. The electric behaviour of a gas discharge is determined by the condition of the plasma (i.e. the number densities of the different kinds of particles and their energy distributions) and its spatial distribution. The equilibrium condition is derived from the balance of Ohmic heating, radiation and heat conduction losses. The response of the discharge to transient changes of the power supply parameters as voltage or frequency can be understood considering the time constants of important elementary processes. Examples demonstrate the use of these effects for the optimization and stabilization of the photometric properties of HID lamps.

Contributed Papers

9:30

LR2 5 Reaction Kinetics in cw Rare-Gas Halogen Lamps M. SALVERMOSER, *Department of Physics, Rutgers University, Newark NJ 07102* D.E. MURNICK, *Department of Physics, Rutgers University, Newark NJ 07102* A. ULRICH, *Physics Department E12, Technische Universitaet Muenchen, Germany* J. WIESER, *Physics Department E12, Technische Universitaet Muenchen, Germany* Pumping with a continuous low energy (< 20keV) electron beam sent through thin ceramic foils into high pressure excimer gas mixtures, the reaction kinetics leading to efficient vuv emission from ArF and F₂ at 193nm and 157nm respectively has been studied. The scaling of the pumping power density with energy to the inverse 2.5 power and cube of the pressure allows a wide range of pumping rates to be considered. And, by studying the spectrum and yield as a function of pressure and gas mixture, optimum conditions for vuv emission can be determined and specific formation and quenching channels can be isolated. Energy transfer efficiency near 10% has been obtained at 193nm for neon-argon-fluorine (1:0.008:0.0004) mixtures and at 157nm for neon-fluorine (1:0.002) at two to three bar pressure. Lamps emitting tens of milliwatts light output from a 0.8mm diameter point have been stable for tens of hours. Scaling to at least 10W/cm²str continuous output is possible.

8:45

LR2 3 Spectroscopic Study of High Pressure Microhollow Cathode Discharges in Argon* U. ERNST, K. FRANK, *University of Erlangen-Nuremberg, Physics Department I, Erwin-Rommel-Str. 1, 91058 Erlangen, Germany* W. HARTMANN, *Siemens AG ZTEN3, Corporate Technology, Paul-Gossen-Strasse 100, 91050 Erlangen, Germany* Reducing the diameter of the cathode opening to values on the order of 100 μm in microhollow cathode discharges allows to operate stable d.c. glow discharges in argon at atmospheric pressure. Current densities up to 100 A/cm² were observed at forward voltages around 200V and discharge currents up to 10mA. Microhollow cathode discharges have proven to be an efficient source of excimer radiation using noble gases. In order to generate excimer radiation in argon at 127 nm, a reasonable large number of high energy electrons (around 10 eV) at high pressure is necessary. To get more information about plasma parameters like electron density and temperature, the spectral light emission at wavelength between 120 and 900 nm was investigated using a monochromator for the vacuum ultraviolet and the visible range. First results regarding the spectral light emission of high pressure microhollow cathode discharges and the observed plasma properties will be presented.

*Funded by DFG FR1273 and Siemens AG Erlangen, Germany

9:45

LR2 6 A Molecular and Atomic Radiative Transfer Module for the General Plasma Model Plasimo HARM VAN DER HEIJDEN, ROBERT HOOGLAND, JAN VAN DIJK, JOOST VAN DER MULLEN, *Department of Applied Physics, Eindhoven University of Technology, The Netherlands* The general modular 2D plasma model Plasimo is being developed to model a wide range of plasmas, including cascaded arcs and inductively coupled plasmas (ICPs). With the introduction of modules for inductively coupled and microwave powered lamps, Plasimo can also be used to simulate these light sources. The work on light source plasmas necessitated the addition of a radiative transfer module. The radiation module calculates local absorption and emission properties at discrete frequencies. For atomic lines, each line profile is sampled with about twenty points while for high pressure (near) LTE molecular spectra, such as seen from the Sulphur lamp and high pressure Sodium discharges, points are sampled from a continuous classical Franck-Condon spectrum. Using the formulation of discrete frequencies, the radiation transport code is able to treat both atomic and molecular transitions in the same way. The effects of radiative transfer are calculated by integrating the radiative transfer equation along well-chosen lines in the plasma. Although Plasimo works with a 2D grid, due to the nature of radiative transfer the transfer properties are calculated in fully three dimensions. Results will be presented of Sulphur lamp (molecular) spectra.

Invited Papers

10:30

MR1 1 Electron Impact Ionization of Molecules for Plasma Processing.MARTIN SCHMIDT, *Institut für Niedertemperatur-Plasmaphysik, Fr.-L.-Jahn-Str. 19, 17489 Greifswald, Germany**

Plasma processing is successfully used in plasma etching, thin film deposition, surface cleaning and surface treatment. One fundamental process in low temperature plasmas is the electron impact ionization of molecules and atoms. This report deals with the methods and results of measurements of the partial and total ionization cross sections of precursor molecules used in plasma etching (halocarbons, fluorine-bearing compounds: CF_4 , C_2F_6 , NF_3) and thin film deposition (silicon-bearing compounds SiH_4 , $\text{Si}(\text{CH}_3)_4$, $\text{Si}(\text{OC}_2\text{H}_5)_4$, $\text{Si}_2\text{O}(\text{CH}_3)_6$ and metal-containing compounds TiCl_4 , $(\text{C}_5\text{H}_5)\text{Pt}(\text{CH}_3)_3$, $(\text{CH}_3\text{C}_5\text{H}_4)_2\text{Fe}$, $(\text{CH}_3\text{C}_5\text{H}_4)_2\text{Ru}$). The measurement of partial ionization cross sections requires the application of mass spectrometry (or some other means of mass selection). Here results received with a double focussing E-B mass spectrometer and with a time-of-flight instrument are presented. The influence of kinetic excess energies of the fragment ions and of pyrolytic decomposition of the target gas on the cross section measurements are discussed. A short review of cross section measurements of free radicals with the fast-beam-technique is given. The results are compared with calculations of the total ionization cross section using additivity rules, semi-classical and semi-empirical formulae, and the BEB method.

*I greatly appreciate the contributions to this work of R. Basner, K. Becker, H. Deutsch, and V. Tarnovsky.

11:00

MR1 2 Electron Impact Ionization Calculations Avoiding the Three-Body Coulomb Asymptotic Form.C. WILLIAM MCCURDY, *Lawrence Berkeley National Laboratory*

The low-energy electron impact ionization problem has resisted accurate numerical treatment for decades because the formal theory of break-up with Coulomb interactions does not provide a viable path for computational approaches. A general method will be described for computing electron impact ionization cross sections which avoids any appeal to the three-body Coulomb asymptotic form. The approach involves exterior complex scaling of the electronic coordinates and direct calculation of the outgoing flux for two electrons. Results will be presented for singly and triply differential ionization cross sections for electron impact ionization of atomic hydrogen, as well as for the Temkin-Poet and other model break-up problems. In addition we will discuss the relationship of this approach to convergent close coupling (CCC) calculations on break-up and ionization processes. By projecting the wave function from our exterior complex scaling calculations onto the close coupling representation, the origin of the "step function" oscillations in CCC calculations will be demonstrated.

11:30

MR1 3 Electron-Impact Ionization of Atomic Ions.*M. S. PINDZOLA, *Department of Physics, Auburn University, AL 36849†*

Both time-dependent and time-independent close-coupling methods are employed to investigate the electron-impact single and double ionization of atoms and their positive ions. The time-dependent method is based on the propagation of wavepackets involving two or three active electrons. Final time projections of the double continuum yield single ionization cross sections, while projections of the triple continuum yield both single and double ionization cross sections. The time-independent method is based on an R-matrix solution of a two active electron wavefunction constructed as an antisymmetrized product of Sturmian pseudo-orbitals and zero-derivative box orbitals. Domain partitioning of the wavepacket and the R-matrix Hamiltonian allows scaling of both methods on distributed-memory parallel computers. Cross sections for the electron-impact single ionization of Be^+ , B^{2+} , and C^{3+} are compared with crossed-beams experimental measurements. Cross section ratios for the electron-impact single and double ionization of the Temkin-Poet model for He are also compared with experiment.

*Work supported in part by the U. S. Department of Energy and the National Science Foundation

†Collaborators include D. M. Mitnik and F. J. Robicheaux of Auburn University, D. C. Griffin of Rollins College, and N. R. Badnell of the University of Strathclyde.

Contributed Papers

12:00

MR1 4 Electron induced ionization and dissociation of molecular ions SARA MATT, *Institute for Ionphysics, University of Innsbruck, Austria* RAINER DAVID, *Institute for Ionphysics, University of Innsbruck, Austria* ALEKSANDER STAMATOVIC, *Institute for Ionphysics, University of Innsbruck, Austria* PAUL SCHEIER, *Institute for Ionphysics, University of Innsbruck, Austria* TILMANN MAERK, *Institute for Ionphysics, University of Innsbruck, Austria* The present study is devoted to the quantitative investigation of electron-induced ionization and dissociation reactions of molecular ions using a novel experimental technique developed in our lab. These reactions are of importance in plasmas where step-wise ionization and dissociation reactions can occur at appreciable rates and thus strongly influence the plasma properties. We have extended studies for the case of electron-induced dissociation reactions of molecular ions from the mere measurement of cross section functions to the simultaneous determination of the kinetic energy distribution (KED) of the product ions formed and the corresponding cross section q . This allows us to obtain three-dimensional plots of the single differential cross section dq/dW versus incident electron energy E and product ion kinetic energy W .

12:15

MR1 5 Calculation of Electron-Impact Ionization Cross Sections of Molecules Using the DM Formalism H. DEUTSCH, *Univ. Greifswald, Germany* K. BECKER, *Stevens Institute of Technology, Hoboken, USA* T.D. MAERK, *Univ. Innsbruck, Austria* Much emphasis has been devoted recently to the experimental determination of absolute electron-impact ionization cross sections of molecules and radicals due to the importance of these cross sections in many applications. Supporting calculations have been lagging to some extent. Due to the complexity of such calculations simplistic additivity rules and semi-empirical methods have often been used. More rigorous methods, i.e. methods that incorporate some quantum mechanically calculated quantities include the BEB formalism of Kim and co-workers, the method of Khare and collaborators, and the semi-classical Deutsch-Maerk (DM)-formalism. We report results of a comprehensive comparison of calculated ionization cross sections for molecules and radicals using the DM-formalism with available experimental data and with available BEB calculations and results from the application of the model of Khare and co-workers. Targets include hydrocarbon and fluorocarbon compounds, radicals and simple di-, tri-, and polyatomic species. *Work supported by OEW-EURATOM Assoc., FWF, OENB, BMWV, and the US DOE.

SESSION MR2: SURFACE WAVE PLASMAS

Thursday morning, 7 October 1999; York Room Sheraton Waterside Hotel at 10:30

I. Ghanashev, Nagaya University, presiding

Invited Papers

10:30

MR2 1 Applications of surface-wave discharges.MICHEL MOISAN, *Groupe de physique des plasmas, Université de Montréal, Montréal H3C 3J7, Québec*

Surface-wave discharges (SWDs) belong to the category of high-frequency (HF) discharges where the sustaining electric field is provided by a wave that creates its own propagating medium. This behavior means a strong self-consistent interaction between the wave field and the discharge, an interesting feature for modeling. Another feature of SWDs is their operating conditions (frequency, discharge vessel configuration and dimensions, gas pressure and composition) which are the widest of all HF discharges. Because of these properties, the initial "application" of SWDs has been modeling, which has improved considerably our insight into all HF discharges. Recent technical developments¹ on SWD plasma sources in Japan and Germany have largely extended their possible applications by introducing flat SWDs and also very large diameter SWDs. Points to be raised are: 1) the superiority of SWDs over other HF discharges for applications in general and 2) applications eventually unique to SWDs. The superiority of SWDs stems from the unprecedented stability and wide-band impedance matching of this plasma source with the generator, extreme flexibility of operating conditions, possibility of achieving large plasma volume and the highest plasma density. However, there appears to be only one application feature restricted to SWDs, which is the setting of the plasma column length by merely adjusting the HF power level to the field applicator (wave launcher), which translates into optimizing the residence time for achieving appropriate chemical reactions in the plasma. The various categories of existing SWD applications are reviewed.

¹M Moisan, J Hubert, J Margot and Z Zakrzewski, The development and use of surface-wave sustained discharges for applications, in *Advanced Technologies Based on Wave and Beam Generated Plasmas*, eds. H. Schlüter and A. Shivarova, Kluwer 1999.

11:00

MR2 2 Mechanisms of Wave-discharge Self-consistency in Surface Wave Produced Plasmas.A. SHIVAROVA, *Faculty of Physics, Sofia University, BG-1164 Sofia, Bulgaria*

The surface-wave sustained discharges with their clear manner of unification of plasma- and wave field- characteristics provide very good basis for studying the self-consistency of high-frequency discharges, in general. In the talk, discharge production by surface wave propagation in stationary and pulsed regimes as well as stationary discharge maintenance by Trivelpiece-Gould mode are discussed. Models of diffusion-controlled discharges in the frameworks of the fluid plasma theory are reviewed. The nonlinear processes (step ionization and recombination) in the charged particle balance or the

longitudinal diffusion are specified in the various cases as being the main mechanisms which interrelate the plasma parameters to the maintenance field intensity. Locality/nonlocality of the electron heating make the difference between self-consistency considered as a relation of the plasma parameters to the maintenance field intensity or to the wave field intensity. In all the cases covered, results for the self-consistent axial structure of the discharges are presented and commented.

Contributed Papers

11:30

MR2 3 Slot-Antenna Excitation of Single and Multi-Mode Surface-Waves in Bounded Planar High-Density Plasmas IVAN GHANASHEV, HIDEO SUGAI, *Nagoya University* Slot-antenna excited planar surface-wave (SW) plasmas can be and are already used for dry processing of large-area flat objects, in particular in Japan.¹ One can operate them in single-mode or multi-mode regimes. The single-mode regime can be obtained only at specific conditions by fine-tuning the control parameters. It has attracted much attention recently because of its easy-to-analyze eigenmode light-emission patterns at discrete plasma densities, which can be predicted by an analytical eigenmode computation,² neglecting the presence of the slot-antennas. For general conditions single mode operation is difficult to obtain due to overlapping resonances of more than one eigenmodes, resulting in multi-mode operation. In order to understand these two SW plasma regimes we analyze theoretically the SW excitation taking into account the presence of the slot antennas. Since the electric field pattern in slots with simple geometry is known to depend only weakly on the slot environment, we treat this field as a (known) source, which allows us to compute the amplitudes of the various SW eigenmodes in the plasma. The relative eigenmode intensities, the total field energy and the absorbed power are shown to vary when changing the plasma density. Cases of single and multi-mode operation are demonstrated.

¹Sugai, Ghanashev, Nagatsu: *Plasma Sources Sci. Technol.* 7 (1998) 192

²Ghanashev, Nagatsu, Sugai: *Jpn. J. Appl. Phys.* 36 (1997) 337

11:45

MR2 4 Propagation of surface waves in two-plasma systems bounded by a metallic enclosure JOËLLE MARGOT, LUC STAFFORD, *Physics Department, Université de Montréal, Montréal, Qc, H3C 3J7* TUDOR W. JOHNSTON, *INRS-Energie et Matériaux, Varennes, Qc, J3X 1S2* The excitation of surface waves (SW) has been the object of intensive research over the last twenty to thirty years because of their interest in sustaining plasmas under various experimental conditions and configurations. Since the pioneering work having reported the theoretical existence of surface waves in 1959 (Trivelpiece and Gould), it is commonly believed that such waves only exist in plasmas bounded by a dielectric layer. However, some recent numerical and experimental investigations by the groups of Birdsall and Sugai, respectively, indicate that surface waves can be excited in plasmas bounded by a metallic enclosure, the plasma sheath then acting as a dielectric layer. In this presentation, we generalize the theory of surface waves to plasma-plasma-metal configurations in cylindrical geometry. Using a full electromagnetic approach in the cold plasma approxi-

mation, we search for SW or pseudo-SW solutions (i.e. solutions that tend toward pure surface waves when the permittivity of the outer plasma approaches unity). We thus determine the dispersion and attenuation characteristics of the waves. We explore situations in which the inner plasma column is either overdense or underdense and we investigate the influence of a magnetic field axial to the plasma columns.

12:00

MR2 5 Surface Wave Plasma Driven by Ring Dielectric Line for Producing Dense, Large Area, Uniform Plasmas NAOKI MATSUMOTO, *Sumitomo Metal Industries Ltd.* Surface Wave excited Plasma (SWP), has been put into practice as a plasma source for the fabrication process of ULSI and LCD devices. This plasma has several advanced features: 1) Very high electron density with relatively low electron temperature; 2) Very uniform plasma density over large areas; 3) Operation from gas pressure of few mT to the order of thousands of mT. We present a newly developed microwave driven surface wave plasma source called a Ring Dielectric Line (RDL). The RDL is a metal ring wave-guide, filled with dielectric material, driven by a microwave. Slots for coupling the microwave power are symmetrically arrayed under the dielectric, facing towards the processing chamber. The electromagnetic power generates an electromagnetic surface wave, which in turn excites a plasma surface wave on the bottom side of the quartz plate in the processing chamber. In terms of its plasma characteristics, the uniformly distributed argon plasma with wide range of pressure of 20, 40 and 80mT as well as with high density about $5 \times 10^{17}/\text{m}^3$ over the cutoff density was observed. The electron temperature was about 2eV. In addition, in the 5000-minutes continuous running test for C_4F_8 etching, it achieved repeatability of $\pm 0.7\%$ and non-uniformity of about $\pm 3\%$.

12:15

MR2 6 On Azimuthal Perturbations in Microwave Discharges at Elevated Pressures HANS SCHL+APW-TER, *Ruhr-Universität Bochum, Institut für Experimentalphysik II* ANDREI V. MAXIMOV, *University of Alberta, Institute of Theoretical Physics* A model of azimuthal perturbations in cylindrical microwave discharges is presented. Instability is shown to be caused by diffusion driven by electron pressure gradients. It might provide a mechanism for the onset of filamentations in surface-wave-sustained discharges. A window for instability exists at medium azimuthal mode numbers, provided the electron density is high enough. Estimates for the influence of radial diffusion are given, and the validity of simplifications made are examined on the basis of scale considerations. The role of recombination entering at high electron densities is discussed.

Invited Papers

13:30

NR1 1 Ionization of and electron capture from He and D₂ studied with COLTRIMS.*C.L. COCKE, *J.R. Macdonald Laboratory, Physics Dept., Kansas State University, Manhattan, KS, 66506*

The COLTRIMS (COLd Target Recoil Ion Momentum Spectroscopy) approach to final-state momentum imaging is now being widely used in at least a dozen accelerator and synchrotron-radiation laboratories in the world and its use is growing rapidly. The technique combines fast imaging detectors with a supersonically cooled gas target to allow the charged particles from a collision, including both recoil ions and electrons, to be collected with extremely high efficiency and with fully measured vector momenta. It allows the investigation of correlations between the momenta of the ejected fragments and in some cases the identification of collective modes of disintegration. When molecular targets are used, it allows the a posteriori determination of the alignment of the molecule at the time of the collision. We will discuss the use of this approach to study photo- and charged-particle ionization of He and D₂ as well as electron capture from these targets by singly and multiply charged projectiles.

*This work was carried out in collaboration with: M.A. Abdallah (1), Matthias Achler (2), H. Braeuning (2), Angela Braeuning-Deminian (2), Achim Czasch (2), R. Doerner (2), A. Landers (1,5), V. Mergel (2), T. Osipov (1), M. Prior (3), H. Schmidt-Boecking (2), M. Singh, T. Weber (2), W. Wolff (4), and H.E. Wolf (4). Supported by the Division of Chemical Sciences, Office of Basic Energy Sciences, Office of Science, U. S. Department of Energy. [(1) J.R. Macdonald Laboratory, Physics Department, Kansas State University, Manhattan, KS 66506; (2) Institut fuer Kernphysik, Univ. Frankfurt, August-Euler-Str. 6, D-60486 Frankfurt, Germany; (3) Lawrence Berkeley National Laboratory, Berkeley, CA 94720; (4) Instituto de Fisica, Universidade Federal do Rio de Janeiro Caixa Postal 68.528, 21945-970, Rio de Janeiro, Brazil; (5) Physics Dept., Western Michigan University, Kalamazoo, MI 49008]

14:00

NR1 2 Dissociative Electron Impact Processes in Molecules.PHILIP C. COSBY, *Molecular Physics Lab, SRI International, 333 Ravenswood Ave, Menlo Park CA 94025*

This abstract not available.

Contributed Papers

14:30

NR1 3 Absolute Cross Section for the Formation of N₂⁺(X) Ground-State Ions Produced by Electron Impact on N₂ N.

ABRAMZON, K. BECKER, *Stevens Institute of Technology, Hoboken, USA* R.B. SIEGEL, *NIST, Gaithersburg, USA* A combination of electron scattering techniques and laser-induced fluorescence (LIF) techniques was used in an absolute experimental determination of the N₂⁺(X) ionization cross section as a function of electron energy from threshold to 200 eV. N₂⁺ ground-state ions, resulting from electron impact on N₂, are detected by LIF of the N₂⁺ transition at 391 nm. The relative cross section obtained from LIF spectra taken at different electron energies is put on an absolute scale by calibration relative to the well-known electron-impact cross section for the formation of He atoms in the 2 3S metastable state from the ground state. The He 2 3S atoms are probed by LIF at 389 nm in the same apparatus using the same equipment and method that is used in the N₂⁺(X) cross section determination. Our cross section peaks at 60 eV with a value of about 80 × 10⁻¹⁸ cm² which has an uncertainty of 10% with two other recent determinations/estimates of this cross section. * Work supported by NSF and NASA.

14:45

NR1 4 Dissociative Electron Attachment to Laser-Excited Benzene* CUMALI TAV, *UT/ORNL LAL PINNADUWAGE, ORNL/UT* We have conducted comprehensive measurements on enhanced electron attachment to ArF and KrF laser excited benzene in the presence of Ar and N₂ buffer gases. At both these laser

lines, two-photon absorption leads to excitation of benzene to energies above its ionization potential. These excitations have been shown to lead to the population of long-lived, core-excited Rydberg states of benzene¹ in addition to the ionization of benzene. Present measurements on the dependency of negative ion yield on laser fluence, benzene pressure, buffer gas pressure, etc. verify that the observed negative ions formation is due to the attachment of the photoelectrons to the concomitantly produced Rydberg states. Furthermore, the ionization yield at the ArF laser line was dependent on the N₂ pressure, but was independent of the Ar pressure. This is likely to be due to the collisional stabilization of "hot benzene" produced at the one photon level at the ArF line only in the presence of N₂.

*Research sponsored by the DOE EMSP program. ORNL is managed by the Lockheed Martin Energy Research Corporation for the US DOE under contract number DE-AC05-96OR22464.

¹L.A. Pinnaduwege and Y. Zhu, *Chem. Phys. Lett.*, 277 (1997) 147.

15:00

NR1 5 Dissociative Recombination of He₂⁺ L. COMAN, M. GUNA, L. SIMONS, KENNETH A. HARDY, *Florida International University, Miami, Fl, 33199** The final product states of the dissociative recombination (DR) of He₂⁺ have been studied by time of flight (TOF) spectroscopy. DR final product state atoms

were seen in six final product states, and from the $V = 2,3,4$, and 5 vibrational levels of the molecular ion. The energy resolution of the TOF method is sufficient to separate the rotational levels built of these vibrational states. Rotational states up to $J=15$ were observed. From the rotational states observed, we made the first

measurements of the rotational constants of the molecule, and find that the vibrational constants are in reasonable agreement with those predicted by theory.

*The authors thank NASA for support under grant NAG 5 3826

SESSION NR2: GLOWS

Thursday afternoon, 7 October 1999; York Room Sheraton Waterside Hotel at 13:30; R. Winkler, INP Greifswald, presiding

Invited Paper

13:30

NR2 1 The Electron Emission and Micro Plasma Formation on a Ferroelectric Disk.

KOICHI YASUOKA, *Tokyo Institute of Technology*

The pulsed electron source using a ferroelectric cathode can easily produce an electron beam of high current density with relatively low driving voltage. The originally proposed mechanism in which the screening electrons captured on the surface of the ferroelectric cathode were pulled away by coulomb potential of spontaneous polarization is not adequate to explain the experimental data. It has been shown that the surface plasma triggered by a reversal of spontaneous polarization is crucial for the electron emission. Microscopic studies have been conducted from a point of view on the mechanism of ferroelectric electron emission (FEE) under the influence of surface microstructures. Commercially available disk shaped PZT ceramics of 500 μm thickness are used as cathodes materials. The gold electrodes were deposited; fully solid on the bottom surface and grid electrode of 100 μm width and 300 μm separations on the top surface. Negative pulsed voltage with the rise time of 100 ns is applied to the bottom electrode. The grid electrode is grounded. The electron emission current is measured at the collector plate mounted above the grid electrode, without accelerating voltage. The luminescence is always observed around the grid electrode whenever the electron emission occurs. The luminescence points are mostly found not on the edge of the grid electrode but on the cutoff points of grid electrode. Many micro cracks are formed near the cutoff points due to the mechanical stress caused by the voltage applications. By scratching the surface of a new cathode having no cracks, however, the light emission and the electron emission are both observed. The data showed above implies that the surface microstructure is one of the important factors for triggering the surface plasma and electron emission.

Contributed Papers

14:00

NR2 2 Charged Species Transport in the Afterglow of Electronegative Plasmas IGOR KAGANOVICH, DEMETRE ECONOMOU, *Plasma Processing Laboratory, Department of Chemical Engineering, University of Houston, 4800 Calhoun Rd., Houston, TX 77204-4792* The spatio-temporal profiles and wall fluxes of charged species during the afterglow of an electronegative discharge have been investigated. Electronegative plasma decay occurs in two stages. During the first stage, electrons dominate plasma diffusion and negative ions are trapped by the electrostatic fields; the flux of negative ions at the wall is zero. Theories for plasma decay have been developed for equal and strongly different ion (Ti) and electron (Te) temperatures. In the case $T_i = T_e$, and when detachment is important in the afterglow, the product of detachment frequency to ion diffusion time critically affects behavior. If this product is greater than unity, negative ions are converted to electrons during their diffusion towards the wall. The presence of these electrons results in "self-trapping" of negative ions, due to emerging electric fields; the negative ion flux at the wall is very small. In the case $T_i \ll T_e$, negative ion fronts form inside the plasma and move towards the wall in the afterglow with nearly constant velocity (assuming that Ti and Te remain constant). During the second stage of the afterglow, electrons have

disappeared and ions diffuse to the wall with the ion-ion ambipolar diffusion coefficient.

14:15

NR2 3 Multiphoton Resonant Enhanced Ionization of Neutral Argon*

ZHEN TANG, RICHARD B. MILES, *Dept. of Mechanical and Aerospace Eng., Princeton Univ.* Multiphoton ionization of neutral argon is being explored as a method to control air plasmas. The resonant multiphoton ionization process in naturally occurring argon is a potential scheme for providing a long ionized channel through the atmosphere, which can be used for the control and guiding of electrical discharges. We will present a preliminary theoretical model and an experimental study on a very promising $3+1$ ionization in neutral argon. The output of a frequency tripled, injection seeded Ti: Sapphire laser was focused to an argon sample cell. REMPI process was monitored by the ionization current through a pair of electrodes. Photo-ionization of argon is greatly enhanced by a three photon resonance between the $3p^6 \ ^1S_0$ and $3p^5 \ 3d \ [5/2]_3$ states of argon at 261.27 nm. The argon pressure was 0-100 torr. A model based on four dominant channels to reach ionization is used to estimate the electron number density in the laser focus region. We outline a method to evaluate the numerical value of the three-photon transition probability from the atomic parameters of argon. The ionization process is modeled by a simple quantum defect approximation.

*Supported by the Plasma Rampart Program of DOD/AFOSR MURI

14:30

NR2 4 E - H discharge mode transition in pulse-modulated inductively coupled plasmas MANABU EDAMURA, *National Institute of Standards and Technology* ERIC BENCK, *National Institute of Standards and Technology* Pulse-modulated plasmas are attractive for plasma etching processes because it provides additional control of the etching. In particular, it has the potential to reduce surface charging damage of devices through the creation of negative ions. But for relatively long pulses, an E mode discharge is found after the start of the rf power (G. A. Hebner, et al., *J. Appl. Phys.* 82, 2814, (1997)), which may cause charging damage of devices and reduced repeatability of etching processes. In this work, the E mode to H mode discharge transition in pulse-modulated O₂/Ar plasmas generated by GEC-ICP cell was studied by Langmuir probe technique. For a 2ms pulse-cycle with a 95E-mode continued almost a half of the pulse cycle before switching to the H mode. Time-dependent electron temperature measurements showed a large spike in the electron temperature at the start of E mode and another broader, lower intensity spike at the transition to H mode. The average electron temperature of the E and H modes were almost the same while electron densities were significantly different. Time-dependent electron energy distribution functions (EEDFs) were also obtained from the probe measurements. In the E mode, the EEDF had two maxima. The lower energy maxima appears to be comprised of low energy electrons left over from the afterglow plasma.

14:45

NR2 5 Modeling of Air Plasmas Generated by Electron Beams: "Fountain" and "Thunderstorm" Discharges SERGEY O. MACHERET, MIKHAIL N. SHNEIDER, RICHARD B. MILES, *Dept. of Mechanical and Aerospace Eng., Princeton University* We suggest a method of using electron beams to generate plasmas at high or moderate pressure. When injected into a gas, electron beams generate not only plasmas, but also a "cloud" of negative charge. Modeling shows 2 distinct discharge regimes, a "fountain" and a "thunderstorm." Beam propagation and plasma formation were modeled using a kinetic equation in the forward-back approximation, plus continuity equations for electrons and positive and negative ions, and the Poisson equation. In a few nanoseconds, the "cloud" can accumulate such charge that electric field near it exceeds the breakdown threshold, creating a streamer between the "cloud" and a positively biased plate. The sparks can be generated with a high repetition rate. With multiple beams, sparks would occur between the "clouds" and between each "cloud" and the "earth" (grounded plate). Without positively biased plates or for weak beams, a discharge would occur between the "cloud" and the foil through which the beam is injected. In this "fountain" discharge, the back current of plasma electrons balances the current of high-energy beam electrons.

15:00

NR2 6 Cold Atmospheric Pressure Plasmas Created by Resonance Laser Optical Pumping I.V. ADAMOVICH, M. CHIDLEY, E. PLOENJES, P. PALM, J.W. RICH, *Dept. of Mechanical Engineering, The Ohio State University, Columbus, OH* Large volume, diffuse, non-thermal plasmas are produced in flowing gases at atmospheric pressures. The plasma is excited by a system of two high power c.w. carbon monoxide gas lasers, directed coaxially into a flowing gas absorption cell. Typical cell gas mixtures are N₂/O₂/CO in ratios of 0.92/0.03/0.05. Plasmas are sustained in such mixtures to 1 atm. total pressure, with the gases are flowing at velocities of 10 cm/sec. With 20 W total laser power, a diffuse glow plasma of 20 cm length and 1 cm diameter is created in the gas. The energy distribution in the translational, rotational, and the three molecular vibrational modes is determined using a

combination of Raman and Fourier Transform Infrared emission spectroscopy. Electron densities are determined by Thomson discharge probes, and are 10¹¹ cm⁻³. The plasma has huge energy content in the molecular vibrational modes, with average mode energies ranging from 0.5 to 5 eV per molecule. The translational/rotational mode temperature remains cold, with average values of 500 K. Such discharges are unconditionally stable, and appear to be scalable to very large volumes. The thermodynamics and molecular energy transfer processes in these systems will be presented in detail.

SESSION OR1:

MAGNETICALLY-ENHANCED PLASMAS

Thursday afternoon, 7 October 1999

Stratford Room Sheraton Waterside Hotel at 15:45

Harold Anderson, University of New Mexico, presiding

15:45

OR1 1 Correct 2-species 2D or 3D quasi-neutral approximation for magnetoplasma diffusion TUDOR WYATT JOHNSTON, *INRS-Energie et Materiaux, C.P. 1020, Varennes, Quebec, CANADA, J3X 1S2* JOELLE MARGOT, *Groupe de Physique des Plasmas, Universite de Montreal, C.P. 6128, Centre-Ville, Montreal, QC, CANADA H3C 3J7* For a 2-species magnetoplasma the basic transport equations are the diffusion/mobility equations for each species charge density, together with the Poisson equation giving the coupling electrostatic field. With near-equality of the positive and negative space charge in the one-dimensional case, it is easy to derive a single equation using as approximation the classic ambipolar (equal-current) condition. This works because in one dimension setting the divergence of the total current (a scalar) equal to zero also implies that the total current (a vector) is itself zero. This is no longer true in two or three dimensions and it is incorrect in general to assume zero total vector current density. The correct quasi-neutral condition has been applied, resulting in two coupled partial differential equations for the mean charge density of either species and the electrostatic potential. As they should, these new equations indeed reduce to previous results in the appropriate limits.

16:00

OR1 2 Ion heating in the HELIX helicon plasma source JOHN KLINE, MATTHEW BALKEY, ROBERT BOIVIN, PAUL KEITER, EARL SCIME, *West Virginia University* Ion heating sources have been developed for many plasma experiments including Tokamaks and Q-machines. These ion heating systems typically create electric fields that resonate with the gyro-motion of the ions to supply energy. However, for a helicon source the ratio of the collision frequency to the gyro frequency is much greater than one. For Tokamaks and Q-machines this ratio is much less than one. Thus, the ions in a helicon source only complete a fraction of the gyro orbit before colliding with another ion. We will present observations of efficient, anisotropic ion heating in a steady-state helicon plasma source for two external loop antennae driven at frequencies just above the ion cyclotron frequency. The ion velocity space distribution is measured by laser induced fluorescence in an argon plasma. The measured bulk ion heating is highly anisotropic (the perpendicular temperature increase is ten times the parallel temperature increase) even though the plasma is moderately collisional. Comparison of laser induced fluorescence measurements of the perturbed distribution function with theoret-

ical calculations for electrostatic ion cyclotron waves indicate that electrostatic ion cyclotron waves are launched into the plasma. This work supported by the U.S. Department of Energy under grant DE-FG02-97ER54420 and the National Science Foundation under grant ATM-9616467.

16:15

OR1 3 Ion Temperature Anisotropies in Helicon Plasmas
MATTHEW M. BALKEY, *West Virginia University* EARL E. SCIME, *West Virginia University* ROBERT BOIVIN, *West Virginia University* PAUL KEITER, *West Virginia University* JOHN KLINE, *West Virginia University* WVU HELICON TEAM, Laser induced fluorescence measurements of the ion temperature in an argon helicon plasma indicate a substantial ion temperature anisotropy (perpendicular over parallel). The perpendicular ion temperature scales linearly with the applied magnetic field strength and also depends on the RF driving frequency and amplitude. We will present measurements of the ion temperature as a function of magnetic field, RF amplitude, and RF frequency. We will also present measurements of the electromagnetic fluctuation spectrum in the source. Preliminary measurements suggest that the RF driving wave may parametrically decay into waves that can couple to the ions, thus providing a path for RF energy directly into the ions.

16:30

OR1 4 Laser and Radiofrequency Production of Seeded Air Plasmas* J. SCHARER, G. DING, H. GUI, K. KELLY, E. PALLER, *Department of Electrical and Computer Engineering, University of Wisconsin, Madison 53706* Seeded gas plasmas and air constituents have been created by a 193 nm laser and by a radiofrequency source. We have obtained $10^{14}/\text{cm}^3$ plasma densities with initial electron temperatures of 0.3 eV in TMAE (tetraakis (dimethylamino) ethylene) by laser photoionization. We developed a fast Langmuir probe analysis of plasma decay independent of ion species mix. Langmuir probe and optical emission data illustrating the density and temperature decay with TMAE mixed with nitrogen is presented. Simulations of antenna

coupling, wave frequencies, wave propagation, and power absorption are compared with experimental observations for radiofrequency plasma sources. The source produces plasma densities of $2 \times 10^{13}/\text{cm}^3$ in an 8500 cm^3 volume at electron temperatures of 5 eV in 10 mTorr Ar with 1 kW coupled power levels in a non-uniform magnetic field. Plasmas production at pressures from 2-760 Torr using Ar and laser initiated TMAE plasmas as seeds will be discussed.

*Supported by Air Force Office of Scientific Research Grant F49620-97-1-0262 in cooperation with the DDRE and in part by NSF Grant ECS-9632377.

16:45

OR1 5 Scaling of Hollow Cathode Magnetrons for Metal Deposition* GABRIEL FONT, *Novellus Systems, Inc., San Jose, CA, 95134 USA* MARK J. KUSHNER, *University of Illinois, Dept. of Electrical and Computer Engr., Urbana, IL, 61801, USA* Hollow Cathode Magnetrons (HCMs) are low pressure, high plasma density sources for deposition of metals for microelectronics fabrication. HCMs typically operate at pressures of < 10 mTorr, biases of 300-400 V and magnetic fields at the surface of the cathode of 150-300 G. With Al and Cu cathodes, metal ionization fractions exceeding 70% can be achieved. To improve the scaling of HCMs to larger diameters, plasma characteristics have been investigated using a 2-dimensional hybrid model and the results have been compared to experimental measurements of electron density and temperature, and deposition uniformity. The model combines particle and fluid simulations to resolve long-mean-free transport of sputtered metal atoms, and secondary electron emission. Simulations and measurements performed for an 8 cm diameter device with a 20 cm substrate-cathode gap show that the electron temperature in the cathode is 4-5 eV while that 1-2 cm above the floating substrate is 2-3 eV. The uniformity of the ion flux to the substrate can be controlled by the cusp magnetic field produced at the mouth of the cathode.

*Work was supported by Novellus and SRC.

SESSION OR2: DUSTY PLASMAS

Thursday afternoon, 7 October 1999; York Room Sheraton Waterside Hotel at 15:45; Gottlieb Oehrlein, SUNY at Albany, presiding

Invited Paper

15:45

OR2 1 Coulomb crystals in a monolayer dusty plasma.*

J GOREE, *Univ. of Iowa*

Dusty plasmas are ionized gases containing small particles of solid matter. These particles become highly charged, and can arrange themselves in a crystalline-like lattice. Experiments and simulations of a monolayer of microspheres suspended in an rf glow discharge were performed. With a small number of particles, ranging from 1-19, we measured the microscopic structure of very small crystals. The crystals have concentric rings. For certain numbers of particles, corresponding to 'closed-shells' in the outermost ring, the configurations are the same as for hard spheres. Yukawa molecular-dynamics simulations accurately reproduce our experimental results. By adding far more particles ($\sim 10,000$) and operating at higher power, we discovered Mach cones. These are V-shaped shocks created by supersonic objects. They were detected in a two-dimensional Coulomb crystal. Most particles were arranged in a monolayer, with a hexagonal lattice in a horizontal plane. Beneath the lattice plane, a sphere moved faster than the lattice sound speed. The resulting Mach cones were double, first compressional then rarefactive, due to the strongly-coupled crystalline state. Molecular dynamics simulations using a Yukawa potential also show multiple Mach cones.

*work supported by NSF and NASA. Experiments performed at MPE, Garching, Germany

16:15

OR2 2 The Interaction of Debye-Shielded Particles* MERLE E. RILEY, *Sandia National Laboratories, Albuquerque, NM 87185* RICHARD J. BUSS, *Sandia National Laboratories, Albuquerque, NM 87185* Macroscopic particles or solid surfaces in contact with a typical low-temperature plasma immediately charge negatively and surround themselves with an electron-depleted region of positive charge. This Debye shielding effect is involved in

the Debye-Huckel theory in liquids and plasma sheath formation in the gas phase. In this report, the interaction between such screened particles is found by using the same basic linearization approximation that is used in constructing the Debye shielding potential itself. The results demonstrate that a small but significant attraction exists between the particles, and, if conditions are right, this attractive force can contribute to the generation of particulate plasma crystals.

*Supported by US DoE under contract DE-AC04-94AL85000

Invited Paper

16:30

OR2 3 Plasmas with Fine Particles.

NORIYOSHI SATO, *Department of Electrical Engineering, Tohoku University, Sendai 980-8579, Japan*

Plasmas with fine particles are of current interest in plasma physics and engineering. Here are presented our experiments done on fine-particle plasmas at Tohoku University, which are concerned with negative-ion plasmas, fullerene plasmas, and dusty plasmas. In these experiments, fine particles are negatively charged in plasmas. There are many common properties among these plasmas with fine particles, although the particle sizes and weights are quite different. Negative-ion plasmas are produced by feeding a SF₆ gas into a Q-machine plasma consisting of electrons and potassium (or sodium) ions. A fraction of the electron to ion density is controlled by changing the SF₆ gas pressure. For such a low electron fraction as 10⁻³ ~ 10⁻⁴,^{1,2} there appear drastic changes of plasma phenomena. Negative-ion plasmas are useful for basic investigations of general properties of fine-particle plasmas, although there is no effect of gravity on fine particles. Fullerene plasmas are produced by injecting fullerenes (C₆₀) also into a Q-machine. Mass number (≈ 720) of fullerene ions (negative) is much larger than that (≈ 146) of SF₆ ions. Fullerene plasmas are used for producing new materials consisting of potassium (or sodium) and fullerene atoms. We are interested in producing endohedral fullerenes K-C₆₀ (or Na-C₆₀) on the endplate (substrate).^{3,4} In case of dusty plasmas, fine particles are huge and have many electrons on the surfaces, depending on the particle size. With an increase in the fine-particle density, there appears a strong coupling among the particles, yielding fluid and solid (Coulomb lattice) behaviors in the presence of gravity. In our work on dusty plasmas, non-dispersive particles of 10 μm in diameter are injected into dc discharge plasmas. Our emphasis has been on active controls of structures and dynamics of fine-particle clouds levitating in weakly-ionized plasmas.⁵ Essential points of our measurements are presented of vertical and radial profiles, phase transition, vortices driven electrostatically and azimuthal rotation in a weak vertical magnetic field, vertical spread of particle clouds, and vertical strings formed by periodic alignments of particles. Now we can establish a simple method of dust removal from dusty plasmas.

¹N. Sato, *A Variety of Plasmas* (edited by A. Sen and P. K. Kaw, Indian Academy of Sciences, Bangalore, 1989), p.79.

²N. Sato, *Plasma Sources Sci. Technol.* **3**, 395 (1994).

³N. Sato, T. Mieno, T. Hirata, Y. Yagi, R. Hatakeyama, and S. Iizuka, *Phys. of Plasmas* **1**, 3480 (1994).

⁴T. Hirata, R. Hatakeyama, T. Mieno, and N. Sato, *J. of Vacuum Sci. Technol.* **14**, 615 (1996).

⁵N. Sato, G. Uchida, R. Ozaki, and S. Iizuka, *Physics of Dusty Plasmas* (edited by M. Horanyi, S. Robertson, and B. Walch, American Institute of Physics, New York, 1998), p.239.

SESSION PR1: RECEPTION AND BANQUET

Thursday evening, 7 October 1999; York Room Sheraton Waterside Hotel at 18:30

SESSION QF1: DIAGNOSTICS II
 Friday morning, 8 October 1999
 Stratford Room Sheraton Waterside Hotel at 8:00
 Ion Abraham, University of Wisconsin, presiding

8:00

QF1 1 Coherent Rayleigh scattering in weakly ionized gases with nearly-degenerate four-wave mixing PETER BARKER, *Department of Mechanical and Aerospace Engineering, Princeton University* RICHARD MILES, *Department of Mechanical and Aerospace Engineering, Princeton University* JAY GRINSTEAD, *Optical Technology Division, National Institute of Standards and Technology* Coherent frequency-resolved Rayleigh scattering is being investigated as a diagnostic for sub-atmospheric pressure gases, and, in particular, for neutral temperature measurements in weakly ionized gases. The process acts upon the nonresonant portion of the third-order polarizability in which the input beams are configured in the backward degenerate four-wave mixing geometry. The nearly-counterpropagating pump beams induce by electrostriction a linear superposition of traveling-wave and stationary density gratings. A narrowband probe laser scatters off these density perturbations. The nonresonant four-wave mixing process is degenerate in the reference frame of the molecules which participate. In the laboratory frame the process is seen as nearly degenerate, with the frequency difference in the pumps which create the traveling grating translated to the frequency difference between the probe and the signal. The spectral distribution of the probe light scattered by the traveling gratings of the broadband pumps carries with it information about the velocity distribution and, hence, the translational temperature. Frequency resolution of the signal is obtained with an etalon. Preliminary results indicate greatly increased sensitivity over spontaneous Rayleigh scattering. For near-atmospheric pressures the four-wave mixing signal could easily be seen on a card and detected with a photodiode. Frequency resolved measurements performed in air and in a discharge down to 60 torr will be presented. The application of the technique to temperature measurements in plasmas will be discussed.

8:15

QF1 2 "IRMA" a Tunable Infrared Multi-Component Acquisition System for Plasma Diagnostics J. RÖPCKE, L. MECHOLD, *INP-Greifswald, 17489 Greifswald* J. ANDERS, F.G. WIENHOLD, *IPM-Freiburg, 79110 Freiburg, Germany* D. NELSON, M. ZAHNISER, *Aerodyne Research, Inc., Billerica MA 01821-3976, USA* The monitoring of transient or stable plasma reaction products, in particular the measurement of their ground state concentrations, is the key to an improved understanding of molecular non-equilibrium plasmas. Infrared tunable diode laser absorption spectroscopy (TDLAS) is a modern promising technique with specific capabilities for on-line process control in research and industry. For plasma diagnostics and control a compact and transportable multi-component TDLAS acquisition system, "IRMA," has been developed. The IRMA system contains 4 independent laser stations. A multi-path cell is included. Based on rapid scan software the absolute concentrations of several molecular species can be measured simultaneously within milliseconds and used as digital output. The contribution gives a survey of the optical subsystem, the data processing and the analysis technique. The flexibility and versatility of IRMA is demonstrated at examples of time-dependent species density measurement.

8:30

QF1 3 Measurements of ne and Te in CF₄ plasmas by laser Thomson scattering M. D. BOWDEN, *Kyushu University* R. TABATA, *Kyushu University* K. UCHINO, *Kyushu University* K. MURAOKA, *Kyushu University* Accurate information of the electron properties of processing plasmas is an essential step in understanding the complex plasma chemistry that occurs in these discharges. In this paper, we report results of electron property measurements made in a low-pressure inductively coupled plasma (ICP) operated in a mixture of CF₄ and Ar, using the method of laser Thomson scattering. Thomson scattering is a reliable method of measuring electron properties in plasmas, but this is the first time that it has been used in this type of reactive plasma. Measurements taken for various discharge conditions will be presented. The various steps that were taken to ensure that the high-energy laser pulse did not perturb the discharge also will be discussed.

8:45

QF1 4 Spatially Resolved Measurements of O₂ Vibrational Distribution and Rotational Temperature in Laser-Sustained Nonequilibrium Plasmas R. LEIWEKE, M. FERNEE, I. ADAMOVIČH, W. LEMPERT, *The Ohio State University, Department of Mechanical Engineering, Columbus, Ohio 43210* It is well known that the CO laser can be used to initiate and sustain electron production in pure CO (or mixtures of CO with buffers such as argon and/or nitrogen) at low to modest translational temperature. In this paper, we will present new results which quantify the influence of spatial inhomogeneity in the CO pump laser intensity on the vibrational distribution of O₂ in high pressure N₂/O₂/CO and Ar/O₂/CO plasmas. This will be accomplished by Planar Laser Induced Fluorescence (PLIF) using the well-known Schumann-Runge bands of molecular oxygen. The primary objective of the work to be presented is the experimental verification of predictions from detailed "Master Equation" kinetic modeling codes. Determination of O₂ vibrational populations for v''=0-3 will be achieved using an ArF excimer laser at ~ 193 nm. Levels 4-7 will be measured using KrF at ~ 248 nm. A secondary objective will be to determine the spatial dependence of the heavy gas translational/rotational temperature, which will be inferred from the rotationally resolved O₂ LIF spectra. Complimentary spatially averaged electron density measurements will be performed by determining classical current-voltage characteristics.

9:00

QF1 5 LIF of OH radicals in a dielectric-barrier discharge RAVI SANKARANARAYANAN, BIJAN PASHAIE, SHIRSHAK DHALI, *Southern Illinois University, Carbondale, Illinois 62901* We present the results of laser induced fluorescence (LIF) measurements of OH radicals in a dielectric-barrier discharge. The discharge consists of a simple dielectric-barrier with one glass dielectric excited with a frequency in the range of 1-3 kHz. A YAG-pumped tunable dye laser is doubled to produce the excitation at 282 nm. The laser beam excites the OH molecule from the 0-vibrational state of the ground electronic state to the 1-vibrational state of the excited electronic state. The broadband radiation due the (1,1) transition is recorded in the 312-330nm range. A gated CCD camera is used to record the LIF with spatial resolution. Results of OH concentration with variation in power supply voltage, oxygen concentration, and flow will be presented. Results show that with increase in power supply voltage, there is a drop in OH concentration. This is likely due to the change in the nature of the discharge at higher powers. Funded by NSF

9:15

QF1 6 Self Absorption Effects on the Detection of Hg and Cd in an Atmospheric Microwave Sustained Plasma* KAMAL HADIDI, *Massachusetts Institute of Technology* PAUL WOSKOV, *Massachusetts Institute of Technology* GUADALUPE FLORES, *Massachusetts Institute of Technology* KAREN GREEN, *Massachusetts Institute of Technology* PAUL THOMAS, *Massachusetts Institute of Technology* The detection limits for cadmium and mercury at the 228.8 nm and 253.65 nm transitions, respectively, in an atmospheric 1.5 kW, 2.45 GHz microwave sustained plasma has been found to depend on the path length between the plasma and the detection system. Atomic emission spectroscopy of such microwave plasma is under development as a real-time monitor of EPA regulated hazardous metals in smokestacks. Measurements of the detection limits for axial and radial side views of the discharge show a clear increase of the axial detection limit. Self absorption by unexcited cadmium and mercury along the longer turbulent axial propagation path is shown to be responsible for the increase of the detection limits.

*Supported by the Office of Science and Technology, U.S. DOE.

9:30

QF1 7 Measurements of Ion Energy and Ion Flux Distributions in Inductively Coupled Plasmas in CF₄/O₂/Ar Mixtures M. V. V. S. RAO,* *NASA-Ames Research Center* J. S. KIM,† *NASA-Ames Research Center* M. A. CAPPELLI,‡ *NASA-Ames Research Center* S. P. SHARMA, *NASA-Ames Research Center* We report mass spectrometric studies of energy distributions and absolute concentrations of ions generated in CF₄/O₂/Ar inductively coupled rf plasmas. The ions were collected through a 100 μm orifice in the grounded and water cooled lower electrode in a GEC cell configuration. The measurements were made at gas pressures in the 10-50 mTorr range and rf coil power in the 100-300 W range. The observed ions are CF₃⁺, CF₂⁺, CF⁺, C⁺, F⁺, COF⁺, CO⁺, O₂⁺, and O⁺. The relative abundance of these ions varies with pressure and rf power. The energy distribution and absolute concentrations are correlated with electron number density and plasma potential measured by a compensated Langmuir probe.

*Thermosciences Institute, NASA-Ames Research Center

†Thermosciences Division, Mechanical Engineering Department, Stanford University

‡Thermosciences Division, Mechanical Engineering Department, Stanford University

9:45

QF1 8 Electrical Characterization of an Ionized Physical Vapor Deposition Reactor S. RAUF, P. L. G. VENTZEK, V. ARUNACHALAM, D. G. CORONELL, *Motorola Inc.* Ionized physical vapor deposition (IPVD) is an important new technology for depositing conformal metallic thin films on patterned wafers during microelectronics manufacturing. IPVD reactors are electrically quite complex with dc power supplies in addition to rf sources at multiple frequencies. These sources are generally coupled to each other through the plasma and they strongly interact in the sheaths at different surfaces. This study aims at characterizing the electrical behavior and sheath dynamics of an IPVD reactor with a plasma-immersed antenna coil, a dc excited sputtering target and an rf biased electrode. The computational tools used for this investigation are the Hybrid Plasma Equipment Model (HPEM) and an external circuit model. It is found that the dc current from the target builds up a large negative dc bias at the coil. Because of this large bias, most of the rf coil voltage drops across the sheath at the coil, accelerating ions to high energies and causing significant sputtering of the coils. The rf from the coil also

contributes to wafer biasing and resputtering of the deposited film. The effects of frequency, power and gas pressure are systematically examined.

SESSION QF2: DC GLOWS

Friday morning, 8 October 1999

York Room Sheraton Waterside Hotel at 8:00

T. Makabe, Keio University, presiding

8:00

QF2 1 Coexistence of Contracted and Diffuse Plasmas in Steady-State Glow Discharges YURY Z. IONIKH, NAIRA V. CHERNYSHEVA, SERGEY O. MACHERET, RICHARD B. MILES, *Dept. of Mechanical and Aerospace Eng., Princeton University* A D.C. glow discharge in argon and Ar-nitrogen and Ar-He mixtures has been studied in cylindrical tubes 1 to 2 inches i.d. at pressures 10 - 200 Torr and currents 1 - 200 mA. In pure Ar, the discharge contracts at any pressure within the studied range, if the current exceeds 30 - 60 mA. Addition of 1 per cent or more of nitrogen causes contraction to cease, so that the discharge is diffuse at all conditions examined. At lower percentages of nitrogen admixture, a new phenomenon could be observed which we called a "partial contraction". The positive column consists of two parts, of which one is contracted and the other is diffuse, with a well-pronounced boundary between the two. The boundary can be moved along the tube by changing the discharge current. Current-voltage characteristics of the discharge in this regime do not exhibit a typical contraction-related jump, but include instead a monotonically increasing region. Preliminary experiments show that the contracted-diffuse coexistence seem to occur also in Ar-He mixtures, and possibly in pure Ar. The phenomenon is studied in detail, and possible mechanisms are proposed.

8:15

QF2 2 Direct Proof of the Thermal Nature of the Effect of a Discharge Plasma on Shock Wave Propagation* YURY IONIKH, ALEXANDER MESHCHANOV, AZER YALIN, RICHARD MILES, *Princeton University* A laser schlieren method has been used for observing shock wave propagation through a longitudinal glow discharge in pure argon and in argon with an admixture (1 per cent) of nitrogen at pressures 30 - 100 Torr and currents 1 - 100 mA. Axial gas temperatures have been measured by ultraviolet Rayleigh scattering. A spark discharge has been used for shock wave generation. Passing the laser beam twice across the discharge allowed us to measure an instantaneous shock wave velocity. A pulsed discharge mode with short pulses was used, which prevented the gas from heating. Shock wave velocity and schlieren signals in this discharge are identical to those in a gas with no discharge. This result proves that the influence of a plasma on shock wave propagating is attributable to thermal mechanism alone. Additional evidence for this is that shock wave parameters in the discharges in Ar and in Ar+nitrogen are identical if, and only if, the gas temperatures in both discharges are equal.

*The work was supported by AFOSR New World Vistas Program

8:30

QF2 3 Atmospheric Pressure Glow Discharges in Air* ROBERT H. STARK, KARL H. SCHOENBACH, *Old Dominion University, Norfolk, VA 23529* DC glow discharges at atmospheric pressure, sustained by microhollow cathode discharges could be generated in argon and in air. The differential electric field strength along the discharge axis has been measured by reducing the distance between anode and cathode and by recording the change in voltage at constant current. The electric field was found to be constant for distances greater than 2 mm from the cathode, as expected for the positive column of a glow discharge. It is 130 V/cm for argon and 1.2 kV/cm for air. For less than this distance the electric field decreases to a small value, indicating an electron beam like transport mechanism in this range. Experiments in air with a gap distance up to 1 cm have been performed. The electrical data allow us to determine the electron density by using information on electron mobility. For a current density of 3.8 A/cm², an electric field of 1.2 kV/cm, and assuming a temperature of 2000 K, the electron density in mid plane of the air glow is 510¹² cm⁻³. The temperature value was estimated from spectral measurements, and through interferometry. The power density, required to sustain this atmospheric pressure air discharge is 4.6 kW/cm³, which is close to the theoretical value of 4.0 kW/cm³.

*This work was funded by the Air Force Office of Scientific Research in Cooperation with the DDR&E Air Plasma Ramparts MURI Program.

8:45

QF2 4 Acoustic Shock Wave Propagation in a Glow Discharge¹ S. POPOVIĆ, L. VUŠKOVIC, *Old Dominion U., Norfolk, VA* Experiments with weak acoustic shock waves propagating through glow discharges^{2,3} have shown unexpected damping, dispersion, and propagation effects that still remain to be understood. Similar effects were observed for both monoatomic and molecular gas discharges. Increase of shock velocity propagation is more pronounced in the cathode region of a d.c. glow discharge than in the positive column.⁴ This and other observations suggested that pure thermal effects only could not explain the observed shock modification. In the present analysis of the observed phenomena, we started from the hypothesis that electronic excitation is the controlling process in the energy storage and transfer along the shock structure. Further, we explored the shock structure similarity of weak shock waves in glow discharges and strong shock waves in monoatomic neutral gases, where the accumulated excited state population was observed in leader and precursor regions. A detailed time-dependent approach for describing the ionization-recombination process was used to demonstrate the possibility of sufficient energy storage to account for the observed shock modification.

¹Supported by Accurate Automation Corporation.

²A. I. Klimov et al., *Sov. Tech Phys. Lett.* **8**, 192 (1982).

³B. N. Ganguly et al., *Phys. Lett. A* **230**, 218 (1997).

⁴S. Popović and L. Vušković, *Physics of Plasmas* **6**, 1448 (1999).

9:00

QF2 5 A New Plasma Column Model Including Wall Interactions DIRK UHRLANDT, MARTIN SCHMIDT, ROLF WINKLER, *Institut für Niedertemperatur-Plasmaphysik Greifswald, Germany* An extended self-consistent model has been developed which comprises the nonlocal kinetic description of the radially inhomogeneous dc column plasma in a cylindrical tube and a

treatment of the interaction of the plasma with the insulated tube wall. The model allows to determine self-consistently the radially dependent kinetic quantities of electrons, ions and excited atoms, the radial space charge field and the axial electric field in the column as well as the charge carrier surface densities on the tube wall. The method is based on the solution of the radially inhomogeneous electron kinetic equation, the balances of the most important excited states, the ion momentum balance and the Poisson's equation. In addition, a balance of electrons on the wall including their reflection, desorption, recombination and their flux onto the wall has been deduced which is used finally to determine the axial field strength self-consistently. A special optimization technique has been developed to find the numerical solution of the full set of non-linearly coupled equations. The capabilities of the model are demonstrated by means of results for a low pressure neon column plasma.

9:15

QF2 6 Self-Consistent Monte Carlo Simulations of Positive Discharges UWE KORTSHAGEN, *Mechanical Engineering, University of Minnesota, MN 55455* JAMES E. LAWLER, *Dept. of Physics, University of Wisconsin-Madison, WI 53706** Fully converged simulations of positive column discharges using single electron or "direct simulation" Monte Carlo codes were reported at GEC98. Initial solutions at low RxN (product of column radius and gas density) were found using only personal computers. Solutions to higher RxN, corresponding to an ion mean-free-path of 1/4 the column radius, have now been found using a supercomputer. Sixteen converged simulations, reaching a Debye length of 1/17 the column radius, are available [1]. The simulations illustrate sheath formation and the negative dynamic resistance of the positive column at low currents. The simulation results have been reproduced using entirely independent codes. No fluid approximations or plasma-sheath boundary conditions are used. The simulations are valuable for comparison to other types of fluid and kinetic theory models.

[1]J. E. Lawler and U. Kortshagen, *J. Phys. D: Appl. Phys.*, submitted.

*Supported by the NSF and the Univ. of Minnesota Supercomputing Center

9:30

QF2 7 Nonequilibrium Positive Column III. J. H. INGOLD, *One Bratenahl Place #610, Bratenahl, OH 44108* Previous work has shown that the first principles nonlocal kinetic method [1] is closely approximated by the nonlocal moment method [2] in positive column analysis, and that the transition from nonequilibrium to equilibrium at sufficiently high NR (gas density × radius) can be studied by the nonlocal moment method [3]. The present paper describes the derivation of a quantitative condition that the parameter NR must satisfy in order for local equilibrium to prevail in the low pressure positive column discharge. The derivation is based on the electron energy balance equation resulting from the two-term Legendre expansion technique of solving the Boltzmann equation for the electron energy distribution function. Use of the

quantitative condition is illustrated by application to a positive column discharge in neon.

[1]D. Uhrlandt and R. Winkler, *J. Phys. D* **29**, 115 (1996).

[2]J. H. Ingold, *Phys. Rev. E* **56**, 5932 (1997).

[3]J. H. Ingold, *Bull. Am. Phys. Soc.* **43**, 1466 (1998).

9:45

QF2 8 Fluid Approach for Modelling a DC Discharge at Low-Pressures G. GOUSSET, *LPGP, Univ. Paris-Sud (France)* L.L. ALVES, *CFP, IST (Portugal)* O. LEROY, *LPGP, Univ. Paris-Sud (France)* A one-dimensional fluid model is used to analyse the radial non-local behaviour of the electron kinetics in a dc positive column at low-pressures. The model solves the first three moments of the inhomogeneous electron Boltzmann equation (EBE), written under the two-term approximation, together with the transport

equations for the ions, and Poisson's equation. In order to include the diffusion term in the ion transport equations, the model variables (particle densities and drift velocities, electron mean energy, and space-charge field) were developed in power series around the small ratio of the ion temperature to the electron characteristic energy¹. Calculations were performed in pure He for a discharge radius of 1 cm and pressures varying between 0.1-5 Torr. We have also used a PIC-MCC code, for the same set of electron-neutral cross sections, as benchmark tests of the fluid model. A good agreement is found between the discharge characteristics predicted by the two approaches. Model results reveal that, for pressures around 1 Torr, a transition occurs from a non-local to a local regime, after which the electron mean energy can be deduced from the solution to the homogeneous EBE.

¹H. B. Valentini, *J Phys D: Appl. Phys.* **21**, 311 (1988)

SESSION RFI: PLASMA-SURFACE INTERACTIONS

Friday morning, 8 October 1999; Stratford Room Sheraton Waterside Hotel at 10:30

K. Tachibana, Kyoto University, presiding

Invited Paper

10:30

RF1 1 Plasma-Surface Interactions in Dielectric Patterning Using High-Density Sources.

GOTTLIEB S. OEHRLEIN, *Physics Department, State University of New York, Albany, 1400 Washington Avenue, Albany, N.Y. 12222**

Low pressure discharges play an essential role for pattern transfer into dielectric layers in integrated circuit production, e.g. for etching of vias and trenches in the formation of high-performance multi-level interconnection schemes. A variety of dielectric materials are being considered for these applications, ranging from conventional SiO₂ and different spin-on glass films, over organic insulators to porous materials. The necessity of different chemical etching environments and the varying spontaneous chemical reactivity of the dielectric materials in the context of demanding technological requirements on the pattern transfer process presents a spectrum of challenges on the control of plasma-surface interactions. We will illustrate these issues by discussing several prototypical pattern transfer applications, the solutions that have been arrived at, and the dominant plasma-surface interaction mechanisms.

*M. F. Doemling, C. Hedlund, Xi Li, P. J. Matsuo, M. Schaepekens, and T.E.F.M. Standaert

Contributed Papers

11:00

RF1 2 Sticking Coefficients of Neutrals in Inductively Coupled Plasma and RIE Reactors*

DA ZHANG, MARK J. KUSHNER, *University of Illinois, Urbana, IL, 61801, USA* The sticking coefficient of neutral radicals in low pressure, inductively-coupled-plasma (ICP) and reactive-ion-etching (RIE) reactors affects both the surface and bulk plasma properties. For example, recent experiments have shown that etching rates in fluorocarbon plasmas are functions of the wall temperature due to the sensitivity of CF_x sticking coefficients to temperature.¹ Other experiments have shown that surfaces can appear to be either sources or sinks of radicals depending on the magnitude to the incident ion flux.² A Surface Kinetics Model (SKM) has been developed and integrated into the the Hybrid Plasma Equipment Model (HPEM) to self-consistently investigate plasma-surface interactions in reactors where surface chemistry is material dependent. The SKM will be described and results will be discussed for C₂F₆ etching of Si in an ICP reactor where the wall temperature is varied to demonstrate the coupling between wall conditions and etch properties. The generation of neutral radicals on surfaces by ion bombardment will also be discussed for fluorocarbon plasmas in RIE reactors.

*Work was supported by SRC, LAM and Applied Materials.

¹M. Schaepekens, et al, *J. Vac. Sci. Technol. A* **16**, 2099 (1998)

²J. Booth, et al, *J. Appl. Phys.* **85**, 3097 (1999)

11:15

RF1 3 Chlorine Plasma-Silicon Surface Interactions on the Angstrom to Micron Scale

VINCENT M. DONNELLY, *Bell Laboratories, Lucent Technologies* KATHERINE H. A. BOGART, *Bell Laboratories, Lucent Technologies* The surface layer formed during chlorine plasma etching of silicon is of interest in understanding and controlling etching of this material. We have investigated this plasma-surface interaction using vacuum sample-transfer and angle-resolved x-ray photoelectron spectroscopy (XPS) to determine absolute coverages of SiCl_x with a depth resolution of 6 Å. Electron shadowing of SiO₂-masked Si features was used to determine Cl-coverage and SiCl_x stoichiometry on sidewalls and trench bottoms with sub-micron resolution. Gas-phase Cl, Cl₂, and SiCl_y (y = 0-3) were monitored by optical emission and mass spectrometry. The ratio of etching product-to-etchant (SiCl_y-to-Cl) flux to the wafer varied from 0.078 to 11 between 10 and 0.4 sccm Cl₂. Surprisingly, SiCl, SiCl₂, and SiCl₃ (1.0:0.45:0.33 on horizontal surfaces) and total Cl were independent of the product-to-etchant flux ratio. The Cl areal density of

the $\bar{16}\text{\AA}$ thick layer was $2.63 \times 10^{15} \text{ cm}^{-2}$ on horizontal surfaces and $1.3 - 1.8 \times 10^{15} \text{ cm}^{-2}$ on Si sidewalls, where SiCl is the overwhelmingly favored SiCl_x species. Reaction pathways are presented to explain constancy of the surface layer with Cl_2 flow rate, as well as the dramatically different stoichiometry of the sidewall layer.

11:30

RF1 4 Plasma-Grid Interaction CHANG-KOO KIM, *Department of Chemical Engineering, University of Houston* DEMETRE ECONOMOU, *Department of Chemical Engineering, University of Houston* JUSTINE JOHANNES, *Sandia National Laboratories* TIMOTHY BARTEL, *Sandia National Laboratories* Plasma interaction with a grid is important in a number of applications. In neutral beam etching, for example, a grid is used to neutralize ions and generate collimated beams of energetic neutrals for aniso-

tropic etch without charge damage. Also, many ion sources and satellite thrusters are based on extraction of an ion beam from a plasma through a grid. The plasma conditions, the grid hole diameter, and aspect ratio determine the effect of the grid on the neutral, ion, or plasma transport through the grid. We have measured the energy and angular distribution of ions effusing from a hole on a wall in contact with a high density plasma. A single hole is thought to be a well defined system capturing the essential aspects of plasma-grid interaction. A hemispherical sectioned electrode is used as the detector. The hole diameter is varied from 25 to 1000 microns and the hole aspect ratio (depth to diameter) is varied from 0.25 to 10. Experimental data are compared to particle based plasma simulation tools. In particular, Icarus, a 2-D transient Direct Simulation Monte Carlo (DSMC) code and Mercury, a computationally fast, steady-state particle code are used to investigate the plasma behavior in front of and behind the grid. Electrons, ions and neutrals are treated as particles and an explicit Poisson solver, based on the boundary element method, is used to compute electric fields.

Invited Paper

11:45

RF1 5 Plasma Immersion Ion Implantation for the Treatment of Metal Surfaces.

WOLFHARD MÖLLER, *Institute of Ion Beam Physics and Materials Research, Forschungszentrum Rossendorf, D-01314 Dresden, Germany*

Plasma Immersion Ion Implantation (PIII) has emerged as a powerful technique not only for a number of electronic applications, but also for the treatment of metallic surfaces, in particular with the purpose of wear protection. The item to be treated is immersed into a low-pressure plasma. By applying a pulsed negative high voltage up to about 40 kV with pulse durations of a few up to a few ten microseconds, high-energy ions are generated for surface modification with a high subsurface penetration. The process can be applied to 3D workpieces and scaled up to large surface areas. The paper will address the experimental validation of simple models of the dynamic plasma boundary evolution during a PIII pulse, and their consequences for the process parameters and the limitations in treating structured surfaces. It will also describe the mechanisms of the plasma- and ion-surface interaction during the PIII nitriding of selected metals such as stainless steel and aluminum alloys, for which conventional plasma nitriding is problematic. Finally, some technical applications will be demonstrated.

Contributed Paper

12:15

RF1 6 Recombination Coefficient Measurements of O and N radicals HARMEET SINGH, *U. C. Berkeley* JOHN COBURN, *U. C. Berkeley* DAVID GRAVES, *U. C. Berkeley* Surface recombination of radicals in low-pressure high-density plasmas has direct influence on the neutral and ionic composition of the plasma. While, electron impact dissociation of molecules is the dominant mechanism for creation of radicals, the surface recombination of radicals is often expected to be the dominant loss mechanism. We have a combination of measurements and a model to determine the recombination coefficients of O and N, to O_2 and N_2 , respectively on the stainless steel walls of our inductively coupled plasma

chamber. The radial variation of the electron energy distribution function (EEDF) is measured using a tuned, cylindrical Langmuir probe. The number density of the molecular species is measured using line-of-sight modulated beam mass spectrometry. The mass spectrometer is differentially pumped in three stages to ensure a good beam to background signal ratio. The radical absolute number density is measured using appearance potential mass spectrometry with the aforementioned mass spectrometer. The recombination coefficient is calculated using a balance of the volume-generation and surface-loss rates of the radicals in the plasma. The generation rate of the radicals is calculated using the number density measurements of the parent molecule and the spatially resolved EEDFs. At approximately 330 K on stainless steel, the recombination coefficient for O is 0.16, and recombination coefficient for N is 0.07.

Invited Paper

10:30

RF2 1 Microdischarges in Silicon: Fabrication and Performance of Single Sub-100 μ m Diameter Devices and Planar Arrays.*

GARY EDEN, *University of Illinois, Dept. of Electrical and Computer Engr., Urbana, IL 61801, USA*

Cylindrical microdischarge devices, 20-400 μ m in diameter, have been fabricated in silicon, glass, Kapton and other materials, and operated in a variety of gases at room temperature. The discharges are typically azimuthally uniform. Continuous operation at pressures exceeding one atmosphere and specific power loadings exceeding several hundred kW cm⁻³ have been realized. This presentation will describe the fabrication and characterization (electrical and spectroscopic) of both single devices and arrays of microdischarges. Also, the application of these novel devices as sensors or microparticle "laboratories" will be briefly discussed.

*Work supported by AFOSR.

Contributed Paper

11:00

RF2 2 The One Atmosphere Glow Discharge in Air: Phenomenology and Applications RAMI BEN GADRI, *University of Tennessee at Knoxville* DANIEL M. SHERMAN, ZHIYU CHEN, FUAT KARAKAYA, J. REECE ROTH, *University of Tennessee at Knoxville* The existence of an atmospheric pressure RF glow plasma with the characteristics of a classical low pressure DC glow discharge has been experimentally and theoretically demonstrated [1,2]. At the UTK Plasma Sciences Laboratory, the One Atmosphere Uniform Glow Discharge Plasma (OAUGDP) in air has been applied to a wide range of plasma processing applications. The technology is simple, technically attractive, and suitable for online treatment of webs and 3-dimensional workpieces. A parallel plate reactor and a Remote Exposure Reactor (RER) have been developed for direct plasma immersion and remote exposure,

respectively. The RER is based on generating active species capable of sterilization and surface treatment in a uniform surface layer of the OAUGDP on planar panels [3], and convecting the active species to a remote chamber where the workpiece is located. A related surface plasma has been developed for indoor air filtration systems. In addition, the surface plasma on flat panels modified the boundary layer in wind tunnel tests to produce electrohydrodynamic (EHD) flow effects that can be used to increase or decrease aerodynamic drag [3].

[1] Massines et al., *J. Appl. Phys.*, Vol. 83, N 6, pp 2950-2957, Mar. 1998.

[2] J. R. Roth, "Industrial Plasma Engineering" Vol. I: Principles. Inst. Phys. Pub., Bristol and Philadelphia, ISBN 0-7503-0318-2, 1995.

[3] Roth et al., AIAA Paper 98-0328, 36th AIAA Meeting, Reno NV, 1998, Jan. 12-15.

Invited Paper

11:15

RF2 3 Novel Biomedical Applications for Plasma-Deposited Thin Organic Films.

BUDDY D. RATNER, *University of Washington Engineered Biomaterials (UWEB), Seattle, Washington 98195, USA**

Biomaterials of the future will control with precision proteins and cells interacting with their surfaces. At the present time, proteins adsorb to biomaterials in an indiscriminate manner leading to a surface mixture of different proteins in different states of denaturation. Stochastic protein layers of this type are never used in living organisms, and may allow the body to identify medical implants as foreign objects. A number of approaches will be presented in this lecture that illustrate the unique potential of plasma deposited films to accurately control protein layers at interfaces. First, plasma-deposited fluoropolymer films as tight binding surfaces will be illustrated. These have special application for blood compatible surfaces and for diagnostic applications. Second, plasma-deposited ether-terminated oligoethylene glycol (glyme) layers will be presented as a means to inhibit protein attachment and subsequent cellular attachment. Finally, plasma-deposited thin films imprinted with template proteins that can recognize their template protein with high specificity will be presented. Such surfaces can direct a protein of choice to the surface and therefore can accurately control biological processes.

*With Huaiqiu Shi, Erika Johnston and Vickie Pan

11:45

RF2 4 Gas Plasma Afterglow Sterilization : A New Approach

S. MOREAU, *Ecole Polytechnique, Montreal, Canada* M. MOISAN, *Universite de Montreal, Montreal, Quebec* M. TABRI-ZIAN, *Ecole Polytechnique, Montreal, Canada* J. BARBEAU, *Universite de Montreal, Montreal, Canada* A. RICARD, *CPAT, Universite Paul-Sabatier, France* L'H. YAHIA, *Ecole Polytechnique, Montreal, Canada* Gas plasma afterglow offers the possibility of sterilizing heat-sensitive polymer-based medical devices. Focusing on the influence of plasma parameters on sterilization efficacy, we have shown that gas composition, pressure and flow, and power density affect the destruction rate of our reference bacterial spores, *Bacillus subtilis* var. *niger*. NO titration method has enabled us distinguishing between two effects : spore coat oxidation by oxygen atoms and DNA denaturation by UV emission from NO_β species. Moreover, we have observed that the maximum emission of atomic nitrogen corresponds to the maximum of UV emission (2% oxygen in nitrogen). We have begun evaluating the influence of the reactor wall material on the sterilization efficacy. Preliminary results prove that atomic recombination on the reactor wall may be an important factor contributing to the loss of active species, thereby decreasing the destruction rate of the bacterial spores.

12:00

RF2 5 The formation of ion-ion plasmas in an argon/chlorine mixture*

JENNIFER L. KLEBER, MARK S. RABALAIS, LAWRENCE J. OVERZET, *University of Texas at Dallas* Electronegative plasmas and ion-ion plasmas in particular have many potential advantages in semiconductor processing.¹ An ion-ion plasma is one in which the density of negative ions greatly exceeds that of electrons so that ions carry a majority of the conduction current to any surface in contact with the plasma. A microwave interferometer, a Langmuir probe, and a CCD camera were used to study pulsed plasmas in a mixture of 95% argon and 5% chlorine.

The plasma parameters of power, pressure, pulsing frequency, and duty cycle were varied to determine under what conditions ion-ion plasmas can form in the afterglow. A simple 0-D model was used to confirm under what conditions the transition to an ion-ion plasma would occur rapidly, the initial negative ion density at the transition would be high, and the negative ion density time averaged over the pulsing period would be high.

*This material is based upon work supported by NSF grant # CTS-9713262

¹S. Samukawa and S. Furuoya, *Plasma Sources Sci. Technol.* **5**, 132 (1996).

12:15

RF2 6 Negative Ion Formation in Pulsed Plasmas*

LAL PINNADUWAGE, ORNL WEIXING DING, ORNL DENNIS MCCORKLE, *UT/ORNL* We have observed enhanced O^- formation in a pulsed glow discharge of O_2 in a Langmuir probe-assisted photodetachment experiment.¹ A large enhancement in O^- formation was observed in the afterglow. The experimental observations are consistent with enhanced electron attachment to high-Rydberg states of O_2 that survive into the afterglow with lifetimes longer than 10 microseconds. We will discuss the survivability of the weakly-bound Rydberg states in plasma environments. We will also point out that, (i) enhanced negative ion formation reported in a number of pulsed discharges (including those of H_2 and SiH_4) can be explained via enhanced electron attachment to high-Rydberg states as well, and (ii) the role of high-Rydberg states should be taken into account in modeling various pulsed and continuous discharges.

*Research Supported by DOE-EMSP Program and the NSF. The ORNL is managed by Lockheed Martin Energy Research Corp. for the U.S. Department of Energy under contract number DE-AC05-96OR22464.

¹W. X. Ding, L. A. Pinnaduwege, and D. L. McCorkle, *Plasma Sources Sci. Technol.* (in press, 1999).

Author Index

A

Abner, Douglas **IWP1 4**
 Abraham, I.C. **ETP7 91**,
 FW1 2
 Abramzon, N. **ETP1 10**,
NR1 3
 Adamovich, I.V. **ETP1 17**,
ETP7 90, **IWP4 34**,
NR2 6, **QF1 4**
 Adams, S.F. **ETP7 80**,
IWP7 53
 Adler, Helmar G. **ETP4 60**,
ETP7 89
 Akashi, Haruaki **IWP8 58**
 Albin, Sacharia **IWP10 71**
 Al-Khateeb, H.M. **JW1 6**
 Alman, Darren A. **IWP7 56**
 Alvarez, I. **IWP1 3**
 Alves, L.L. **ETP3 29**,
IWP4 32, **QF2 8**
 Amatuucci, W.E. **IWP12 86**,
IWP12 88
 Anders, J. **QF1 2**
 Anderson, H **BT2 1**
 Anderson, L.W. **IWP3 12**,
IWP3 13
 Andrew, Y. **ETP7 91**,
FW1 2
 Angel, G. **IWP10 78**
 Angel, Gordon **IWP10 76**
 Arnold, Susan **IWP11 80**
 Arnush, D. **ETP3 54**
 Arunachalam, V. **BT2 1**,
QF1 8
 Ash, R.L. **ETP3 35**
 Avdonina, Nina **IWP3 20**

B

Babb, J.F. **ETP4 64**
 Babb, Jim **ETP2 23**
 Bahia, J.E. **IWP12 83**
 Bahrim, C. **IWP3 21**
 Bailey, Wm.F. **ETP3 27**
 Bakker, Leon **DT2 2**
 Bakshi, Vivek **ETP7 74**
 Balkey, Matthew **OR1 2**
 Balkey, Matthew M.
IWP6 40, **IWP6 41**,
OR1 3
 Balkey, M.M. **IWP6 42**
 Baravian, G. **IWP11 82**
 Barbeau, J. **RF2 4**
 Barker, Peter **IWP13 89**,
QF1 1
 Bartel, Timothy **FW2 6**,
RF1 4
 Bartschat, K. **IWP3 16**

Basner, R. **ETP1 11**,
ETP1 12
 Basurto, E. **IWP1 3**
 Becker, K. **ETP1 3**,
ETP1 10, **ETP1 11**, **ETP1**
12, **IWP3 18**, **IWP4 30**,
MR1 5, **NR1 3**
 Ben Gadri, Rami **RF2 2**
 Benck, Eric **DT1 3**,
IWP4 33, **NR2 4**
 Bengtson, Roger D.
ETP7 74
 Bereznoi, Stanislav
FW2 7, **IWP6 39**
 Berger, J.A. **ETP1 5**
 Bettega, Marcio H.F.
ETP1 7
 Bhandarkar, Upendra
IWP2 9
 Biennier, Ludovic **ETP7 84**
 Bilwatsch, O. **ETP4 59**
 Birdsall, C.K. **IWP4 24**
 Birdsey, B.G. **JW1 6**
 Blackburn, M.A. **IWP6 42**
 Blackwell, D.D. **ETP3 54**
 Blagoev, A.B. **IWP7 54**
 Blagoev, Alexander
ETP3 32
 Bletzinger, B.N. **BT2 4**
 Boffard, John B. **IWP3 12**,
IWP3 13
 Bogaerts, Annemie **FW2 3**,
FW2 4
 Bogart, Katherine H.A.
AT2 6, **RF1 3**
 Boivin, R.F. **IWP6 42**
 Boivin, Robert **IWP6 40**,
IWP6 41, **OR1 2**, **OR1 3**
 Boogaarts, Maarten **GW1 2**
 Booske, J.H. **ETP7 91**,
FW1 2
 Booth, Jean-Paul **ETP7 84**
 Bose, Deepak **AT2 3**,
BT1 2, **BT2 2**
 Božin, J. **IWP3 23**
 Bowden, M.D. **ETP3 43**,
ETP7 76, **QF1 3**
 Braithwaite, N.St.J.
IWP4 28
 Brake, M.L. **ETP3 40**
 Bratescu, Maria Antoaneta
IWP4 26
 Bratescu, Maria-Antoaneta
ETP7 87
 Brock, Lori R. **ETP7 89**
 Brooke, G.M. **IWP13 94**
 Brown, D. **IWP10 78**

Buckman, Stephen J.
AT1 4, **AT1 5**, **ETP1 1**
 Buenker, R.J. **ETP2 20**
 Buenker, Robert J. **ETP2 21**
 Buff, J. **IWP10 78**
 Buff, Jim **IWP10 76**
 Burrow, Paul D. **AT1 2**
 Buss, Richard J. **OR2 2**

C

Calzada, M.D. **ETP3 42**
 Campillo, Celine **IWP10 70**
 Candler, Graham **JW2 5**
 Cappelli, M.A. **ETP7 88**,
IWP12 84, **QF1 7**
 Cappelli, Mark A.
IWP13 93, **IWP5 36**,
IWP9 67
 Carman, R.J. **DT2 5**
 Cekić, M. **DT2 7**
 Chadderton, Lewis T.
AT1 4
 Chae Hwa, Shon **IWP9 66**
 Chaker, Mohamed **FW1 3**
 Champion, R.L. **ETP2 18**
 Champion, Roy **LR1 3**
 Chang, C.S. **ETP3 50**
 Chang, Hong-Young
ETP3 49, **ETP3 50**
 Chatterjee, Barun K.
ETP7 92
 Chen, F.F. **ETP3 54**
 Chen, Z. **IWP13 90**
 Chen, Zhiyu **RF2 2**
 Chernysheva, Naira V.
QF2 1
 Chidley, M. **NR2 6**
 Chilton, J. Ethan **IWP3 14**
 Chiu, Y.-H. **LR1 4**
 Chiu, Yu-Hui **ETP2 22**,
ETP2 26
 Choi, Seung **FW2 6**
 Choi, Y.W. **ETP7 76**
 Christlieb, A.J. **IWP1 5**
 Christophorou, Loucas
ETP1 6, **JW1 4**, **JW1 5**
 Chung, Chin-Wook
ETP3 49
 Chung, H-K. **ETP4 64**
 Chung, Hyun-Kyung
ETP2 23
 Chutjian, Ara **AT1 1**
 Cisneros, C. **IWP1 3**
 Coburn, John **RF1 6**
 Cocke, C.L. **NR1 1**
 Collard, Corey **ETP3 40**

Collins, G.J. **ETP3 48**,
IWP12 83, **IWP13 98**,
IWP7 48
 Coman, L. **NR1 5**
 Compaan, A.D. **IWP9 63**
 Coronell, D. G. **BT2 1**
 Coronell, D.G. **QF1 8**
 Cosby, Philip C. **NR1 2**
 Costa i Bricha, E **ETP3 36**
 Cronin, Daniel **IWP9 65**
 Crowe, A. **IWP3 16**
 Crowley, B. **BT1 6**,
ETP3 46, **ETP3 53**
 Cummings, J. **IWP10 78**
 Cunge, G. **BT1 6**, **ETP3**
46, **ETP3 53**
 Cunge, Gilles **ETP7 84**
 Curry, John J. **DT2 6**,
LR2 5

D

Dalgarno, A. **CT1 1**
 Dandapani, Eshwar
IWP10 74
 Date, Hiroyuki **GW1 4**
 David, Rainer **MR1 4**
 Davies, P.B. **IWP2 8**
 de Urquijo, J. **IWP1 3**
 DeJoseph Jr., C.A.
ETP1 15, **ETP2 19**,
ETP7 80, **ETP7 86**
 Deutsch, H. **ETP1 11**,
ETP1 12, **IWP3 18**,
MR1 5
 Dhali, Shirshak **QF1 5**
 Ding, G. **OR1 4**
 Ding, Guowen **IWP5 35**
 Ding, Weixing **IWP11 79**,
RF2 6
 Dinh, T. **ETP3 35**
 Döbele, H.F. **DT1 1**,
DT1 4, **ETP7 79**
 Donkó, Zoltán **IWP4 29**
 Donnelly, Vincent M.
AT2 6, **RF1 3**
 Dorai, Rajesh **IWP11 80**
 Doughty, Douglas **ETP4 61**
 Drakes, James **LR1 5**
 Dressler, R.A. **LR1 4**
 Dressler, Rainer **ETP2 22**,
ETP2 26
 Duffy, A. **ETP3 47**
 Dyakov, Ilya **LR1 3**
 Dyakov, I.V. **ETP2 18**

E

Economou, Demetre **NR2 2**,
RF1 4

Author Index

- Edamura, Manabu
IWP4 33, **NR2 4**
- Eden, Gary **RF2 1**
- Edgell, Robert ETP1 2
- Eggs, Christoph IWP2 7
- Elakshar, F.F. IWP13 95
- El-Dakroui, A. **ETP4 57**
- El-Habachi, A. ETP4 57,
ETP4 58, **LR2 2**
- El-Habachi, Ahmed
ETP3 31, ETP3 33
- Eliasson, Baldur IWP2 10
- Ellefson, Robert E. BT2 5
- Engeln, Richard **GW1 2**
- Entley, William R. **FW1 4**
- Ernst, U. ETP4 59, **LR2 3**
- F**
- Fabrikant, I.I. ETP1 16,
IWP3 21, JW1 7
- Farley, John W. IWP13 92
- Felfli, Zineb **IWP3 20**
- Feng, S.-J. DT2 8
- Ferne, M. QF1 4
- Fernsler, R.F. FW1 5,
FW1 6, IWP12 86,
IWP12 87, IWP12 88
- Ferreira, C.M. ETP3 29,
IWP4 32
- Filipović, D.V. **IWP3 15**
- Flores, Guadalupe QF1 6
- Flores III, G.J. IWP5 37
- Font, Gabriel IWP1 1,
OR1 5
- Fontes, C.J. IWP3 16
- Frank, K. ETP4 59, **LR2 3**
- Frees, Louis C. BT2 5
- Fresnet, F. **IWP11 82**
- Fu, Weihai **IWP10 71**
- Fujita, T. FW2 2
- Fukuyama, T. **ETP2 25**
- Fuller, Nicholas C.M.
AT2 6
- G**
- Gallis, Michael FW2 6
- Gallup, G.A. ETP1 16
- Gambús, G. IWP7 50
- Ganguly, Biswa ETP7 86
- Ganguly, B.N. ETP7 83
- Ganguly, J.D. **BT2 4**
- Garamoon, A.A. **IWP13 95**
- Garscadden, A. ETP1 15,
ETP2 19
- Gay, T.J. JW1 6
- Ghanashev, Ivan **MR2 3**
- Gibson, Jennifer ETP1 1
- Gijbels, Renaat FW2 3,
FW2 4, IWP6 39
- Gilgenbach, R.M. **ETP7 93**
- Girard, Frédéric **ETP2 24**
- Girshick, Steven L. IWP2 9
- Giuliani, J.L. **IWP10 72**
- Godyak, V. ETP3 47
- Godyak, Valery **AT2 2**
- Goedheer, Wim FW2 3
- Gogineni, Prasad BT2 3
- Gomez, S **IWP7 52**
- Gordon, Matthew DT1 5
- Goree, J **OR2 1**
- Goto, Toshio DT1 6,
DT1 7, ETP7 85,
IWP10 69
- Gottschalk, J.R. **IWP9 63**,
JW2 6
- Goussset, G. ETP3 29,
IWP4 32, **QF2 8**
- Govindan, T.R. AT2 3,
BT1 2, BT2 2
- Graham, W.G. ETP3 36,
ETP3 45, ETP7 77,
IWP7 52
- Grapperhaus, Michael
FW1 1
- Graves, David **JW2 2**,
RF1 6
- Green, Karen QF1 6
- Green, K.M. **IWP5 37**
- Grinstead, Jay QF1 1
- Grossjohann, Rico ETP4 62
- Gu, Jian-ping ETP2 21
- Gu, J.-P. ETP2 20
- Guberman, Steven **LR1 1**
- Guenther, Klaus **LR2 4**
- Guerra, V. IWP1 2
- Gui, H. OR1 4
- Gulley, Robert **AT1 5**,
ETP1 1
- Guna, M. NR1 5
- Guo, X. **IWP3 16**
- H**
- Haaland, P.D. ETP2 19
- Haas, F.A. **IWP4 28**
- Hadidi, K. IWP5 37
- Hadidi, Kamal **QF1 6**
- Hagelaar, Gerjan **DT2 9**
- Hala, Ahmed **IWP12 85**
- Hamada, Akira ETP1 4
- Hanna, Jeremy IWP6 43
- Hannemann, Mario
IWP10 68
- Hardt, Peter IWP10 68
- Hardy, Kenneth A. NR1 5
- Hartgers, Bart IWP8 61,
IWP8 62
- Hartig, M BT2 1
- Hartmann, W. LR2 3
- Hassouni, Khaled DT1 5
- Hatae, A. ETP6 68
- Hayashi, Makoto ETP1 6
- Hebner, Greg **ETP3 51**,
ETP7 75
- Heggemeier, J.P. ETP1 5
- Heil, Brian AT2 4
- Hennessy, William J.
FW1 4
- Herman, Irving P. AT2 6,
DT1 2
- Hershkowitz, Noah **BT1 4**,
IWP12 85, IWP7 47
- Hikosaka, Y. BT2 6, BT2 7
- Hioki, K. **ETP7 73**
- Hirsch, G. ETP2 20
- Hirsch, Gerhard ETP2 21
- Hitchon, W.N.G. **IWP1 5**
- Hojnacki, D. IWP3 22
- Holloway, James Paul
ETP3 40
- Hong, Jung-In ETP3 50
- Hongsheng, Guo **IWP13 97**
- Hoogland, Robert LR2 6
- Hori, Masaru DT1 6,
DT1 7, ETP7 85,
IWP10 69
- Horie, I **ETP3 37**
- Huebschman, M.L.
ETP7 74
- Huo, Winifred **ETP1 13**
- Hwang, Helen BT2 1,
BT2 2
- I**
- Ianno, N.J. IWP4 25
- Iizuka, Satoru ETP3 34,
ETP6 67
- Ilias, Samir IWP10 70
- Imai, S. IWP7 51
- Ingold, J.H. DT2 1, **QF2 7**
- Ionikh, Yuriy DT1 8
- Ionikh, Yury Z. **QF2 1**,
QF2 2
- Isaacs, W.A. **AT1 3**
- Ishii, Nobuo DT1 7
- Islam, T. **IWP4 25**
- Itazu, N. ETP7 73
- Ito, Masafumi DT1 6,
DT1 7, ETP7 85,
IWP10 69
- Itoh, H. ETP2 25
- Iwatani, Kazuki ETP3 44
- J**
- Jae Koo, Lee IWP9 66
- James, B.W. ETP3 43
- Janssen, Ger IWP8 61
- Jayaraman, RaviPrakash
IWP10 74
- Ji, J.S. **IWP12 84**
- Jiao, C.Q. **ETP1 15**,
ETP2 19
- Jin Ho, Kang IWP9 66
- Johannes, Justine FW2 6,
RF1 4
- Johnsen, Rainer **ETP7 92**
- Johnston, Colin IWP8 61
- Johnston, C.W. **ETP4 63**
- Johnston, M.D. ETP7 93
- Johnston, M.E. **ETP1 5**
- Johnston, Tudor W. MR2 4
- Johnston, Tudor Wyatt
OR1 1
- Joost, van der Mullen
ETP4 63
- Jovančić, P. IWP13 99
- Jović, D. IWP13 99
- K**
- Kabouzi, Y. **ETP3 42**
- Kaganovich, Igor FW2 7,
IWP6 39, **NR2 2**
- Kaiser, D. BT1 5
- Kajiwara, Toshinori
ETP7 82
- Kalatchev, M. ETP7 71
- Kamada, Takahiro ETP7 87
- Kanakasabapathy,
Sivananda K. **IWP13 91**
- Kanik, I. IWP3 16
- Karakaya, F. IWP13 90
- Karakaya, Fuat RF2 2
- Kastenmeier, Bernd E.E.
BT2 5
- Katachanov, Alexander
ETP7 84
- Kato, Kohgi ETP3 34
- Kato, T. IWP3 19
- Kawamoto, Shinji FW2 5
- Kawamura, K. ETP7 76
- Kawetzki, T. DT1 4
- Kedzierski, W **IWP3 17**
- Keeler, M.L. **IWP3 12**,
IWP3 13
- Keiter, P.A. IWP6 42
- Keiter, Paul IWP6 40,
OR1 2, OR1 3
- Kelly, K. OR1 4
- Kelly, Kurt IWP5 35
- Kettlitz, Manfred **ETP4 62**

- Khabibrakhmanov, I.
 ETP3 47
 Khachan, J. ETP3 43
 Khakoo, M.A. IWP3 16,
 JW1 3
 Khater, Marwan **IWP10 73**
 Killer, Eric IWP2 10
 Kim, Chang-Koo **RF1 4**
 Kim, J.B. **ETP7 76**
 Kim, J.S. **ETP7 88**,
 IWP12 84, QF1 7
 Kim, S.S. ETP3 50
 Kim, Yong-Ki **JW2 4**
 Kimura, M. ETP2 20
 Kimura, Mineo **ETP1 4**,
 ETP2 21
 Kinoshita, K. BT2 6, BT2 7
 Kitajima, Masashi ETP1 4
 Kitajima, T. **FW2 2**
 Kitamori, K ETP3 37,
 ETP3 38
 Kleber, Jennifer L. **RF2 5**
 Klein, M. IWP9 64
 Klein, T.M. ETP1 5
 Kline, J.L. IWP6 42
 Kline, John IWP6 40,
 OR1 2, OR1 3
 Koga, K. ETP6 68,
 ETP6 69
 Kogelschatz, Ulrich
 IWP2 10
 Kondo, Kei-ichi GW1 4
 Kono, Akihiro DT1 6,
 ETP7 78, ETP7 85
 Kortshagen, Uwe **AT2 4**,
 IWP2 7, IWP2 9, **QF2 6**
 Kotp, E.F. IWP13 95
 Kouchi, N. **JW1 2**
 Kovalski, S.D. ETP7 93
 Kroesen, Gerrit DT2 2,
 DT2 9
 Kruger, C. GW1 1
 Kruger, Charles JW2 5
 Kucheriavy, Andrew
 ETP1 2
 Kull, Alan **IWP5 36**
 Kurihara, M. **DT2 10**
 Kuroki, Yukinori ETP3 44
 Kurunczi, P. ETP1 3,
 IWP4 30
 Kushner, Mark J. **GW2 1**,
 IWP11 80, IWP8 59,
 IWP9 65, **JW2 3**, OR1 5,
 RF1 2
- L**
 Lacoste, A. **IWP4 32**
 Lampe, M. FW1 5, FW1 6
- Lang, N. **ETP7 71**
 Langan, John G. FW1 4
 Lange, Hartmut **ETP3 55**
 Lapatovich, Walter
 ETP2 23
 Laux, C. **GW1 1**
 Laux, Christophe JW2 5
 Lavarias, Arnel IWP10 71
 Laverty, S. ETP3 45
 Lavrov, B.P. ETP7 71
 Lawler, James E. QF2 6
 Lawler, J.E. DT2 6,
 GW2 2, LR2 5
 Le Guyadec, Erick ETP2 24
 Lee, W.C. ETP6 70,
 ETP7 90, IWP4 34
 Lee, Yao-Sheng **BT2 3**
 Leipold, Frank **ETP3 31**
 Leiweke, R. **QF1 4**
 Lémpert, W. ETP6 70,
 ETP7 90, IWP4 34,
 QF1 4
 Leonhardt, D. FW1 5,
 IWP12 86, IWP12 87,
 IWP12 88
 Leou, K.C. **IWP6 38**
 Leroy, O. QF2 8
 Letourneur, Karine GW1 2
 Levandier, Dale **ETP2 22**,
 ETP2 26
 Levandier, D.J. LR1 4
 Levin, Debbie **LR1 5**
 Li, Y. ETP2 20
 Li, Yan-Ming **DT2 3**
 Li, Yunlong **DT1 5**,
 ETP3 34
 Lichtenberg, A.J. BT1 8
 Lieberman, M.A. AT2 5,
 BT1 8
 Lieberman, Michael A.
 JW2 1
 Lilly, J. **ETP6 70**
 Lin, Chun C. IWP3 12,
 IWP3 13, IWP3 14,
 JW1 1
 Lin, T.L. IWP6 38
 Lipshultz, Bruce ETP7 74
 Lister, G.G. DT2 6, LR2 5
 Lister, Graeme **GW2 3**,
 IWP8 60
 Lo, T.Y. IWP6 38
 Loffhagen, D. IWP2 8
 Loffhagen, Detlef **GW1 3**,
 IWP10 68
 Loureiro, J. **IWP1 2**
 Lu, S. ETP7 91, FW1 2
 Lukas, Ch. **ETP7 79**
- Lungu, A.M. ETP7 72,
 IWP11 81
 Lungu, C.P. **ETP7 72**,
 IWP11 81
- M**
 Ma, Cheng-Yu IWP11 79
 Macheret, Sergey O.
 IWP13 89, **IWP4 27**,
 NR2 5, QF2 1
 Madziwa, T.G. **ETP3 54**
 Maeda, Mitsuo ETP7 82
 Maeda, S. ETP6 69
 Maerk, T.D. IWP3 18,
 MR1 5
 Maerk, Tilmann MR1 4
 Maeshige, K. **IWP7 49**
 Magne, L. IWP11 82
 Maguire, P.D. ETP3 45
 Mahony, C.M.O. ETP3 36,
 ETP3 45
 Makabe, T. **BT1 1**, DT2 10,
 ETP7 73, FW2 2,
 IWP7 49
 Malović, G. IWP3 23
 Malyshev, Mikhail V.
 AT2 6
 Manheimer, W.M. FW1 5,
 FW1 6
 Mano, T. FW2 2
 Mansour, M.A. ETP3 43
 Marakhtanov, A.M. **BT1 8**
 Margot, Joëlle **MR2 4**
 Margot, Joelle OR1 1
 Marinković, B. IWP3 15
 Märk, Tilmann AT1 6
 Martus, K.E. **ETP1 3**,
 ETP1 10
 Mason, Nigel AT1 6
 Mathews, D.F. IWP3 16
 Matsui, J. BT1 1
 Matsumoto, Naoki **MR2 5**
 Matsuo, Peter J. BT2 5
 Matsuzaki, H. IWP7 55
 Matt, S. IWP3 18
 Matt, Sara **MR1 4**
 Matuoka, Y. ETP6 69
 Maximov, Andrei V.
 MR2 6
 McConkey, J W IWP3 17
 McCorkle, Dennis
 IWP11 79, RF2 6
 McCurdy, C. William
 MR1 2
 McCurdy, C.W. AT1 3
 McGrath, Robert IWP10 74
 McInerney, Jack E GW1 5
 McKoy, Vincent ETP1 7
- Mechold, L. **IWP2 8**,
 QF1 2
 Meezan, Nathan IWP13 93
 Meger, R.A. **FW1 5**,
 FW1 6, IWP12 86,
 IWP12 87, IWP12 88
 Mérel, Philippe **FW1 3**
 Meshchanov, Alexander
 QF2 2
 Meyyappan, M. AT2 3,
 BT1 2
 Michael, J.D. **DT2 1**
 Mikaelian, G. IWP3 16
 Mildren, R.P. **DT2 5**
 Miles, Richard B. DT1 8,
 IWP13 89, IWP4 27,
 NR2 3, NR2 5, QF1 1,
 QF2 1, QF2 2
 Millard, Michael **ETP7 86**
 Miller, T.A. ETP7 80,
 IWP7 53
 Misakian, Martin ETP3 41,
 IWP4 33
 Misina, Martin IWP6 39
 Mitchell, J. Brian A. **LR1 2**
 Mitchell, Stephen E.
 IWP13 92
 Miyamoto, M. IWP11 81
 Mizuno, Manabu IWP4 26
 Mizutani, Yuko IWP10 69
 Moisan, M. ETP3 42,
 RF2 4
 Moisan, Michel FW1 3,
 IWP10 70, **MR2 1**
 Möller, Wolfhard **RF1 5**
 Monaco, Elizabeth M.
 IWP2 11
 Moreau, S. **RF2 4**
 Morgan, W.L. **ETP1 8**,
 ETP1 9
 Morris, Robert IWP11 80
 Morrow, R. DT2 5
 Morrow, T. ETP7 77
 Moselhy, M. **ETP4 58**,
 LR2 2
 Moshkalyov, S. **ETP7 77**
 Moskowitz, Phil **IWP8 60**
 Motomura, H. IWP7 51
 Motoyama, Y. **IWP7 55**
 Msezane, Alfred IWP3 20
 Murakami, I. IWP3 19
 Muraoka, K. ETP3 43,
 ETP7 76, QF1 3
 Muraoka, Katsunori
 ETP7 82
 Murnick, D.E. DT2 4

Author Index

- Murphy, D.P. FW1 5,
IWP12 86, IWP12 87,
IWP12 88
- N**
- Nagesha, Kannadaguli
ETP1 14
- Nagulapally, Manoj JW2 5
- Nakamura, Masayuki
DT1 7
- Nakamura, S ETP3 38
- Nakamura, Yoshiharu
ETP1 6
- Nakano, N. BT1 1,
ETP7 73, IWP7 49
- Nakano, Nobuhiko FW2 1
- Nakatani, Keigo ETP7 78
- Narishige, S. ETP3 43
- Nelson, D. QF1 2
- Nishimura, Naoki IWP6 44
- Nishimura, Takuma
IWP4 26
- Noda, S. BT2 6, BT2 7
- Nordheden, Karen BT2 3
- Nossair, A.M. IWP13 95
- O**
- Oda, Akinori IWP8 58
- Oehrlein, Gottlieb S.
BT2 5, RF1 1
- Ogoyski, Alexander
ETP3 32
- Ohkubo, Mitsuyuki
ETP7 87
- Ohmori, Y ETP3 37
- Okada, Tatsuo ETP7 82
- Okpalugo, O.A. ETP3 45
- Oksuz, Lutfi IWP7 47
- Olthoff, James ETP1 6,
ETP3 41, IWP4 33,
JW1 4, JW1 5
- Olthoff, J.K. ETP2 18
- Overzet, Lawrence J.
IWP10 73, IWP10 75,
RF2 5
- Overzet, L.J. IWP13 91
- Ozaki, Ryoichi ETP6 67
- Ozawa, N. BT2 6, BT2 7
- P**
- Packan, D. GW1 1
- Paller, E. OR1 4
- Palm, P. ETP1 17, NR2 6
- Pashaie, Bijan QF1 5
- Pasquiers, S. IWP11 82
- Patiño, P. IWP7 50
- Pechacek, R.E. FW1 5
- Pejčev, V. IWP3 15
- Peko, B.L. ETP2 18,
IWP13 96
- Peko, Brian LR1 3
- Petrov, George ETP3 32
- Petrova, Tsvetelina
ETP3 32
- Petrović, Z.Lj. ETP3 56,
IWP1 6
- Petrović, Z.Lj. IWP13 99
- Petrović, Z.Lj. IWP3 23,
IWP7 57
- Phelps, A.V. ETP3 30
- Pierrot, L. GW1 1
- Pindzola, M.S. MR1 3
- Pinnaduwege, Lal ETP1 14,
IWP11 79, NR1 4, RF2 6
- Ploenjes, E. ETP1 17,
NR2 6
- Popović, S. DT2 7,
ETP3 35, IWP13 94,
QF2 4
- Postel, C. IWP11 82
- Postel, Olivier B. IWP9 67
- Puech, V. IWP11 82
- Pullins, S. LR1 4
- Pullins, Steve ETP2 22,
ETP2 26
- Punset, C. ETP3 29
- R**
- Rabalais, Mark S. RF2 5
- Radetić, M. IWP13 99
- Radmilović, M. IWP1 6
- Radovanov, S. IWP10 78
- Radovanov, Svetlana B.
IWP10 76
- Rao, M.V.V.S. ETP2 18,
ETP7 88, IWP12 84,
QF1 7
- Raspopović, Z.M. ETP3 56
- Ratner, Buddy D. RF2 3
- Rauf, S. BT2 1, IWP7 45,
QF1 8
- Rescigno, T.N. AT1 3
- Ricard, A. RF2 4
- Rich, J.W. ETP1 17,
IWP4 34, NR2 6
- Riley, Merle E. LR1 6,
OR2 2
- Ritchie, Burke LR1 6
- Roe, Larry DT1 5
- Romanini, Daniele ETP7 84
- Röpcke, J. ETP7 71,
IWP2 8, QF1 2
- Rosati, Richard ETP7 92
- Roth, J. Reece RF2 2
- Roth, J.R. IWP13 90
- Rousseau, A. IWP11 82
- Rozoy, M. IWP11 82
- Rusinov, I.M. IWP7 54
- Ruzic, David N. IWP7 56
- S**
- Sá, P.A. IWP1 2
- Sakadžić, S. ETP3 56
- Sakai, T. DT2 8
- Sakai, Y. ETP3 39,
ETP7 72, IWP11 81
- Sakai, Yosuke ETP7 87,
IWP4 26, IWP8 58
- Sakoda, T. ETP3 43
- Salvermoser, M. DT2 4
- Samukawa, Seiji IWP10 69
- Sankaranarayanan, Ravi
QF1 5
- Sasaki, Tai IWP8 58
- Sato, Hiroshi ETP2 21
- Sato, Noriyoshi ETP3 34,
ETP6 67, OR2 3
- Sato, Shoichi IWP6 44
- Sawada, Keiji ETP7 74
- Schappe, R. Scott ETP1 2
- Scharer, J. OR1 4
- Scharer, John IWP5 35
- Scheier, Paul AT1 6,
MR1 4
- Schermerhorn, J.D.
IWP9 63
- Schl+APw-ter, Hans
MR2 6
- Schmidt, Dan IWP13 93
- Schmidt, M. ETP1 11,
ETP1 12
- Schmidt, Martin IWP10 68,
MR1 1, QF2 5
- Schoenbach, Karl H.
ETP3 31, ETP3 33,
LR2 1, QF2 3
- Schoenbach, K.H. ETP4 57,
ETP4 58, LR2 2
- Schram, Daniel GW1 2
- Schultz, D.R. ETP2 20
- Schulz-von der Gathen, V.
DT1 4, ETP7 79
- Scime, Earl E. IWP6 40,
IWP6 41, OR1 2, OR1 3
- Scime, E.E. IWP6 42
- Seki, M. IWP7 55
- Sekine, M. BT2 6, BT2 7
- Senn, Gilbert AT1 6
- Seo, Sang-Hun ETP3 49,
ETP3 50
- Serikov, Vladimir FW2 5
- Shannon, S. ETP3 40
- Shao, M. IWP9 63
- Sharma, S.P. ETP7 88,
IWP12 84, QF1 7
- Shaw, D.M. ETP3 48,
IWP12 83, IWP13 98,
IWP7 48
- Shcherbakov, Yu.V.
ETP5 66
- Sheman, D.M. IWP13 90
- Sherman, Daniel M. RF2 2
- Shi, Wenhui ETP3 33
- Shilova, A.V. ETP5 66
- Shimizu, Tetsuji ETP3 34
- Shimoda, T. ETP3 39
- Shimozuma, Mitsuo GW1 4
- Shiratani, M. ETP6 68,
ETP6 69
- Shivarova, A. MR2 2
- Shneider, Mikhail N.
ETP5 65, NR2 5
- Shurgalin, M. ETP4 64
- Shurgalin, Max ETP2 23
- Siegel, Ralph ETP1 6
- Siegel, R.B. NR1 3
- Sifontes, A. IWP7 50
- Simons, L. NR1 5
- Singh, Harmeet RF1 6
- Skalny, Jan Dusan AT1 6
- Skrzypkowski, Miroslaw P.
ETP7 92
- Slemrod, Marshall BT1 3
- Smith, H.B. IWP4 24
- Smithro, C.G. ETP3 27
- Smolyakov, A.I. ETP3 47
- Snijkers, R.J.M.M.
IWP9 64
- Snodgrass, T.G. ETP7 91,
FW1 2
- Sobolewski, Mark ETP7 81,
IWP7 46
- Sosov, Yu. IWP3 22,
JW2 6
- Spaan, M. ETP7 79
- Spangler, R. IWP6 42
- Spangler, Robert IWP6 41
- Sparks, T BT2 1
- Stafford, Luc MR2 4
- Stamatovic, Aleksandar
AT1 6
- Stamatovic, Aleksander
MR1 4
- Stancil, P.C. ETP2 20
- Stancil, Phil ETP2 21
- Stark, R.H. ETP4 57
- Stark, Robert H. ETP3 31,
QF2 3
- Steen, P.G. ETP3 36,
IWP7 52

Steffens, Kristen L.
ETP7 81
 Stephen, Thomas **BT2 8**
 Stephen, T.M. IWP13 96
 Sternberg, Natalia **BT1 3**
 Stojanović, V. IWP1 6
 Stoykov, Svetoslav **IWP2 7**
 Strinić, A. **IWP3 23**
 Subramaniam, V.V.
 ETP6 70, IWP4 34
 Suda, Yoshiyuki **IWP4 26**
 Sueoka, Osamu ETP1 4
 Sugai, Hideo MR2 3
 Sugawara, H. **ETP3 39**,
 ETP7 72, IWP11 81
 Sumiya, Shigeaki IWP10 69
 Suzuki, Reiko ETP2 21
 Suzuki, T **ETP3 38**
 Swihart, Mark T. IWP2 9

T

Tabata, R. QF1 3
 Tabrizian, M. RF2 4
 Tachibana, K. **DT2 8**,
IWP7 51
 Tagashira, Hiroaki GW1 4
 Takagi, Ken-Ichi **ETP3 44**
 Takahashi, Nobuaki
 IWP8 58
 Takano, Y. IWP7 55
 Takashima, Seigou **DT1 6**,
ETP7 85
 Takemoto, Hiroki IWP6 44
 Tanaka, Hiroshi ETP1 4
 Tanaka, K. ETP6 69
 Tang, Zhen **NR2 3**
 Tarnovsky, V. **ETP1 11**,
ETP1 12
 Tav, Cumali **NR1 4**
 Team, CRD on expanding
 plasmas GW1 2
 Team, Dept. of Mech. and
 Aerospace Eng. Princeton
 Univ. DT1 8
 Team, University of
 Tennessee IWP13 90
 Team, WVU Helicon
 OR1 3
 Terry, J. ETP7 74

Theodosiou, C.E. IWP3 22,
 JW2 6
 Thomas, P. IWP5 37
 Thomas, Paul QF1 6
 Thompson, C. ETP7 77
 Thompson, Keith
IWP10 75
 Thompson, Matthew S.
 IWP2 11
 Thornhill, J.W.
 IWP10 72
 Thumm, U. **IWP3 21**
 Tokuyama, S. ETP3 43
 Toyozawa, A. ETP6 68
 Trajmar, S. IWP3 16
 Tran, K.C. ETP3 42
 Trassy, C. ETP3 42
 Truxon, J.M. IWP3 22,
JW2 6
 Tsai, C.H. IWP6 38
 Tsendin, Lev FW2 7
 Tsuboi, H. BT2 6, BT2 7
 Tsukada, Tsutomu
 IWP10 69
 Turner, M.M. **BT1 6**,
BT1 7, ETP3 46,
 ETP3 53

U

Uchida, Giichiro **ETP6 67**
 Uchino, K. ETP3 43, QF1 3
 Uchino, Kiichirou ETP7 82
 Uchiyama, H. ETP3 48,
IWP12 83, IWP7 48
 Uhrlandt, Dirk **ETP3 28**,
 ETP3 55, **QF2 5**
 Ulrich, A. DT2 4
 Upadhyaya, Kaushal BT2 3
 Ushirozawa, M. IWP7 55

V

Valentini, H.-B. **BT1 5**
 van de Sanden, Richard
 GW1 2
 van der Heijden, H.
 ETP4 63
 Van der Heijden, Harm
 IWP8 61, **LR2 6**
 Van der Mullen, Joost
 IWP8 61, IWP8 62,
 LR2 6

van der Straaten, Trudy
IWP8 59, IWP9 65
 van Dijk, Jan ETP4 63,
IWP8 61, IWP8 62,
 LR2 6
 Van Doren, Jane M.
IWP2 11
 Van Zyl, Bert BT2 8
 Vender, D. BT1 6, ETP3
 46, ETP3 53
 Ventzek, P. L. G. **BT2 1**
 Ventzek, Peter GW1 4
 Ventzek, PLG ETP3 37,
 ETP3 38
 Ventzek, P.L.G. IWP7 45,
 QF1 8
 Viggiano, A.A. IWP11 80
 Vitello, Peter **ETP3 52**
 Vrhovac, S. IWP7 57
 Vukovic, Mirko **IWP4 31**
 Vušković, L. ETP3 35,
 IWP13 94, IWP3 15,
 QF2 4
 Živanov, S. **IWP7 57**
 Živanović, J. IWP7 57

W

Walker, Thad IWP3 12
 Walton, S.G. FW1 5,
 IWP12 86, **IWP12 87**,
 IWP12 88
 Wang, J.G. **IWP3 19**
 Wang, S.-B. AT2 1
 Wang, Yicheng **ETP3 41**,
IWP4 33
 Watanabe, Ayako ETP2 21
 Watanabe, M. **ETP3 48**,
 IWP12 83, IWP7 48
 Watanabe, Y. **ETP6 68**,
ETP6 69
 Waters, K BT2 1
 Watts, Christopher
IWP6 43
 Wendt, A.E. **AT2 1**,
 ETP7 91, FW1 2
 Werking, J. AT2 1
 White, A. ETP6 70,
IWP4 34

Wienhold, F.G. QF1 2
 Wieser, J. DT2 4
 Wilde, R.S. **ETP1 16**
 Williams, P.F. IWP4 25
 Williams, Skip **IWP11 80**
 Williams, Steve ETP1 2
 Williamson, J.M. **ETP7 83**
 Williamson Jr., W.
 IWP3 22, JW2 6
 Winkler, Rolf ETP3 28,
 GW1 3, IWP10 68, QF2 5
 Winstead, Carl **ETP1 7**
 Woong, Kim IWP9 66
 Woskov, Paul QF1 6
 Woskov, P.P. IWP5 37
 Wszolek, Matthew F.
 IWP2 11
 Wu, Han-Ming **GW1 5**,
IWP1 1
 Wu, Yaoxi **AT2 5**

X

Xu, Y. **JW1 7**

Y

Yahia, L'H. RF2 4
 Yalin, Azer **DT1 8**, QF2 2
 Yamashiro, Yasumasa
 IWP6 44
 Yan, Min **FW2 3**
 Yaney, Perry ETP7 86
 Yasuoka, Koichi **NR2 1**
 Yoneda, Katsumi DT1 6,
 ETP7 85
 Yonesu, Akira **IWP6 44**
 Yoon, N.S. ETP3 50
 Young Kyo, Shin IWP9 66
 Yu, L. GW1 1
 Yu, Z. IWP13 98

Z

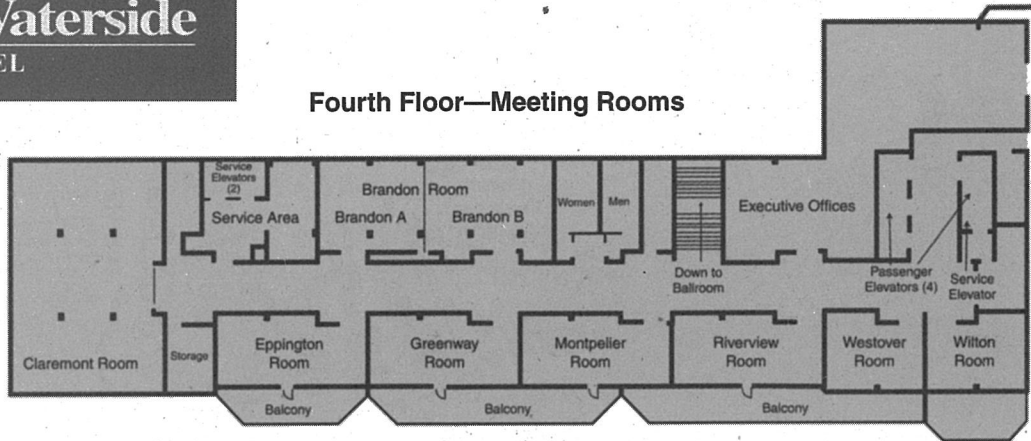
Zahniser, M. QF1 2
 Zare, R. GW1 1
 Zeman, V. IWP3 16
 Zhang, Da **RF1 2**
 Zimmerman, Todd A.
 IWP3 12
 Zou, Jizou IWP13 89

NOTES

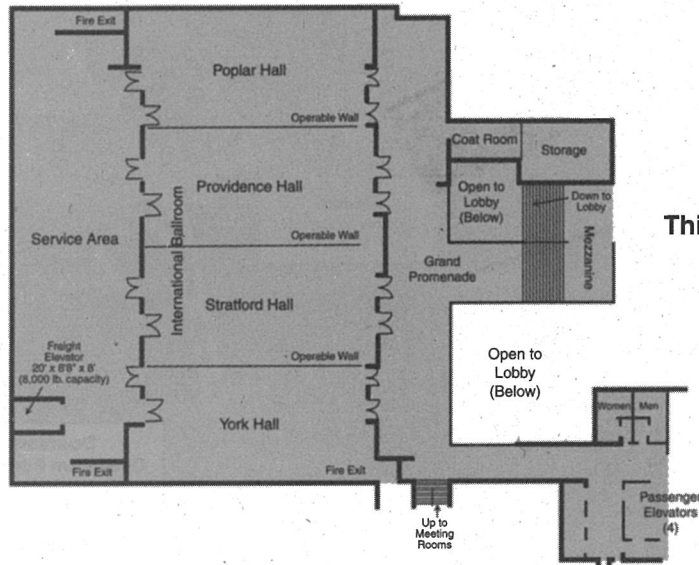


Sheraton Norfolk Waterside HOTEL

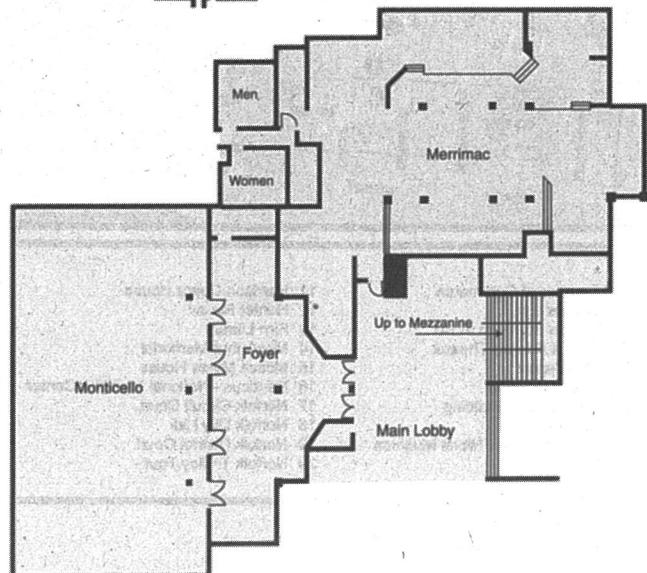
Fourth Floor—Meeting Rooms



Third Floor—Ballrooms



Lobby Level— Merrimac & Monticello



OR2 **Dusty Plasmas**
Goree, Sato
York Room

18:30 THURSDAY EVENING
7 OCTOBER

PR1 **Reception and Banquet**
York and Stratford Rooms

8:00 FRIDAY MORNING
8 OCTOBER

QF1 **Diagnostics II**
Stratford Room

QF2 **DC Glows**
York Room

10:30 FRIDAY MORNING
8 OCTOBER

RF1 **Plasma-Surface Interactions**
Oehrlein, Möller
Stratford Room

RF2 **Innovative Plasma Applications/Negative Ion Formations**
Eden, Ratner
York Room

Epitome of the 1999 GEC Meeting

8:00 TUESDAY MORNING 5 OCTOBER

- AT1 **Electron-Molecule Collisions**
Chutjian, Burrow
Stratford Room
- AT2 **Glows: Inductively Coupled Plasmas**
Wendt, Godyak
York Room

10:30 TUESDAY MORNING 5 OCTOBER

- BT1 **Sheaths and Instabilities**
Stratford Room
- BT2 **Etching**
York Room

13:30 TUESDAY AFTERNOON 5 OCTOBER

- CT1 **Foundations of Gaseous Electronics**
Dalgarno
York and Stratford Rooms

15:00 TUESDAY AFTERNOON 5 OCTOBER

- DT1 **Diagnostics I**
Döbele, Herman
Stratford Room
- DT2 **Lighting and Plasma Displays**
York Room

19:30 TUESDAY EVENING 5 OCTOBER

- ETP1 **Electron-Molecule Collisions**
Poplar Room
- ETP2 **Heavy Particle Collisions**
Poplar Room
- ETP3 **Glows I**
Poplar Room
- ETP4 **High Intensity Light Sources**
Poplar Room
- ETP5 **Spark Channel Temporal Variations**
Poplar Room
- ETP6 **Dusty Plasmas**
Poplar Room
- ETP7 **Optical Diagnostics**
Poplar Room

8:00 WEDNESDAY MORNING 6 OCTOBER

- FW1 **Deposition/Materials Processing**
Grappnerhaus
Stratford Room
- FW2 **RF Glows**
York Room

10:15 WEDNESDAY MORNING 6 OCTOBER

- GW1 **Chemistry and Transport Processes**
Stratford Room
- GW2 **Will Allis Memorial Session**
Lawler, Lister
York Room

11:30 WEDNESDAY MORNING 6 OCTOBER

- HW1 **Business Meeting**
York Room

13:30 WEDNESDAY AFTERNOON 6 OCTOBER

- IWP1 **Transport Effects**
Poplar Room
- IWP2 **Gas Phase Chemistry**
Poplar Room
- IWP3 **Electron-Atom Collisions**
Poplar Room
- IWP4 **Glows II**
Poplar Room
- IWP5 **Laser Media and Thermal Plasmas**
Poplar Room
- IWP6 **Magnetically-Enhanced Plasmas**
Poplar Room
- IWP7 **Plasma-Surface Interactions**
Poplar Room
- IWP8 **Lighting-Related Discharges**
Poplar Room
- IWP9 **Plasma Displays**
Poplar Room
- IWP10 **Plasma Processing and Surface Modifications**
Poplar Room
- IWP11 **Environmental Applications**
Poplar Room
- IWP12 **Electrical Diagnostics and Mass Spectrometry**
Poplar Room
- IWP13 **Innovative Plasma Applications**
Poplar Room

16:00 WEDNESDAY AFTERNOON 6 OCTOBER

- JW1 **Electron Collisions With Excited Atoms and Molecules**
Lin, Kouchi, Khakoo
Stratford Room
- JW2 **Simulations and Modeling**
Lieberman, Graves, Kushner, Kim
York Room

20:00 WEDNESDAY EVENING 6 OCTOBER

- KW1 **Laboratory Tours**
Old Dominion University Campus

8:00 THURSDAY MORNING 7 OCTOBER

- LR1 **Recombination and Heavy Particle Collisions**
Guberman, Mitchell
Stratford Room
- LR2 **High Pressure Lighting Plasmas**
Schoenbach, Guenther
York Room

10:30 THURSDAY MORNING 7 OCTOBER

- MR1 **Electron Impact Ionization**
Schmidt, McCurdy, Pindzola
Stratford Room
- MR2 **Surface Wave Plasmas**
Moisan, Shivarova
York Room

13:30 THURSDAY AFTERNOON 7 OCTOBER

- NR1 **Dissociation and Ionization**
Cocke, Cosby
Stratford Room
- NR2 **Glows**
Yasuoka
York Room

15:45 THURSDAY AFTERNOON 7 OCTOBER

- OR1 **Magnetically-Enhanced Plasmas**
Stratford Room



0003-0503(199910)44:4:1-M